Modelling altered Glucocorticoid Sensitivity: From HPA axis to metabolic abnormalities in mice and humans

Zoi Michailidou

Doctor of Philosophy
University of Edinburgh
2007

Acknowledgements

I am grateful to the Wellcome Trust for generously funding me for 4 years to pursue my PhD.

In the first year of my training, I had the pleasure to work with 3 very challenging supervisors (Dr Norah Spears, Dr Nik Morton and Dr Steve Anderton) in 3 very different projects but equally stimulating. My gratitude to all of them for challenging me and teaching me an awful lot about science and supervision and also for encourage me to freely explore their projects.

Working in Jonathan's lab has been a privilege. Jonathan, I have to say it has been a pleasure meeting you. Thank you for your enthusiasm, guidance and support on my research. But most of all I want to say *ευχαριστώ πολύ* for your generosity and for all the philosophical chats about life in general.

I also want to thank all the members of the ENDO lab, for genoursly helping me whenever I asked. Special thanks go to Lynne Ramage, an amazing person and a brilliant technician, that always had time to teach me and answer any of my questions. I will miss you Lynne! Val Lyons was the first person to teach me anything that had to do with plasmids and transfections, thanks Val for your patience and enormous help. Maggie Lai for her kindness, help and sharing her knowledge on any scientific aspect we have discussed the last 3 years. Meeting and working with Chris Kenyon was simply a pleasure. Thank you Chris for your kindness, calmness (!!!!!!) and all the help either technical or intellectual or for simply listening. Many thanks to Rod Carter for all the help with the restraint stress experiments and….Rod… sorry for all these early starts in the animal house. Oooo… it was fun exposing me to Scottish football.What an experience!

Supervising an autonomous Greek- that has a mind of their own- is not an easy job. Many thanks to Karen Chapman for her patience, supervision throughout my PhD, her thorough and critical views on my Thesis. Karen, I also want to say thank you for giving me the opportunity to experience supervising Liz Owen and Jenny Richardson, 2 great MSc students and a pleasure to work with them, I learned a lot.

I cannot thank enough Nik, first of all for believing and supporting my self-ruling nature, for his liberal guidance through my PhD, for teaching me what makes a good scientist with integrity and that good things come to those who wait. E*υχαριστώ Nik.*

My running fellows Elaine Smith (what can I say…I am impressed with you!), Julie Nixon (the one who introduced me to running back in the Western days…) and Nik for our long runs around Arthur Seat and the endorphins overload to keep me going. E*υχαριστώ!!!*

Special thanks to Heidi Sutherland and Sheila Boyle (MRC HCU, Edinburgh) for their generous and enormous help in the characterisation of the ESKN92 cells.

I was lucky to meet four extremely different people, but sharing a common characteristic…having a great heart, that not only we had fun pub/dinner times but more importantly supported me in a very difficult time in my life. What can I say…thanks is not enough… Julie, Janet, Ricky and Nik.

Last but not least I want to say… E*υχαριστώ*
Κώστα για την αγάπη σου και που ήρθες μαζί μου στα ξένα.
και
μπαμπά, μαμά, Χρύσα που πιστεύετε σε εμένα και με στηρίζετε.

Declaration

I declare that this Thesis and the work presented in it are entirely the result of my own independent investigation, except where stated in the text. This work has not been and is not currently submitted for any other degree.

Zoi Michailidou

dedicated to

Those who came the hard way…

Table of contents

List of Tables

List of Figures

List of Abbreviations

5'-RACE	5' rapid amplification of cDNA ends
11β-HSD1/2	11β-hydroxysteroid dehydrogenase type 1/2
ACTH	Adrenocorticotropic hormone
Adx	Adrenalectomy
AF1/2	Activation function 1 /2
AGT	Angiotensinogen
AP1/2	Activator protein 1 /2
AT	Adipose tissue
ATP	Adenosine triphosphate
AVP	Arginine vasopressin
β-gal	beta-galactosidase
bp	Base pairs
cAMP	Cyclic adenosine monophosphate
CBG	Corticosteroid-binding protein
cDNA	Complementary DNA
CNS	Central nervous system
CRH	Corticotrophin-releasing hormone
CT	Computerised single sliced tomography
DBD	DNA binding domain
DEPC	Diethylpyrocarbonate
DEX	Dexamethasone
DG	Dentate gyrus
DNA	Deoxyribonucleic acid
DNase	Deoxyribonuclease
dNTP	Deoxyribonucleotide triphosphate
DTT	Dithiothreitol
EDL	Extensor longus digitalis muscle
EDTA	Ethylenediaminetetraacetic acid
En-2	Engrailed- 2 gene
ER	Oestrogen receptor
ESC	Embryonic Stem Cell

ESKN92	GR-trapped embryonic stem cell line
FCS	Fat cell size
FISH	Fluorescence in situ hybridization
GABA	γ-amino butiric acid
GAPDH	Glyceraldehyde-3-phosphate dehydrogenase
GC	Glucocorticoid
G6Pase	Glucose-6-phosphatase
GR	Glucocorticoid receptor
GRE	Glucocorticoid response element
HPA	Hypothalamic-pituitary-adrenal
Hsp	Heat shock protein
IκB	Inhibitory κB
IL-2/8/10	Interleukins 2/8/10
kb	Kilobase
LBD	Ligand binding domain
LIF	Leukimia Inhibitory Factor
LPS	Lipopolysaccharide
MMTV (LTR)	Mouse mammary tumour virus (long terminal repeat)
MOPS	3-(N-Morpholino) propanesulfonic acid
mRNA	Messenger RNA
MR	Mineralocorticoid receptor
NF-κB	Nuclear factor κB
NLS	Nuclear Localization Signal
PBS	Phosphate buffered saline
PCR	Polymerase chain reaction
PEPCK	Phosphoenolpyruvate carboxykinase
PNMT	Phenyethanolamine-N-methyl-transferase
POMC	Pro-pionomelanocortin
PVN	Paraventricular nucleus of the hypothalamus
RA	Retinoic Acid
RAAS	Renin-angiotensin-aldosterone system
RNA	Ribonucleic acid

PRA	Plasma Renin Activity
PRC	Plasma Renin Concentration
RT-PCR	Reverse transcription PCR
SAT	Subcutaneous adipose tissue area
SBP	Systolic Blood Pressure
SCCE	Side chain cleavage enzyme
SDS	Sodium dodecyl sulfate
SEM	Standard error of the mean
SSC	Saline sodium citrate
STAT	Signal transducer and activator of transcription
TAT	Tyrosine aminotransferase
TBE	TRIS boric acid EDTA
TBP	TATA binding protein
TCR	T cell receptor
TEMED	N,N,N',N'-Tetramethyl-1-,2-diaminomethane
TG	Triglycerides
TNF-α	Tumour necrosis factor α
VAT	Visceral adipose tissue area
X-gal	5-bromo-4-chloro-3-indolyl-β-D-galactopyranoside
YAC	Yeast artificial chromosome

Publications from this Thesis

Papers

1. **Michailidou Z**, Coll AP, Kenyon CJ, Morton NM, O' Rahilly S, Seckl JR, Chapman KE. Peripheral mechanisms contributing to glucocorticoid hypersensitivity in Pomc-null mice treated with corticosterone. J Endocrinology 194, 161-170 (2007).

2. **Michailidou Z**, Jensen MD, Dumesic DA, Chapman KE, Seckl JR, Walker BR, Morton NM. Omental 11beta-hydroxysteroid dehydrogenase 1 correlates with fat cell size independently of obesity. Obesity May; 15(5); 1155-1160 (2007).

3. **Michailidou Z,** Southerland HGE, Marshall E, Carter R, Owen E, Holmes MC, Kenyon CJ, Morton NM, Seckl JR, Chapman KE. Glucocorticoid Receptor Heterozygosity causes Hypertension through RAS activation. *In preparation*

Abstracts

1. **Michailidou Z,** Southerland HGE, Carter R, Owen E, Kenyon CJ, Holmes MC, Morton NM, Seckl JR, Chapman KE. A novel glucocorticoid receptor allele: From HPA axis hyperactivity to metabolic abnormalities? *Abstract*, American Endocrine Society, June 2007, Toronto.

2. **Michailidou Z,** Southerland HGE, Carter R, Marshall E, Owen E, Kenyon CJ, Holmes MC, Morton NM, Seckl JR, Chapman KE. Gene trap-mediated Glucocorticoid Receptor Heterozygosity Exaggerates aspects of the Metabolic Syndrome. *Abstract Oral presentation (awarded 1st prize presentation)*, 2ND Integrative Physiology Meeting, May 2007, Aberdeen

3. **Michailidou Z**, Jensen MD, Chapman KC, Seckl JR, Walker BR, Morton, NM. Omental fat 11β-hydroxysteroid dehydrogenase type 1, but not Glucocorticoid Receptor, is correlated with fat cell size independently of obesity. *Abstract,* American Endocrine Society, June 2006, Boston.

4. **Michailidou Z**., Coll A.P, Morton NM, Kenyon C.J., O'Rahilly S., Seckl J.R., Chapman K.E. A selective increase in adipose 11β-HSD1 expression in corticosterone-treated POMC-null mice is associated with worsening of metabolic disease. Abstract O*ral presentation.* British Endocrinology Society, Glasgow, April 2006.

5. **Michailidou Z**., Coll A.P, Morton NM, Kenyon C.J., O'Rahilly S., Seckl J.R., Chapman K.E. Corticosterone treatment in *Pomc*$^{-/-}$ mice selectively increases adipose 11β-HSD1 expression and promotes the metabolic syndrome. *Abstract Oral presentation*, North Am. Ass. Study of Obesity, Vancouver, October 2005.

Abstract

The primary determinants of tissue glucocorticoid action are glucocorticoid receptor (GR) density and intracellular levels of ligand, the latter determined both by activity of the hypothalamic-pituitary-adrenal (HPA) axis and cellular activity of 11β-hydroxysteroid dehydrogenase (11β-HSD) enzymes that interconvert active 11-hydroxy (corticosterone, cortisol) and inactive 11-keto (11-dehydrocorticosterone, cortisone) glucocorticoids. Here, the contribution of GR density and ligand levels in determining body composition and metabolic phenotype have been investigated in mice and in humans.

Genetic evidence in humans implicates variations in the GR gene in the regulation of the HPA axis as well as the control of body fat distribution, metabolic parameters and blood pressure. Although GR deficient mouse models have been previously generated (with homozygous nulls dying at birth), the effects of altered GR density upon fat distribution and blood pressure have not been described. This study addresses the relationship between GR density and metabolic parameters, including body fat distribution, insulin resistance and hypertension. A novel line of mice harbouring a null mutation in the GR gene ($GR^{+/-}$) was generated from an ES cell line in which a β-galactosidase-neomycin phosphotransferase (βgeo) reporter cassette was fused with GR. The resulting fusion protein lacks part of the DNA binding domain and the entire ligand binding domain and is transcriptionally inactive. In addition, the β-galactosidase enzyme activity "reports" activity of the GR gene promoter. $GR^{-/-}$ mice are present in a normal Mendelian ratio before birth. Intriguingly, 1 (of 36/146 expected if null allele not lethal) survived to adulthood suggesting this might be a hypomorphic rather than a null allele. Heterozygous

($GR^{+/-}$) mice showed 40-45% reductions in GR mRNA levels in the hippocampus, paraventricular nucleus of the hypothalamus, pituitary gland and adipose tissue, 30% in liver, 56% in muscle and 67% in adrenals. X-gal staining of $GR^{+/-}$ brain sections showed that GR-βgal is present throughout, mirroring GR mRNA expression. Adult $GR^{+/-}$ mice had larger adrenals, higher evening plasma corticosterone levels and greater corticosterone responses following 10 minute restraint suggesting a hyperactive HPA axis. Compared to $GR^{+/+}$ littermates, $GR^{+/-}$ mice had similar body weight gain on normal chow or high fat diet, with unaltered fat depot (inguinal, epididymal, mesenteric) weights and similar glucose and insulin tolerance. However, $GR^{+/-}$ mice had higher (10%) systolic blood pressure, associated with activation of the renin-angiotensin system. Thus GR haploinsufficiency in mice causes increased blood pressure and accords with data associating GR polymorphisms with hypertension in humans.

The role of altered GC sensitivity was also investigated in a mouse model of HPA axis hypoactivity pro-opiomelanocortin null (POMC) mice. POMC-null mice are obese due to central melanocortin deficiency. In contrast to most rodent models of obesity, POMC-null mice are also glucocorticoid deficient due to ACTH deficiency. Previous data have shown that glucocorticoid replacement in POMC-null mice exaggerated hyperphagia, obesity and insulin resistance and caused hypertension. Here, the contribution of peripheral glucocorticoid sensitivity was investigated. POMC-null mice have increased liver and retroperitoneal fat GR mRNA levels but, specifically in adipose tissue, *decreased* levels of mRNA encoding 11β-HSD1, a reductase which regenerates active glucocorticoids, thus amplifying their action.

Adipose tissue expression of 11β-HSD1 mRNA and other glucocorticoid target genes (e.g. lipoprotein lipase) was increased following glucocorticoid replacement in POMC-null mice, possibly contributing to increased fat accumulation and exacerbated metabolic abnormalities.

Finally, the relationship between intra-adipose glucocorticoid action and obesity in humans was explored, specifically comparing intra-abdominal and subcutaneous depots. 11β-HSD1 mRNA expression in omental (visceral) fat was positively associated with body mass index, visceral adiposity, fat cell size and plasma triglyceride levels. In contrast, GR mRNA levels were negatively correlated with these parameters. The novel correlation of 11β-HSD1 with omental fat cell size independently of obesity suggests that intracellular GC regeneration is a stronger predictor of adipocyte hypertrophy than GR levels in the omentum in these individuals.

In conclusion, altered tissue GC sensitivity, mediated through altered GR density, altered ligand availability or 11β-HSD1-mediated ligand regeneration, can differentially result in a variety of phenotypic changes. These may not lead to a disease state *per se* but may explain, in part, an individual's susceptibility to a favourable or unfavourable body composition and cardio-metabolic risk, including hypertension.

Chapter 1

Introduction

1. Glucocorticoids

Glucocorticoids (GCs) are multi-tasking steroid hormones secreted from the adrenal glands. Cortisol and corticosterone are the principal active glucocorticoids produced by most mammalian species and probably have analogous roles. Cortisol is the major active glucocorticoid produced by humans and most mammals, whereas rodents synthesize corticosterone. Corticosterone is also a minor glucocorticoid (10-15%) in humans. GCs have pleiotropic and profound physiological effects that are essential for the maintenance of homeostasis and adaptation under physical and emotional stress. They are key regulators of the development and maturation of tissues/organs. They exert crucial modulatory effects on intermediate metabolism, immune and inflammatory processes and the cardiovascular system. They have central (brain) effects on mood and behaviour and food intake. Dysregulation of GC production and secretion is involved in the pathogenesis of diseases. Hypersecretion of GCs, as in the Cushing's Syndrome, leads to a plethora of pathological features such as redistribution of body fat (visceral obesity), protein catabolism (wasting of skeletal muscle), hyperglycaemia, insulin resistance, hypertension, increased serum lipids, salt and water retention, osteoporosis, impaired cognitive function, depression and reproductive abnormalities (reviewed in Buckingham 2006). In contrast, GC insufficiency, as in Addison's disease, is characterised by weight loss, hypoglycaemia, hypotension, weakness/generalised fatigue and mood abnormalities (reviewed in Buckingham 2006). However, more subtle alterations in GC action are also implicated in the pathogenesis of common diseases, such as the Metabolic Syndrome (a cluster of related conditions including visceral obesity, hypertension,

insulin resistance, hyper/dyslipidaemia and atheromatous cardiovascular diseases), autoimmune disorders, depression and reproductive abnormalities (reviewed in Reaven, 2006, Seckl, 2004; De Kloet et al., 1998).

GCs act on target cells via intracellular receptors, which belong to the superfamily of ligand-activated nuclear receptors (Manglesdorf et al., 1995). GCs bind to and interact with 2 receptors; the glucocorticoid (GR) and mineralocorticoid (MR) receptor. GR has a lower affinity (cortisol/corticosterone kd~5nM) and is glucocorticoid selective, whereas MR has a higher affinity (kd~0.5nM) and binds to cortisol, corticosterone and the mineralocorticoid, aldosterone (Arriza et al., 1987; Rupprecht et al., 1993) with high and roughly equal affinity. Both receptors regulate the transcription of a number of target genes when activated (reviewed in Beato et al., 1996 and also see sections 1.5.1.5 & 1.5.1.6).

The main focus of this Thesis was to investigate the effects of altered GC sensitivity on metabolism and HPA axis function. Thus, in this chapter (a) the biosynthesis and physiological functions of GC (b) the mechanisms that regulate GC secretion, (c) the mechanisms of GC action, with main emphasis given to the GR and (d) the modulation of GC sensitivity and downstream physiological consequences are discussed.

1.1 Production and secretion

The zona fasiculata and reticularis of the adrenal cortex are the main sites of cortisol/corticosterone production. As with all steroid hormones, the precursor for

GC biosynthesis is cholesterol. The first step in the biosynthetic pathway, is the cleavage of the cholesterol side chain by the side chain cleavage (SCC) enzyme (also known as cytochrome P450, or CYP11A1) to produce pregnenolone (fig. 1.1). Next, a series of reactions occur to give rise to cortisol and corticosterone (fig. 1.1). Rodents do not produce cortisol due to a lack of the 17α-hydroxylase (CYP17) enzyme in the adrenal gland. When GCs are produced, they are immediately released into the circulation by diffusion (Orth et al., 1992). GCs release occurs in a pulsatile manner and follows a circadian rhythm with maximal levels in the morning and nadir levels (3-5 fold lower) early in the sleep phase, in humans. Conversely in rodents, peak levels of GC secretion are in the evening (active phase) and nadir levels in the morning. Furthermore, GCs are released in response to fasting, physical/emotional stress, and the magnitude of the response depends on the intensity and duration of the stimulus and the individual's previous "exposure" to stress (reviewed in McEwen et al., 1997).

1.2 Regulation of secretion

GC secretion is under the tight control of the hypothalamus-pituitary-adrenal (HPA) axis (fig.1.2). The hypothalamus integrates a variety of neural and humoral signals, processessing the information received and responding by activating the synthesis of GCs. A forward drive of the HPA axis stimulates the release of corticotrophin-releasing hormone (CRH) and arginine vasopressin (AVP) from parvocellular neurons of the hypothalamic paraventicular nucleus (PVN) into the hypophyseal portal blood vessels (reviewed in McEwen et al., 1997). CRH and AVP are thus delivered to the anterior pituitary gland where they bind to the corticotrophin-

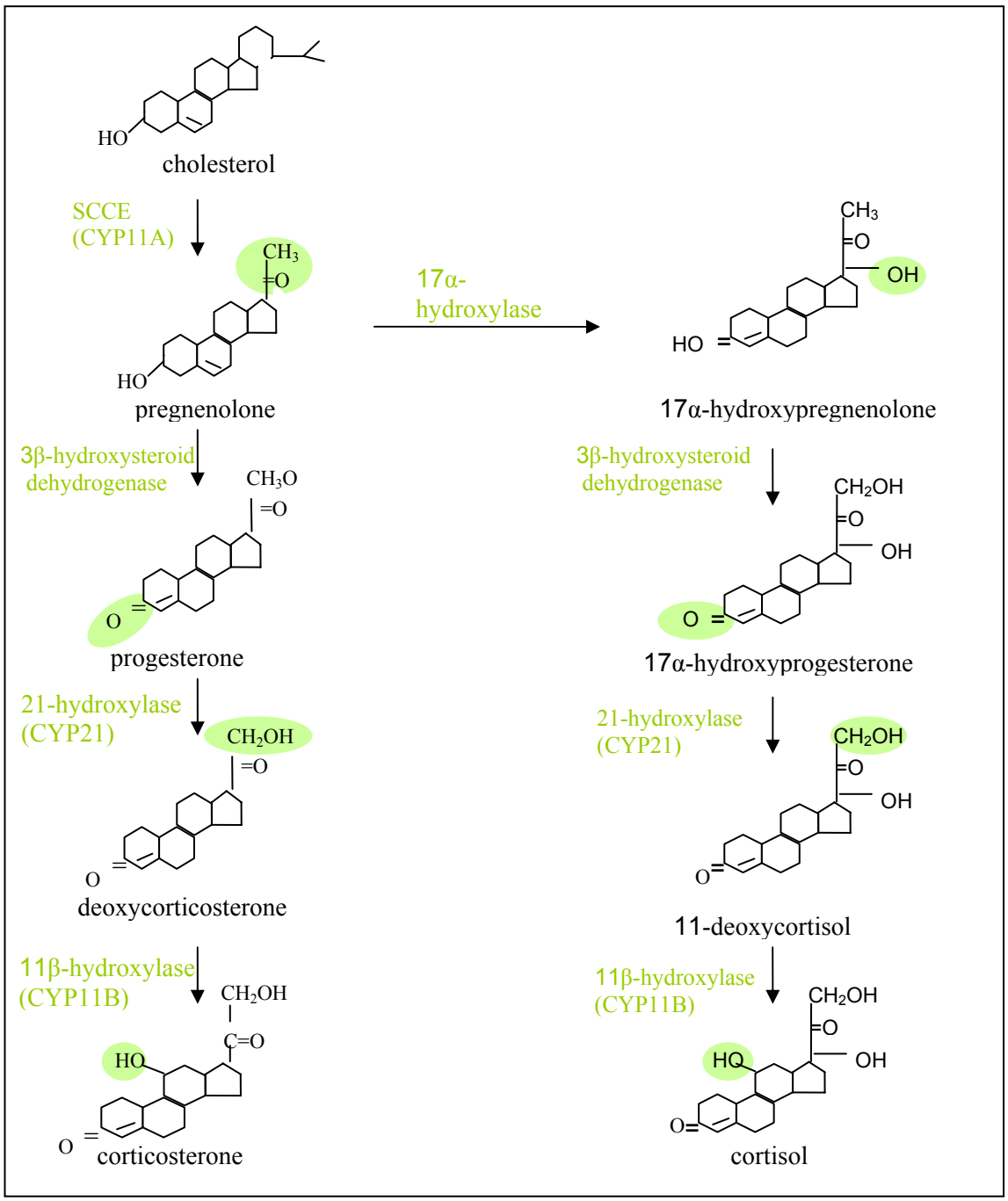

Figure 1.1 Biosynthesis of glucocorticoids.

Cortisol/corticosterone are synthesized in the zona fasciculata of the adrenal cortex from cholesterol. This schematic view illustrates the principal enzymes (in green) involved and the reactions they catalyze. The highlighted substituents on each molecular structure indicate the chemical change occurring in each reaction. SCCE; side chain cleavage enzyme. Adapted from Brook and Marshall, 2001.

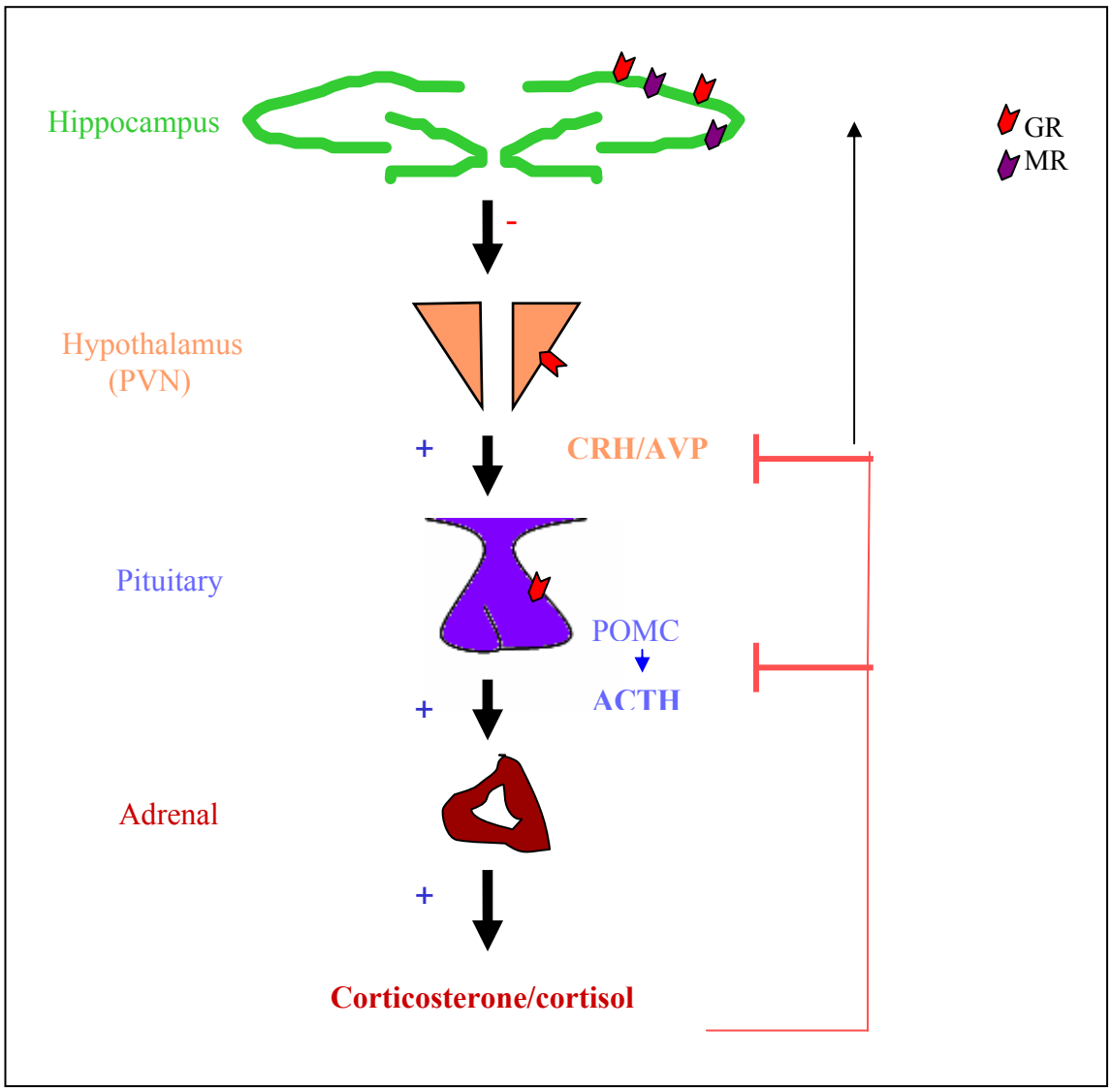

Figure 1.2 Regulation of glucocorticoid secretion by the HPA axis

A simplified schematic view of the hypothalamus-pituitary-adrenal (HPA) axis showing principal loci involved in glucocorticoid feedback control. A forward drive stimulates (black thick arrows) the production and secretion of cortisol/corticosterone from the adrenal glands. Glucocorticoid secretion is auto-regulated by negative feedback (blunt red arrows) at the level of the pituitary (suppressing POMC expression and ACTH release) and the hypothalamus (suppressing CRH expression). The negative feedback depends on the levels of GR (red block arrow) in the pituitary, hypothalamus and hippocampus and MR (purple block arrow) levels in the hippocampus. CRH; corticotrophin releasing hormone, AVP;arginine vasopressin, POMC; proopiomelanocortin peptide, ACTH; adrenocorticotrophin, GR; glucocorticoid receptor, MR; mineralocorticoid receptor.

releasing hormone receptor 1 and vasopressin receptor 1, respectively (McEwen et al., 1997). This triggers the production of proopiomelanocortin (POMC), the precursor for adrenocorticocotrophic hormone (ACTH), which in turn is secreted by the corticotrophs into the circulation. ACTH binds to melanocortin receptor type 2 and stimulates the synthesis of cortisol/corticosterone from the adrenal cortex (McEwen et al., 1997).

GC secretion is autoregulated by negative feedback acting principally at the level of the pituitary and hypothalamus, by suppressing the release of ACTH and CRH/AVP respectively (Keller-Wood and Dallman, 1984). This negative feedback system is sensitive to the rise of cortisol levels. There is a fast feedback, by which ACTH suppression occurs within minutes to 2h, and a delayed feedback which happens in two phases; an early (2-4h of cortisol elevation) and a late (after 4h of cortisol increase) phase (Jones and Gilham, 1988). The feedback system is regulated by both MR and GR. MR mainly regulates the basal circadian secretion whereas GR is involved in the peak circadian and stressed-induced cortisol secretion (Reul and De Kloet, 1985; reviewed in de Kloet, 2004).

GCs also exert rapid effects on the hippocampus, thus inhibiting the HPA axis. Paradoxically, the effects of GCs on the hippocampus are primarily excitatory, causing a rapid transcription-independent increase in the release of glutamate on CA1 neurons and thus inducing excitatory synaptic inputs to these cells (reviewed in Tasker et al., 2006). However, the hippocampal regulation of the HPA axis is mainly inhibitory. Excitatory hippocampal output is transformed to an inhibitory

hypothalamic input by hippocampal projections relaying through γ-aminobutiric acid (GABA)ergic inhibitory neurons in the PVN (Tasker et al., 2006). Thus, GCs induce a rapid increase in the hippocampal excitatory output to the hypothalamus which in turn inhibits hypothalamic neuroendocrine cells (CRH neurons) and results in a rapid GC feedback inhibition of the HPA axis (Tasker et al., 2006).

1.3 Physiological functions of glucocorticoids

1.3.1 Development

Prenatally, GCs are essential for the structural development of organs and for the maturation of tissues. GCs regulate the growth and maturation of tissues especially at critical phases where proliferation and terminal differentiation occur. Adequate GC exposure *in utero* is essential for lung maturation (reviewed in Brown and Seckl, 2005). Clinically, in situations of premature birth, GCs are administered to the mother in late gestation to accelerate the maturation of the prenatal lungs and ameliorate respiratory distress (Halliday, 2004). GR is essential for foetal lung maturation as evidenced by GR hypomorphic ($GR^{hypo/hypo}$) mice which die at birth from atelectasis of the lungs and cannot be rescued by GC treatment (Cole et al., 1995; details on this model in section 1.6.1). Moreover, mice with low GC exposure *in utero* ($CRH^{-/-}$) die at birth from respiratory distress but can be rescued by glucocorticoid replacement (Muglia et al., 1995). GCs affect a number of processes involved in lung maturation. They up-regulate respiratory epithelial sodium channels and genes involved in lung expansion (ie surfactant proteins, fatty acid synthase). They also reduce lung cellularity leaving larger and fewer alveoli, by reducing type II alveolar cell proliferation, promoting their terminal differentiation, increasing

apoptosis and reducing angiogenesis (reviewed in Brown and Seckl, 2005). GCs play a key role in triggering the differentiation of neural crest epithelial cells into chromaffin cells. The proposed mechanisms were that they do this, by (a) suppressing neuronal markers in the sympathoadrenal progenitors, shifting them into a chromaffin cell phenotype and (b) inducing the adrenaline-synthesizing enzyme, phenylethanolamine-N-methyl transferase (PNMT) in a subpopulation of chromaffin cells (Unsicker et al., 1978; Anderson, 1993). However, analyses of chromaffin cell development in $GR^{hypo/hypo}$ and GR-deficient mice ($GR^{null/null}$, details in section 1.6.1) mice showed that loss of *GR*-mediated signalling does not reduce or deplete adrenal chromaffin cell numbers (Finotto et al., 1999). On the other hand, PMNT immunoreactivity was undetectable in E18.5 $GR^{null/null}$ or $GR^{hypo/hypo}$ adrenals (while in wild type mice PNMT immunoreactivity is clearly detectable at E15.5), and consequently did not also contain any adrenaline (Finotto et al., 1999).

1.3.2. Metabolism

During fasting and exercise, when glucose and insulin levels are low, GCs are released into the circulation to antagonize the anabolic effects of insulin and promote hepatic glucose production. In contrast, after food intake, GCs induce energy storage in the form of glycogen by activating glycogen synthase (Orth et al., 1992). In skeletal muscle, GCs modulate both protein and glucose metabolism. They suppress protein synthesis and promote protein degradation and amino acid export and inhibit glucose uptake and glycogen synthesis (reviewed in Vegiopoulos and Herzig, 2007).

The central role of GCs to maintain glucose levels comes from evidence from Addison's disease (GC deficient) patients that have low glucose levels while Cushing's (GC excess) patients exhibit glucose intolerance (reviewed in Andrews and Walker, 1999). Moreover, CRH knock out mice, that lack GCs, fail to counteract hypoglycaemia (Jacobson et al., 2006). The potential mechanisms involved in the maintenance of glucose by GCs can be summarized as follows: First, GCs can promote gluconeogenesis by inducing phosphoenolpyruvate (PEPCK) (reviewed in Hanson and Reshef, 1997) and glucose-6-phosphatase expression (G6Pase) (Garland, 1986). The GC effects on hepatic glucose metabolism are mediated by the GR, since GR liver-specific ablation results in hypoglycaemia during fasting accompanied by down-regulation of gluconeogenic enzymes (Opherk et al., 2004; details in section 1.6.1). Second, GCs can decrease glucose transport by causing translocation of glucose transporter (GLUT4) from the cell membrane to an internal location and thus inhibit glucose transport in peripheral tissues (Horner et al., 1987). Third, GCs can prevent insulin production and secretion , as evident from mice over-expressing GR in pancreatic β-cells (Delaunay et al., 1997, details in section 1.6.1). However, whether this function occurs under normal GR levels with excess GCs still remains to be addressed. Fourth, GCs can induce the synthesis and promote liver and portal circulation accumulation of the sphingolipid, ceramide (Zierath, 2007; Holland et al., 2007), which has been suggested to antagonise insulin stimulation of glucose uptake and glycogen synthesis by inhibiting phosphorylation and activation of Akt/protein kinase B signalling thus contributing to the development of insulin resistance (Summers et al., 1998; Hajduch at al., 2001; Powell et al., 2003; Stratford et al., 2004). Recent data from Des1 (dihydroceramide desaturase; converts inactive

dihydroceramide to active ceramide) knock out mice showed that they were unresponsive to GC-induced insulin resistance (Holland et al., 2007). This is an interesting study linking GC-induced insulin resistance and ceramide, but will need further investigation, for example testing the ceramide synthesis/sectretion in tissue-specific (liver, pancreas, adipose) GR transgenic models. In adipose tissue, GCs affect lipid metabolism. In peripheral (eg subcutaneous, gluteal and thigh) fat depots, they increase lipolysis by up-regulating hormone sensitive lipase (Slavin et al., 1994; and reviewed in Leung and Munk, 1975; Mattsson and Olsson, 2007), whereas in central (abdominal, visceral) fat depots they induce pre-adipocyte differentiation (Gaillard et al., 1991), lipogenic activity and hypertrophy (Samra et al., 1998; Masuzaki et al., 2001). Finally, in brown adipose tissue glucocorticoids reduce thermogenesis by down-regulating uncoupling protein 1 (UCP-1) (Soumano et al., 2000).

1.3.3 Immune system

GCs are one of the most frequently prescribed drugs and are used to treat a range of immune/inflammatory disorders, mainly allergic and autoimmune disorders such as asthma, rheumatoid arthritis and also acute inflammation because of their potent immunosuppressive action. GCs modulate genes involved in the priming of the innate immune response, suppress T lymphocytes (or T cells) (of the Th (helper)1 lineage) while they promote humoral (Th2 cells) immunity and tolerance (reviewed in Franchimont et al., 2002). Firstly, the role of GCs in innate immunity, has been demonstrated in adrenalectomised animals, which were more sensitive to the lethal effects of LPS administration (Abernathy et al., 1957; Sambhi et al., 1964) and LPS-

mediated poinflammatory (IL-1, TNF-α) cytokine secretion by macrophages (Bertini et al., 1988). This highlighted the macrophage as a key cell type for GC-mediated increased survival after LPS challenge. Consistent with the increased mortality of adrenalectomized animals to LPS administration, macrophage-specific GR knock out mice (MGRKO) mice die when challenged with LPS (Bhattacharyya et al, 2007). Moreover, GR-deficient macrophages treated with dexamethasone (DEX; synthetic GC) fail to inhibit LPS-mediated induction of inflammatory genes (Bhattacharyya et al, 2007) suggesting an essential role of GR in mediating immunosuppression in macrophages. Secondly, with respect to adaptive immunity, GCs promote a Th2 response by increasing IL-10 secretion by macrophages or Th2 cells (Ramirez et al., 1996). Additionally, GCs may induce the development of regulatory T cells (Treg: produce high IL-10 levels), that in turn suppress immune responses, prevent self-reactivity and promote immune tolerance (Barrat et al., 2002). They can also block dendritic cell maturation, thus reducing the ability of the latter to present antigens to T lymphocytes and induce an immune response (Piemonti et al., 1999). Moreover, GCs can promote T cell survival or apoptosis depending on the type of T cell, the degree of activation and the timing of GC exposure (Ashwell et al., 2000). It has been hypothesized that endogenous GCs are involved in thymocyte development and positive/negative selection (Godfrey et al., 2000). However, GR knockout mice display normal thymocyte development and selection (Purton et al., 2000) and this remains a controversial field. The mechanisms by which GCs exert their anti-inflammatory effects are beyond the scope of this thesis. Briefly, many of their effects are mediated though interference with the key inflammatory transcription factor, NF-kB (McEwen et al., 1997).

1.3.4 Cardiovascular system

The direct effects of GCs on the cardiovascular system are difficult to dissect since any changes in GC plasma levels have multiple central and systemic consequences. GC excess raises blood pressure (Whitworth et al., 1995; Ferrari, 2003; Baid and Nieman, 2004). They may do this either by altering tissue sensitivity to catecholamines or by exerting aldosterone-like actions modulating water and electrolyte balance through illicit activation of MR in kidney (Brilla and Weber, 1992; Young et al., 1994; Young et al., 1995). Additionally, cortisol increases plasma erythropoietin levels, which in turn has direct vasoconstrictor effects, thus contributing to cortisol-induced hypertension (Kelly et al., 2000). GCs also increase the number of β-adrenergic receptors in vascular smooth muscle cells thus increasing vascular tone (reviewed in Magiakou et al., 2006). They reduce atrial natriuretic peptide (vasodilator), inhibit membrane transport of L-arginine and nitric oxide synthase (eNOS) synthesis which impairs peripheral vasodilation hence leading to blood pressure elevation (reviewed in Magiakou et al., 2006). Observations in rodents suggest that GCs contribute to the maintenance of normal cardiac contraction by modulating membrane calcium transport and potassium channel activity (Penefsky and Kahn, 1971; Wang et al., 1999). Furthermore, in healthy volunteers short-term glucocorticoid treatment decreased resting heart rate suggesting that GCs may be involved in regulation of cardiac electrical activity (Brotman et al., 2005). Recently, selective overexpression of GR in cardiomyocytes resulted in enhanced cell contractility and increased heart rate, atrio-ventricular block and ion-channel remodelling, suggesting a direct role of GR in cardiac function (Sainte-Marie et al.,

2007, also see section 1.6.1). However, the direct effects of GCs on the heart require further investigation.

1.3.5 Behaviour

Although GC production and secretion is strictly regulated by the HPA axis, impairment of the latter leads to abnormal GC levels that induce structural remodelling in the brain (reviewed in McEwen, 2005). GR is widely expressed in the brain (hypothalamus, thalamus, cerebellum, amygdala, cortex) with the highest expression observed in the hippocampus (Herman et al., 1989). MR is also expressed in the hippocampus where it acts as a glucocorticoid receptor because the tissue does not contain 11β-hydroxysteroid dehydrogenase type 2 (Holmes et al., 2003; for details refer to section 1.4), and therefore little cortisol is converted into cortisone (Arriza et al., 1988; De Kloet et al., 1998). The hippocampus is a key locus for learning, memory, reasoning, mood and behaviour (reviewed in McEwen, 1999). The hippocampus is also sensitive to GC alterations, and susceptible to stress (McEwen, 1999). Chronic overexposure to GCs (as in Cushing's disease) causes long-lasting deficits in memory, attention and depressive symptoms. Conversely, low GC levels are associated with chronic fatigue, antisocial personality disorder (aggressiveness), with the amygdala being a key target (reviewed in Kim and Haller, 2007).

1.3.6 Stress response

Physical or emotional stress leads to HPA axis activation and increased GC secretion. In the short term, the stress-protective effects of GCs promote survival by

ensuring energy availability and limiting potentially threatening processes such as inflammation. Following a stress response, homeostasis is restored by the negative feedback system of GCs through the HPA axis. This is an essential mechanism since long term exposure to excessive circulating GCs leads to pathological consequences (ie diabetes, hypertension, osteoporosis etc).

1.4 Regulation of glucocorticoid action

The primary determinants of GC action are the GR density and intracellular levels of ligand, the latter determined both by activity of the HPA axis (as described in section 1.2) and cellular activity of 11β-hydroxysteroid dehydrogenase (11β-HSD) enzymes (reviewed in Seckl et al., 2004). The GR-mediated GC action is extensively described in the following section (1.5). Tissue-specific GC availability is regulated by the intracellular enzymes, 11β-HSDs (fig. 1.3). 11β-HSD1 is predominantly a reductase in intact cells, regenerating cortisol/corticosterone (active GCs) from cortisone/11-dehydrocorticosterone (inactive GCs) (Low et al., 1994; Kotelevtsev et al., 1997; Jamieson et al., 2000; Hundertmark, 1995). It is highly expressed in liver, adipose tissue, lung and central nervous system, classical GR target tissues, where it amplifies local GC action (Cole, 1995; Krozowski et al., 1995a, b, c). Conversely, 11β-HSD2 limits cortisol/corticosterone availability and action in placenta and mineralocorticoid-target tissues such as kidney, colon and salivary glands by converting active to inactive GCs (reviewed in Seckl and Walker, 2001). Following interconversion of cortisol and cortisone, both steroids undergo A-ring reduction by 5α- and 5β-reductases and the resulting dihydro-metabolites are then reduced further by 3α-hydroxysteroid dehydrogenase (3α-HSD) to yield tetrahydrometabolites, 5β-

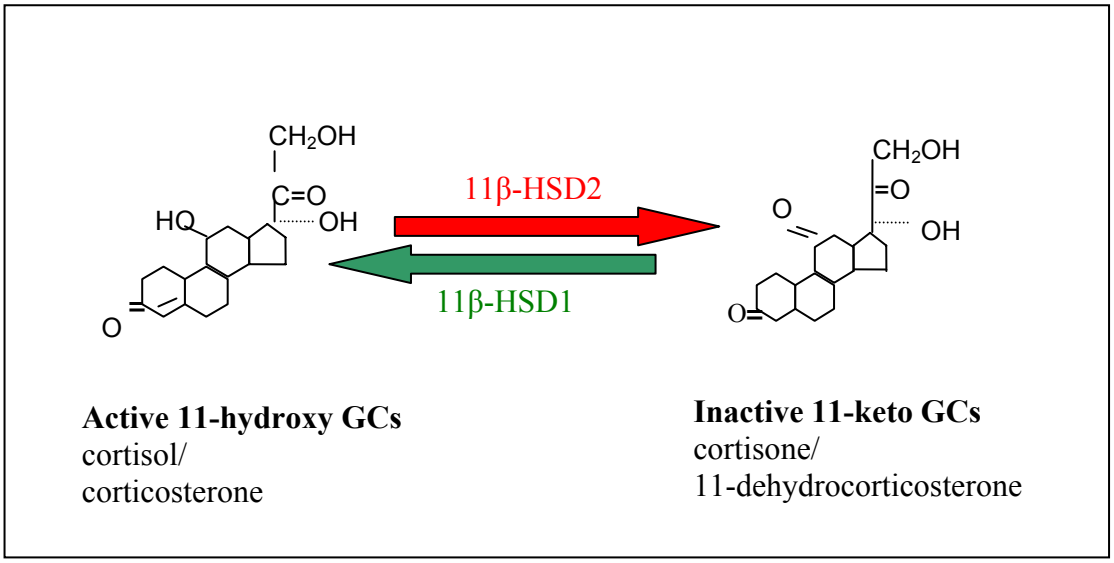

Figure1.3Interconversion of corticosterone/cortisol to 11β-hydrocorticosterone / cortisone by 11β-hydroxysteroind dehydrogenases (11β-HSDs).

The active 11-hydroxy glucocorticoids are converted to inactive 11-keto glucocorticoids by the high affinity 11β-HSD2 (nicotinamide adenine dinucleotide – dependent dehydrogenase) enzyme. 11β-HSD2 is mainly expressed in mineralcorticoid target tissues like kidney, colon and salivary glands and also in the placenta. The regeneration of active glucocorticoids is catalysed by the lower affinity 11β-HSD1. In tissue homogenates 11β-HSD1 is a NADP(H)-dependent bidirectional enzyme while in intact cells and tissues it acts as a 11-ketoreductase. 11β-HSD1 is mainly expressed in tissues with high sensitivity to glucocorticoids (liver, adipose tissue, lung and brain). The catalytic moiety of 11β-HSD2 faces the cytoplasm while 11β-HSD1 is directed into the endoplasmic reticulum (ER) lumen which is important for cofactor availability and bidirectionality of the enzyme (reviewed in Odermatt et al., 2006). Adapted from Seckl & Walker, 2004.

tetrahydrocortisol (THF), 5α-tetrahydrocortisol (allo-THF) and 5β-tetrahydrocortisone (THE) (Andersson et al., 1991; Normington and Russell, 1992 and reviewed in Hammer and Stewart, 2006). The activity of 11β-HSD in the body is classically reflected by the ratio of total urinary cortisol and cortisone metabolites: [THF + allo-THF]/THE (Hammer and Stewart, 2006), although this is a rather rough measure of net action of both isoenzyes in all tissues as well as A-ring reductases.

Furhermore, corticosteroid binding globulin (CBG) modulates the availability of GCs (Dunn et al., 1981). In the circulation, approximately 90% of active GCs are bound to CBG, with the remainder either bound to albumin or found in a "free" form (Dunn et al., 1981). While CBG might act as a "sink" it has been suggested that GCs can only enter the cells by dissociating from CBG (Pardridge, 1987). Evidence to support the latter hypothesis comes from observations that receptors for CBG are present on target cell membranes and that serine protease- mediated cleavage of CBG results in the release of bound GC (Singer et al, 1988; Hammond, 1988). CBG knockout mice revealed a more active role of the protein than previously thought. Apart form a cargo transporter, CBG is important for bioavailability, local delivery, and/or cellular signal transduction of GCs (Petersen et al., 2006).

1.5 The Glucocorticoid Receptor

GR was the first mammalian transcription factor isolated and studied in great detail (Miesfeld et al., 1984) and it is highly conserved between species (http//www.NURSA.org). In humans, the gene encoding GR is located on chromosome 5 (Gehring et al., 1985) and comprises of 9 exons, spread over ~124kb

DNA. GR, as for all nuclear receptors, has a three domain structure (fig. 1.4). The N-terminal domain consists of sequences required for target-gene activation (Giguere et al., 1986), the DNA binding domain (DBD), encodes 2 highly conserved Zn fingers absolutely essential for DNA binding and which are also required for dimerization of the receptor (Tsai et al., 1988), nuclear translocation (Picard and Yamamoto, 1987) and transactivation (Hollenberg et al., 1987; Lefstin et al., 1994).

The third domain of GR is the C-terminal or ligand binding domain (LBD), which is responsible for hormonal binding (Giguere et al., 1986; Warriar et al., 1994) and nuclear translocation (Picard and Yamamoto, 1987). Additionally, the LBD is involved in heat shock protein binding (Dalman et al., 1991; Pratt, 1993), transactivation (Hollenberg and Evans, 1988; Webster et al., 1988), dimerization (Dahlman-Wright et al., 1992) and, in the absence of the hormone, silencing of the receptor (Godowski et al., 1987; Danielson, 1986).

1.5.1 Mechanisms of GR action

1.5.1.1 GR is activated when it binds to glucocorticoids

In the absence of its ligand, GR is present in a multiprotein complex of several heat shock proteins (hsp) including hsp90, hsp70, hsp56 and hsp40, immunophilins (Cyp40, FKBP52) and molecular chaperones (eg hsp90) (Pratt, 1993; Hutchison et al., 1994a,b; Pratt, 1998) that retains the unligated GR in the cytoplasm in an inactive (partly unfolded) state (Hutchison et al., 1993). The unliganded, hsp-complexed GRs exist in a dynamic equilibrium between nucleus and cytoplasm and shuttle continuously across the nuclear membrane (Hache et al., 1999).

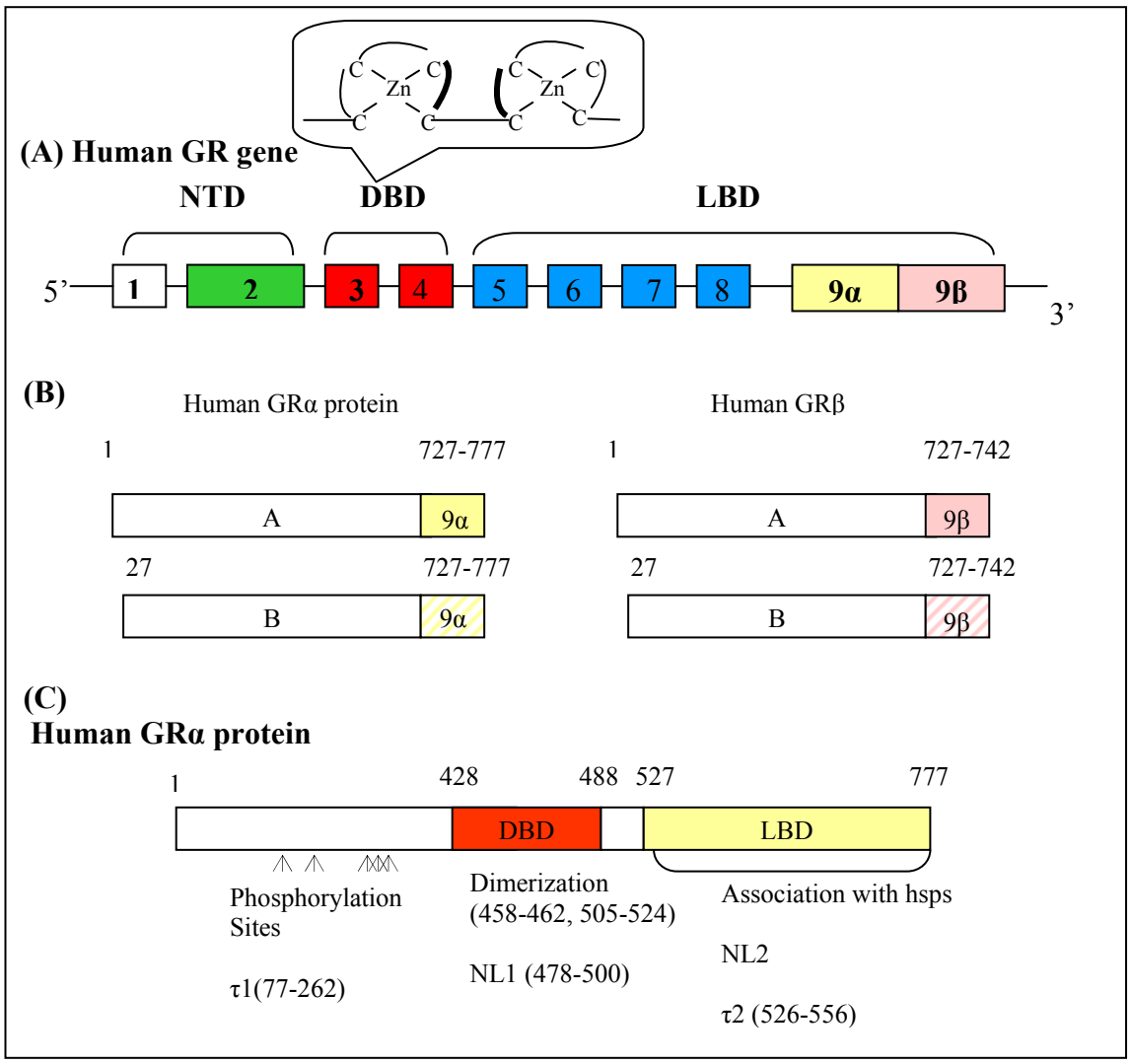

Figure 1.4 Human GR gene and protein structures.

(A) Schematic representation of the hGR gene. (B) Alternative splicing results in two mRNA isoforms GRα and GRβ. Alternative translation starts, result in GR proteins differing at N-terminus; GR-A and GR-B protein isoforms. (C) Structure of the GRα protein, indicating the different domains and functions mapped to specific regions (amino acid numbers) of the protein. NTD; N-terminal domain (exons 1-2), DBD; DNA-binding domain (exons 3-4) with the 2 zing fingers (insert), LBD; ligand binding domain (exons 5-9); NL; nuclear localization signals; hsps; heat shock proteins, τ1 & τ2 ; transactivation domains. Adapted from deRijk et al., 2002.

Recent evidence suggest that hsp90 appears to be an essential component of the multisubunit chaperone machine that functions in the nucleus to maintain the mobility of GR, therefore assisting in the assembly and disassembly of the macromolecular complexes that are recruited to GR-responsive promoters (Elbi et al., 2004). Additionally, hsp90 has been shown to be essential for steroid binding to GR (Pratt and Toft, 1997), and thus changes in hsp90 binding affinity for GR, and in hsp90 levels can alter the EC50 value (concentration of agonist for half maximal induction of gene expression) and the partial activity of the agonist (Kaul et al., 2002). In the absence of ligand, GR is generally accepted to be located in the cytoplasm (Lukola et al., 1985; Cidlowski et al., 1990; Akner et al., 1994), although there are some contradictory reports that suggest a bidirectional shuttling between the cytoplasm and the nucleus (Madan and DeFranco, 1993; Pratt, 1993). For unliganded wild type (WT) receptors expressed at physiological levels, this equilibrium is normally expected to strongly favor cytoplasmic localization of the receptor (Hache et al., 1999), while overexpression of GR in some cells showed partial transfer of GR to the nucleus in the absence of ligand (Sanchez et al., 1990; Martins et al., 1991).

Upon binding of the GC to the GR (GC/GR), conformational changes of the latter take place that lead to a) GC/GR dissociation from the hsp complex which is now unable to reassemble b) GR protein hyperphosphorylation and c) the nuclear localization sites (NLS) in the GR are unmasked and the GC/GR translocates into the nucleus, where it binds as a homodimer to glucocorticoid response elements (GREs) on target genes and regulates their transcription (reviewed in Bamberger et al., 1996).

1.5.1.2 Hormone binding, GR conformational change and dissociation from hsps

The crystal structure of the LBD revealed that it contains 12 α-helices that are folded to generate a hydrophobic pocket for the ligand (Bledsoe et al., 2002). When the hormone binds the receptor, a conformational change of helix 12 occur (folds back trapping the ligand in its binding pocket) and consequently the pocket "shuts" (Bledsoe et al., 2002). Hormone binding affinity determines the potency of transcriptional activity. Point mutations in the LBD of GR lead to reduced or increased glucocorticoid binding affinity (Hurley et al., 1991; Warriar et al., 1994; Lind et al., 2000) or GC/GR complex stability (Ashraf and Thompson, 1993). These alterations are associated with clinical syndromes of GC hypo- or hyper-sensitivity (section 1.6).

1.5.1.3 Phosphorylation of GR

In the absence of the hormone, GR is partially phosphorylated (in the NTD), and after binding to an agonist and dissociation from the hsp complex becomes highly phosphorylated (Orti et al., 1992). GR phosphorylation does not seem to be essential for nuclear translocation since mouse GR that lacks all phosphorylation sites is able to translocate to the nucleus after hormone binding (Webster et al., 1997). Furthermore, it is still debatable if the GR phosphorylation state alters the receptor's transcriptional activity since mutations of single, multiple or all phosporylation sites of mouse or human GR resulted in very subtle reductions of its transcriptional activity at least in transfected cells (Mason and Housley, 1993; Almlof et al., 1995).

1.5.1.4 Nuclear translocation, dimerization and GRE binding to target genes

Following hormone binding, nuclear translocation occurs after a nuclear localization signal (NLS) is unmasked (Picard and Yamamoto, 1987; reviewed in Akner et al., 1995). Two NLSs have been identified in the glucocorticoid receptor, the first (NL1) located in the DBD (exon 4) and the second (NL2) in the LBD, but its exact location is unknown (Picard and Yamamoto, 1987). In most *in vitro* experiments following agonist treatment, GR nuclear translocation and saturation (complete translocation) occurs within 10-20 min and 30-60min respectively (Ucker and Yamamoto, 1984; Picard and Yamamoto, 1987, Htun et al., 1996 and reviewed in Stahn et al., 2007). In the nucleus the activated GR interacts with the DNA/chromatin and subsequently with GREs on target genes. The "classical" model of this interaction is thought to be dependent on the GR DBD, where a GRE (consists of a pair of DNA half sites) binds GR as a homodimer (Luisi et al., 1991). Briefly, a GR monomer binds to the higher affinity half-site, followed by binding of the second monomer and its stabilization by protein-protein interaction within the second zinc finger of the DBD (Wrange et al., 1989; Dahlman-Wright et al., 1991; Dahlman-Wright et al., 1993). However, there are a subset of GREs that do not require dimerization at least in a conventional arrangement (Adams et al., 2003; also section 1.5.1.7).

1.5.1.5 Transactivation

Transactivation by GR is mediated via "positive" GREs and is thought to be responsible for many of the effects of GCs. Transactivation depends on the τ1 and τ2 domains in GR. The former is located in the N-terminal region and is hormone-

independent (Hollenberg and Evans, 1988), while the latter locates to the LBD (fig. 1. 4) and requires hormone binding (Giguere et al., 1988). When GR binds to GREs, the transcription process is initiated by a complex mechanism. GR itself is capable of recruiting and stabilising the transcriptional pre-initiation complex (Freedman, 1999), and also make contacts with numerous components of the transcriptional machinery *in vitro* (Robyr et al., 2000). Studies using the mouse mammary tumour virus long terminal repeat (MMTV LTR), which contains several GREs, showed that transcriptional activation by GR requires DNA binding, disruption of local chromatin structure and assembly of the initiation complex at a TATA box (Hebbar and Archer, 2003). The interaction between GR and MMTV LTR is dynamic; after ligand activation, GR first binds to the chromatin, recruits remodelling activity and is then lost from the template (Hager et al., 2000).

The GR transcriptional activity depends on co-activators that mediate the recruitment of the basic (eg RNA polymerase II, TATA-box binding protein) transcriptional machinery (Robyr et al., 2000) or chromatin remodelling (eg histone acetylation; Yao et al., 1996). Apart from the recruitment of co-activators of the basic transcriptional machinery, the transcriptional activity of GR is enhanced by other co-activators, for example of the p160 family (Kurihara et al., 2000). The p160 family consists of steroid receptor activator SRC-1, SRC-2 and SRC-3 (Onate et al., 1995; Anzick et al., 1997; Hong et al., 1996), which could act as a docking platform for the recruitment of other associated co-regulators such as CBP (cAMP response element binding protein) or p300 and thus enhance GR-mediated gene expression (Wu et al., 2007). P160 knock out experiments (using siRNA) showed that the effect of p160 in GR transactivation is promoter and cell type specific (Trousson et al., 2007). For

example, inhibition of SRC-1 expression induced a 40% and 50% inhibition in GRE2-TATA promoter activity in astrocytes and Schwann cells respectively, whereas SRC-2 or SRC-3 inhibition affected only one or the other cell type (Trousson et al., 2007). Regarding the MMTV promoter, SRC knock down gave similar results in both cell types, with siSRC-1 and siSRC-2 inhibiting (50%-60%) DEX activation while siSRC-3 did not affect GR signalling (Trousson et al., 2007).

1.5.1.6 Transrepression

The transcription of genes can be inhibited by GCs through direct interaction between the GR and negative GREs, such as in the pro-opiomelanocortin, α-fetoprotein and prolactin gene (Sakai et al., 1988). However, more recent studies suggest that in the case of POMC and prolactin, repression occurs by tethering, in which positive transcriptional regulators bind DNA and are then targeted by GR in a process termed "transrepression" (Chandran et al., 1999). Transrepression refers to molecular mechanisms in which monomers of the GC/GR complex directly or indirectly interact with transcription factors, for example those that regulate the expression of pro-inflammatory genes (activator protein 1; AP1 and nuclear factor-κB; NF-κB) (reviewed in Newton and Holden, 2007). Negative regulation by the GR receptor complexes results in reduced transcriptional activities of target genes and thus the inhibition of inflammatory mediators such as cytokines (eg IL1, IL2, TNF-α, IFN-γ) and prostaglandin synthesis. Briefly, the following mechanisms are thought to mediate transrepression: (1) inhibition of a transcription factor binding to specific DNA sequences through direct protein–protein interaction (2) increased IκB synthesis (an inhibitor of NF-κB), by the GRE and the GC/GR complex interaction

and (3) competition for nuclear coactivators between the GC/GR complex and other transcription factors (reviewed in Stahn et al., 2007).

1.5.1.7 Trans-repression by protein-protein Interactions

A popular view is that transrepression by GR is through protein-protein interactions between monomers of activated GR and "pro-inflammatory" transcription factors, particularly NF-kB and AP-1. The "dissociation" of DNA-binding versus protein-protein interactions have been studied in transgenic mice carrying a mutation in the D-loop of the second Zn finger (dimerization interface) in the DBD of GR ($GR^{dim/dim}$ mice; details in section 1.6.1 & Table 1.1) (Reichardt et al., 1998). The GR dimerization and DNA-binding to target genes was partially impaired in this model (Adam et al., 2003). Although exhibiting less than total impairment of dimerization, $GR^{dim/dim}$ mice showed a lack of responsiveness of TAT under GC exposure and thus impaired transactivation, while the protein-protein-dependent suppression of AP-1 activity was unaffected (Reichardt et al., 1998). Interestingly, this model showed that HPA axis feedback depends on both DNA-binding and protein-protein interactions since CRH expression was unaffected (thus its suppression does not require DNA-binding) whereas POMC expression was increased (requires GR DNA-binding activity) (Reichardt et al., 1998). This mechanism of transrepression apparently does not require DNA-binding by GR (Reichardt et al., 1998). The main line of evidence is from studies in transfected cells and from the $GR^{dim/dim}$ mice. However, caution should be exerted when interpreting these data. Firstly, many of these initial experiments were in transfected cells where GR was over-expressed in cell types that are not directly relevant to the inflammatory response (eg HEK293). Secondly, the

interpretation of the $GR^{dim/dim}$ phenotype has been called into question (Adams et al., 2003) by experiments showing that activation of the PMNT gene is dependent upon non-classical GREs (not the conventional inverted repeat arrangement) and thirdly, by recent data, on macrophage-specific GR knockout mice (MGRKO), demonstrating the importance of p38-GR interaction for mediating GC immunosuppression, thus providing an alternative mechanism, based on gene induction for suppression of NF-kB **(**Bhattacharyya et al., 2007).

1.5.2 Regulation of GR action

1.5.2.1 GR splicing variants

Cloning of the human GR gene revealed two splicing isoforms, designated GRα and GRβ (Hollenberg et al., 1985), with the first considered as the classical GR (fig. 1.4). The GRα protein consists of 777 amino acids and is the primary mediator of GC action (Hollenberg et al., 1985). GRβ is generated by alternative splicing of exon 9 (Hollenberg et al., 1985). The GRα and GRβ proteins are identical for the first 727 amino acids (fig. 1.4). They differ only at the C-terminal domain, where GRβ has a unique 15 amino acid sequence replacing the last 50 amino acids of GRα (Hollenberg et al., 1985; Encio and Detera-Wadleigh, 1991). GRβ cannot bind ligand and in several promoter/transactivation systems it has been shown that is transcriptionally inactive (Oakley et al., 1999; Yudt and Cidloowski et al., 2001). Another difference between GRα and GRβ isoforms is that the latter is located in the nucleus in the absence of the hormone (Oakly et al., 1999; Yudt and Cidlowski et al., 2001). However, although GRβ mRNA is widely expressed in human tissues, levels are less than for GRα, and it has not been identified in mice (Bamberger et al., 1995; de Castro et al., 1996; Oakley et al., 1996; Oakley et al., 1997). There is controversy

regarding the functional significance of GRβ. It has been proposed that GRβ exerts a dominant-negative effect on GRα activity (Bamberger et al., 1995) by forming GRα/GRβ heterodimers (Bamberger et al., 1995; Oakley et al., 1996). Furthermore, in human neutrophils, which are less sensitive to GCs compared to T cells, GRβ expression is higher than that of GRα, and treatment with IL-8 increased only the expression of the former (Strickland et al., 2001). Transfection of GRβ into mouse neutrophils (do not express GRβ) resulted in reduction in cell death when cells were exposed to dexamethasone (Strickland et al., 2001). Thus, high expression of GRβ may be a potential mechanism by which neutrophils could escape GC-induced cell death and further IL-8-mediated GRβ induction may contribute to enhanced survival in the presence of GCs during inflammation (Stickland et al., 2001).

Finally, a third spicing variant, GRγ, has been described (Rivers et al., 1999). This variant results from an additional codon between exons 3 and 4, coding for arginine. GRγ is widely expressed in different tissues but its function is still unknown (Rivers et al., 1999).

1.5.2.2 GR translational variants

Variants of GR are also generated through use of alternative translation starts (fig. 1.4). GR-B lacks the 27 amino acids in the N-terminal domain compared to GR-A (major and longer protein product), due to translation starting from a second in frame ATG, 71bp downstream of the first ATG (Yudt and Cidlowski, 2001). Distribution of the GR-B in various tissues has not been investigated and its physiological role is still questionable. However, GR-B was shown to be an efficient GRE transactivator

and to have equal potency to GR-A in a transrepression assay with NF-kB (Yudt and Cidlowski, 2001).

1.5.3 Regulation of GR levels

GR is widely expressed (Ballard et al., 1974), but the expression levels vary in a tissue-specific manner with the greatest mRNA levels seen in the lung (Funder, 1992) and thymus (Miller et al., 1990). In rat tissues, the GR mRNA expression levels are highest in lung (100%), with lower levels as follows: spleen (70%)>brain (55%)>liver (50%)>kidney (43%)>heart (35%)>adrenal (13%)>testis (8%) (Kalinyak et al., 1987). Moreover, GR levels vary within a tissue, with the most well studied being the hippocampal subfields (Herman and Spencer, 1998). In the following sections (1.5.3.1 and 1.5.3.2) the regulation of GR levels by GCs and perinatal "programming" are discussed.

1.5.3.1 Down-regulation of GR by glucocorticoids

GCs seem to be the most potent regulators of GR levels. GCs down-regulate GR expression levels in the majority of cell lines and in human and animal tissues and cells (Burnstein et al., 1991). The physiological role of this negative regulation may be to protect the tissues from excessive GC levels (Burnstein et al., 1991; Silva et al., 1994 and references therein). The proposed autoregulatory mechanisms include a) inhibition of GR mRNA by interfering with an AP-1 and/or AP-2 mediated transcriptional activation of the GR gene (Vig et al., 1994; Nobukuni et al., 1995; Freeman et al., 2005), b) reduction of GR mRNA stability and translation (Burnstein

et al., 1990; Burnstein et al., 1994) and c) reduction of the half-life of the GR protein (McIntyre and Samuels, 1985; Wallace and Cidlowski, 2001). Of these, the latter is still debatable since other groups showed no apparent effect (Rosewicz et al., 1988; Hoeck et al., 1989).

The time of GC exposure seems to be an important parameter in the regulation of GR levels by its ligand. For example, in rat hepatoma cells treated with DEX, it has been observed that there is a small increase in the GR mRNA levels after 6h exposure, followed by a 50-90% decrease after 24h and a restoration of GR levels to basal after 72h (Okret et al., 1986). However, the initial increase in GR levels after DEX-treatment has not been confirmed in rat livers *in vivo* (Dong et al., 1988). Moreover, in a variety of rat tissues GCs caused a decrease in GR mRNA levels up to 72h, reaching a plateau thereafter (Kalinyak et al., 1987).

While in most cells and tissues GCs down-regulate GR levels, in human T-lymphoma and myeloma cell lines (Eisen et al., 1988; Denton et al., 1993; Gomi et al., 1990) and a mouse thymoma cell line (Gruol et al., 1989), as well as double positive thymocytes (Cole et al., 2001), they up-regulate GR expression. Since T cells are sensitive to GC-induced apoptosis, this up-regulating effect on GR levels might be a cell/tissue-specific response regulating T cell homeostasis (Pedersen et al., 2004).

1.5.3.2 Perinatal programming of GR levels

Events that occur around the time of birth, pre-natally or post-natally, can permanently "set" or "programme" GR levels in a tissue-specific manner throughout the lifespan (reviewed in Seckl and Holmes 2006). An adverse maternal environment (either GC overexposure or poor nutritional status) leads to low birth weight offspring and has been associated with the development of a range of pathologies later in life (Seckl and Holmes, 2006). This phenomenon is widely known as the foetal origins of disease. There is strong evidence that prenatal overexposure to GCs permanently "programmes" GR levels. When pregnant rats are exposed to DEX in the third week of gestation, their offspring have reduced birth weights and develop hyperglycaemia as adults. Hepatic GR and PEPCK levels (Nyrienda et al., 1998), as well as adipose tissue GR levels (Cleasby et al., 2003) are permanently elevated, whereas hippocampal GR levels are decreased (Holmes et al., 1997, Levitt et al., 1996) indicating a tissue-specific regulation of GR levels. Events in the immediate post-natal period can also programme GR levels. Removal of pups for a short period, daily, for 7d, alters maternal care and permanently increases GR levels in the hippocampus resulting in a more efficient negative feedback of the HPA axis following stress (Stanton et al., 1988; Meaney et al., 1988). The mechanisms involved in GR "programming" may involve epigenetic alterations in the GR promoter but are beyond the scope of this Thesis, therefore are not discussed further.

1.6 Altered glucocorticoid sensitivity and physiological consequences

As described in previous sections, the regulation of GC secretion and metabolism is determined by the GR, the HPA axis and at the peripheral level by the 11β-HSD enzymes. In the following sections the effects on GC sensitivity and metabolic

parameters of modulating GR (section 1.6.1.1) or 11β-HSD1 levels (section 1.6.1.2) in mice are described. Furthermore, the effects of GR polymorphisms on GC sensitivity and associated pathologies in humans are reviewed.

1.6.1 GR transgenic mice models elucidating the role of altered GR levels on a number of systems involved in HPA axis regulation & metabolism

There are a number of GR mutant mice generated over the past 15 years. Table 1.1 summarizes the GR transgenic mouse models published to date and their phenotype with respect to metabolic parameters and HPA axis function. Most of these models have been used to study the effects of altered GR levels on behaviour but this aspect is not discussed here. The main focus of this Thesis was to investigate the effects of altered GC sensitivity on metabolism and HPA axis function.

The first transgenic GR mouse model was generated by expressing, under the control of the neurofilament promoter, antisense RNA to the 3-prime non-coding region of GR (Pepin et al., 1992). This led to a 40-60% reduction in GR levels, not only in neuronal tissue but also liver. The mice displayed HPA axis hyperactivity and late onset obesity (Pepin et al., 1992) with increased fat mass and plasma triglycerides (Richard et al., 1993). However, in this model, GR density is only partially reduced, the degree of down-regulation of the receptor varies with the tissues examined and levels have not been assessed in many tissues, thus limiting the utility of this model.
Cole et al., (1995) used a gene targeting (insertion of neomycin phosphotransferase cassette into exon 2) approach with the aim of inactivating GR. This strategy resulted in incomplete inactivation (hypomorphic allele) of the GR gene ($GR^{hypo/hypo}$) due to

expression of a truncated protein (39kD GR fragment) with residual activity (Cole et al., 2001). 10-20% of homozygous mice survived (Cole et al., 1995; 2001). $GR^{hypo/hypo}$ mice were profoundly GC resistant, displayed HPA axis hyperactivity, adrenal hypertrophy and reduced hepatic gluconeogenic enzyme expression (Cole et al., 1995; 2001). To ensure complete inactivation of GR function, another model was generated by deleting exon 3 ($GR^{null/null}$) (Finotto et al., 1999). This resulted in 100% lethality shortly after birth due to atelectasis of the lungs (Finotto et al., 1999). $GR^{null/null}$ mice exhibited a similar phenotype to $GR^{hypo/hypo}$ mice, with glucocorticoid resistance, an absent HPA axis negative feedback and impaired gluconeogenic enzyme expression (Tronche et al., 1998). Since GR is reported to affect transcription both by DNA binding-dependent and independent mechanisms, Reichardt et al., (1998) used gene targeting to create a point mutation in the D-loop of the second zinc finger ($GR^{dim/dim}$), which abolishes GR dimerization, with the aim of separating these modes of action. The $GR^{dim/dim}$ mice are apparently unable to transactivate gene transcription through DNA binding of GR, but retain the repressing function of GR attributed to the action of GR monomers, independent of DNA binding (as discussed in section 1.5.1.7). Mice homozygous for this mutation survive, have normal lung and adrenal development but increased corticosterone (CORT) levels and upregulated POMC mRNA expression in the pituitary while CRH expression was unaltered (Reichardt et al., 1998). Oddly, PNMT, a classically GC up-regulated gene, was normally expressed in $GR^{dim/dim}$ mice (Reichardt et al., 1998). These data has been called into question by Adams et al., (2003) who reported that the mutation in the D-loop, whilst it abolishes transactivation through a conventional inverted repeat (or palindromic) GRE, still permits transactivation, via DNA binding-

dependent manner from "non-classical" GREs such as present in the PNMT gene (Adams et al., 2003, also see section 1.5.1.7). It remains to be established whether the repressive effects of GR are mediated via DNA-independent mechanisms or through non-conventional GREs as in the PNMT gene.

Heterozygous mice ($GR^{+/-}$) with a 50% GR reduction, showed normal basal CORT levels, but CORT was increased after restraint stress indicating a disinhibited HPA axis (Ridder et al., 2005). Conversely, mice with a 2-fold increase in GR gene dosage (using a yeast artificial chromosome; YGR) displayed reduced expression of the main components of the HPA axis, 4-fold lower circulating CORT and enhanced HPA feedback regulation after immobilization stress (Reichardt et al., 2000; Ridder et al., 2005).

Because complete inactivation of the GR gene is incompatible with survival, a number of conditional GR gene targeting models have been generated to dissect the role of GR in specific tissues (Table 1.1). A nervous-system-specific inactivation of GR gene was created by flanking exon 3 with loxP sites and crossing the line with nestin-Cre mice (Tronche et al., 1999). This trangene manipulation resulted in viable mice that lack GR in neurons and glial cells (GR^{NesCre}). Loss of GR function in the nervous system resulted in plasma glucocorticoid excess, HPA axis hyperactivity, growth retardation, reduced size, fat redistribution (similar to Cushing's disease) and osteoporosis (Tronche et al., 1999; Kellendonk et al., 2002). However, this model had a complex phenotype with different metabolic phenotypes during suckling, after weaning and in adulthood. Briefly, during suckling GR^{NesCre} displayed a 60%

increase of percent body fat, associated with elevated plasma leptin and insulin levels but normal fat distribution and reduced lean mass (Kellendonk et al., 2002). After weaning, the lean mass was reduced further along with marked reduction in fat mass but persistent hyperleptineamia. Reaching adulthood the GR^{NesCre} mice had reduced fat and lean mass but normalized leptin and insulin levels (Kellendonk et al., 2002). The reduced fat/lean mass in the GR^{NesCre} was probably due to the catabolic signals of elevated hypothalamic CRH and plasma GC levels (Kellendonk et al., 2002). Another 2 models, with altered forebrain GR density have been generated. FBGRKO mice (loss of GR in forebrain) displayed elevated circulating CORT and ACTH levels, impaired negative feedback regulation of the HPA axis and glucocorticoid resistance (Boyle et al, 2005). This time-inducible (CaMKIIa promoter) disruption of GR in the forebrain was an elegant strategy showing that there is a threshold effect: that is, the HPA system and the susceptibility to depression-related disorders is not compromised until GR expression falls below a specific level (Boyle et al., 2005). Conversely, the GRov (increased GR) showed normal HPA axis activity basally and after a mild stress and unaltered expression of HPA axis components (Wei et al., 2004).

Less attention has been focused on the effects of peripheral alterations in GR density in metabolically relevant tissues/organs. To elucidate the role of GR in liver, a hepatocyte-specific GR knockout model was created by crossing GR^{loxP} (exon3-floxed) mice with albumin-α-fetoprotein- Cre mice ($GR^{AlfpCre}$) in which the albumin enhancer and αFP promoter drive Cre expression in hepatocytes (Opherk et al., 2004). Half of the $GR^{AlfpCre}$ mice died shortly after birth due to hypoglycaemia

demonstrating that GR is essential to activate gluconeogenic genes neonatally. Under basal (normally fed) conditions adult transgenic mice had normal glucose levels indicating sufficient compensation by GC-independent mechanisms (ie an increase in glucagon and a decrease in insulin levels). However, $GR^{AlfpCre}$ mice developed hypoglycaemia after prolonged fasting, indicating that GR plays an essential role in liver glucose metabolism only during fasting (Opherk et al., 2004). Moreover, they developed milder hyperglycaemia after streptozotocin-induced diabetes due to impaired induction of gluconeogeneis, suggesting that liver-specific GC-antagonists might be beneficial for the treatment of hyperglycaemia in diabetic patients (Opherk et al., 2004). The role of GR in pancreatic β-cells has been explored in mice overexpressing GR in the β-cells (GRTG) under the rat insulin promoter (Delaunay et al., 1997; Davani et al., 2004). Young adult GRTG mice displayed impaired glucose tolerance and reduced insulin secretion, but unaltered fed or fasted plasma glucose levels (Delaunay et al., 1997). Aged GRTG mice had unaltered body weight, elevated blood glucose levels, reduced insulin secretion and reduced insulin responses to glucose treatment in the islets (Davani et al., 2004), clearly indicating that the elevated GR causes impaired insulin secretion in β-cells. Finally, a transgenic model with conditional inducible cardiac-specific expression of the human GR (hGR) was generated by crossing tetracycline-inducible hGR mice (tetO-hGR) with αMHC-τTA transactivator (expression of the τTA transactivator under the control of cardiac-specific αMHC promoter) mouse line (double transgenic; DT) to evaluate the direct cardiovascular function of increased GR (Sainte-Marie et al., 2007). DT mice had normal survival rates, circulating CORT levels and blood pressure (Sainte-Marie et al., 2007). Cardiac hGR overexpression led to conduction

defects, reduced heart rate, atrio-ventricular block, altered calcium (Ca^{2+}) homeostasis and in isolated cardiomyocytes, cardiac remodelling (Sainte-Marie et al., 2007). Despite the plethora of models of altered GR density, the effects of reduced/increased GR in adipose tissue function/metabolism have not been examined.

In summary, the model that is more relavent, with respect to altered GC sensitivity and the effects on metabolic parameters, to the system I generated and presenting in the following chapters are the $GR^{+/null}$ mice. However, comparisons could not be performed with respect to metabolic effects of altered GR density between the 2 models since data from $GR^{+/null}$ mice are unavailable. The advantage of the model presented in the next chapters is that the LacZ reporter can provide a visual mean of monitoring the expression of the GR in cells, tissues or whole organs or at different developmental stages.

Table 1.1 GR transgenic mice and their phenotype with respect to metabolic parameters and HPA axis (other phenotypes are not listed here).

MODEL	GENETIC	SURVIVAL	GR LEVELS	OBSERVATIONS		REFERENCES
				Metabolic	**HPA axis**	
GR antisense (transgenic) neurofilament promoter	C3HxC57BL/6 (F2) 6mo old	Not compromised	Variable:30-70% ↓, 50-60% ↓, liver hypothalamus, cortex, depending on tissue	↑BW(x2), ↑fat weight, ↓food intake (15% less)	↑ACTH,↑CORT	Pepin et a., 1992
	3-4mo old			↔BW, ↑fat weight, ↓heart & muscle weight ↓food intake, ↓energy expenditure ↑plasma TGs		Richard et al., 1993
GR$^{hypo/hypo}$ (Targeted) insertion mutation in exon 2	C57BL/6x129	most die at birth 10-20% survive	Absent GR mRNA and protein But some residual GR expression (truncated protein) in surviving	↓gluconeogenic enzyme in liver	↑CORT (3 fold), ↑ACTH (15-20 fold), ↑CRH mRNA ↑POMC/ACTH mRNA Adrenal cortical hypertrophy with ↑11β-hydroxylase & ↑aldosterone synthase	Cole et al., 1995 Cole et al., 2001
GR $^{null/null}$ (Targeted) exon 3deleted (loxP/Cre)		Die shortly after birth	Not detected	↓gluconeogenic enzyme in liver	↑CORT, ↑ACTH, ↑POMC/ACTH mRNA	Finotto et al., 1999 Tronche et al., 1998

Table 1.1 GR transgenic mice and their phenotype with respect to metabolic parameters and HPA axis (continue)

MODEL	GENETIC	SURVIVAL	GR LEVELS	METABOLIC PHENOTYPE	HPA AXIS PHENOTYPE	REFERENCES
$GR^{dim/dim}$ (Targeted) Point mutation in exon 4		normal survival		ND	↑CORT, ↔ACTH ↔CRH mRNA ↑POMC/ACTH	Reichardt et al., 1998
GR^{NesCre} (Targeted) exon3- floxed x rat nestin-Cre	C57BL/6xSJF2	Normal postnatal survival	Loss of GR in brain	↓size, ↑ fat distribution in the neck, osteoporosis	↑CORT (am&pm), ↓ACTH (am), ↑CRH ↑POMC mRNA Normal adrenal morphology	Tronche et al., 1999
	Post-weaning to 1month old			↓body mass, ↓FI & EE, ↑plasma leptin & insulin		Kellendonk et al., 2002
	Adults			↓body mass (↓plasma IGF-1), ↓fat mass (75%)	↑NPY(ARC), ↑CRH(PVN)	
$GR^{+/-}$ (targeted) these are the $GR^{null/null}$ (Tronche et al., 1998)	C57BL/6 x FVB/N >10 generations of interbreeding 3-6 month old		GR mRNA: ↓ 33% GR protein: ↓ 50% in hippocampus	ND	↔CORT ↑CORT after restraint stress Fail to suppress CORT after DEX/CRH test	Ridder et al., 2005
YGR (transgenic) (2 copies of YAC encoding GR)	FVB/N x C57BL/6 (F1) 3-6 month old	Normal	↑GR mRNA: 60% brain, 43% pit, 20% liver,spleen,thymus, ↑GR protein: 50%HC	ND	↓CORT, ↑ACTH ↓CRH/ACTH prot ↓POMC mRNA ↓CORT restraint	Reichardt et al., 2000 Ridder et al., 2005

Table 1.1 GR transgenic mice and their phenotype with respect to metabolic parameters and HPA axis (continue)

MODEL	STRAIN BACK/D & AGE	SURVIVAL	GR LEVELS	METABOLIC PHENOTYPE	HPA AXIS PHENOTYPE	REFERENCES
FBGRKO (targeted) CaMKIIa-Cre x floxed	C57BL/6 x 129 x CBA 6 month old 2 month old		Loss of forebrain GR 60% of neurons w/o GR –complete deletion occurs at 4-6 months of age	ND	↑CORT (am&pm), ↑ACTH (am&pm) ↑AVP mRNA in PVN (65%), ↔CRH mRNA in PVN ↔CORT	Boyle et al., 2005
GRov (transgenic) CaMKIIa-HA-tagged GR	C57BL/6		GR forebrain overexpression (78% ↑), including the hypothalamus	ND	↔CORT, ↔ACTH ↔POMC mRNA ↔CRH mRNA ↔MR mRNA (HC)	Wei et al., 2004
GR^{AlfpCre} (targeted) exon 3-floxed x albumin/ α-fectoprotein-Cre	1.5-6month old	½ mice die 2days after birth (hypoglycaemia)	Loss of GR in hepatocytes & biliary duct cells	↓BW, ↓TGs, ↓insulin,↑glucagon ↔ liver PEPCK, TAT, G6Pase mRNA under basal or after DEX treatment Hypoglycemia after fasting Protected from streptozytocin-induced diabetes	↔CORT	Kellondonk et al., 2000; Opherk et al., 2004

Table 1.1 GR transgenic mice and their phenotype with respect to metabolic parameters and HPA axis (continue)

MODEL	STRAIN BACK/G & AGE	SURVIVAL	GR LEVELS	METABOLIC PHENOTYPE	HPA AXIS PHENOTYPE	REFERENCES
GR β-cell TG (transgenic) rat insulin I promoter	C57BL/6J x CBA/J 3 month old	normal growth rate and survival	↑β-cell GR (2-10 copy number)	Impaired glucose tolerance, ↓insulin secretion, ↔fed & fasted blood glucose	ND	Delaunay et al., 1997
	12-15 month			↔BW, ↑blood glucose, ↓insulin Diabetic (α-AR overexpression in islets), ↓insulin response to glucose in islets	ND	Davani et al., 2004
DTGR (double transgenic) tetO-hGR x αMHC –τTA cardiac-specific	B6D2 2month old	normal survival	hGR in cardiomyocytes is Dox-dependent ↔mouse endogenous GR	Bradycardia, cardiomyocyte remodelling, atrio-ventricular block, altered Ca^{2+} homeostasis ↔Blood pressure	↔CORT	Sainte-Marie et al., 2007

BW; body weight, HC; hippocampus, PVN; paraventricular nucleus of the hypothalamus, TGs; triglycerides, PEPCK; phosphoenolpyrouvate carboxylase,TAT;, G6Pase; glucose-6-phosphatase, DEX; dexamethasone (synthetic glucocorticoid), AR; adrenergic receptor, IGF; insulin growth factor, YAC; yeast artificial chromosome, ND; not determined, w/o; without. Note that GR transgenic mice with phenotypes not directly relevant to HPA/metabolic (eg macrophage or Tcell specific GR knock out) are not included.

1.6.2 GR polymorphisms and associations with altered GC sensitivity and pathologies in humans.

Data from GR transgenic mice have clearly shown that altered GR density results in altered glucocorticoid sensitivity and HPA axis dysregulation (where brain GR density is altered). In humans, GC sensitivity (measured by the DEX suppression test) varies between but not within individuals suggesting that there is a set-point for GC sensitivity which might be genetically determined (Huizenga et al., 1998). Impaired GC sensitivity has been associated with mutations/polymorphisms in the GR gene, and has been hypothesized to be the cause or a contributing factor to pathological conditions or subtle metabolic abnormalities (reviewed in van Rossum and Lamberts, 2004). Rare mutations in the GR gene have been identified in a small number of patients diagnosed with general glucocorticoid resistance (or hyposensitivity) (van Rossum and Lamberts, 2006). These mutations are associated with elevated cortisol production, and impaired central negative feedback (van Rossum and Lamberts, 2004). Clinical features in these patients include hypertension (due to increased mineralocorticoid production), hypokalemic alkalosis, fatigue and, in females, hyperandrogenism (van Rossum and Lamberts, 2004). Severe generalized glucocorticoid resistance is not well studied since it is extremely rare. However, 2 patients have been identified, with symptoms of Cushing's syndrome despite low or normal plasma cortisol levels (Iida et al., 1990; Newfield et al., 2000). Lymphocytes from one of these patients, with normal cortisol levels, showed increased GR number per cell (but normal binding affinity), suggesting that the presence of peripheral Cushingoid phenotype might be explained by differential GC sensitivity at the peripheral *vs* the hypothalamic-pituitary level either by tissue-specific differences in

GR numbers or by hypothalamic desensitization (Newfield et al., 2000). Additionally, i*n vitro* experiments (lymphoid cell lines) showed that increasing the quantity of GR induces enhanced responses to glucocorticoids (Pfahl et al., 1978; Nieman et al., 1985). Common polymorphisms linked to or within the GR gene have been implicated in altered GC sensitivity (van Rossum and Lamberts, 2004).

Figure 1.5 shows the location of polymorphisms in the GR gene identified to date that cause GC resistance or altered GC sensitivity. Here the discussion focuses on the 3 most well studied GR polymorphisms which are associated with altered GC sensitivity and alterations in body composition and metabolic parameters.

The ER22/23EK polymorphism in the GR gene is associated with relative glucocorticoid resistance (fig. 1.5). This polymorphism consists of 2 linked single nucleotide changes/substitutions in codons 22 and 23 (exon 2), with only the second substitution causing an amino acid change from arginine (R) to lysine (K) (Koper et al., 1997). A population-based study in elderly Dutch men showed that carriers of the ER22/23EK polymorphism had impaired cortisol suppression after a DEX suppression test, lower risk of dementia, lower fasting insulin levels, increased insulin sensitivity, lower total and low density cholesterol levels and lower C-reactive protein that could protect them from cardiovascular abnormalities and increase their survival (van Rossum et al., 2002; van Rossum et al, 2004a, b; Wust et al., 2004; Koeijvoets et al., 2006). When younger male and female (followed from 13years to 36 years of age)

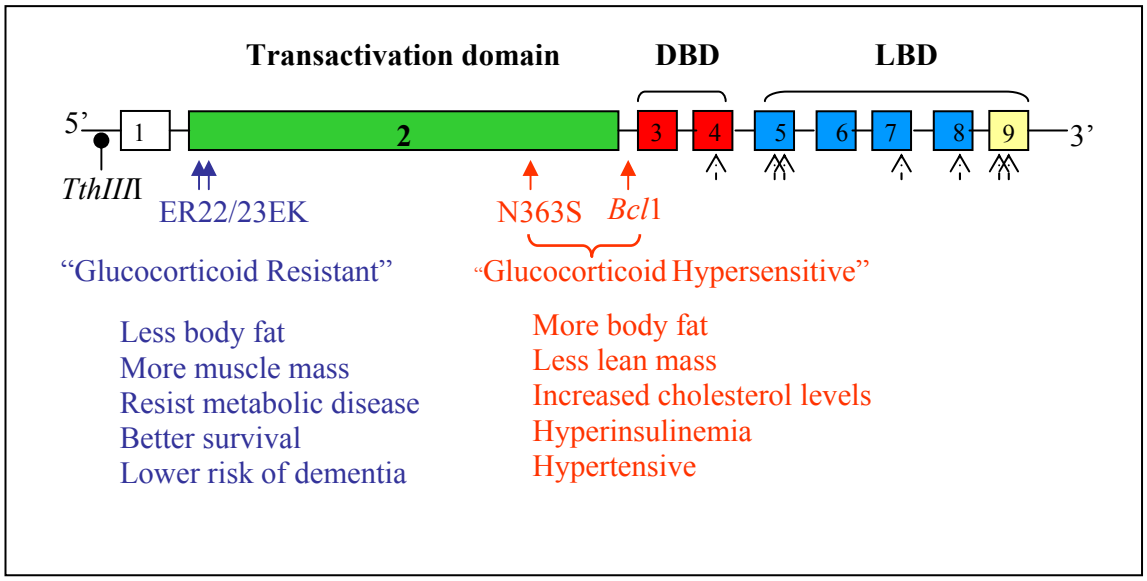

Figure 1.5 Polymorphisms in the GR gene and their clinical associations

A simplified view of the GR gene showing the locations of polymorphisms associated with altered glucocorticoid sensitivity and their effects on body composition and metabolic parameters. The 3 intensively studied and characterized polymorphisms are presented. ER22/23EK (highlighted in blue) carriers show reduced glucocorticoid sensitivity and have a healthy metabolic profile, while N363S or *Bcl*I (highlighted in red) carriers show increased glucocorticoid sensitivity and an unfavourable metabolic profile. Please note that the fourth polymorphism, *TtIII*Ι (oval arrow) in the GR promoter region is much less studied. However, it is believed to be non-functional itself and might be functionally relevant only in combination with the ER22/23EK, since it was found that all ER22/23EK carriers also carry the *TtIII*Ι polymorphism (van Rossum et al., 2004c). The dashed arrows indicate mutations in the GR gene that lead to the syndrome of cortisol resistance (adapted from van Rossum & Lamberts, 2004).

carriers were studied, the male carriers were taller, had more lean body mass and increased muscle strength, and the females had smaller waist circumference (used as a measure for visceral adiposity and a risk factor for the Metabolic Syndrome; reviewed in Reaven, 2005). In all carriers studied, this polymorphism was associated with a healthier metabolic/body composition profile, possibly attributable to glucocorticoid resistance in tissues such as adipose and liver (van Rossum and Lamberts, 2004). However, it has also been associated with a more aggressive multiple sclerosis phenotype (van Winsen et al., 2007), as well as increased risk of dementia (van Rossum 2006). The mechanisms involved in mediating the effects of ER22/23EK polymorphism have been recently elucidated. Transfection experiments showed a reduced capacity for GRE-luciferase activation, indicating decreased transactivation ability (Russcher et al., 2005a). Dexamethasone treatment of peripheral blood mononuclear lymphocytes (PBMLs) from homozygous or heterozygous ER22/23EK carriers showed a dose-dependent reduction in the transcriptional activation of the GC-responsive gene, leukine Zipper protein (GILZ), but normal transrepression of NF-kB (Russcher et al., 2005a). Interestingly, overall GR expression levels in lymphocytes (measured by [^{3}H]-DEX binding of PBMLs) did not differ between control, heterozygous or homozygous carriers (Russcher et al., 2005a). However, the ER22/23EK polymorphism resulted in a shift in favour of the GR-A translational variant over the GR-B (Russcher et al., 2005b; described in section 1.5.2.2) with the former having a less potent transactivator effect (Yudt and Cidlowski, 2001)

The N363S and *Bcl*I-restriction fragment polymorphisms (fig. 1.5) have been associated with increased GC sensitivity and a generally unfavourable metabolic profile (reviewed in van Rossum and Lamberts, 2004). The N363S polymorphism was first identified in an elderly Dutch population and is located in codon 363 of GR exon 2, resulting in an asparagine to serine amino acid change (Koper et al., 1997; Huizenga et al., 1998). The N363S polymorphism is present with allele frequencies ranging from 0.7% to 27% in South Asian (Dhawan et al., 1994; Syed et al., 2004) and Australian (Morris et al., 2003) subjects respectively, and 4-15% in European carriers (Bhopal et al., 1999). The findings regarding this polymorphism and associations with obesity and metabolic abnormalities are contradictory, with some reporting higher BMI (body mass index), increased waist-to -hip ratio (WHR), increased insulin responses to exogenous DEX, elevated plasma lipids and increased CAD risk (Lin et al., 1999; Di Blasio et al., 2003, van Rossum et al., 2003), and others showing no associations with the above parameters in carriers (Rosmond et al., 2001; Dobson et al., 2001). The proposed molecular mechanism by which the N363S variant exerts its effects is by increasing the transactivating capacity of GR (Russcher et al., 2005) or by regulating different genes (Jewell and Cidlowski, 2007). However, recently a meta-analysis study (included 5,909 individuals), performed to evaluate the association between the polymorphism and obesity risk, showed that homo-/hererozygous carriers of the N363S allele did not have a higher risk of developing obesity compared to non-carriers, although they pointed out that there maybe certain genotypic effects that are population-specific (Marti et al., 2006).

The *Bcl*I polymorphism is an intronic restriction fragment length polymorphism of the GR gene in which a C to G nucleotide mutation has occurred 646 nucleotides downstream of exon 2 resulting in 2.2 kb and 3.9 kb fragments following a *Bcl*I digest (Murray et al., 1987; van Rossum et al., 2003). The C allele is the most frequently (65%) occurring (van Rossum and Lamberts, 2004). This polymorphism has shown clear associations with increased GC sensitivity (Buemman et al., 1997, Rosmond et al., 2000; Fleury et al., 2003; van Rossum et al., 2003; Trembley et al., 2003) but the data with respect to alterations in adiposity over time are contrasting. The controversy is probably due to different consequences of *Bcl*I-induced hypersensitivity to GCs during life (van Rossum and Lamberts, 2004). For example, it might be possible that early in life, fat mass (especially visceral) is predominately affected (G-allele carriers have more fat) while later in life (middle-age carriers), lean mass is more profoundly affected (G-allele carriers have less lean mass)(van Rossum and Lamberts, 2004). Interestingly, homozygosity of the G allele was more frequent in subjects with heritable hypertension (Watt et al., 1992). The molecular mechanisms by which the *Bcl*I polymorphism exerts its effects are unknown. Being in an intron limits the use of transfection experiments. One hypothesis proposed that this intronic polymorphism is linked to another polymorphism in the GR promoter region which could increase GR expression and in turn increase mRNA stability, but still waits to be confirmed (van Rossum and Lamberts, 2004).

Finally, it should be noted that the phenotypic changes (especially with respect to metabolic parameters and body composition) and the severity of pathological consequences associated with polymorphisms in the GR gene are complicated and

vary, dependent upon the age, gender and general health status (obese, over- or normal weight) of the carrier, and are population-specific therefore here the review of the literature has been simplified.

1.6.3 11β-hydroxysteroid dehydrogenase type 1 transgenic mice, altered GC sensitivity and the Metabolic Syndrome

GCs that have diffused through the cell membrane must engage with the GR to exert their effects. As mentioned above, apart from the GR determining GC sensitivity, intracellular GC sensitivity is determined by the levels of 11β-HSD enzymes (section 1.4). In this section the focus is on 11β-HSD type 1 since its manipulation is of greatest relevance to explain tissue-specific alterations in GC sensitivity and associations with the Metabolic Syndrome. Studies on adipose-specific 11β-HSD1 over-expressing mice (ap2-11β-HSD1) showed increased corticosterone levels in adipose tissue and the portal system, but not in the peripheral circulation (Masuzaki et al., 2001). The mice developed visceral obesity, glucose intolerance, insulin resistance, dyslipideamia and hypertension (Masuzaki et al., 2001; Masuzaki et al., 2003). Interestingly, GR levels were unaltered in adipose tissue (Masuzaki et al., 2001), suggesting that 11β-HSD1-mediated amplification of GCs in adipose does not affect the level of the receptor in fat in this model. Conversely, 11β-HSD1 knockout mice (11β-HSD1$^{-/-}$; unable to convert inactive to active GCs) showed an improved lipid profile and resisted obesity and glucose intolerance when challenged with high fat diet (Kotelevtsev et al., 1997; Morton et al., 2001; Morton et al., 2004). With respect to circulating GC levels and HPA axis phenotype, 11β-HSD1$^{-/-}$ mice exhibited adrenal hypertrophy and elevated basal ACTH and CORT levels at their nadir and, *in vitro*, 11β-HSD1$^{-/-}$ adrenals were hyper-responsive to ACTH, indicating

a compensation for the lack of active GCs (Kotelevtsev et al., 1997; Harris et al., 2001). However, CRH mRNA levels in the paraventricular nucleus (PVN) of the hypothalamus are unaltered suggesting maintenance of central drive (Harris et al., 2001). Similar to ap2-11β-HSD1 mice, 11β-HSD1$^{-/-}$ mice had unchanged GR levels (Harris et al., 2001). However, the HPA phenotype appears to be strain-dependent. The original observations were made in a mixed background (129 and the outbred MF1). When the 11β-HSD1 disruption was backcrossed onto a C57BL/6J background, only the adrenal hypertrophy was maintained (Carter et al., submitted for publication). Additionally, GR was increased in the hippocampus and PVN, which possibly led to improved GC feedback, thus explaining the unaltered plasma corticosterone (CORT) and ACTH levels (Holmes and Seckl, 2006). Metabolic studies on a C57BL/6 background confirmed the insulin-sensitive phenotype of the 11β-HSD1$^{-/-}$ mice. It seems that the phenotype (either metabolic or HPA axis) in 11β-HSD1$^{-/-}$ mice is strongly affected by the genetic background in which the gene is deleted. However, it is clear that adipose-specific amplification of GCs, by increased 11β-HSD1 activity, in mice causes obesity and all the adverse consequences widely known as the Metabolic Syndrome. What are the parallels with idiopathic obesity in humans?

1.6.4 11β-HSD1 and human obesity

Exposure to high circulating GC levels, as found in Cushing's disease, causes a metabolic disease that resembles features of idiopathic metabolic syndrome including pronounced visceral obesity (reviewed in Seckl et al., 2004; Stewart, 2005).

However, idiopathic obesity is not associated with high circulating GC levels (Marin et al., 1992; Homma et al., 2001; reviewed in Bjorntorp, 2000). Rather, it appears that intra-cellular generation of active from inactive GCs by 11βHSD1 is aberrantly elevated in adipose tissue of obese individuals (reviewed in Seckl et al., 2004; Stewart, 2005). Thus, it has been extensively shown that 11β-HSD1 mRNA and activity are elevated in abdominal subcutaneous adipose tissue from obese compared with non-obese individuals (Rask et al., 2002; Paulmyer-Lacroix et al., 2002; Lindsay et al., 2003; Wake et al., 2003; Engeli et al., 2004; Kannisto et al., 2004). *In vivo* microdialysis confirmed increased regeneration of cortisol from cortisone in abdominal subcutaneous adipose from obese humans (Sandeep et al., 2005). Given the key association of intra-abdominal (visceral) adipose tissue with metabolic and cardiovascular disease risk, it has been hypothesized that increased 11βHSD1 in the visceral, rather than subcutaneous, adipose depot causes the adverse metabolic consequences of idiopathic obesity and the metabolic syndrome (Bujalska et al., 1997). However, Tomlinson et al. reported a negative association between 11β-HSD1 activity and BMI in primary omental human adipocytes cultured *in vitro*, though there was no correlation in whole adipose biopsies (Tomlinson et al., 2002). A further study could not detect increased portal vein cortisol (Aldhahi et al., 2004) or increased splanchnic cortisol production rates (Basu et al., 2005) in obesity suggesting that if cortisol generation is indeed elevated in the visceral fat, it is further metabolised or is not released at higher rates from adipocytes. Together, these data have engendered some confusion as to whether visceral as well as subcutaneous 11β-HSD1 is elevated in human obesity.

Finally, in contrast to the plethora of studies of 11β-HSD1 in adipose tissue and Metabolic Syndrome, curiously few studies have examined associations between tissue GR levels and metabolic parameters. As reviewed here, genetic studies strongly support a role for GR in determining body composition and fat distribution (section 1.6.2). Higher levels of GR found in omental compared to subcutaneous fat (Rebuffe-Scrive et al., 1990) would further be expected to have a more pronounced effect on GC action in the omental depot. However, a previous study in this lab showed no correlation between adipose tissue GR mRNA in abdominal sc adipose tissue and obesity (Wake et al., 2003), whereas another group reported an inverse correlation between sc adipose GRα mRNA and BMI (Kannisto et al., 2004). Therefore, assessing the levels of GR in different adipose depots (central *vs* peripheral) and studying the GR associations with metabolic parameters as well as the relationship between GR and 11β-HSD1 levels is crucial to our understanding of adipose GC disregulation and its consequences in human obesity.

1.7 Thesis Aims

As described in this chapter GCs have a variety of physiological roles and cause a number of responses, primarily through the GR. One major concept, presented here is the sensitivity to the effects of GCs and downstream metabolic consequences. This is of great importance since GCs are used routinely for the treatment of many conditions. However in certain individuals they cause deleterious side effects.

Genetic studies in humans and studies following manipulation of GR in transgenic mice provided compelling evidence that the absolute level of GR protein expressed in a cell can have a dramatic impact on the cellular responsiveness to GCs with consequent downstream effects on a plethora of physiological processes. Therefore the aim of my PhD was to use mouse models of altered GC sensitivity to investigate the effects primarily on metabolism/susceptibility to metabolic disease and HPA axis function, and crucially a human population study to investigate how mechanisms "dissected" from mouse models could be applied to humans.

Specifically the aims of this Thesis were to:

(1) investigate the effect of global reduction in GR density upon tissue GC sensitivity, HPA axis regulation, susceptibility to dietary-induced obesity (DIO) and body fat distribution (*chapters 3, 4 and 5*).

(2) investigate GC sensitivity and determine key parameters of GC action (GR and 11βHSD1) in metabolically important tissues (liver and adipose) and their role in body fat distribution in POMC-deficient mice (*chapter 6*), an established model of HPA hypo-activity which also shows hyperphagic obesity (Challis et al., 2004; Coll et al., 2004; Coll et al., 2005).

(3) address if adipose (biopsies form 4 distinct adipose depots:omental, abdominal subcutaneous, gluteal and thigh) GR levels are altered in obesity, and whether they associate with 11βHSD1 levels and metabolic parameters in human obesity (*chapter 7*).

Chapter 2

Materials and Methods

2.1 Materials

Except where stated otherwise, all chemicals were from Sigma (suppliers addresses can be found in Appendix D).

2.1.1 General chemicals

NICK columns Scintillation proximity assay reagent (anti-rabbit reagent) Hybond-C nitrocellulose membrane	Amersham Pharmacia Biotech UK Ltd.
Protein assay dye reagent concentrate	Bio-Rad Laboratories Ltd.
SeaKem™ LE agarose	Cambrex Bio Science Wokingham Ltd.
1 kb DNA ladder Superscript III cDNA synthesis kit Lyophilised desalted primers (1µg/µl stock)	Invitrogen
Formamide Loading Buffer Reverse Transcription System *Taq*Bead™ Hot Start Polymerase Beetle Luciferin X-gal Nuclease-free water dNTPs (100mM stock)	Promega Ltd.
Lightcycler 480 Probes Master Mix	Roche
Kodak MS-1 autoradiographic film Dexamethasone 20xSSC Oil Red O	Sigma-Aldrich Company Ltd.
ACTH ELISA Kit	Biomerica
DNeasy Tissue extraction kit	Qiagen
RNA Matrix and wash	Anachem
RIA cups	Sarstedt
Whatman 3MM paper 1ml eppendorf tubes 0.5ml eppendorf tubes Superfrost slides	VWR International Ltd.

2.1.2 Miscellaneous equipment

Hyperprocessor GeneQuant RNA/DNA Calculator	Amersham Pharmacia Biotech UK Ltd.
Lumat LB9501 Luminometer	Berthold Technologies (U.K.) Ltd.
Agarose gel electrophoresis equipment 583 Gel Drier	Bio-Rad Laboratories Ltd.
Eppendorf Mastercycler	Eppendorf AG.
Ultra-turrax TD Homogeniser	IKA Labortechnik
Shimadzu spectrophotometer 160A	Shimadzu Europa U.K.
Techne Genius Thermocycler Hybridisation oven HB-1D Hybridisation bottles	Techne

2.1.3 Radiochemicals with their specific activities

[α^{32}P] dCTP 110TBq/mmol (or 3000Ci/mmol)	Amersham Pharmacia Biotech UK Ltd.
[^{3}H]-corticosterone (2.8-3.9TBq/mmol or 75-105Ci/mmol)	
[^{125}I]-iodotyrosyl Angiotensin I (2000Ci/mmol or 74TBq/mmol)	GE Healthcare

2.1.4 Enzymes

All enzymes were obtained from Promega Ltd., unless otherwise stated.

DNase	Invitrogen
AmpliTaq DNA polymerase	Applied Biosystems
Proteinase K RNaseA	Promega Ltd

2.1.5 ES cell tissue culture reagents & equipment

Fetal Calf Serum (FCS) L-Glutamine Penicillin/Streptomycin Trypsin	Invitrogen
Porcrine Gelatin MEM non essential amino acid Sodium Pyruvate Glasgow MEM (G-MEM) Retinoic Acid	Sigma-Aldrich Ltd
T25 Flasks T75 Vented Flasks Quadriperm 4x12 chambers	Greiner Bio-One Ltd.
2ml Cryotubes	Nalgene Labware

2.1.6 Immunofluoresence general

DAPI Horse Serum Donkey Serum EGTA $MgCl_2$ $CaCl_2$ Igepal (NP40)	Sigma
Chromosome paints	Gambio
Vectashield	Vector

2.1.7 Solutions & buffers

SOLUTIONS & BUFFERS	RECIPE
DEPC dH_2O	0.5ml DEPC in 500ml ultrapure dH_2O. Leave for 1-24 h, autoclave.
DNA Loading Buffer	40% v/v glycerol, 0.3% w/v Orange G
1kb ladder buffer	1:2; 1kb ladder:loading buffer, make vol with dH_2O
Oil Red O	210ml ORO in 140ml dH_2O

Borate buffer	8.25g boric acid, 2.7g NaOH, 5g BSA in 1lt dH_2O, pH 7.4
Phosphate buffer	13.8g NaH2PO4-1-hydrate, 42.6g Na2HPO4-anhydrous, 0.93g EDTA in 500ml dH_2O
Tris (50mM, pH 7.4 @ 22°C) for angiotensinogen & renin assays	Tris (12.14g) in 1l dH_2O. Add 10ml 5M HCl, 3.5g neomycin sulphate, 1.75g serum albumin (sprinkle). Adjust to pH 7.4, make up to 2l. Aliquot 10ml and store at -20°C.
Charcoal for agiotensinogen and renin assays	Tris (6.07g) in 500ml dH_2O , add 5ml 5M HCl, 2g neomycin sulphate,1.85g EDTA, 5g BSA (sprinkle).Adjust pH to 7.4, make up to 1l; store 100ml aliquots. Dissolve 0.062g dextran T70 in 5.0ml buffer (0.6g Norit charcoal + 95ml buffer + 5ml Dextran T70 soln.).Store @ 5°C.
10 x MOPS	200mM MOPS acid, 50mM $C_2H_3O_2Na$, 10mM EDTA. pH adjusted to 7.2.
1 x PBS	1 x PBS tablet (Sigma) dissolved in 200ml dH_2O to give 10mM phosphate buffer, 2.7mM KCl, 137mM NaCl
Potassium Acetate (5M acetate, 3M potassium)	245.6g $KC_2H_3O_2$ dissolved in 442.5ml dH_2O, 57.5ml glacial acetic acid.
Prehybridisation Buffer	5 x SSC, 0.5% SDS, 5 x Denhardt's Solution (50 x Denhardt's Solution = 5g Ficoll, 5g polyvinylpyrrolidone, 5g BSA to 500ml with dH_20).
RNase -free Loading Buffer	2g Ficoll 400, 100mg SDS, 25mg bromophenol blue 25mg xylene xyanol in 10ml 0.1M EDTA pH 8 (made with DEPC dH_2O)

20 x SSC	3M NaCl, 0.3M sodium citrate. pH adjusted to 7.0 with 10M NaOH.
50 x TAE	121.1g Tris dissolved in 421.5ml dH_2O, 50ml 0.5M EDTA, 28.6ml glacial acetic acid
10 x TBE	0.9M Tris, 0.9M Boric Acid, 12.5mM EDTA
TE Buffer	10mM Tris-HCl pH 8.0, 1mM EDTA

2.2 Methods

2.2.1 Molecular Biology

2.2.1.1 RNA methods

2.2.1.1.1 RNA isolation by TRIzol extraction

Total RNA was extracted from frozen tissues and cells using TRIzol reagent (Invitrogen). Tissues (50-100mg) were homogenised in 1ml of TRIzol in pre-chilled eppendorf tubes, using an Ultra-turrax homogenizer. Cells (from a confluent T25 flask) were washed once in 1x PBS before 1ml TRIzol was added. Cells were scraped into an eppendorf tube and then 0.2 ml of chloroform was added per 1ml TRIzol. Tubes were vortexed for 20-30s, incubated for 3min at room temperature (RT) then for 15min on ice. Tubes were centrifuged at 12000g for 30min at 4^0C. The aqueous (top) layer was transferred to new pre-chilled eppendorfs. 20-30µl of RNA Matrix (RNaid Plus kit, BIO 101; Anachem, UK) per 500µl sample was added, and tubes were gently inverted for 5min at RT. Samples were then centrifuged at 14000g for 1min at 4^0C to pellet the matrix. 500µl of wash ethanol solution (Anachem) was added to the pellets which were gently re-suspended, then centrifuged for 1min at 14000g at 4^0C. Another two rounds of washes were performed. Finally, RNA was

recovered from the matrix by re-suspending the final washed pellet in 20µl of diethylpyrocarbonate-treated water (DEPC H_2O) containing 400 U/ml RNasin and 10mmol/l dithiothreitol. A final centrifugation (14000g, 2min, 4^0C) to remove the matrix allowed the RNA in the supernatant to be transferred to fresh eppendorfs in 3x6µl aliquots. RNA was quantified using a GeneQuant spectrophotometer (Amersham, Pharmacia Biotech, UK Ltd) and stored at -80^0C for further analysis.

2.2.1.1.2 RNA gel electrophoresis

For each RNA (5 µg) sample, 2.5µl formaldehyde (37%), 2.5µl 10x MOPS buffer and 10µl of de-ionised formamide were added and mixed thoroughly. Samples were then heated to 65°C for 15 min in order to denature RNA secondary structure and the samples were rapidly chilled on ice. 1 µl of DEPC treated loading buffer was added. The samples were resolved on a denaturing 1% agarose 1xMOPS/18% formaldehyde gel. Brielfy, agarose was melted in a microwave, allowed to cool down and MOPS and formaldehyde were added. The gel was allowed to set for 1h and immersed in 1x MOPS buffer for at least 30 min before loading of samples. Samples were run for 3-4 hr until the first band of bromophenol blue dye reach ¾ of the length of the gel. For analysis of transcripts of larger size (>4kb) 0.7% agarose gels were used.

2.2.1.1.3 Northern blotting and hybridisation

To allow RNA capillary transfer, a nylon membrane (Hybond N) and three pieces of Whatman No.3 filter paper of identical size to the gel were immersed in 20x SSC. A "wick" (similar width to the gel but longer length) was placed above an RNAse free

gel tray. The ends of the wick were immersed in the reservoir of 20x SSC which was used as the source of transfer buffer. On completion of electrophoresis, the gel was washed in 20x SSC, inverted, and placed onto the wick. The nylon membrane was placed on top of the gel surface. The assembly was then covered with saran wrap to isolate the buffer chamber, leaving a 'window' uncovered with the gel, membrane and wet Whatman papers at the centre so that capillary transfer would occur only through the gel and up into the membrane when dry paper towels were placed above it. Layers of filter paper were placed on top of the nylon membrane followed by a stack of dry paper towels. A glass plate (to maintain a flat, even transfer) was placed on top with extra weight on top to maximize capillary force. A small spirit level was used to maintain the balance of the transfer and thus even transfer of RNA to the membrane. Following transfer, the memebrane was washed in 2xSCC and then allowed to dry. The RNA was cross-linked to the membrane by UV transilluminator with an irradiation of $7x10^5$ J.

[α^{32}P]-dCTP-labelled cDNA probes were synthesized by adding 15ng of denatured template to the RediVue kit (Amersham) and left incubating at 37°C for 30 minutes. cDNA probes for mouse 11β-HSD1, GR, angiotensinogen, phosphoenolpyruvate carboxykinase (PEPCK), lipoprotein lipase (LPL) and 18S were generated by PCR using gene and exon specific primers. Identities of all PCR products were verified by sequencing as previously described (Morton et al., 2005). Probes were purified using Nick columns (Amersham) into 400μl of water and specific activity of the probe was estimated using a scintillation counter with 1μl of the probe in 1ml of scintillant (Pico-fluor 40). The probe's labelling efficiency was measured by a β-counter, and

10^5 counts were added to the blot. The nylon membrane was soaked in 20x SSC for 10 minutes and then pre-hybridised by placing it in a pre-warmed (55ºC) hybridisation bottle containing 12ml phosphate buffer and 6ml 20% SDS at 55°C. Sonicated Salmon Testis DNA (10mg/ml; 1ml) was denatured at 105° for 15 min, cooled on ice and added to the pre- hybridisation mixture at 65°C for at least 3-4 h prior to adding the probe. Following addition of the ^{32}P-labelled probe, blots were hybridized at 65°C overnight, washed at 65°C to a stringency of 0.5x SSC, 0.1% SDS and exposed to phosphoimager screen, and read with a phosphoimager (Fuji BAS FLA 2000). Analysis was performed using quantitative imaging software (AIDA 2.0, Raytek, Sheffield, UK). Transcript levels were expressed in arbitrary units (A.U.) relative to 18S RNA.

2.2.1.1.4 Real time PCR

2.2.1.1.4.1 cDNA synthesis

For reverse transcription (RT) PCR, 1 μg RNA was pre-treated with DNaseI (Invitrogen) and was then transcribed into cDNA using oligo-dT primers (or random hexamers if 18S was used as an internal control) and a Superscript III First Strand Synthesis kit (Invitrogen) according to the manufacturer instructions in a total volume of 20μl.

2.2.1.1.4.2 Real time PCR analysis

In the human study, GRα and 11β-HSD1 mRNA levels were quantified by Real Time PCR primer-probe sets using the ABI PRISM 7700/ 7900 Sequence Detection

System (PE Applied Biosystems, Cheshire, UK). The primers and probes used are listed in Table 2.1. The PCR reaction contained 5μl of commercial Taqman mix, 4.5 μl of Nuclease-free H_2O and 0.5 μl of cDNA per sample. The PCR programme is described in Table 2.1. The relative amplification of each sample was measured. After each cycle, a probe signal indicates how much cDNA has been amplified for each individual sample. The program generates a threshold level (typically this is set within or slightly above this exponential phase), and a C_T value was calculated as the number of cycles at which exponential amplification began. One primary assumption of the C_T threshold is that amplification efficiency is identical in all samples. The more cycles the sample has to complete to reach that threshold the lower the initial expression. Data acquisition was by Sequence Detector 2.03 software. Levels of GRα or 11βHSD1 mRNA are reported relative to human cyclophilin A mRNA (Hs99999904_m1, Applied Biosystems, Cheshire, UK), the latter previously optimized as an appropriate internal control for human fat (Wake et al., 2003), and are expressed in arbitrary units (A.U.). Each sample was run in duplicate, and the mean values of the duplicates were used to calculate transcript level. Values were calculated relative to the levels of the internal control. Negative controls, omitted RT or cDNA were used to identify genomic DNA contamination. A standard curve for each primer probe set was generated in triplicate by serial dilution of cDNA pooled from all subjects.

For animal experiments, quantitative (real time) PCR was carried out using a LightCycler 480 (Roche). Primer-probe sets used to measure transcripts were as follows: β-actin (20x assay; Mm00607939_s1), 18S (20x assay; Hs99999901_s1), TATA binding protein (TBP; 20xassay; Mm00446973_m1), GR (20xassay;

Table 2.1 Primer-probe mixes used for human adipose transcript levels as previously described (Wake et al., 2003)

GENE	FORWARD PRIMER (5' TO 3')	REVERSE PRIMER (5' TO 3')	PROBE (5' TO 3')
11β-HSD1	GGAATATTCAGTGTCCAGGGTCAA	TGATCTCCAGGGCACATTCCT	6-FAM-CATTGACAACCTTCGCTGGGAGG-TAMRA
GRα	CATTGTCAAGAGGGAAGGAAACTC	ATTTTCAACCACTTCATGCATAGAA	6-FAM-TGTCAGTTGATAAAACCGCTGCCAGTTCT-TAMRA
PCR programme: incubation @ 50^{o}C (2 min) Denaturation @ 95^{o} C (10 min) 40 cycles of PCR (95^{o} C for 15 s, and 60^{o} C for 1 min)			

Mm01260497_m1), 11β-HSD1 (20xassay; Mm00476182_m1) and angiotensinogen (20xassay; Mm00599662_m1). For all the amplification of transcripts a commercial 20xassay (Applied Biosystems) and a commercial master mix was used (FAM-hydrolysis probe, Roche). Each PCR reaction consisted of 0.5µl 20x assay, 5 µl master PCR mix, 2.5 µl nuclease-free water and 2µl cDNA. Each sample was assayed in triplicate. The Lightcycler 480 PCR programme was as follows: pre-incubation at 95^{o}C,5min, amplification 50x (95^{o}C, 10sec; 60 ^{o}C, 30sec; 7 2^{o}C, 1sec) and cooling, 40 ^{o}C, 30sec. Data were analyzed using the 2nd derivative maximum method. Briefly, in this method a fractional cycle (CP) is determined from the amplification curve's second derivative max instead of the threshold crossing (figure 2.1). The 2nd derivative max indicates the cycle at which exponential amplification can no longer be sustained and starts to decline towards linear growth. In this

method, information from the curve shape promotes a better prediction of the starting concentration than the fluorescence level of the curve (in contrast to the threshold method). Moreover, since the CP value depends on the shape of the curve rather than on fluorescence level, this method rejects the assumptions of (a) identical amplification efficiency in all samples and (b) fluorescence-amplicon proportionality (Rasmussen et al., 2001; Luu-The et al., 2005). The ratio of the gene of interest divided by the housekeeping gene concentrations was determined for each sample. The reasons for using two different real time PCR analysis methods and equipment were (a) the availability of the PCR equipment at the time and (b) for the human experiment to have consistency and comparable results with previous data published from this lab (eg Wake et al., 2003).

2.2.1.1.4.3 Validation of internal controls

The internal control used to correct for equal RNA concentrations between samples in the animal experiments (chapters 4 and 5) was β-actin. Overall, 3 internal controls, β-actin, TBP and 18S were tested. Figure 2.2 shows examples of the amplification plots for the 3 internal controls and also GR and 11β-HSD1 and figure 2.3 shows standard curves for actin, GR and 11β-HSD1. All the internal controls tested had similar CP values between genotypes (fig. 2.4A), but actin and TBP had a cycle-amplification profile (mean CP~28 and 32, respectively) in the same range as 11β–HSD1 and GR (CP~28), whereas mean CP for 18S was 15. Therefore actin was selected for internal control in all experiments. Negative samples (no RT, no cDNA) did not amplify (data not shown). Figure 2.4B confirms that concentration of actin is similar between heterozygous and wild type mice in any tissue tested.

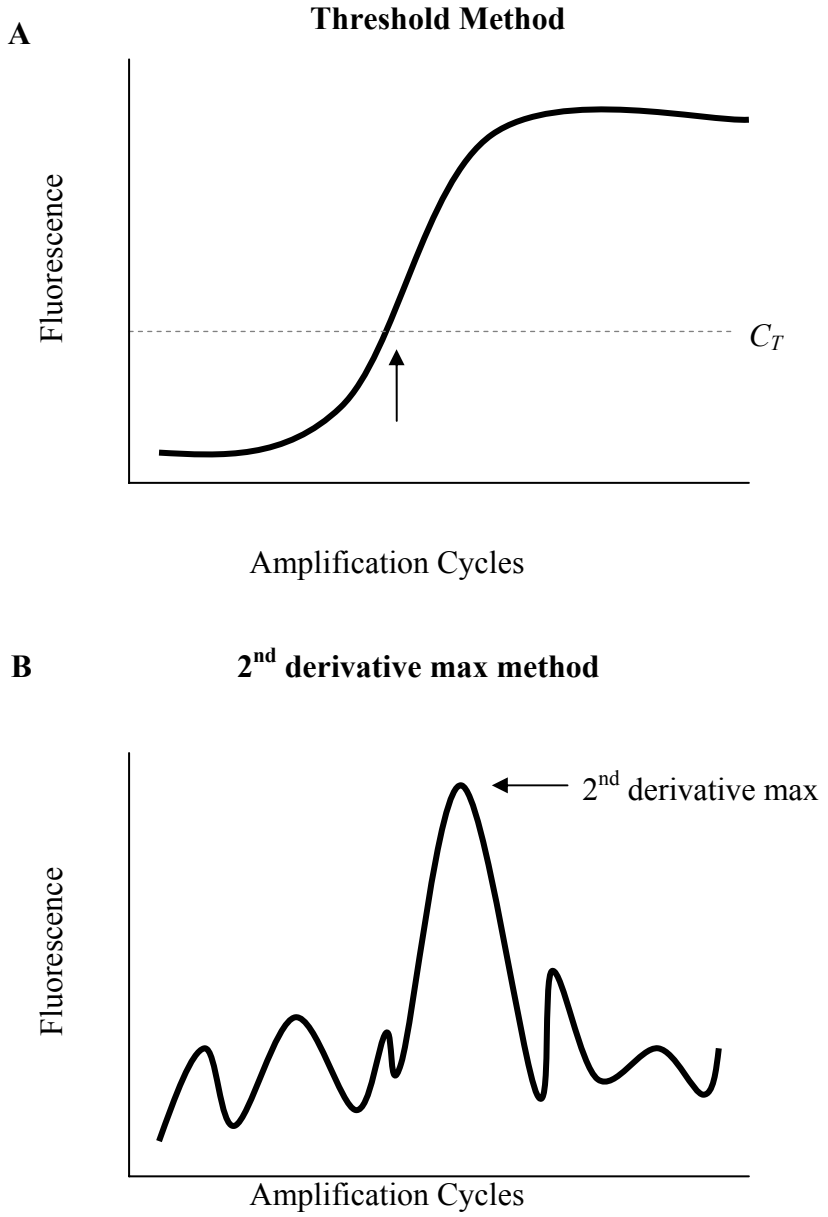

Figure 2.1 Schematic of a real-time PCR fluorescence amplification curve analyzed by two different analysis methods.

The thick black line in each panel shows the same amplification data set with amplification cycle along the x axis and fluorescence on the y axis. Each analysis method identifies a fractional cycle (Cfrac) used to quantify sample copy number, as indicated by black arrows. (A) Threshold method. The arrow indicates Cfrac at the threshold crossing. (B) Second derivative maximum method with the amplification curve second derivative shown. The arrow indicates Cfrac at the second derivative maximum (adapted from Durtschi et al., 2007).

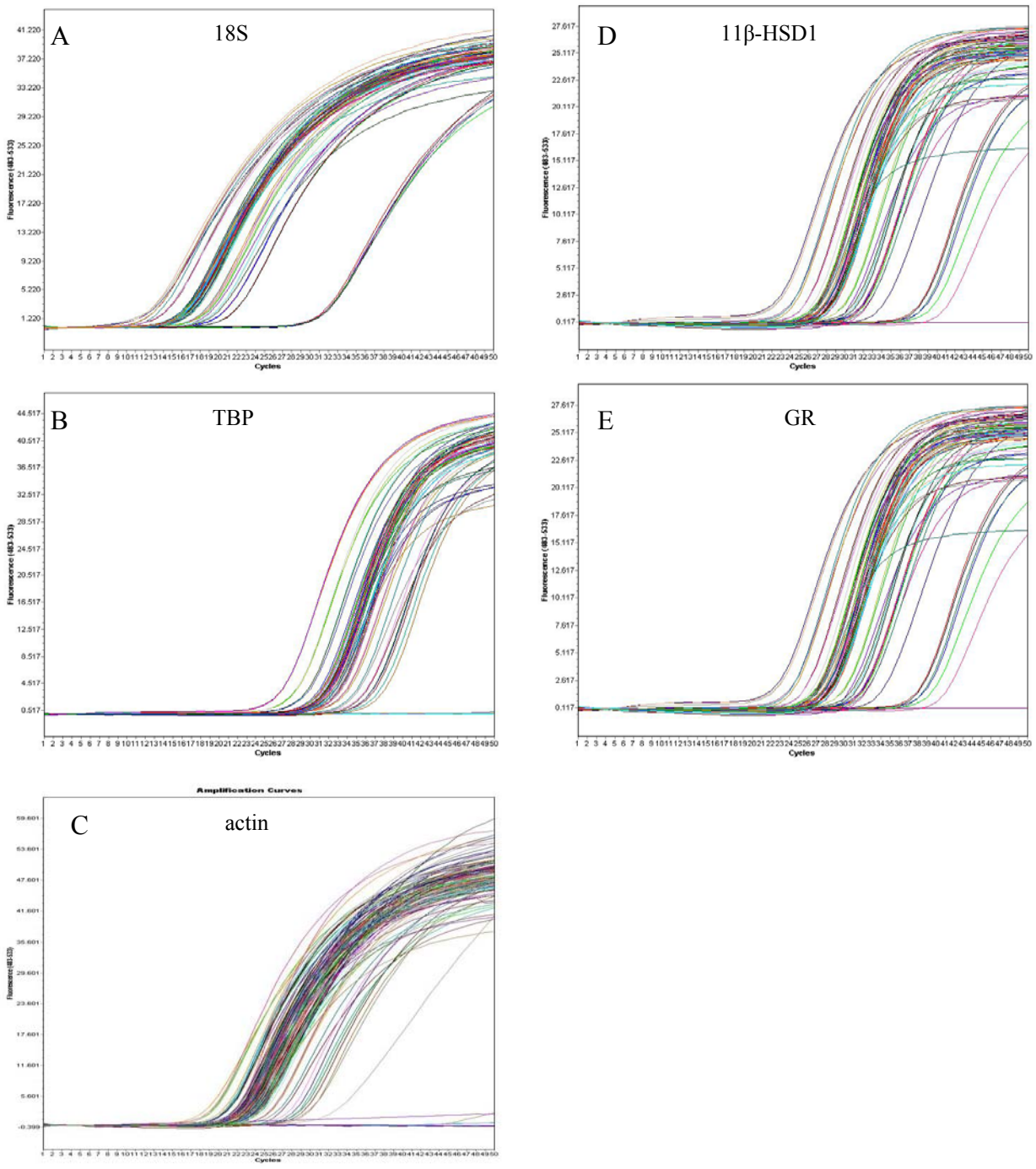

Figure 2.2 Amplification curves for internal controls and genes of interest. Representative amplification curves with x axis showing cycles of amplification and y-axis showing fluorescence level of (A) 18S, (B) TBP, (C) beta-actin (D) 11β-HSD1 and (E) GR. cDNA samples were form mouse epididymal fat.

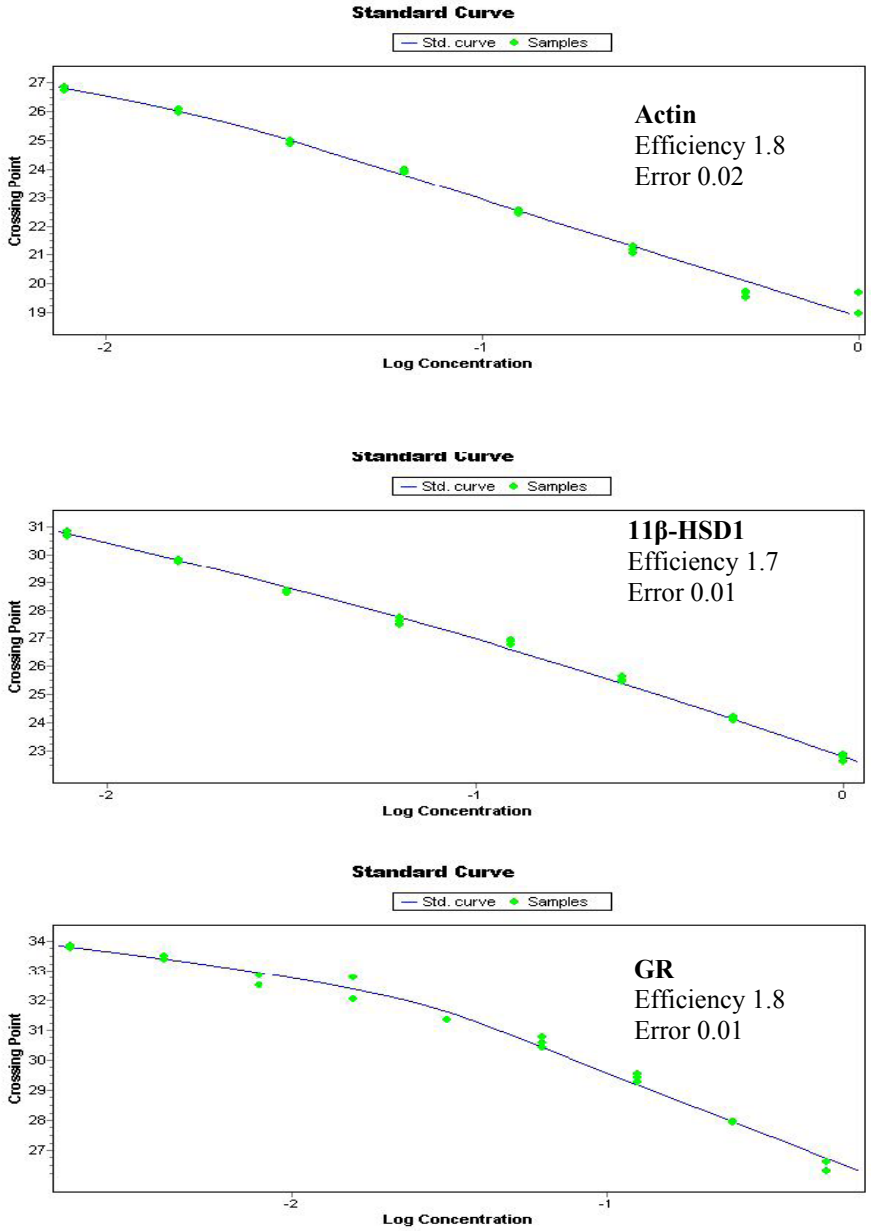

Figure 2.3 Standard curves.

Representative standard curves (SC) for actin, 11β-HSD1 and GR in mouse epididymal fat. SC constructed by serial dilutions (neat, 1:2, 1:4, 1:8, 1:16, 1:32, 1:64, 1:168, 1:336). cDNA samples (lime dots) were diluted 1:20.

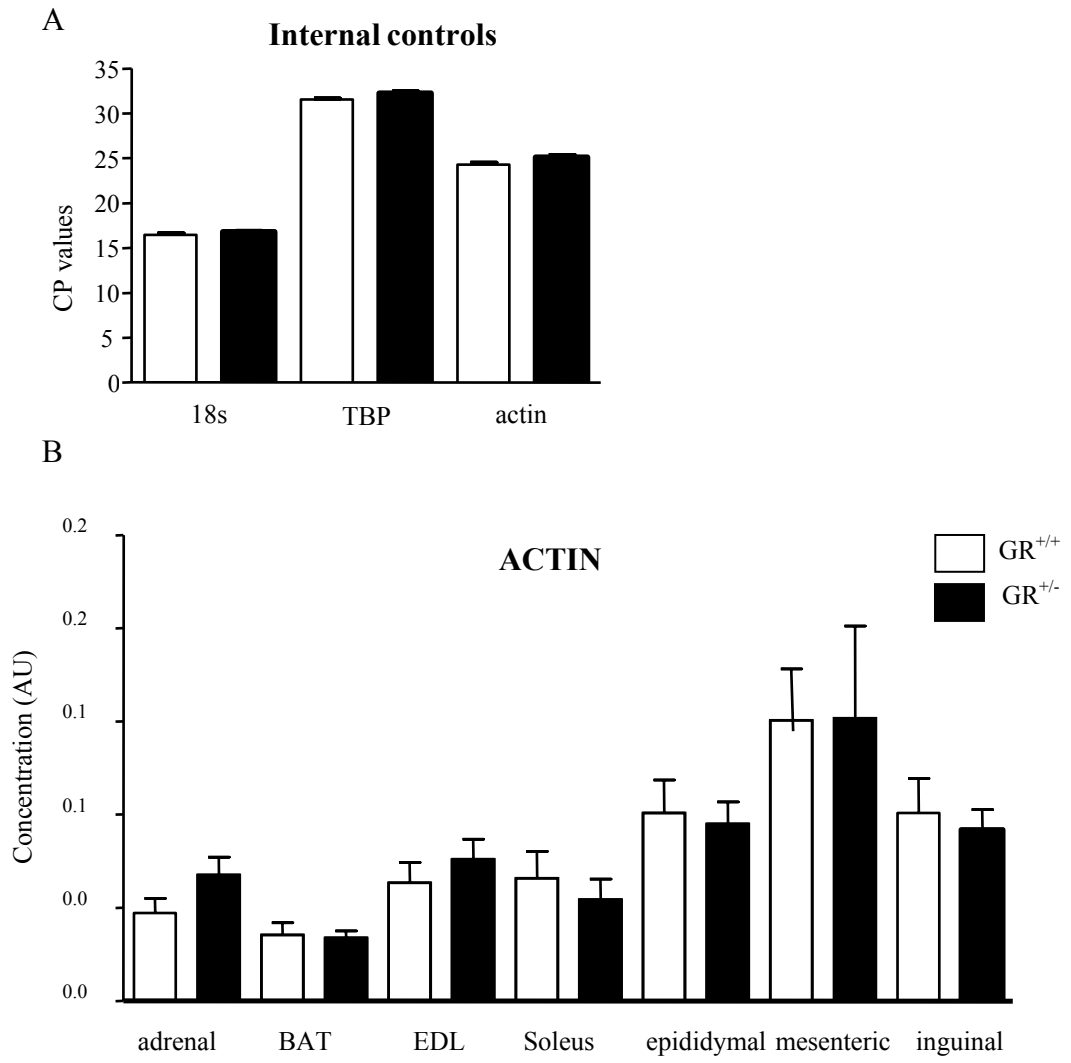

Figure 2.4 Validation of Real time PCR internal controls.

(A) Mean Crossing point (CP) values for internal controls. Actin and TBP appear to be better internal controls since they had a cycle-amplification profile in the same range as GR and 11βHSD1 (section 2.2.1.1.4.3), but the former was selected for all the experiments described in this Thesis. (B) mean concentration of actin in every tissue measured is similar between genotypes and therefore appropriate internal to correct for RNA concentrations between samples.

2.2.1.1.5 In situ mRNA hybridization

In situ GR mRNA hybridization was performed by E. Owen according to a standard protocol used in the lab (Seckl et al., 1990). Briefly, coronal brain sections (10µm) were fixed in 4% paraformaldehyde in 0.1M phosphate buffer and washed in 3x with 2xSSC containing 0.02% diethylpyrocarbonate. Hybridization was carried out in buffer containing 50% deionized formamide, 600mM NaCl, 10mM Tris (pH 7.5), 1mM EDTA, 0.02% Ficoll, 0.02% polyvinylpyrrodine, 0.1% bovine serum albumin, 100µg/ml denatured sonicated salmon sperm DNA, 50µg/ml yeast tRNA, and 10% dextran sulphate. The GR probe was transcribed in vitro from a plasmid encoding a 674bp Pst 1-Eco R1 fragment of rat GR cDNA (ligand binding domain) (Seckl et al., 1990). For sense RNA, the plasmid was linearized with Ava I and cRNA was transcribed with T7 RNA polymerase, in a 10µl reaction containing 1µg linearized plasmid and 25µM [^{35}S]-UTP. Probe (4x 10^6 cpm) was denatured (90^{o}C), added to hybridisation buffer, cooled at 55 ^{o}C prior to adding 10mM dithiothreitol and 200µl of mix was added per slide. Hybridization was performed o/n at 55^{o}C in sealed humidified boxes. The following day, slides were washed in 2x SSC, then treated with RNase A (20µg/ml) for 45min at 37 ^{o}C. Slides were then washed in 2x SSC to a final stringency of 0.1x SSC at 60 ^{o}C. Radiolabelled sections were exposed to a film for ~2weeks. For densitometry, autoradiographs were viewed on a lightbox fitted and imaged using a coolsnap photometrics camera, then analysed using MCID software (Imaging Research Inc.). Control sense RNA was prepared from the same GR plasmid used for the antisense RNA (Seckl et al., 1990). The plasmid was linearized with EcoRI and cRNA was transcribed with SP2 RNA polymerase.

2.2.1.1.6 5'-Rapid amplification of cDNA ends (5'-RACE)

5'-RACE was carried out essentially as previously described (Tate *et al*., 1998 and Sutherland *et al*., 2001). Table 2.2 details the sequences of primers used in 5' RACE. Figure 2.5 illustrates the location of the primers used in the 5'-RACE protocol. Briefly, for reverse transcription, 10 ng P456 primer (specific for *LacZ)* was annealed to 5 µg total RNA, from ESKN92 cells, in a 12µl volume at 70°C . Reverse transcription was carried out in a final volume of 20µl by the addition of 10 mM DTT, 10 mM dNTPs and 200 U of Superscript II reverse transcriptase (Invitrogen) at 37°C for 1 h 0.1 M NaOH was added to hydrolyse the RNA, and reactions incubated at 65°C for 20 min, before neutralising with 0.1 M HCl. DNA was microdialysed for 4 h on 0.025 µm nitrocellulose discs against TE to remove dNTPs and salt. Following dialysis the volume was adjusted to 20 µl with dH_2O. To add a poly A tail, first strand cDNA (20µl) was incubated with 2 mM dATP and 30 U of recombinant terminal deoxynucleotidyl transferase (TdT) (Invitrogen) at 37°C for 10 min. TdT catalyses the template-independent addition of dNTPs to the 3' hydroxyl terminus of single stranded (ss) DNA. 10ng of primer 56 (containing Ts at 3' complementary to the added polyA) was added to 15µl tailed DNA to synthesise the second strand cDNA. Two rounds of PCR reaction (summarized in Table 2.3) with nested *LacZ* primers (59, 80, and 79) followed by microdialysis steps on 0.1 µm nitrocellulose disks to size select larger PCR products, were used to amplify the specific 5'RACE product. These RACE products were directly sequenced (15µl RACE product & 4µl Big Dye) with a –40 *LacZ* sequencing primer (100ng) (ABISEQ, sequencing performed by MRC Human Genetic Unit sequencing service).

The sequence of the 5'-RACE product was compared with other sequences in Ensembl database using the BLAST algorithm. To assess the protein sequence for the GR-trapped gene, the SMART (Simple Modular Architecture Research Tool) was used.

Table 2.2 Primers used in 5'RACE

PRIMERS	**SEQUENCE 5'-3'**
P456	CCGTGCATCTGCCAGTTTGAGGGGA
56	GGTTGTGAGCTCTTCTAGATGGT
80	AGTATCGGCCTCAGGAAGATCG
59	GGTTGTGAGCTCTTCTAGATGG
79	ATTCAGGCTGCGCAACTGTTGG
-40 *LacZ* sequencing primer	GTTTTCCCAGTCACGAC

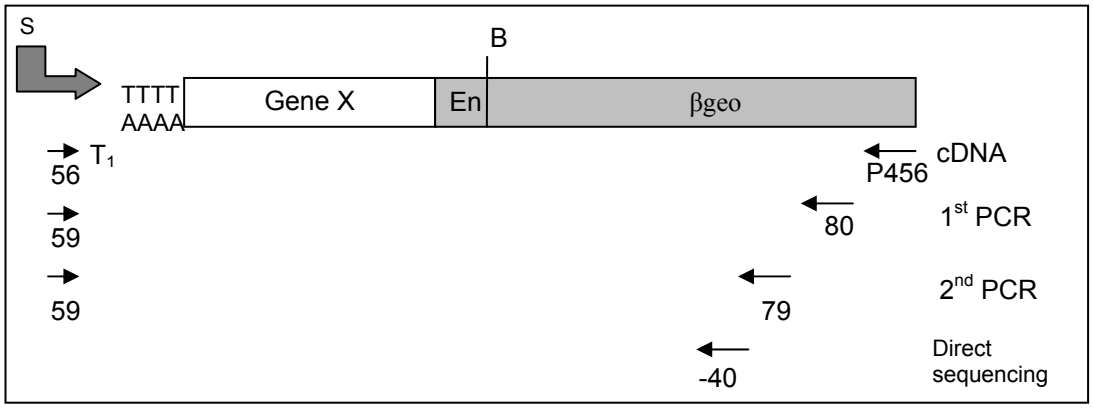

Figure 2.5 Primers used to identify the sequence of trapped genes by 5'RACE (adapted from Sutherland et al, 2001)

Table 2.3 Nested PCR for 5'RACE

PCR MIX	PCR PROGRAMME
1st round PCR: 37µl cDNA, 5µl 10xbuffer, 4µl 25mM MgCl2, 1µl 10mM dNTPs, 100ng primer 59, 100ng primer 80, 0.5µl ampliTaq. dH2O to final vol 50 µl	94°C, 5min Cycles 30x ([94 °C, 90s], [60 °C, 90s], [72 °C, 3min])
2nd round PCR: 5 µl 1st PCR reaction, 5 µl 10xPCR buffer, 4µl 25mM MgCl2, 1µl 10mM dNTPs, 100ng primer 59, 100ng primer 79, 0.5µl. dH2O to final vol 50 µl	94°C, 5min Cycles 30x ([94 °C, 90s], [60 °C, 90s], [72 °C, 3min])

2.2.1.2 DNA methods

2.2.1.2.1 Mouse genomic DNA extraction

DNA was extracted using a commercial kit (DNeasy tissue extraction, Qiagen) according to the manufacturer's instructions. Briefly, tissue samples (mouse ear biopsy) were incubated o/n at 55°C in lysis buffer with proteinase K (0.3mg/ml) (both provided in the kit). Genomic DNA was eluted in an appropriate volume of elution buffer provided (100µl per ear biopsy). DNA was stored at -20 °C for further analysis.

2.2.1.2.2 Genotyping of GR transgenic animals by PCR

PCR primers for LacZ genotyping were designed by Heidi Sutherland (MRC Human Genetics Unit, Edinburgh) and were 20 nucleotides in length with similar [G+C]:[A+T] ratios (H. Sutherland, personal communication). All genotyping PCR reactions were performed in 0.5 ml micro-centrifuge tubes in a volume of 25 µl. Reactions contained 1µl genomic DNA prepared from ear biopsy, 1U AmpliTaq® DNA polymerase (Applied Biosystems), 2.5µl 10x PCR buffer (supplied with the enzyme), 1.6µl of 2.5 mM MgCl2 (supplied with the enzyme), 2µl of 2.5mM dNTPs and 1µl of 25ng/µl each primer. The primer sequences and the respective amplification programme used in genotyping PCR is presented in Table 2.4. β-globin was used as an internal control (primers sequences in Table 2.4). For the genotyping of GR-/- mice, GR primers were designed (details in Table 2.4) that amplified a 470bp product in wild type and heterozygous mice but not in the homozygous (discussed in section 4.2.2.1).

2.2.1.2.3 Agarose gel electrophoresis

2% (w/v) horizontal agarose gels in ½ xTBE (section 2.1.7) electrophoresis buffer were used to resolve cDNA PCR samples. Ethidium bromide (EtBr) was added to the molten agarose to a final concentration of 0.5 µg/ml to allow visualisation of the DNA under ultraviolet light (UV). 5µl loading buffer per sample (section 2.1.7) was added to each DNA sample before loading. 1kb of the DNA size markers (section 2.1.7) were loaded into a well on each gel to enable the sizing and quantification of DNA fragments. Stained DNA was visualized on a UV transilluminator at 260nm and imaged using UviPro 12.4 software.

Table 2.4 The primers and amplification programme for genotyping PCR

PRIMER	SEQUENCE 5'-3'	AMPLIFICATION PROGRAMME
LacZ F	GTTGCGCAGCCTGAATGGCG	1x (92[3min]) 32x (92[30sec]60[45sec]72[45sec]) 1x (72[5min])
LacZ R	GCCGTCACTCCAACGCAGCA	
GR primers for GR$^{-/-}$ genotyping		
GR F	TGTTCCAACTGGTGAACTGACTG	
GR R	TGTTACCAACTTCTAGCCACTGG	
β-globin primers		
Globin F	CCAATCTGCTCACACAGGATAGAGAGGGCAGG	
Globin R	CCTTGAGGCTGTCCAAGTGATTCAGGCCATCG	

2.2.1.2. Transfections

All the plasmids used in the transfections assays (chapter 3) were generated by Val Lyons. Details of plasmids encoding the wild type GR and the GR-βgeo are provided in Appendix A with details of their construction. Transfections were performed as previously described (Bruley et al., 2006).

2.2.1.3 Protein methods

2.2.1.3.1 Total protein extracts from mammalian cells or tissues

ESKN92 cells were grown in T25 flasks. Cells were washed once with PBS, lysed by the addition of 600 µl of cell lysis buffer and harvested by scraping from the surface

of the flasks. Total protein samples were filtered and stored at -20°C until required For epididymal fat tissue protein extraction, tissue samples were weighed and 50mg of tissue was homogenized in 600µl of protein extraction buffer. The homogenate was then centrifuged at 4krpm for 10 min at 4°C to remove any debris. The supernatant was then removed and 50µl aliquots frozen at -20°C for future use and protein quantification.

Total protein concentration was measured by a Bio Rad protein assay. This is a colorimetric assay for protein determination. Sample concentrations were determined from a standard curve created from a series of Bovine serum albumin (BSA) dilutions, ranging from 0-1.2mg/ml. All samples were diluted according to the test assay and done in duplicated in 96 wells plates. 5µl of diluted samples and standards were added to each wells. 50µl of reagent A and 200µl of reagent B were added to each well. The plate was then incubated at room temperature for 15min before reading at a spectrometer at 750nm (Molecular device, OPTImax). The protein concentration was then determined off the standard cure. Typically, lysates contained 1.5-3.0mg/ml protein.

2.2.1.3.2 Resolution of proteins by SDS-PAGE and western blotting

Proteins from ESKN92 (20-40µg total cell protein extracts) and 25µg of protein from epididymal fat tissue was adjusted to 6.5µl using ultra pure H_2O and added to 6µl of a pre-prepared mix of 5µl NuPAGE® LDS sample buffer (Invitrogen) and 1µl of NuPAGE® Reducing agent (Invitrogen). Samples and 10µl of Plus2® pre-stained

protein standard (Invitrogen) were incubated at 70 ºC for 10 min to denature the protein. Samples were loaded onto a 4-12% (for ESKN92, 5-8% resolving and 4% stacking gels were used) Bris-Tris Novex® pre-cast Gel (Invitrogen) which locked to the buffer core in a vertical electrophoresis tank. The inner chamber filled with 200ml of 1x Novex® MOPs running buffer (Invitrogen) and 500µl of NuPAGE® antioxidant (Invitrogen) and the outer chamber filled with 600ml of 1x Novex® MOPs running buffer. Samples were electrophoresed at 200V until the Bromophenol blue band had migrated to the bottom of the gel. Gel was then removed form plastic cassettes and proteins transferred from the gel to a nitrocellulose membrane using a wet transfer system. Transfer was effected at 30V for 90min. Following transfer, the membrane was rinsed in ultra pure H_2O and left dry on Whatman No.3 filter paper.

To reduce non-specific antibody binding, the membrane was rehydrated with 1xTBS for 5 min, then incubated with blocking solution (1xTBS, 5% Blocking grade blocker (Bio-rad), 0.1% Tween) for 1h at RT or overnight at 4°C with agitation. The blocking solution was then removed and the membrane was incubated with primary antibody diluted (Table 2.5) into blocking buffer for 2h at room temperature with agitation. Next, the membrane was rinsed in blocking solution three times, each for 10 min then incubated with agitation for 2h at room temperature with secondary antibody (Table 2.5) diluted into blocker buffer. Finally, the membrane was rinsed in 1x TBS for 15 min, followed by three washes in 1x TBS each for 5min. Protein bands were visualized by incubating the membrane in 1ml of ECL detection mix (reagent1:2 50:50; ECL kit- Amersham Biosciences UK) for 1 min before exposing against autoradiographic film for 5min and then developing. Autoradipgraphs were

scanned using scanner and quantitated using Aida software (Advance image data analyzer Version 3.44.035). In ESKN92, positive/negative control, depending on the antibody used (GR/βgal, respectively) rat liver protein extract was also examined.

Table 2.5 Primary and secondary antibodies used in Western Blots

ANTIBODY	SPECIES	DILUTION	SOURCE
Primary:			
Anti-GR (M-20)	Rabbit polyclonal	1:400	Santa Cruz Biotechnology, UK
Anti-βgalactosodase	Rabbit polyclonal	1:2000	Europa Bioproducts
Secondary: ECL Anti-rabbit IgG	donkey	1:1000	Amersham Biosciences, UK

2.2.2 Embryonic Stem Cell Culture

2.2.2.1 Maintenance of cell lines

ESKN92 and E14 (parental WT) ES cells were frozen in 10% DMSO/90%FCS, and stored in cryotubes in liquid N_2. To retrieve cell lines from liquid N_2, cells were rapidly thawed and centrifuged in culture medium to remove the DMSO. Then cells were seeded into T25 cm^2 culture flasks coated with 0.1% gelatin (Sigma, G-1890), prepared by firstly layering a solution of 0.1% gelatin in PBS over the bottom of the flask and aspirating off before adding cells and media.

All cells were incubated at 37°C in 5% CO_2 and tissue culture medium as described in Table 2.6. ES cells were grown in Glasgow Modified Eagle Medium (GMEM, Invitrogen™) with supplements (Table 2.6) as described (Smith *et al*. in 1988). Cells were grown to near confluence before splitting into fresh tissue culture flasks coated in gelatin if required. To split the cells, medium was poured off, flasks were rinsed

with PBS and monolayers were then covered with 1.5 ml of trypsin-EDTA and incubated at 37°C for 5 min. Gentle agitation dislodged the cells, fresh medium was added, and the cells pelleted at 1000 *g* for 5 min before being replated or harvested for experiments.

Cells were counted before seeded at the relevant density onto microscope slides for immunofluorescence (ES cells, 10^6 cells per slide). Slides were prepared by soaking in 100% ethanol before being left to dry in QuadriPerm slide chambers (2.1.5) inside a laminar flow cabinet. The slides were coated with gelatin for growth of ES cells.

Table 2.6 Sources and maintainance of ES cells

ES CELL LINES	**DESCRIPTION**	**PASSAGE**	**MEDIUM**	**SOURCE**
E14	wt mouse ES cell, (129/Ola).	1:5 every other day	GMEM, 10% FCS (v/v), 100 U/ml LIF (prepared in house, MRC HGU, Edinburgh, pers. com.), 2 mM glutamine, 50 μM β-ME, 100 mM sodium pyruvate (Sigma), 1% NEAA (non-essential amino acids) (v/v) (Sigma)	Gifts from Heidi Sutherland (MRC, HGU Edinburgh)
ESKN92	Gene trap insertion in GR (129/ Ola)	1:5 every other day		

2.2.2.2 In vitro differentiation of ES cells (Strickland and Mahdavi, 1978)

Cells were passaged as described (section 2.2.2.1), seeded (10^4 cells/cm^2) onto gelatin-coated flasks and were grown overnight in normal media. The next day, cells were rinsed with PBS and the media changed to LIF free medium supplemented with 5x 10^{-6} M retinoic acid (all-trans-retinoic acid, stock solution 3.3x 10^{-3} M in DMSO, stored in the dark at -20°C). The retinoic acid containing medium was renewed every 24h for a period of four to six days following induction.

2.2.2.3 Fluorescence *in situ* hybridization (FISH) of ESKN92 cells

2.2.2.3.1 Cell fixation in 3:1 methanol: acetic acid

Cells for two-dimensional (2-D) fluorescence in situ hybridisation (FISH) were prepared as follows: cells were harvested and resuspended in 10ml hypotonic solution (0.033 M KCl, 0.017M tri-sodium citrate), which was added drop-wise with constant agitation (the concentration of cells should be <2x 10^7/ml). The cells were left to swell for 10min at RT before centrifugation at 400g for 5min. Cells were then fixed in fresh 3:1 methanol:glacial acetic acid (MAA), again added drop-wise with constant agitation before incubating on ice for 20min. After centrifugation, the cells were resuspended in 8ml of MAA and the cells placed at 4°C o/n. Cells were fixed twice more and stored indefinitely at -20°C.

2.2.2.3.2 Preparation of FISH probes

2.2.2.3.2.1 Nick translation

DNA was labelled using biotin-16-dUTP or digoxigenin-11-dUTP incorporation by nick translation. 1-1.5µg of DNA was added to 4µl 10x nick translation salts (0.5M Tris-HCl [pH7.5], 0.1M MgS04, 1mM DTT, 500µg/ml BSA), 4µl each of 2mM dATP, dGTP and dCTP, 2µl of 0.5mM dTTP and 4µl biotin-16-dUTP or digoxigenin-11-dUTP (Roche). DNase I was added to a final concentration of 1U/ml along with 1µl of T4 DNA polymerase I (Invitrogen™, 10 U/µl). The total volume was made up to 40µl with dH20 and mixed thoroughly before being incubated at 16°C for 90min. The reaction was terminated by placing at -20°C or immediately processed for the removal of unincorporated label. Quick Spin columns (Roche) containing G-50 Sephadex beads were used in accordance with the manufacturer's instructions to remove any free biotin-16-dUTP, digoxigenin-11-dUTP or dNTPs remaining in the solution. Cleaned probes were eluted in 40µl TE (pH 8).

2.2.2.3.2.2 Quantification of label incorporation

Gridded nitrocellulose membranes were prepared by brief soaking in dH20 followed by 20x SSC for 10min. Labelled DNA probes were diluted to 1x10-3 and 1x10-4 in TE and 1 and 2µl of each were spotted onto the gridded membrane. On the same membrane 20, 10, 2 and 1 pg of labelled lambda DNA standards (Roche) were also spotted. DNA was cross-linked onto the membrane by exposure to 30mJ of UV irradiation. The membrane was immersed in buffer 1 (0.1M Tris-HCl [pH7.5], 0.15M NaCl) for 5min at RT, then blocked in 5% Marvel (w/v) in buffer 1 at 37°C for 30min. 10µl streptavidin-alkaline phosphatase (Boehringer) and/or anti-digoxigenin-alkaline phosphatase (Boehringer) were added to 10ml of buffer 1 and placed in a sealed polythene bag with the membrane for 30min at RT. The

membrane was washed twice in buffer 1 then equilibrated for 5min in 0.1M Tris-HCl (pH 9.5). The colour reaction was developed by incubation of the membrane in a sealed polythene bag, with 5ml of 0.1M Tris-HCl (pH 9.5) and two drops from bottles 1-3 from the alkaline phosphatase substrate kit IV (Vector). The substrates in this colour reaction are 5-bromo-4-chloro-3-indolyl phosphate and nitroblue tetrazolium, which produce a blue reaction product. A complete colour reaction was observed within a few hours of incubation at RT in the dark and an estimate of the concentration of DNA labelled probe was made by comparison with known lambda standards.

2.2.2.3.2.3 The FISH protocol

2.2.2.3.2.3.1 Slide preparation

Glass slides were stored in a dilute solution of HCl in ethanol and were dried and polished with muslin before use. MAA fixed cells (section 2.2.2.3.1) were removed from storage at -20°C and centrifuged at 400g for 5min. Fresh MAA fix was added until the cell suspension reached a 'milky' appearance. One drop of suspension from a fine tipped pastette was dropped onto a horizontal microscope slide from a 30cm height (the best chromosomal spreads were achieved when the air humidity was ~50% and by breathing on the slides initially). Slides were stored for 2-6 days prior to hybridisation.

2.2.2.3.2.3.2 Hybridisation and detection of FISH signal

Slides were treated with 100µg/ml RNaseA in 2x SSC for 1h at 37°C, washed briefly in 2x SSC and dehydrated through an ethanol series (2min each in 70%, 90% and

100% ethanol). Slides were dried under a vacuum for 10min before being heated in a 70°C oven for 5min and immediately denatured in 70% formamide (v/v) in 2x SSC (pH 7.8) at 70°C for 1-2min. Slides were plunged in 70% ethanol at 4°C for 2min before dehydration through 90% and 100% ethanol.

Labelled probes (section 2.2.2.3.2) were prepared by precipitation of ~75 ng probe with 5µg salmon sperm DNA and mouse Cot 1 DNA (Invitrogen™, 2.5-10µg depending on repeat content of probe). After the addition of 2x vol of ethanol, probes were centrifuged under a vacuum before resuspension in 10µl hybridisation mix (50% deionised formamide [v/v], 10% dextran sulphate [v/v], 1% Tween 20 [v/v], in 2x SSC) or 13µl of commercial mouse chromosome paints supplied in hybridisation buffer (Cambio). All probes were denatured at 70°C for 5min and reannealed at 37°C for 15min before being spotted onto coverslips and picked up by the slides. Slides were sealed with rubber solution (TipTop) before incubation o/n in a covered tray in a 37°C water bath.

Rubber solution was removed from the slides and they were immersed in 2x SSC at 45°C for 4 x 3min. The coverslips fall off naturally. Slides were washed a further 4 x 3min in 0.1x SSC at 60°C before transfer to 0.1% Tween 20 [v/v] in 4x SSC. Detection was carried out in a moist chamber pre-heated to 37°C. Biotin was detected with sequential layers of fluorochrome-conjugated avidin (FITC- or TxR-avidin), biotinylated anti-avidin, and a further layer of fluorochrome-conjugated avidin. Digoxigenin was detected with sequential layers of Rhodamine (R)-conjugated anti-digoxigenin and TxR-conjugated anti-sheep IgG. Detection reagents

were diluted in SSCM (4x SSC, 5% Marvel milk powder [w/v]) to the appropriate concentration (Table 2.7). After blocking with 40µl of SSCM for 5min at RT, 40µl of the appropriate detection layer was applied to each slide. Slides were incubated in the same way at 37°C for 60min followed by 3 x 2min washes of 0.1% Tween 20 [v/v] in 4x SSC at 37°C. All slides were mounted in 0.5 µg/ml of DAPI in Vectashield. Coverslips were sealed with rubber solution (PANG) and slides were stored in the dark at 4°C until imaged.

The probe to detect pGT-3 DNA (the gene trap vector; Sutherland et al., 2001; details in Appendix, fig. A4) was labelled with digoxygenin-11-dUTP (DIG) and the probe to detect GR DNA (a 6 kb genomic clone located at the 5' end of the gene, gift from H. Reichardt; details in Appendix, fig. A.5) was labelled with biotin-16-dUTP. A mouse chromosome 18 paint, pre-labelled with biotin-16-dUTP was also used to distinguish chromosome 18 from the rest of the chromosomes. DIG was detected with Rhodamine-conjugated anti-digoxigenin primary antibody followed by Texas Red-conjugated anti-sheep IgG. Biotin was detected with fluorochrome-conjugated avidin (FITC), biotylated anti-avidin antibody followed by a further layer of fluorochrome-conjugated avidin.

2.2.2.4 Immunofluorescence on fixed cells

Mammalian cells were grown on slides as described (section 2.2.2.1). For the dexamethasone (DEX) experiments, ESKN92 or WT (ES14; parental ES cell line) cells were maintained in glucocorticoid-free (FCS treated with charcoal to remove GC) medium for 24h. The next day the cells were treated for 10min with 1µM DEX,

a synthetic glucocorticoid, and then immediately fixed and immunostained. All subsequent incubations were performed at RT. Slides were rinsed in PBS containing 1.5mM $MgCl_2$ and 1mM $CaCl_2$ and fixed for either 10 or 20min in 4% or 3% paraformaldehyde (pFa) (w/v) in PBS respectively. All steps were performed with PBS containing Mg^{2+} and Ca^{2+}.

Table 2.7 FISH antibodies and fluorochrome-conjugates

ANTIBODY OR FLUOROCHROME-CONJUGATE	SPECIES	SOURCE	STOCK (MG/ML)	DILUTION
FITC-avidin	Goat	Vector	2.0	1:500
TR-avidin	Goat	Vector	2.0	1:500
Biotinylated anti-avidin	Goat	Vector	0.5	1:100
R-anti- digoxigenin	Sheep	Roche	0.2	1:20
TR-anti-sheep (IgG, H&L)	Rabbit	Vector	0.5	1:100

After a further 3 washes in PBS, the slides were quenched in 50mM NH_4Cl in PBS for 10min and permeabilised for 12min in 0.1% Triton X-100 (v/v) in PBS. Slides were washed a further 3 times in PBS before blocking in 5% donkey serum (v/v) in PBS for 20 min. Slides were then incubated o/n in moistened chambers with primary antibody (diluted in 5% block) under a parafilm coverslip (Table 2.8). After washing, slides were incubated in secondary antibody (Table 2.8) diluted in the same way but with incubation for 1h. All secondary antibodies were species-specific fluorescein isothiocyanate (FITC) or Texas Red (TR) conjugates obtained from the

Jackson Laboratories or Vector Lab. Secondary antibody was washed as above and all slides were mounted with 0.5 μg/ml 4,6-diamidino-2-phenylindole (DAPI) in Vectashield (Vector). Coverslips were sealed with rubber solution (PANG) and slides were stored in the dark at 4°C until imaged (section 2.2.2.5).

Table 2.8 Primary and secondary antibodies used in immunofluorescence

ANTIBODY	SPECIES	SOURCE	DILUTION FACTOR
Primary:			
Anti-β-gal	Rabbit polyclonal	Europa	1:2000
Anti-GR (M20)	Rabbit polyclonal	Santa Cruz	1:50
Secondary:			
Anti-rabbit FITC conjugate (IgG, heavy & light chain specific [H&L])	Donkey	Jackson Labs, 711-095-152	1:75

2.2.2.5 Fluorescence imaging of cells or nuclei

2-D FISH slides or immunofluorescence experiments were examined using a Zeiss Axioplan fluorescence microscope (MRC HGU microscope facility, Edinburgh) both with 100 watt mercury bulb, and equipped with a triple band-pass filter (Chroma # 83000). Images were collected with a cooled CCD camera depending on the model of microscope (Pentamax with a Kodak KAF 1400 sensor or Micromax with Kodak KAF 1400e sensor respectively, Princeton Instruments) using IPLAB software v. 3.6 (Scanlytics, USA).

2.2.3. Animals

2.2.3.1 Pomc-null mice

Pomc-null tissues were provided by Dr Tony Coll (University of Cambridge). The animals were generated on a 129/SvEv background and maintained as described (Challis et al., 2004; Coll et al, 2005). Eight week-old male mice (n=5/group) were treated with corticosterone (25μg/ml) in their drinking water, a dose that results in similar plasma glucocorticoid levels and hypothalamic CRH mRNA levels in *Pomc*$^{-/-}$ and wild type mice (Coll et al. 2005). All animal protocols used in these studies were approved under the auspices of the UK Home Office Animals (Scientific Procedures) Act, 1986. Animals were killed between 8:00 and 9:00am by cervical dislocation. Trunk blood samples were collected into EDTA coated tubes (Sarstedt, Germany), centrifuged (6000g x 10min) and plasma stored at -80 C until required for assay.

2.2.3.2 B6N92 mouse line generation

Blastocyst injection of embryonic stem cells (ESKN92) and generation of chimeric mice was carried by the transgenic service (BRR, Phase I, Edinburgh University). Genomic DNA form chimeric mice was tested for the presence of the pGT1-3 transgene by PCR amplification using primers that amplify a 413 bp fragment within the *LacZ* gene (section 2.2.1.2.2). Chimeras were mated to C57BL/6 female mice to achieve germ line transmission, and further backcrossed to C57BL/6 to generate an inbred colony. The conony was maintained as heterozygous (GR$^{+/-}$) by backcrossing to C57BL/6. To generate GR$^{-/-}$, F3 or F7 GR$^{+/-}$mice were intercrossed.

2.2.3.3 Housing and diets

Animals were housed in standard cages with controlled lighting (12h light: 12h dark, lights on at 7am), and were fed standard chow from weaning. For unstressed plasma corticosterone, ACTH and glucose sampling experiments, animals were acclimated to single housing and tail nicks performed within 1min of disturbing the cage. For diet induced obesity (DIO) experiments mice were weaned on either high fat diet (58% kcal as fat, D12331; Research Diets, New Brunswick, NJ) or a low fat diet (11% kcal as fat, with corn startch, D12328; Research Diets). These diets are not isocaloric, the LF is 4.07kcal/g, the HF is 5.56kcal/g. Information on the exact composition of the diets can be found in http://www.researchdiets.com/. Mice remained on the diet for 22 weeks with *ad libitum* access to water and diet. Body weight was monitored weekly throughout the experiment and food intake was measured using singly housed mice for 3 weeks. Mice were culled by decapitation between 8-10 am. Tissues were rapidly frozen in dry ice for RNA or protein analysis or in formalin for histology.

2.2.3.4 Biochemistry

2.2.3.4.1 Hormone Assays

For morning corticosterone and ACTH measurements, animals were killed between 0800 and 0900h by decapitation. Trunk blood samples were collected into EDTA coated tubes (Sarstedt, Germany), centrifuged (6000g x 10min) and plasma stored at -80^{o}C until required for assay. Evening corticosterone was sampled between 19:00 and 20:00 pm.

2.2.3.4.1.1 Corticosterone (B) Assay

B levels were measured by an in-house radioimmunoassay, in which unlabelled sample B and [^{3}H]-B compete for anti-B antibody. The concentration of B in each sample was determined from the standard curve. However, this method is not a quantitative method for determining free plasma B levels, since B is dissociated from CBG in the assay procedure. It therefore measures total B concentration.

Plasma samples were diluted (1:10 for am cort and for the 120min after restraint time point, 1:20 for pm CORT and for the 20min after restraint stress time point) in borate buffer and heated at 65°C for 30min to denature CBG and allow dissociation of B. A series of B standards were prepared (0-320nM) to allow production of a standard curve. Samples and standards were incubated in duplicate in flexible 96-well plates with a mixture of [^{3}H]-B (10,000cpm added per sample) and B antibody (1 in 10,000 dilution of rabbit anti-rat B antiserum in borate buffer; kindly provided by Dr. Chris Kenyon) in borate buffer in a total volume of 70µl for 1h at 37°C. Anti-rabbit scintillation proximity assay beads were then added to each sample and the plates sealed and incubated overnight at 37°C. The beads bind to the primary antibody and, if the primary antibody is bound to [^{3}H]-B, the radioactive signal is detected by the beads in close proximity and the resulting scintillation signal detected by β-scintillation counter, and analysed using Multicalc software. The inter- and intra-assay coefficients of variation were <10%, and the detection limit was 0.15µg/dl.

2.2.3.4.1.2 ACTH Assay

ACTH was measured with an enzyme-linked immunosorbent (ELISA) commercial assay (Biomerica, Newport Beach, CA), according to the manufacture's instructions. Briefly, the assay measures the biologically active 39 amino acid chain of ACTH by a 2-site ELISA. The assay uses, a biotinylated goat polyclonal antibody to human ACTH (binds the C-terminal 34-39aa of ACTH) and a horseradish peroxidase-labelled mouse monoclonal antibody to human ACTH (binds the mid-region and N-terminal 1-24aa of ACTH) the latter used for detection. 200µl of plasma samples, calibrators (0, 5, 18, 55, 165 and 500pg/ml) and controls (33 and 150pg/ml) were incubated (for 4.5h at RT on an orbital shaker) with the enzyme labelled antibody and a biotin coupled antibody in a streptavidin-coated microplate well. At the end of incubation, the microwell was washed to remove unbound components and the enzyme bound to the solid phase was incubated with the tetramethylbenzidine (TMB) substrate for 30min at RT, in an orbital shaker. An acidic (sulfuric acid) solution (provided in the kit) was then added to stop the reaction and converts the colour to yellow. The intensity of the colour is directly proportional to the concentration of the ACTH in the sample. The absorbance at 450nm was read within 10min of adding the stop solution. A dose response curve of absorbance *vs* concentration was generated from the calibrators and the sample concentration was calculated by point-to-point interpolation. The sensitivity or minimum detection limit of this assay is 0.46pg/ml.

2.2.3.4.1.3 Renin and angiotensinogen assays

Renin and angiotensinogen assays were developed in house (by Dr Chris Kenyon), and involve radioimmunoassay of angiotensin I generated from renin + angiotensinogen. Plasma renin activity, plasma renin concentration and angiotensinogen concentration were measured.

For quantitative conversion of ***plasma angiotensinogen*** to angiotensin I, a small aliquot (1µl diluted plasma) of plasma is incubated with excess renin. Depending on the concentration of plasma angiotensinogen, which varies between mouse strains, plasma was diluted (1:5) with Tris buffer (section 2.1.7). The excess renin was either from mouse kidney or submaxillary glands and was prepared (by Dr Chris Kenyon) by homogenising tissues with 5vol of Tris and using the resultant supernatant after centrifugation (105,000g for 60min). The amount of renin added to the assay must be optimised. Addition of excess renin causes complete conversion of angiotensinogen to angiotensin I, even at 0˚C, whereas addition of too little renin causes the reaction to be incomplete. The optimised Ang I generating system for measuring angiotensinogen in these studies was 1µl dilute plasma + 9µl renin extract (a 100 fold dilution of cytosol from submaxillary glands). ***Plasma renin concentration*** measures the generation of angiotensin I when plasma is incubated with excess angiotensinogen. Plasma was diluted 5-fold with Tris buffer and incubated with plasma from a binephrectomised rat (BNX) which contains no renin but high angiotensinogen levels (prepared by Dr Chris Kenyon). The optimised Ang I generating system for measuring plasma renin concentration in these studies was 1µl dilute plasma + 9µl BNX. ***Plasma renin activity*** measures angiotensin I generated

from endogenous renin and endogenous angiotensinogen. The optimised angiotensin I generating system used in these studies was with 10µl undiluted plasma.

Briefly the assay protocol was as follows: In 10µl Ang I generating system or standards (400pg/10µl, double dilutions with Tris), 10µl Ang I antibody in RIA cups (x4 tubes) was added at 0°C. The samples/standards were then centrifugated at 2000rpm for 1min. 2 of 4 tubes were incubated at 0° and the other 2 tubes at 37 °C for 30min with shaking. Following, 150µl Tris (0°C) containing approx 4-5000cpm ^{125}I-Angiotensin I (section 2.1.3) was added and briefly agitated. All samples were incubated at 2°C for 18h. The next day, separation was carried by using 250µl of charcoal suspension (section 2.1.7), following samples were centrifugated at 3000 rpm for 15min, the supernatant was aspirated and the free charcoal pellet was counted.

2.2.3.4.2 Glucose and insulin tolerance tests

For glucose tolerance tests (GTT), animals were fasted for 6h and 2mg/g body weight D-glucose was injected (from a 25% D-glucose solution) intraperitoneally (ip). Blood sampling (a drop) was performed from a tail venesection at time 0 (prior to injection), 15, 30, 60 and 120min after injection. For insulin tolerance tests, fasted (6h) animals were injected ip with 1mU/g BW (females) or 1.5mU/g BW (males) human insulin (Humulin 100IU/ml, *Lilly*) and blood sampling was taken from a tail venesection at time 0, 15, 30 and 60min after injection. Plasma glucose was measured using a Glucose Monitoring System (One Touch Ultra, Lifescan, Johnson & Johnson) or a glucose assay in a 96 well plate as follows. Duplicates of 20µl of

plasma, or a series of dilutions from the stock glucose solution used to generate a glucose standard curve (0, 50, 100, 150, 200, 250, 300, 400 mg/dL, were incubated with 250µl of Thermo-infinity hexokinase reagent (Alpha Laboratories) for 5 min. The reagent causes the glucose present in the sample to be phosphorylated and NADH is generated, and consequently absorbance of the latter is measured at 340nm using a spectrophotometer. Sample concentrations (mg/dL) were extrapolated from the standard curve.

2.2.3.4.3 Lipid Assays and Hepatic Tissue Morphology

Hepatic triglycerides (TG) were extracted following homogenisation of 100mg of liver in isopropanol (10vol) and then incubation for 45min at 37^{o}C. Following centrifugation (3000g x 10 min), 10µl supernatant was incubated at 37^{o}C for 5min with 1ml Thermotrace triglyceride reagent (Alpha Laboratories, Hampshire, UK) and absorbance at 500nm was spectrophotometrically measured. A blank and a triglyceride calibrator or standard (2.5mmol/l) provided in the kit were also included in the assay. Sample triglycerides were calculated using the following formula: Liver TG=absorbance of the sample/absorbance of calibrator x2.5x10, where 2.5 is the concentration of calibrator and 10 the volume of isopropanol used.

Levels of non-esterified fatty acid (NEFA) and triglyceride levels were determined by commercial kits (NEFA, Roche Diagnostics, West Suffolk, UK; triglyceride, Dade Behring, Marburg, Germany).

Neutral lipids, cholesterol and fatty acids were identified by light microscopy at x 40 magnification in cryostat liver sections (30μm) stained with Oil red O (Sigma) and counter-stained with haematoxylin. Briefly, frozen liver sections were rinsed in H_2O, then 60% (v/v) isopropyl alcohol and stained for 10min with Oil Red O (section 2.1.7). Following, sections were washed briefly in 60% isopropyl alcohol and then washed well in H_2O. After washes, sections were stained with haematoxylin for 1min washed in 1%(v/v) ammonia for 30sec, briefly washed in H_2O and mounted.

2.2.3.5 Blood pressure measurements

In the Pomc-null experiment (chapter 6) blood pressure was measured by Dr Tony Coll (Cambridge). Systolic blood pressure was measured photoelectrically in the tail of restrained conscious mice using an IITC model 179 analyser (Woodland Hills, California, USA). In the $GR^{+/-}$ experiment (chapter 5) blood pressure was measured by Dr Elaine Marshall (Endocrinology Unit, Edinburgh) using IITC Non Invasive Blood Pressure measuring system (Harvard Apparatus, Edenbridge, Kent, UK. Prior to recording measurements, all mice underwent 3 periods of training to acclimate them to the procedure.

Non-invasive blood pressure (BP) measurements were determined by detection of return of tail pulsations (RTP) using tail cuff plethysmography, which can reliable detect systolic BP within <5mmHg in concordance with inter-arterial measuring systems. The computerised RTP-computerised model was calibrated for sensitivity (maximum inflation, rate of deflation) and programmed to measure four single

inflation/ deflation cycles per experimental recording (giving eight measurements). The tail cuff plethysmographam has an integrated sensor-cuff occluder inflation and detects the return of tail pulsations passing through the occluder cuff on each deflation cycle. This method has been validated by several methods, more recently by radiotelemetry (Pfeffer, 1971; Whitesall et al, 2004). Variability in testing was minimized by: 1) a conditioning period of 3-5 days where mice restrained without, and then eventually with, BP being measured with tail cuff inflation to familiarise the mice to the procedure prior to commencing treatment and BP is recorded at the approximate normal level for a C57BL6 mouse (by use of 20-30 consecutive inflation and deflation cycles if tail cuff balloon and using the average) 2) other measures to reduce alarm reaction of mice were the use of a quite room with dimmed lighting and measurements taken at the same time of each day, by the same person. Blood pressure was recorded as follows. After 5-10 minutes in a heated chamber (30-35^{o}C), mice were placed on the heated blood pressure platform and held in place with an opaque restraining chamber. The mean arterial blood pressure (mm Hg) and pulse rate (beats per minute) was recorded for each mouse. Data measurements were averaged and presented as mean arterial pressure (MAP).

2.2.3.6 Tissue morphology

Tissues were fixed in formalin and processed for histopathology. The left adrenal was sectioned (4μm) and stained with haematoxylin and eosin (H&E) by the histology service (QMRI, University of Edinburgh) for histopathological examination.

2.2.3.7 Tissue fixation and X-gal Staining

X-gal staining to detect β-galactosidase activity was carried out on frozen coronal brain sections and whole embryos. Embryos were washed twice at RT for 15 min in wash solution (0.05% BSA [w/v], 2mM $MgCl_2$, 0.02% NP40 (v/v), 0.1% sodium desoxycholate [w/v] in 0.1M phosphate buffer) before staining. Brain sections were transferred directly from -80ºC into fixative (4% paraformaldehyde, 0.02% NP40, 0.01% sodium deoxycholate, 5mM EGTA, 2mM $MgCl_2$) for 15min at 4ºC, washed twice in PBS containing 2mM $MgCl_2$, 0.02% NP40, 0.01% sodium deoxycholate and stained for 6h in PBS containing 2mM $MgCl_2$, 0.02% NP40, 0.01% sodium deoxycholate, 5mM potassium ferricyanide, 5mM potassium ferrocyanide, 1mg/ml X-gal, protected from light. Staining solution was removed and the samples stored in PBS until required. Embryos or brain sections were visualised with a conventional light microscope.

2.2.4 Human Study

2.2.4.1 Subjects

Informed, written consent was obtained from 21 women undergoing elective, laparascopic tubal ligation surgery; the study which was approved by the Mayo Clinic IRB. Tubal ligation surgery is done routinely in the follicular phase of the menstrual cycle to eliminate the risk of pregnancy. Prior to surgery, body composition was assessed by measuring weight, height, body fatness (% fat) using dual x-ray absorptiometry (DEXA; DPX-IQ; Lunar Radiation, Madison, WI) and abdomial fat distribution using a single sliced computerized tomography scan at the

L_{2-3} level as described (Jensen et al., 1995; Jensen et al., 1993). Visceral and subcutaneous adipose tissue areas were calculated as previously described (Jensen et al., 1993). All the data were kindly provided by Prof Michael Jensen (Mayo Clinic, Rochester, USA). Although 8 of 21 subjects were taking oral contraceptives (OC), there was no effect on the variables by t-test, therefore the data were pooled.

2.2.4.2 Biochemistry

Fasting plasma triglycerides, glucose and insulin levels were assayed as previously described (Jensen et al., 2003). HOMA-IR was calculated by the equation [fasting insulin (μU/ml) x fasting glucose (mmol/L)/22.5] (Matthews et al., 1985). All the data were kindly provided by Prof Michael Jensen (Mayo Clinic, Rochester, USA).

2.2.4.3 Adipose tissue Biopsies

Tissues were provided by Prof M. Jensen (Mayo Clinic). Subcutaneous fat from abdominal (n=13), thigh (n=16) and gluteal (n=18) regions were collected just prior to surgery and omental (n=21) adipose biopsies were obtained intra-operatively. Fat cell size (mean diameter of mature adipocytes in μm) was determined using the AdCount (Biomedical Imaging Resource, Mayo Clinic) approach as previously described (Tchoukalova et al., 2003) and data were provided by Prof Michael Jensen. For RNA, biopsies were washed to remove blood and then snap frozen in liquid nitrogen and stored at -80^{o}C. Biopsies were homogenized in 1-2mls Trizol®, RNA

was extracted, quantified and integrity verified as described in section 2.2.1.1. Real time PCR was performed and analysed as described in section 2.2.1.1.4.

2.2.5 Computational methods and Statistical analysis

The Bioinformatics programmes and resources, with their website addresses, used in this thesis are listed below.

Ensembl	http://www.ensembl.org/
NCBI (BLASTN/P, TBLASTN)	http://www.ncbi.nih.gov/BLAST/
NCBI (Entrez)	http://www.ncbi.nlm.nih.gov/Entrez/index.html
SMART	http://smart.embl-heidelberg.de/
NURSA	http://www.nursa.org
GraphPad	http://www.graphpad.com/quickcalcs/index.cfm

For the statistical analysis of the data obtained in this thesis, 2 main statistical software were used, Sigma Stat 3.1 and GraphPad Prism 4. Comparisons between 2 groups (heterozygous *vs* control mice), was done by Students t-test. For the effect of genotype x treatment (either CORT or diet), 2-way ANOVA followed by post-hoc Tukeys' tests for group differences. For GTT or ITT comparisons, the area under the curve (AUC) was calculated for every animal and then the means of groups compared with either Students t test (genotype comparisons) or 2-way ANOVA (genotype x diet). For the analysis of data obtained in the human study (chapter 7), repeated measures ANOVA followed by post hoc Tukey test were performed to determine differences in transcript levels in paired adipose compartments. Pearson

correlation was performed to examine the relationships between anthropometric and metabolic parameters with 11βHSD1 or GRα mRNA levels in different fat depots according to a priori hypotheses to minimize multiple interdependent. Multiple linear regression was performed to test if relationships between fat cell sizes or triglycerides with transcript levels are independent of obesity. In the transfection experiments, analysis was performed as follows. After subtraction of background levels (determined from Gem negative controls), reporter activity (firefly luciferase) was divided by the internal standard (renilla luciferase) to control for variation in transfection efficiency and cell number in each sample. Data from separate experiments were combined by arbitrarily setting the empty vector value in absence of dexamethasone (DEX) equal to 1 for the PNMT data. MMTV data set the value of wild type GR in the absence of DEX equal to 1 (as empty vector data were not available). Values are means± SEM of 9 individual transfections (from 3 experiments, each carried out in triplicate), and data analysed for statistical significance by one-way ANOVA. All data presented in this Thesis was tested for normality and were normalized by log transformation where appropriate. Significance was set at $p<0.05$. Values are means ± SEM. For full details of statistical analysis please refer to figure legends in each chapter. The details of the statistical methods used are presented in each experimental chapter, in the figure legends.

Chapter 3

Characterization of GR “Trapped” cells (ESKN92)

3.1 Introduction and Aims

3.1.1. What is gene trapping: advantages & limitations

The International Gene Trap Consortium provides a thorough overview/tutorials regarding gene trap technology (http://www.genetrap.org/tutorials/overview.html). Briefly, gene trapping is a method of randomly generating embryonic stem cells with insertional mutations by inserting a gene trap vector construct into an intronic or coding region of genomic DNA (Skarnes et al., 1992). The gene trap vector constructs contain selectable reporter tags (ie *lacZ*) that provide the advantage of easily identifing cell lines where the vector has successfully interrupted a gene. Additionally, if the tag expression mimics that of the endogenous gene, then monitoring the tag-fusion gene activity in cells, tissues or the whole organism (ie embryos) would enable easy visualization of the endogenous gene expression in an organ of interest in any developmental stage or during disease (Skarnes et al., 1992). Furthermore, gene traps seem to represent a more powrful insertional mutagenes (than other transgenes), since (a) the tag-endogenous gene fusion products may interfere with the normal coding capasity of the endogenous gene and generate a mutation (Skarnes et al., 1992) and (b) is less labor-intensive because cloning a portion of endogenous gene from the tag-fusion transcript limits the time-consuming process of searching for exons in flanking genomic DNA (Skarnes et al., 1992). Gene trap sequences are derived from cDNA or genomic DNA from the trapped locus using primer sequences from vector ends. These sequences are used to identify and annotate the trapped gene (Skarnes et al., 1992 and http://www.genetrap.org). Gene trap cell lines are used to produce mutant mouse strains that are useful "tools"

for the functional characterization of genes. Although the insertion of the vector construct in region of a gene typically results in complete inactivation of the "trapped" gene (a null allele), this is not always the case (http://www.genetrap.org). For example, there is a possibility that the vector insertion might lead to a hypomorphic gene function, or result in a dominant negative phenotype. Generally, if the vector is inserted close to the 5' end of a gene, but downstream of the untranslated region before the first exon, is more likely to create a null allele than insertion near the 3' end (http://www.genetrap.org).

Limitations that should be considered when using a gene trap mutagenesis approach are as follows: (a) the genomic region surrounding the vector insertion in embryonic stem cell line should be carefully investigated to ensure that the gene of interest is fully and solely inactivated. Because a greater percentage of a gene's exons are prevented from being transcribed and translated, vector insertions near the 5' end of a gene are more likely to result in complete gene inactivation than insertion at the 3' end and (b) there is the possibility of inactivating multiple genes. This can happen if the vector insertion is in a region where the coding regions of multiple genes overlap, or is upstream of an RNA gene such as a microRNA that would normally be transcribed along with the gene that has been identified as inactivated and (c) genes coding on the opposite strand can also be inactivated by vector insertion threfore ideally the strand orientation of the gene of interest should be checked (extensive information on gene traps can be found in http://www.genetrap.org).

3.1.2. "Trapping" the glucocorticoid receptor in ES cells

To generate mice lacking one functional GR allele ($GR^{+/-}$ mice), an existing embryonic stem (ES) cell line (ESKN92) was used generously provided by Heidi Sutherland and Wendy Bickmore (MRC Human Genetics Unit, Edinburgh, UK). ESKN92 cells arose from a gene trap screen to identify chromosomal and nuclear proteins in mouse cells (Sutherland et al, 2001). A schematic representation of the gene trap screening strategy is shown in Figure 3.1. Briefly, a β-galactosidase-neomycin phosphotransferase (βgeo or referred here as βgal) reporter cassette lacking a promoter and translation start, but with a splice acceptor site at the 5' end of the cassette, was randomly integrated into the genome of mouse ES cells (129Ola). If the cassette integrated into an intron of an expressed endogenous gene, splicing (fusion of the endogenous and βgeo transcript) may occur from the splice donor site of the endogenous gene to the splice acceptor site of the cassette. The presence of a poly- adenylation (pA) site at the 3' end of the cassette ensure that transcription terminated at the end of the cassette. If the resulting spliced transcript maintained the open reading frame (ie is in phase with the triplet codon message), then a chimaeric protein would be generated in which the N-terminal amino acids are derived from the endogeneous gene and the C-terminal amino acids derived from the *β-geo* cassette (Tate et al, 1998). This approach allowed the resulting fusion protein to be expressed from the endogenous gene promoter and additionally confers β-gal activity (for cell specific identification) and neomycin resistance (neo^R; for subsequent selection of the gene-trap ES cell line). Thus, clones in which chimericproteins have been generated can be selected for neo^R and localization of the

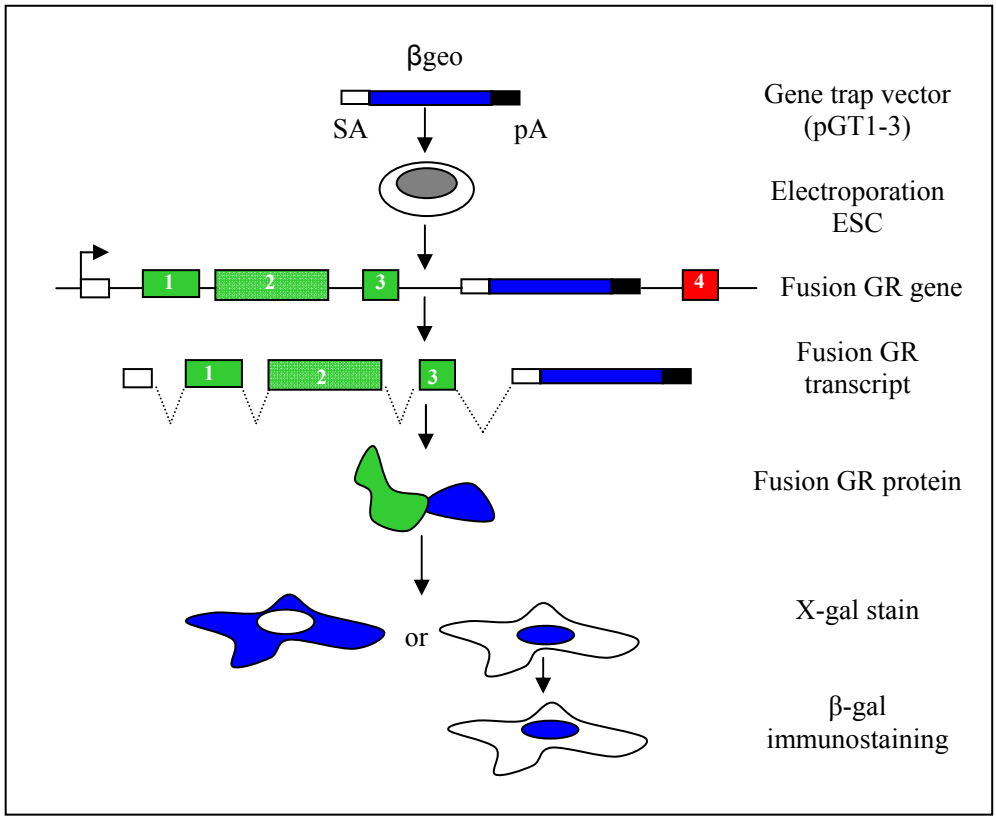

Figure 3.1 Gene-trapping strategy.

The gene trap vectors (pGT1-3, Sutherland et al., 2001) contain a splice acceptor site (SA), a βgeo cassette and a poly-adenylation signal (pA). The gene targeting vector integrated into an intron of the GR gene downstream of coding exons. This led to the splicing of the βgeo reporter in frame with the gene transcript. Translation results in a chimeric/fusion protein, comprising GR at the N terminus and βgeo at the C terminus, expressed from the endogenous GR promoter (modified from Sutherland et al, 2001).Numbers 1, 2, 3 and 4 correspond to exons 1, 2, 3, 4 of the GR gene. Integration of the gene trap in the intro between exon 3-4 (DBD) results in the loss of exons 4-9 and therefore part of the DNA binding domain (exon 4) and the entire ligand binding domain (exons 5-9).

fusion protein is determined by virtue of the β-gal activity using X-gal staining or immunofluorescence using a β-gal antibody. Frequently, the fusion of the endogenous gene with the β-geo reporter is mutagenic and alters or abolishes the normal function of the endogenous protein if domains critical for normal function are deleted by the fusion (Tate et al, 1998). In the ESKN92 cell line it was reported that the β-geo cassette had integrated into the GR gene (Sutherland et al, 2001), generating a fusion protein lacking part of the DNA binding domain (DBD) and the entire ligand binding domain (LBD). The fusion protein was predicted to be non-functional and because it lacks both known nuclear localization signals (NLS) is predicted to be cytoplasmic (Picard and Yamamoto, 1987). However, the apparent diffuse nuclear localisation of the fusion protein (Sutherland et al, 2001) suggested that it might retain some residual DNA binding activity, or possibly a novel NLS, and may not be completely non-functional.

The experiments described in this chapter (fig 3.2) were designed to characterise the ESKN92 cell line, prior to using the cells to generate a line of GR mutant mice.

Specifically I aimed to:

- confirm a single gene trap integration in ESKN92 cells, and that the insertion was in the GR gene on chromosome 18.
- determine the precise site of the splice junction (where βgeo fuses to the GR transcript), thereby identifying the intron into which the cassette had inserted.

- examine the cellular localization pattern of the fusion protein and whether it was affected by the presence of either ligand or the presence of endogenous GR (eg the wild type GR allele from the non-targetted chromosome).
- determine the size of the expressed fusion protein
- characterise the nature of the GR-βgeo allele (null, dominant negative or hypomorphic) by recreating the fusion protein and testing its ability to activate a GC responsive promoter in transiently transfected HEK293 cells.

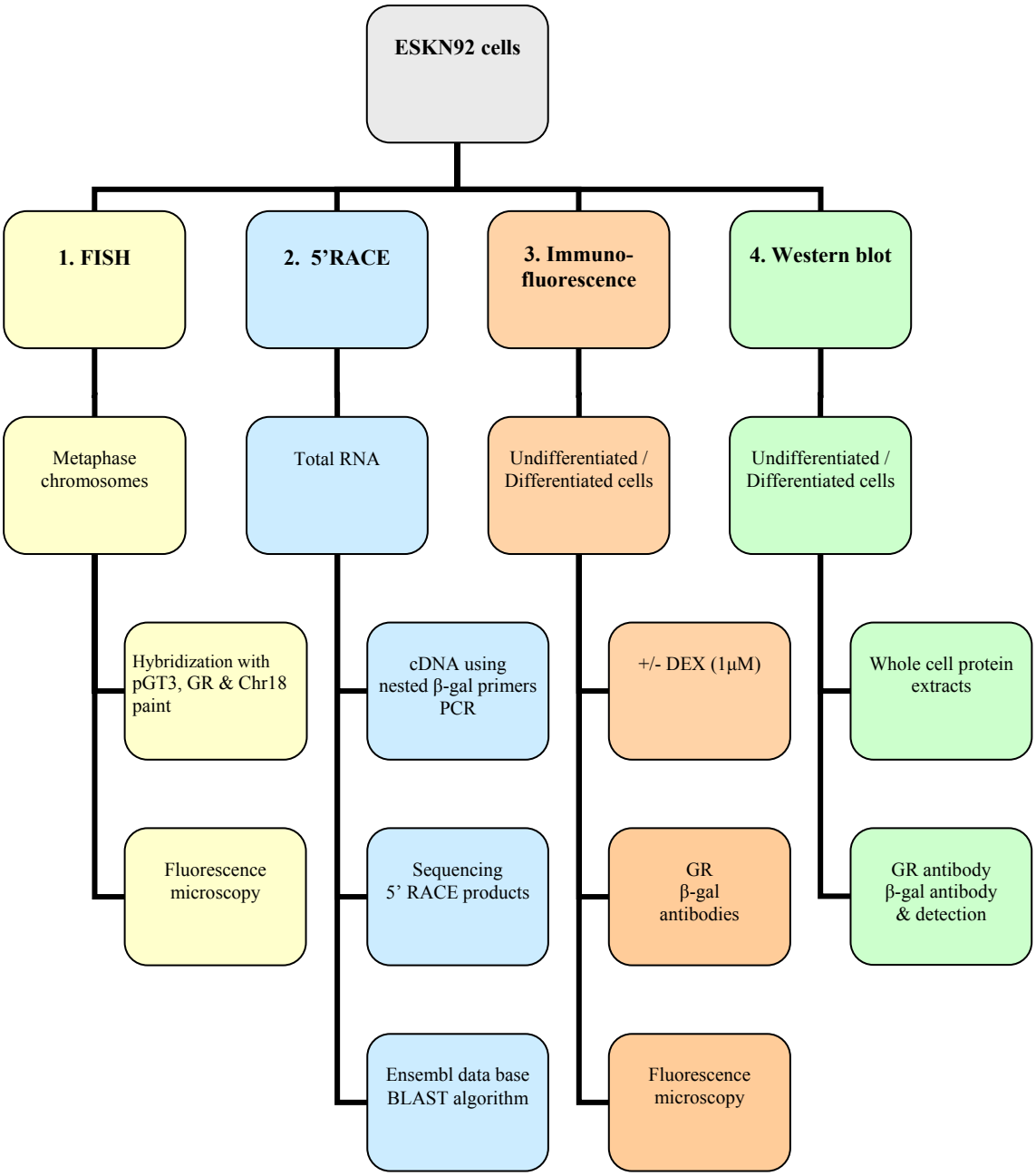

Figure 3.2 Flow Chart of ESKN92 characterization experiments.

(1) FISH was performed to confirm a single integration of the βgeo cassette and confirm localization to the GR locus on chromosome 18. (2). 5'RACE was performed to identify the integration site in the GR locus. (3). Immunofluorescence was used to examine the cellular localization of the fusion protein, using antibodies against GR and/or β-gal, and to determine whether this was influenced by cellular differentiation and glucocorticoid ligand (DEX). Briefly, undifferentiated or differentiated ESKN92 or a wild type parental cell line (ES14) were treated with 1μM DEX for 10 min to test if fusion protein responds to ligand by translocating to the nucleus and (4). Whole extract ESKN92 protein was analyzed by western blot to check the size of the fusion protein.

3.2 Results

3.2.1 ESKN92 cells contain a single integration of the gene trap cassette in the GR locus, on chromosome 18

The chromosomal location of the gene trap was determined by metaphase FISH analysis of DNA in ESKN92 cells, using probes specific for the gene trap vector (pGT-3), the GR and chromosome 18 (Table 3.1). To confirm that the gene trap insert was on chromosome 18, FISH was carried out using the pGT-3 probe together with a chromosome 18 'paint'. Both chromosomes 18 showed green diffuse staining along their length (fig. 3.3A). The gene trap (red signal) is present only in one copy of chromosome 18 (fig. 3.3A). No other red signals were seen confirming a single gene trap integration site on chromosome 18. To confirm that the insertion is at the GR locus, metaphase chromosomes were hybridized with both the pGT-3 probe and a GR specific probe. Both probes hybridize to the same site (merged the red and green signals to appear as a yellow signal) on both the two sister chromatids of chromosome 18 (fig. 3.3B), confirming integration into the glucocorticoid receptor locus. Finally, figure 3.3C shows a GR specific probe hybridized to both chromatids of chromosome 18, used as a positive control.

Table 3.1 Probes used to detect the insertion site of the pGT-3 (gene trap vector) into ESKN92 chromosomes by FISH.

PROBE 1	PROBE 2
pGT3-DIG-TxR	Chromosome 18-BIOTIN-FITC
pGT3-DIG-TxR	Chromosome 18-BIOTIN-FITC
GR-BIOTIN-FITC	pGT3-DIG-TxR
GR-BIOTIN-FITC	pGT3-DIG-TxR
GR-BIOTIN-FITC	-

DIG is digoxygenin-11-dUTP, TxR is Texas Red-conjugated anti-sheep IgG. FITC is fluorochrome-conjugated avidin. The GR probe used is a 6kb genomic fragment located at the 5' end of the gene (for FISH details please refer to section 2.2.2.3.)

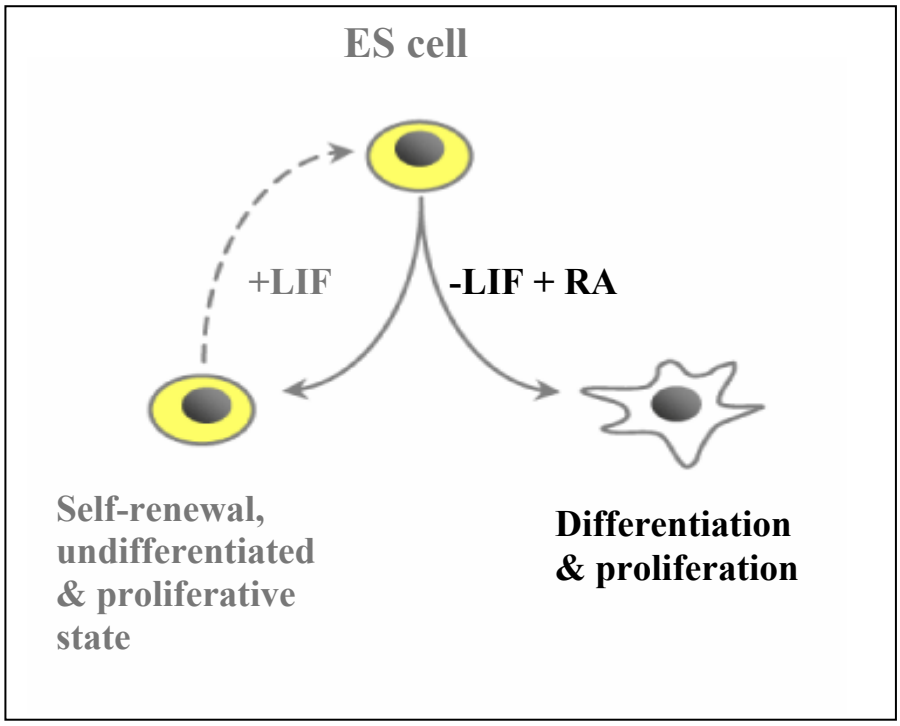

Figure 3.3 Maintenance and differentiation of mouse Embryonic Stem (ES) cells. Cells are cultured in the presence of Leukemia Inhibitory Factor (LIF) to maintain the undifferentiated state or in the absence of LIF and the presence of retinoic acid (RA) to differentiate them along a non-specific pathway. Cells are allowed to differentiate for 8 days and their differentiation state is microscopically examined. The majority of cells in the ESKN92 cell line grown in the presence of LIF, formed densely packed clusters. When cells were supplemented with 5x 10^{-6} M RA for 6-8 days morphological changes were observed; densely packed cells became much less compact and moved apart from each other as reported previously (Strickland and Mahdavi, 1978). Cell morphology also altered so that cells become larger, flatter and more irregularly shaped.

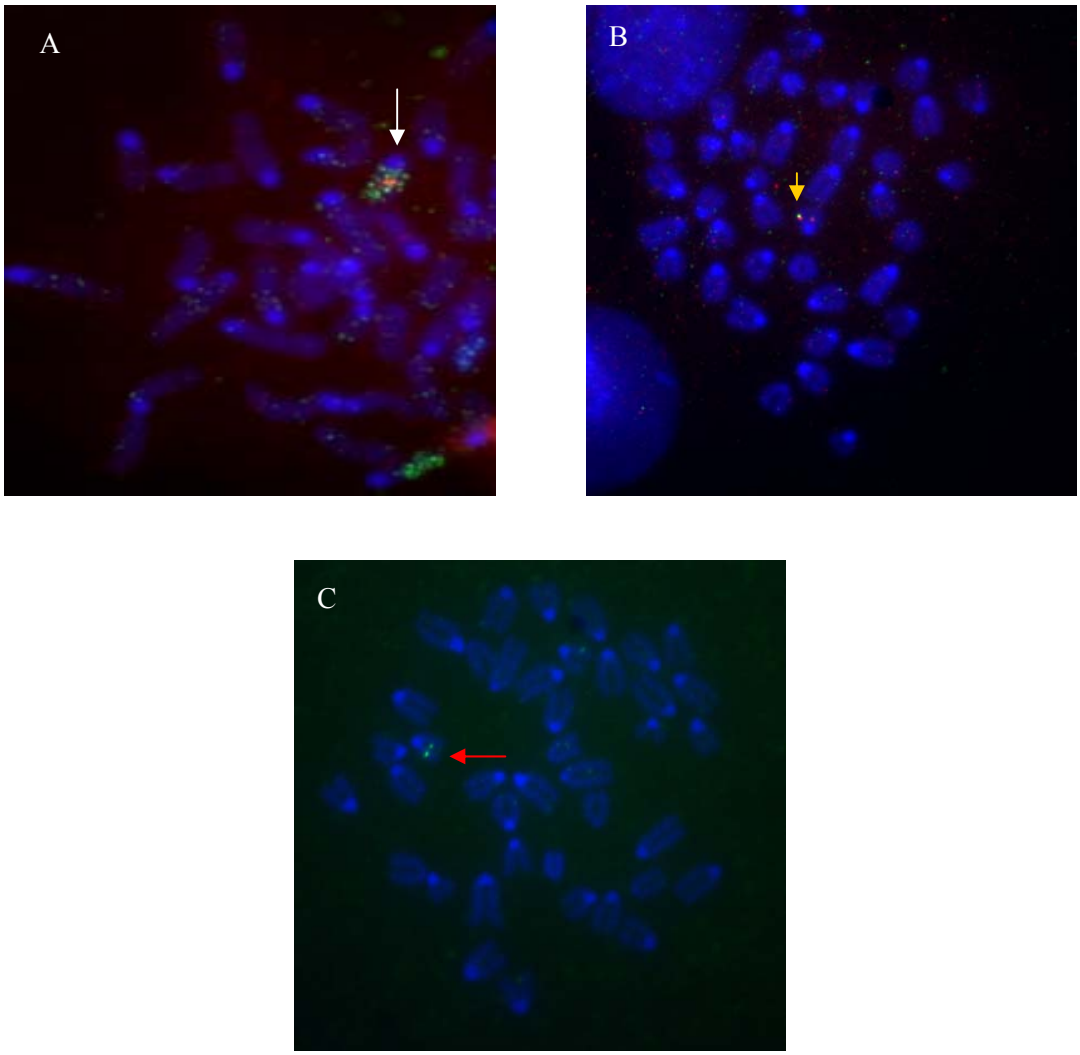

Figure 3.4 Single integration of the gene trap into chromosome 18 at the GR locus in ESKN92 cells.

Representative images of metaphase chromosomes hybridised with (A) both the pGT-3 probe (labelled with DIG-TxR; red dot) and a "paint" for chromosome 18 (biotin-FITC labelled; green diffuse stain); 2 copies of chromosome 18 are fluorescent along their entire length but only one contains the trap (white arrow)**, (**B) both the pGT-3 probe (labelled as above; red dot) and a GR probe (biotin-FITC labelled; green dot), indicating colocalization of the trap with the GR (yellow arrow) and (C) a GR specific probe (labelled as above) showed 2 copies, one in each chromatid (red arrow). Chromosomes are 4,6-diamidino-2-phenylindole (DAPI) stained. The images were acquired using filters appropriate for DAPI, FITC and Texas Red. Magnification x 100

3.2.2 Insertion of the gene trap into intron C of GR results in the removal of the second Zn finger of DBD and the entire LBD.

5'-RACE was used to identify the insertion site of the βgeo cassette into the GR gene. cDNA was synthesized from ESKN92 cells using a βgal specific primer. A universal primer (section 2.2.1.1.6) was ligated to the 3' end of the cDNA and a nested PCR carried out, again using a universal primer and an internal βgal primer. A single PCR product was obtained (not shown). This was sequenced using the nested βgal primer to identify the junction between the βgeo cassette and the GR mRNA. ~400bp of the sequence is shown in figure 3.4A. The BLAST algorithm was used to compare with the Ensembl database. This verified that the gene trap was inserted in the GR gene in the ESKN92 cell line. Examination of the sequence revealed that the βgeo cassette was spliced onto the end of exon 3 of GR (fig. 3.4A). Therefore the cassette integrated into intron C, resulting in an mRNA encoding a fusion protein in which the second zinc finger (ZF), encoded by exon 4, of the DNA binding domain (DBD) and the entire ligand binding domain (LBD), encoded by exons 5-9, of GR were replaced by βgeo (fig. 3.4B). Thus, the fusion protein lacks both known nuclear localization signals (NLS; Picard and Yamamoto, 1987). Translation is predicted to result in a GR-βgeo fusion protein (referred as GR-βgal throughout this Thesis) expressed from the endogenous GR promoter.

A

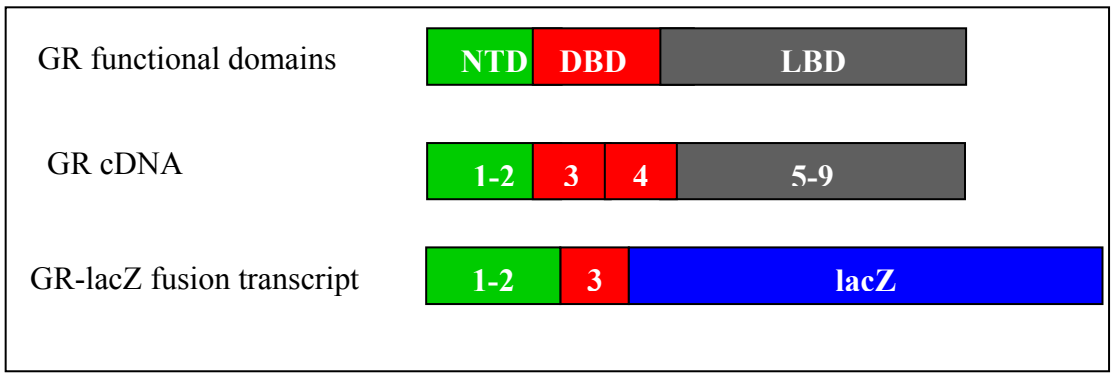

B

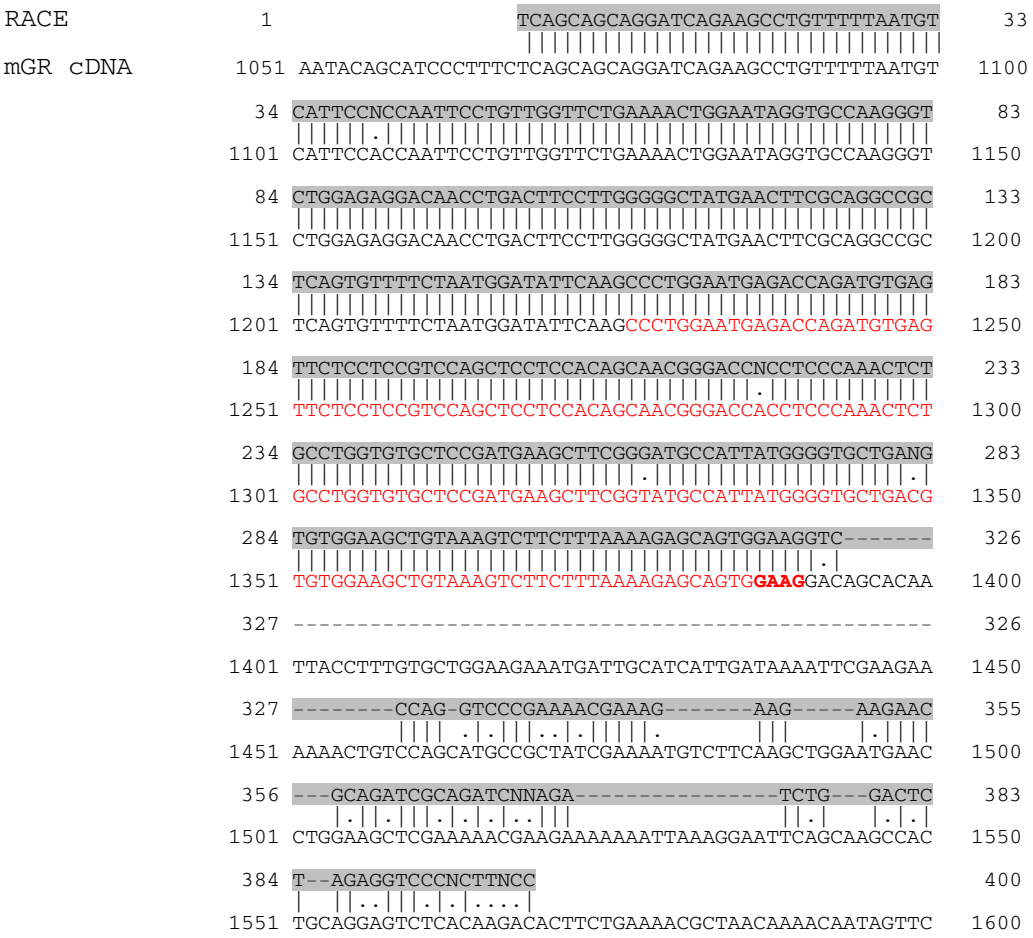

Figure 3.5 5'RACE shows the βgeo cassette has replaced exons 4-9 of GR in the encoding mRNA.

Figure 3.5 5'RACE shows the βgeo cassette has replaced exons 4-9 of GR in the encoding mRNA.

(A) A schematic view of the functional domains of GR (upper), the GR cDNA, showing the regions encoded by individual exons (middle) and the predicted structure

of the fusion protein. Green corresponds to the N-terminal domain (NTD; encoded by exon 2), red is the DNA binding domain (DBD; exons 3 and 4), grey is the ligand binding domain (LBD; exons 5 to 9) and blue is the lacZ with neo attached at the end of the fusion protein. Note that exon 1 is non-coding.) and (B) Alignment of mouse GR (black letters; starting from 1051bp) with the 5'RACE sequence product (grey shaded portion; 1-400bp). Briefly, the alignment performed by firstly reverse complementing the RACE sequence (reading from the LacZ) using http://bioinformatics.org/sms/rev_comp.html, accessing the FASTA mGR cDNA (accession number: X04435) sequence. Then pasted both reverce complement of the RACE and the FASTA GR cDNA into the EBI alignment programme (http://www.ebi.ac.uk). Note that the first nucleotide of the RACE aligns with nucleotide 1068 of mGR and the red letters are exon 3 of GR. The alignment ends at GAAG of exon 3 (bold red letters). After the end of exon 3, the sequense corresponds to the splice site of the engrailed 2 gene of the gene trap vector. The dash (-) indicates that there is no corresponding nucleotide in a sequence. For complete information on the whole mGR cDNA, 5'RACE and the gene trap vector sequences refer to Appendix B.

3.2.3 GR-βgal fusion protein is located both in the cytoplasm and the nucleus.

3.2.3.1 Localization of wild type GR and GR-βgal fusion proteins in undifferentiated ESKN92 cells.

Previous data have shown diffuse nuclear localization of fusion protein (Sutherland et al, 2001) yet, as stated above, both the known GR NLSs (Picard and Yamamoto, 1987) were not present. To examine localization, immunofluorescence was performed on undifferentiated ESKN92 using β-gal and GR specific antibodies. Contrary to expectations, in the absence of its ligand (dexamethasone), intact (wild type) GR was located in the nucleus in large, round spots (foci or clusters), distributed in a punctuate manner in both undifferentiated ESKN92 (fig. 3.6) and ES14 cells (wild type cell line; WT) (fig. 3.7). The GR antibody also showed some diffuse fluorescence in the cytoplasm of ESKN92 cells, probably detecting the fusion protein (not seen in the wild type cells; fig.3.7) with some strong fluorescence along lines at the periphery of the cytoplasmic membrane (possibly the cytoskeleton). In contrast, the fusion protein (detected using a βgal antibody), showed a diffuse localisation throughout the cytoplasm and the nucleus in undifferentiated ESKN92 cells (fig. 3.8). As expected, no βgal immunofluorescence was apparent in WT cells (fig. 3.9) nor was there any specific fluorescence detected when the primary antibody was omitted. Residual immunofluorescence is probably due to autofluorescence (fig. 3.10).

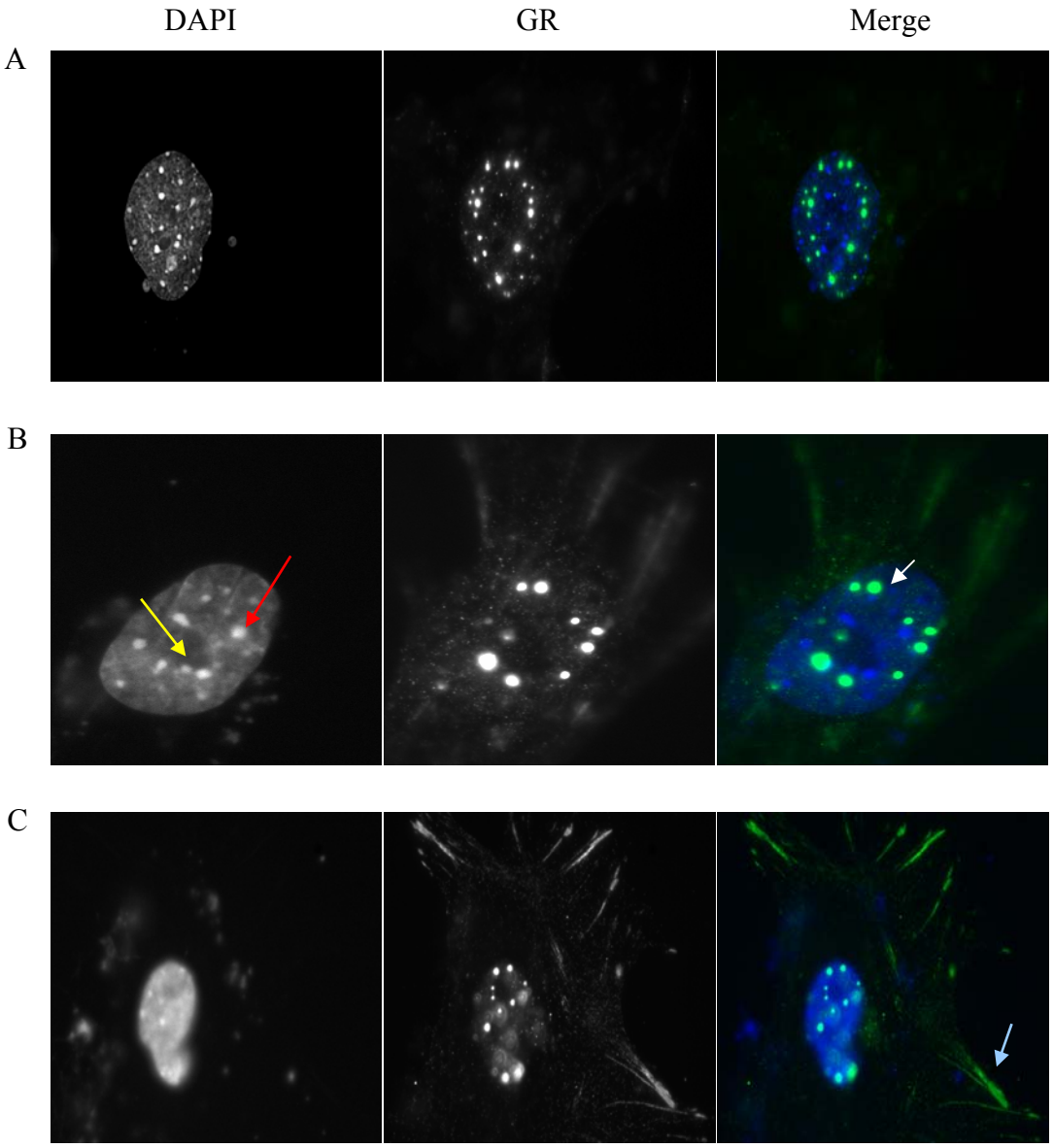

Figure 3.6 GR immunostaining in undifferentiated ESKN92 cells detecting intact GR and GR-βgal fusion protein reveals discrete nuclear foci.

Representative photographs of 3 independent ESKN92 cells (A, B and C, from top to bottom). The left *column* of each shows DAPI (labelling DNA), the *middle* column is FITC (attached to the secondary antibody, detecting GR) and the *right* column is the merged picture (DAPI is blue and FITC is green). White arrow (B, right image) indicates nuclear GR foci, and red and yellow arrows (B, left photo) shows a nucleolus (with the appearance of a hole in the DAPI staining) and heterochromatin respectively. Light blue arrow (C, right image) indicates the GR fluorescence along the cytoskeleton. The GR antibody detects both the intact and fusion protein in ESKN92 cells. Images captured from a conventional fluorescence microscope at magnification x100.

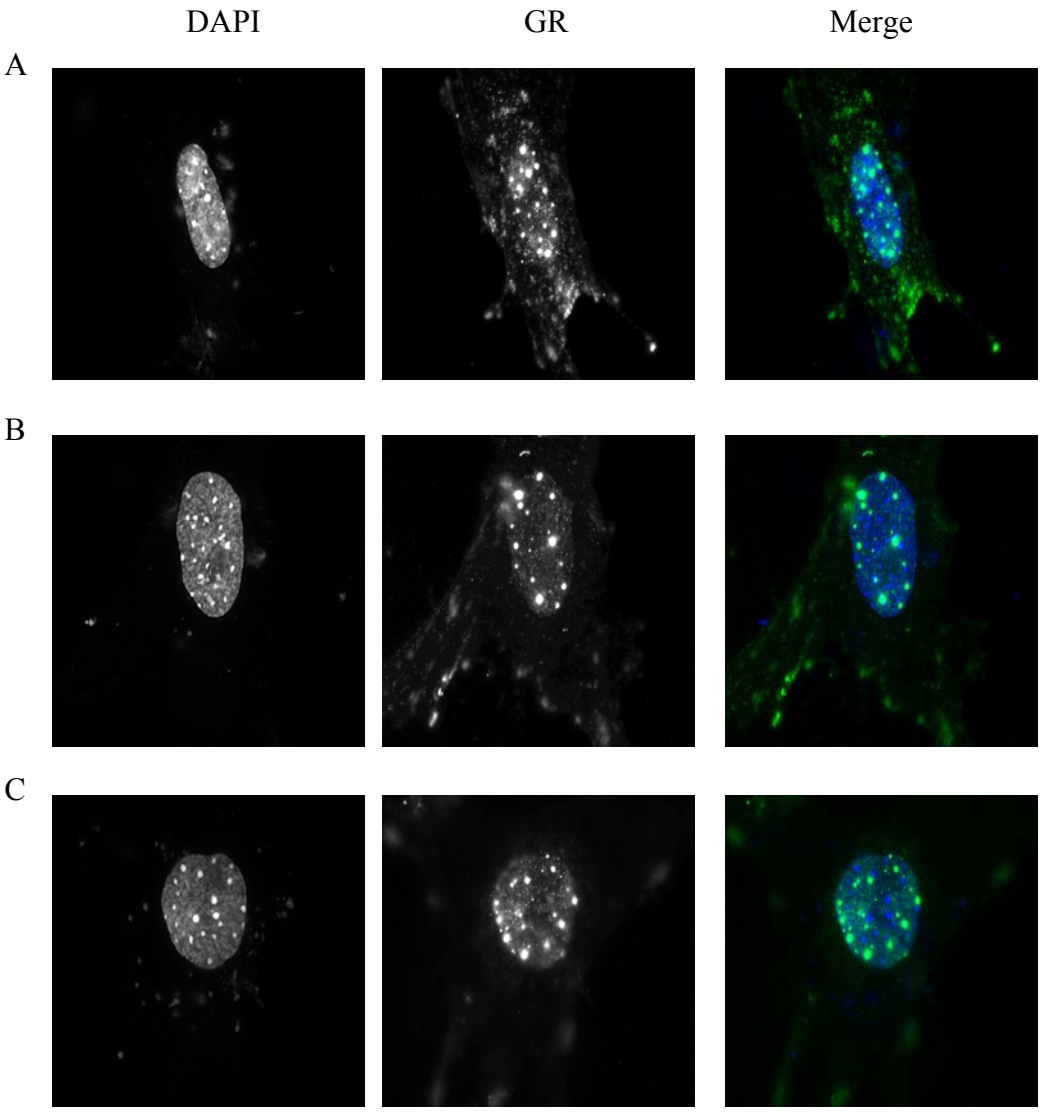

Figure 3.7 Immunostaining of GR in undifferentiated WT ES cells reveals intact GR in discrete nuclear foci.

Representative photographs of 3 independent WT cells (A, B and C, from top to bottom). The left *column* of each shows DAPI (labelling DNA), the *middle* column is FITC (attached to the secondary antibody, detecting GR) and the *right* column is the merged picture (DAPI is blue and FITC is green). The GR antibody detects the intact protein in WT cells. Images captured from a conventional fluorescence microscope at magnification x100.

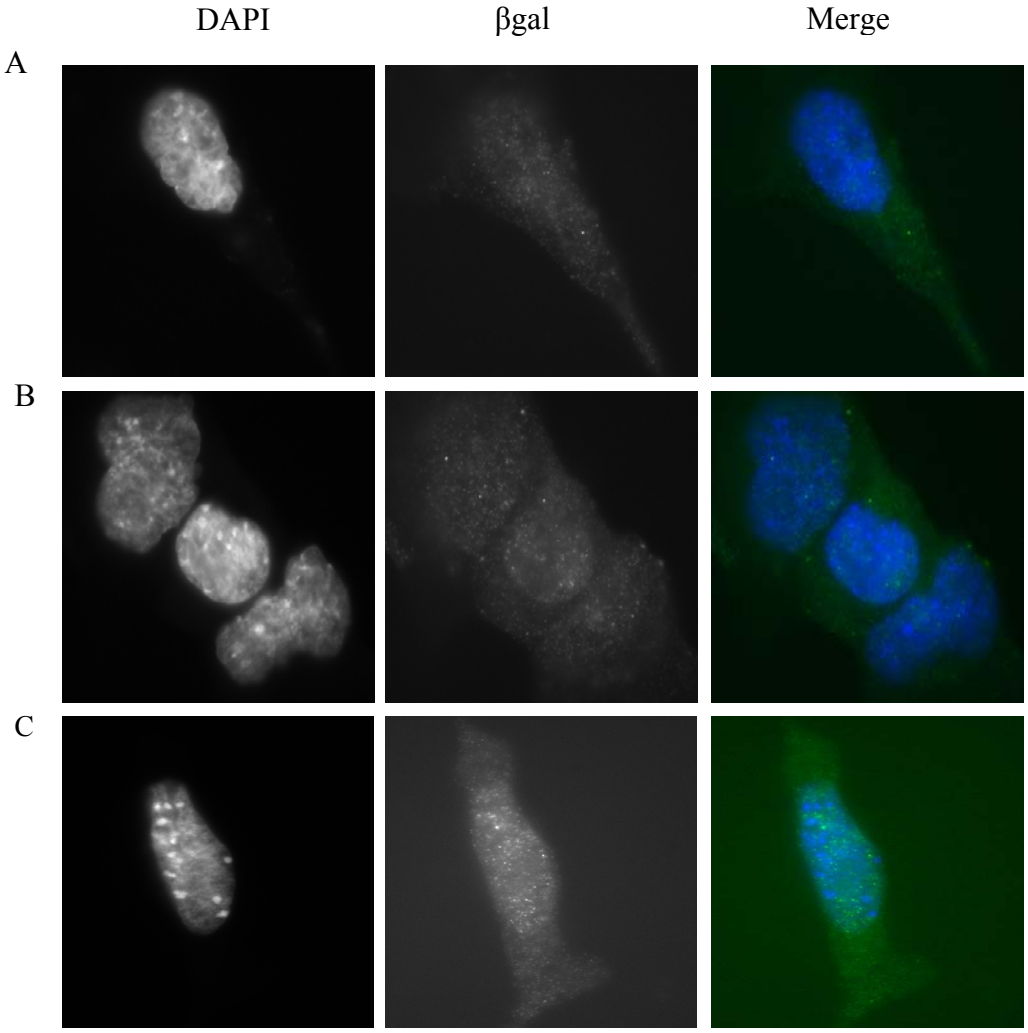

Figure 3.8 βgal immunostaining of undifferentiated ESKN92 cells reveals diffuse nuclear and cytoplasmic GR- βgal fusion protein localization.

Representative photographs of 3 independent undifferentiated ESKN92 cells (A, B and C, from top to bottom). The left *column* of each shows DAPI (labelling DNA), the *middle* column is FITC (attached to the secondary antibody, detecting βgal) and the *right* column is the merged picture (DAPI is blue and FITC is green). The βgal antibody detects the fusion protein in ESKN92 cells. Images captured from a conventional fluorescence microscope at magnification x100.

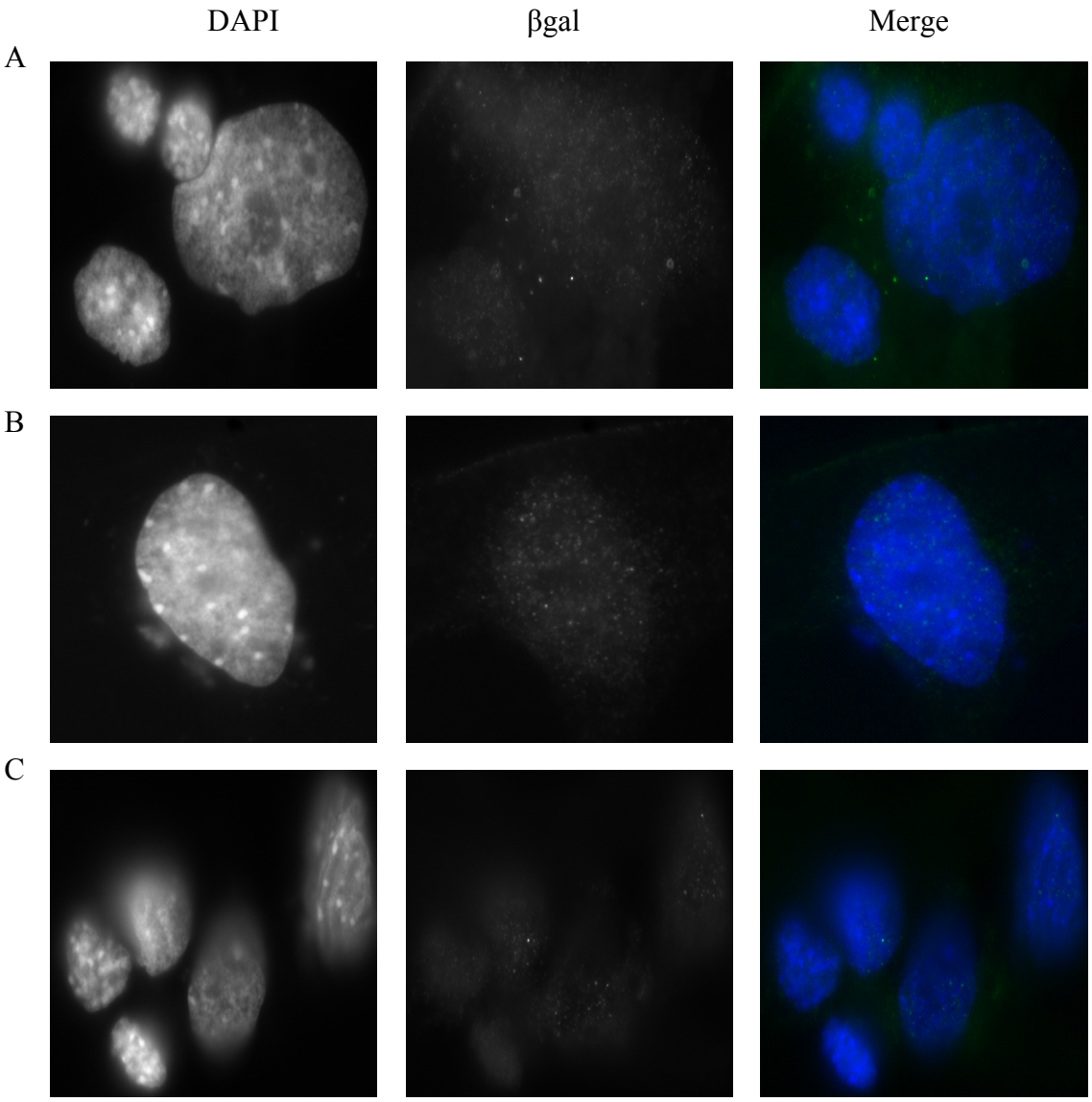

Figure 3.9 No βgal immunostaining is detected in undifferentiated WT cells (used as a negative control for the fusion protein).

Representative photographs of 3 independent undifferentiated WT cells (A, B and C, from top to bottom). The left *column* of each shows DAPI (labelling DNA), the *middle* column is FITC (attached to the secondary antibody, detecting βgal) and the *right* column is the merged picture (DAPI is blue and FITC is green). Absent βgal immunoreactivity in WT cells. Images captured from a conventional fluorescence microscope at magnification x100.

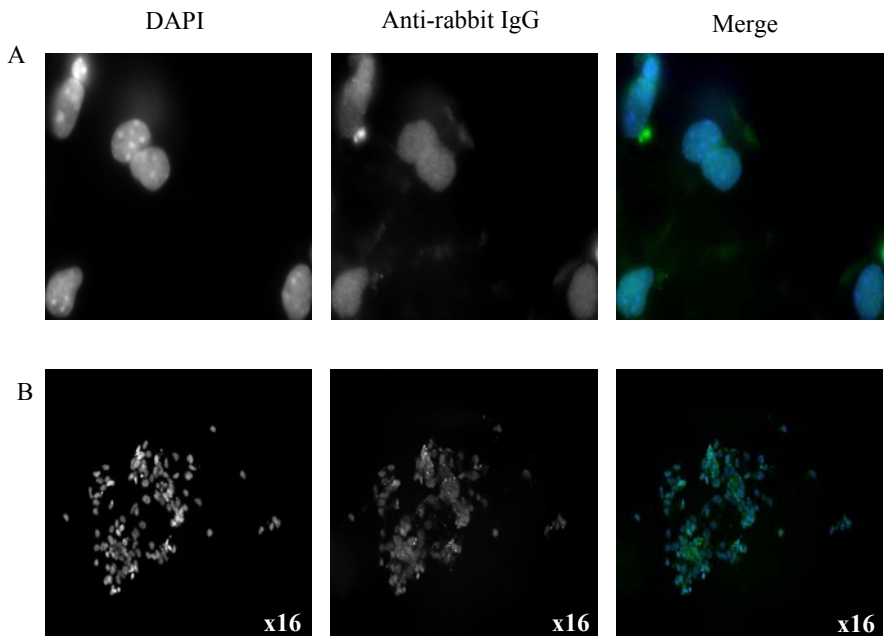

Figure 3.10 Omission of primary antibodies.

Immunofluorescence performed on differentiated ESKN92 cells. Omitting the primary antibodies (GR or β-gal) and incubating only with secondary antibody (anti-rabbit IgG). Channels have been split; on the left side is DAPI, middle is the FITC (attached to secondary antibody) and right is the two pictures merged.

3.2.3.2 Fusion and intact GR protein localization in differentiated ESKN92 cells.

To determine whether the unexpected nuclear immunofluorescence of endogenous GR is unique to undifferentiated ESKN92 cells, cells were differentiated and the localization pattern examined using GR and βgal specific antibodies**.** When cells were induced to differentiate, endogenous GR was evenly and diffusely distributed in the cytoplasm and the nucleus in both cell lines (fig. 3.11 and fig. 3.12). Cytoplasmic immunofluorescence seemed to be more prominent in the differentiated cells but this could be due to larger cytoplasmic volume in differentiated ES cells. In contrast, the fusion protein, detected using a βgal antibody, showed a diffuse localisation throughout the cytoplasm and the nucleus in differentiated (fig. 3.13) ESKN92 cells. As expected, no βgal immunofluorescence was apparent in differentiated WT cells (fig. 3.12).

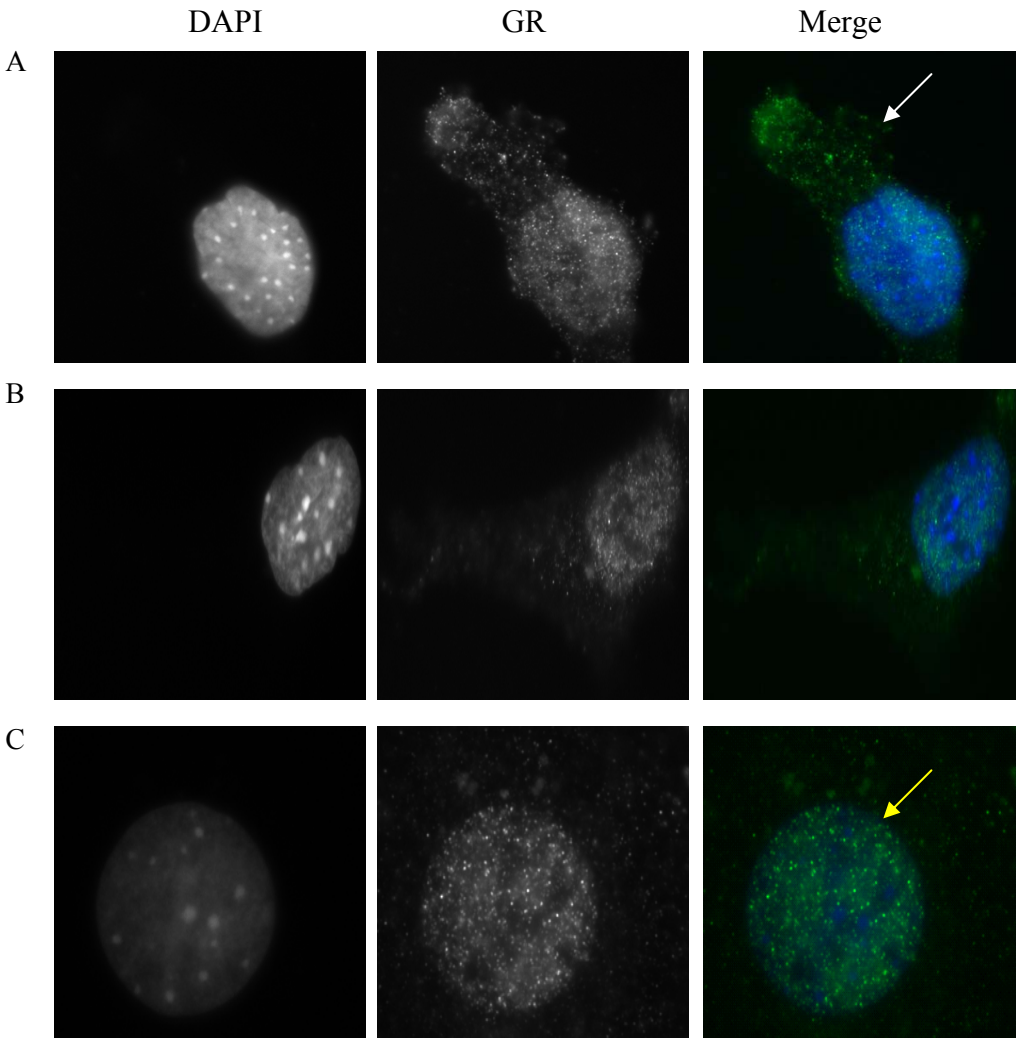

Figure 3.11 GR immunostaining in differentiated ESKN92 cells reveals diffuse nuclear and cytoplasmic intact GR and GR-βgal fusion protein distribution.

Representative photographs of 3 independent ESKN92 cells (A, B and C, from top to bottom). The *left* column of each shows DAPI (labelling DNA), the *middle* column is FITC (attached to the secondary antibody, detecting GR) and the *right* column is the merged picture (DAPI is blue and FITC is green). White arrow (A, right image) indicates diffuse cytoplasmic staining, and yellow arrow (C, right image) shows diffuse nuclear staining. The GR antibody detects both the intact and fusion protein in ESKN92 cells. Images captured from a conventional fluorescence microscope at magnification x100.

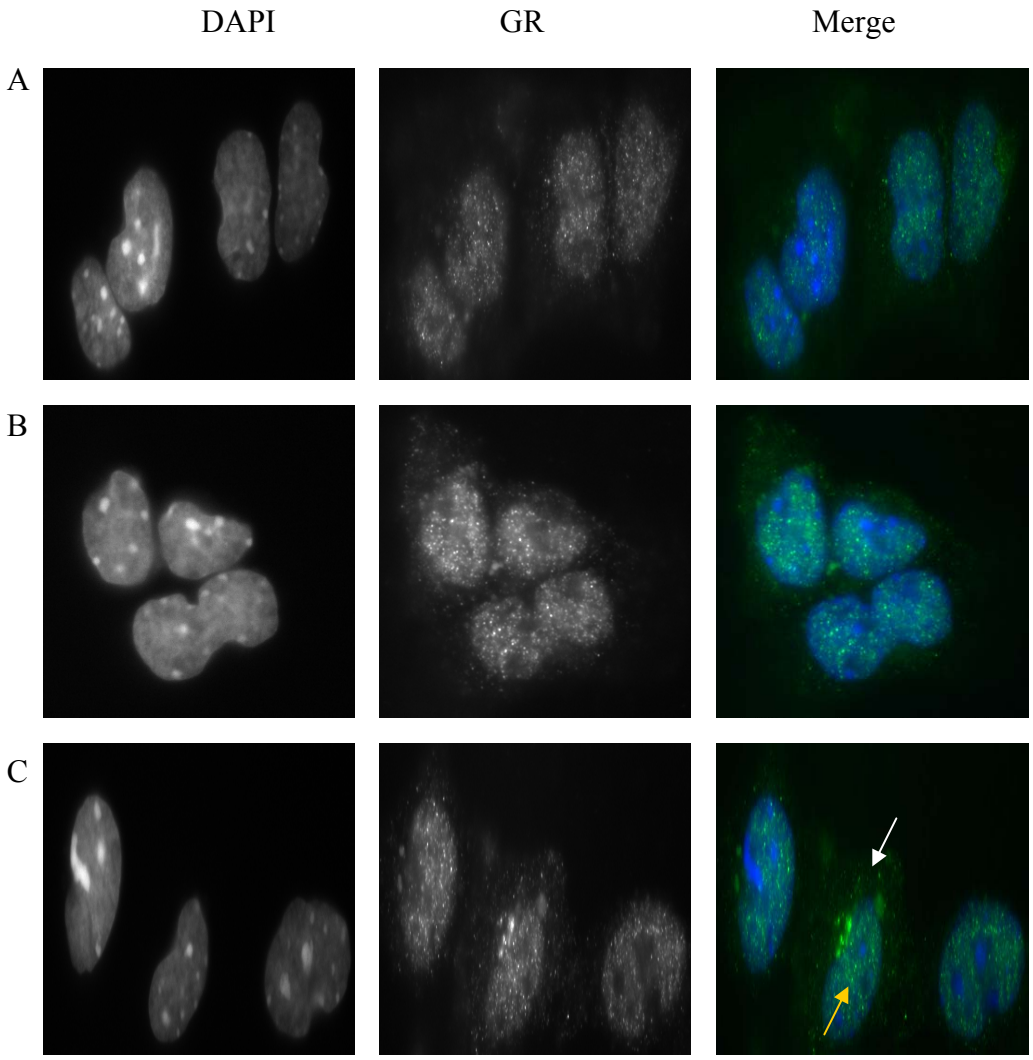

Figure 3.12 GR immunostaining in differentiated WT cells reveals diffuse nuclear and cytoplasmic intact GR protein distribution.

Representative photographs of 3 independent WT cells (A, B and C, from top to bottom). The *left* column of each shows DAPI (labelling DNA), the *middle* column is FITC (attached to the secondary antibody, detecting GR) and the *right* column is the merged picture (DAPI is blue and FITC is green). White arrow (C, right image) indicates diffuse cytoplasmic staining, and yellow arrow (C, right image) shows diffuse nuclear staining. The GR antibody detects the intact GR protein in WT cells. Images captured from a conventional fluorescence microscope at magnification x100.

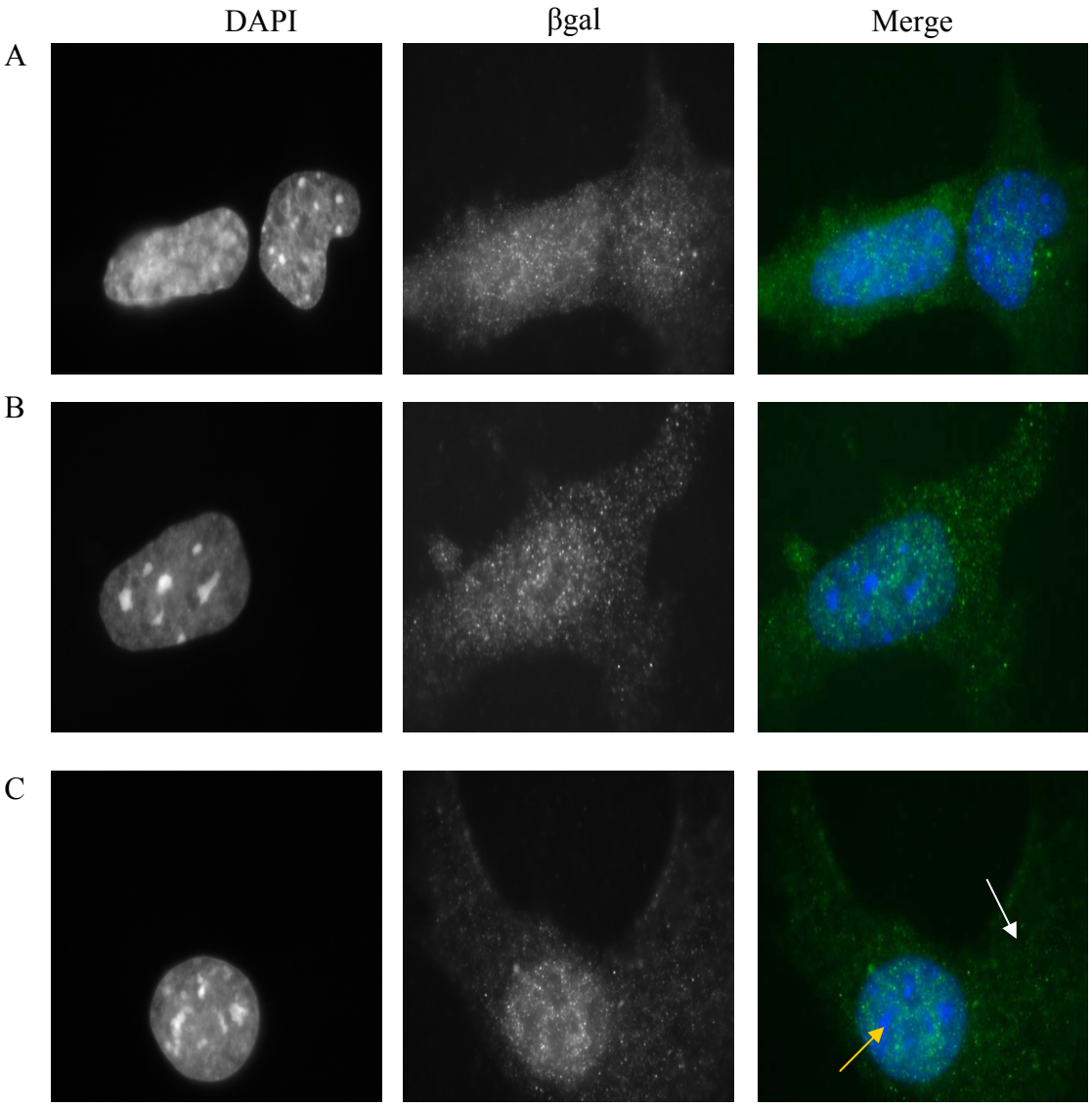

Figure 3.13 βgal immunostaining in differentiated ESKN92 cells reveals diffuse nuclear and cytoplasmic GR-βgal protein distribution.

Representative photographs of 3 independent ESKN92 cells (A, B and C, from top to bottom). The *left* column of each shows DAPI (labelling DNA), the *middle* column is FITC (attached to the secondary antibody, detecting βgal) and the *right* column is the merged picture (DAPI is blue and FITC is green). White arrow (C, right image) indicates diffuse cytoplasmic staining, and yellow arrow (C, right image) shows diffuse nuclear staining. The βgal antibody detects the GR-βgal fusion protein in ESKN92 cells. Images captured from a conventional fluorescence microscope at magnification x100.

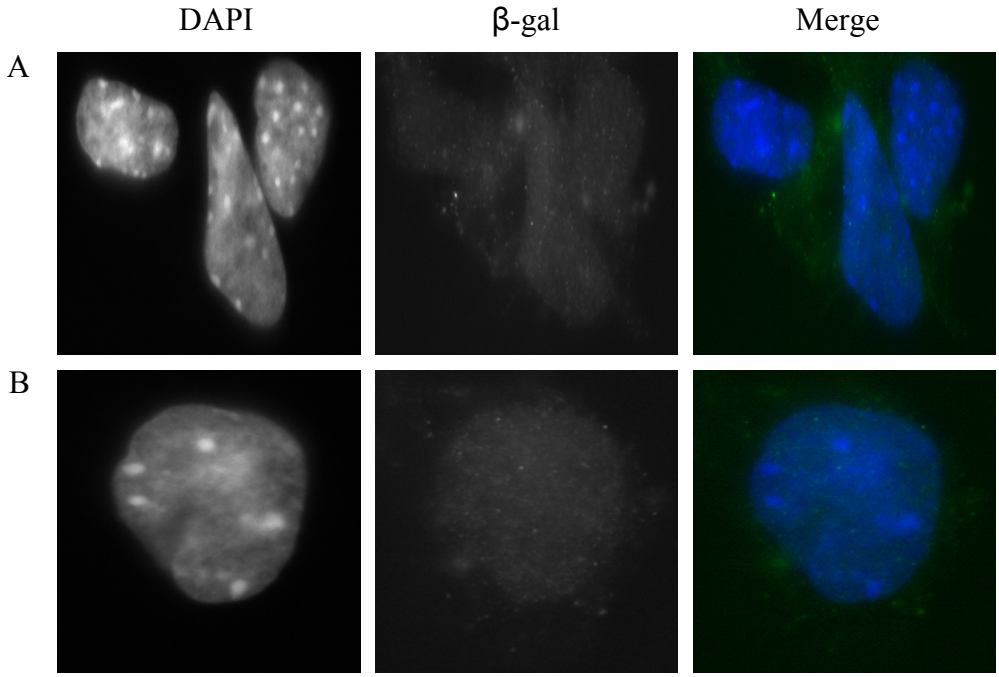

Figure 3.14 GR-βgal fusion protein is not detected in differentiated WT cells (negative control for the GR- βgal fusion protein).

Representative photographs WT cells (A and B; from top to bottom). The *left* column of each shows DAPI (labelling DNA), the *middle* column is FITC (attached to the secondary antibody, detecting βgal) and the *right* column is the merged picture (DAPI is blue and FITC is green). Images captured from a conventional fluorescence microscope at magnification x100.

3.2.3.3 Fusion and intact GR protein localization in DEX-treated ESKN92

The nuclear localization of GR in undifferentiated or differentiated ES cells was unexpected. To determine if this was due to the presence of residual glucocorticoid (GC) in the foetal calf serum of the culture medium, endogenous and fusion GR localisation was investigated in the absence of serum GC (removal by dextran-coated charcoal). In addition, DEX was used to induce nuclear localization of GR. Since the GR-βgal fusion protein lacked the entire LBD, it was predicted to be unresponsive to DEX. Removal of GC from serum had no effect on the localization of either intact or GR-βgal fusion protein in undifferentiated ESKN92 (fig. 3.15A, E) or WT ES cells (fig.3.15C) No differences in immunofluorescence were observed with 1μM DEX-treatment in either undifferentiated (fig. 3.15A-B) or differentiated (fig. 3.16A-B) ESKN92 cells. In contrast, DEX treatment of WT cells increased GR immunofluorescence in the nucleus and decreased GR immunofluorescence in the cytoplasm. This occurred in both undifferentiated (fig. 3.15C-D) and differentiated WT cells (fig. 3.16C-D). However, as noted above, GR immunostaining, whether in the nucleus or the cytoplasm was more diffuse in differentiated cells (fig. 3.16), with much smaller foci when compared to undifferentiated WT cells (fig. 3.15). There was no effect of DEX upon the pattern of βgal immunostaining in the nucleus of undifferentiated (fig. 3.15E-F) or differentiated ESKN92 cells (fig. 3.16E-F). As expected, no β-gal immunostaining was seen in WT cells under any conditions (fig. 3.15G-H and fig. 3.16G-H).

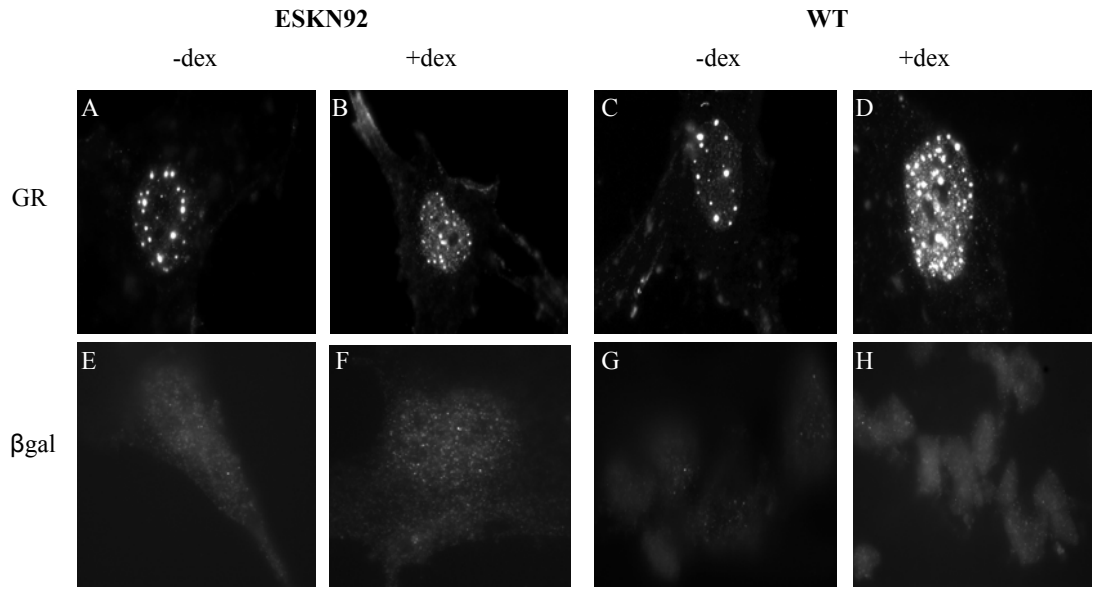

Figure 3.15 DEX has no effect on the distribution of GR-βgal fusion protein in undifferentiated ESKN92 cells *but* WT cells respond to DEX with increased GR immunostaining in the nucleus.

GR immunofluorescence in (A) ESKN92 cells before DEX and (B) 10 min after addition of 1μM DEX; (C) WT cells before DEX and (D) WT cells after DEX treatment. βgal immunofluorescence in (E) ESKN92 cells before DEX and (F) 10 min after DEX; (G) and (H) showing no βgal immunostaining in WT cells before or after DEX treatment (-ve control). One representative image per treatment, capturing the FITC channel (grey scale). Magnification x100. Note that the GR antibody detects both intact GR and GR-βgal fusion protein in ESKN92 cells, but only intact GR in WT cells. Therefore by a subtraction process the fusion protein distribution can be deduced, and also determine whether the presence of the intact affects the distribution of the fusion protein.

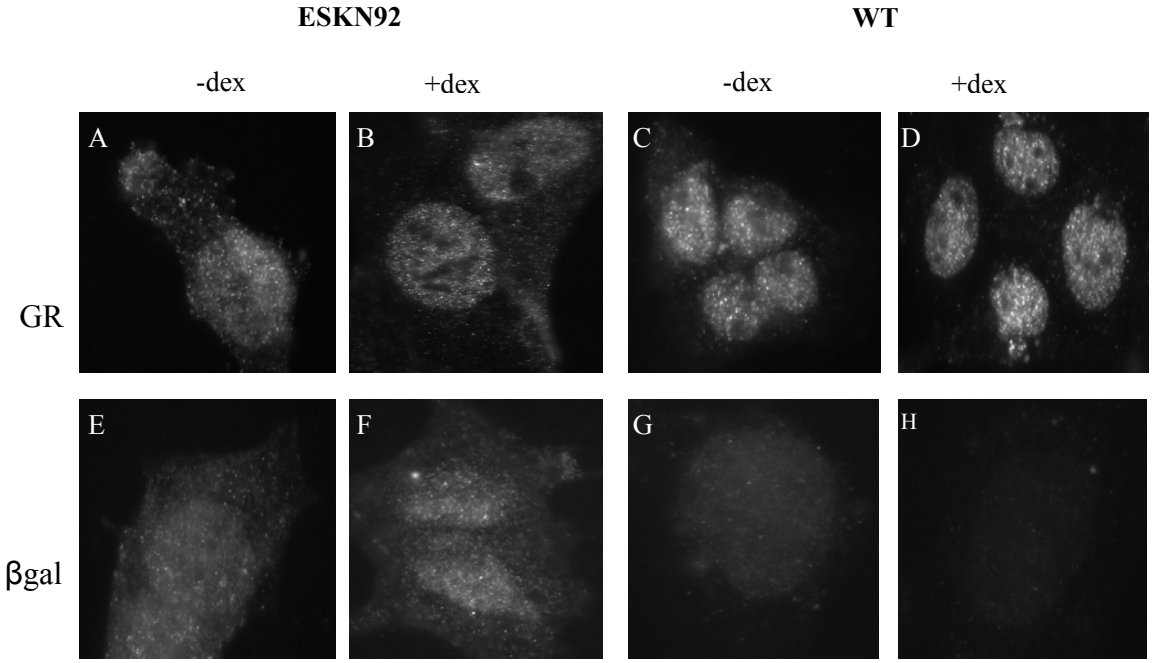

Figure 3.16 DEX has no effect on the translocation of intact or fusion GR protein in the nucleus of differentiated ESKN92 cells *but* WT cells respond to DEX with increased GR immunostaining in the nucleus and subsequently decreased cytoplasmic GR signal.

GR immunofluorescence in (A) ESKN92 cells before DEX and (B) 10 min after addition of 1μM DEX; (C) WT cells before DEX and (D) WT cells after DEX treatment. βgal immunofluorescence in (E) ESKN92 cells before DEX and (F) 10 min after DEX; (G) and (H) showing no βgal immunostaining in WT cells before or after DEX treatment (-ve control). One representative image per treatment, capturing the FITC channel (grey scale). Magnification x100. Note that the GR antibody detects both intact GR and GR-βgal fusion protein in ESKN92 cells, but only intact GR in WT cells. Therefore by a subtraction process the fusion protein distribution can be deduced, and also determine whether the presence of the intact affects the distribution of the fusion protein.

3.3 Immunoblotting demonstrates the presence of a 200kDa protein corresponding to the GR-β-gal fusion protein in ESKN92 cells.

Western blot of whole protein ESKN92 cell extracts was performed in order to detect the intact GRa (~ 95 kDa) and also the GR-βgal fusion protein (predicted size ~200 kDa). Because of the large predicted size of the chimeric protein, a 5% polyacrylamide gel was used to resolve proteins. Following transfer, the membrane was incubated with either GR antibody (epitope located at the N-terminus of GR) or an antibody against β-galactosidase. However, only the blot incubated with the GR antibody is presented because the β-galactosidase antibody bound to a variety of non-specific proteins (data not shown). Immunoblotting with the GR antibody detected a protein of the predicted size (figure 3.17) in differentiated (-LIF) and a weaker band in undifferentiated (+LIF) ESKN92 cells.

3.2.5 The nature of the GR-βgal fusion allele

3.2.5.1 Construction of plasmids expressing normal GR and the GR-βgal fusion protein.

Expression plasmids expressing intact GR and the GR-βgal fusion protein were constructed in the pcDNA 3.1(-) vector by Val Lyons, using DNA fragments derived from mouse GR expression plasmids, the 5'RACE PCR product from ESKN92 cells and the pGT-3 gene trap vector (see Appendix for details and fig. A1-3 for illustrations oftheplasmids).

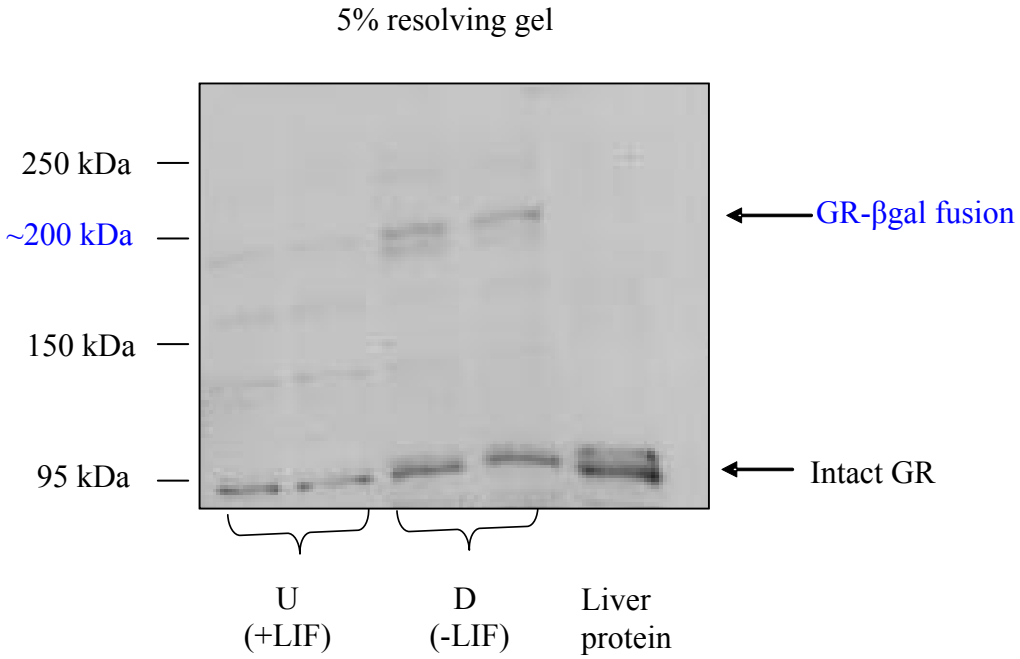

Figure 3.17 Western blotting with anti-GR antibody shows the presence of the predicted 200 kDa GR-βgal fusion protein in ESKN92 cells.

Whole protein extracts (10μg) from duplicate samples of undifferentiated (U; +LIF) and differentiated (D; -LIF+Retinoic Acid) ESKN92 cells were resolved by 5% PAGE, transferred to membrane and incubated with anti-GR antibody. Rat liver protein extract was used as a positive and negative control for the intact GR and the GR-βgal fusion proteins, respectively. Molecular weights are indicated (determined by colour marker) at the left side of the picture. Black arrows indicate the intact GR protein (95kD) and the fusion protein (200kDa) respectively.

3.2.5.2 Transfection experiments show that GR-βgal is transcriptionally inactive.

To address the nature of the GR-βgal allele, the ability of the fusion protein to activate transcription in transfected HEK293 cells, which lack functional GR, was tested. HEK293 cells were transiently co-transfected with either a PNMT (Adams et al., 2003; kindly provided by D. Pearce) or MMTV-LTR luciferase reporter (Lefebvre et al., 1991) and either of the following constructs (a) pcDNA3.1, the empty vector for wild type (WT) GR or GR-βgal to test if there is any functional GR in the cells (b) WT-GR to confirm normal GR induction by DEX or (c) GR- βgal mutant (lacks the ligand binding domain therefore should not be activated by DEX) to test the nature of mutant GR and (d) WT-GR co-transfected with GR-βgal to test if there is a dominant negative activity. All experiments were performed with or without 1μM DEX in charcoal stripped serum (fig. 3.19). Results using the PNMT-luciferase reporter (fig. 3.20) show a small induction of GR promoter activity with the vector alone suggesting that there is a low level of functional GR in the HEK293 cells. This was not apparent in the ransfection experiments with the MMTV-luciferase reporter (fig. 3.21). The GR-βgal fusion protein had no effect on promoter activity in the absence of DEX, indicating that it was not constitutively active(fig. 3.20 and fig.3. 21). As expected, DEX treatment had no effect on GR-βgal activity. Importantly, addition of GR-βgal fusion protein had no effect upon the DEX induction via WT-GR of either MMTV-LTR (fig. 3.21) or PNMT (fig. 3.20), indicating that it had no dominant negative activity. Overall, these results show that the GR- βgal mutant is transcriptionally inactive, and therefore predicted to act as a null allele.

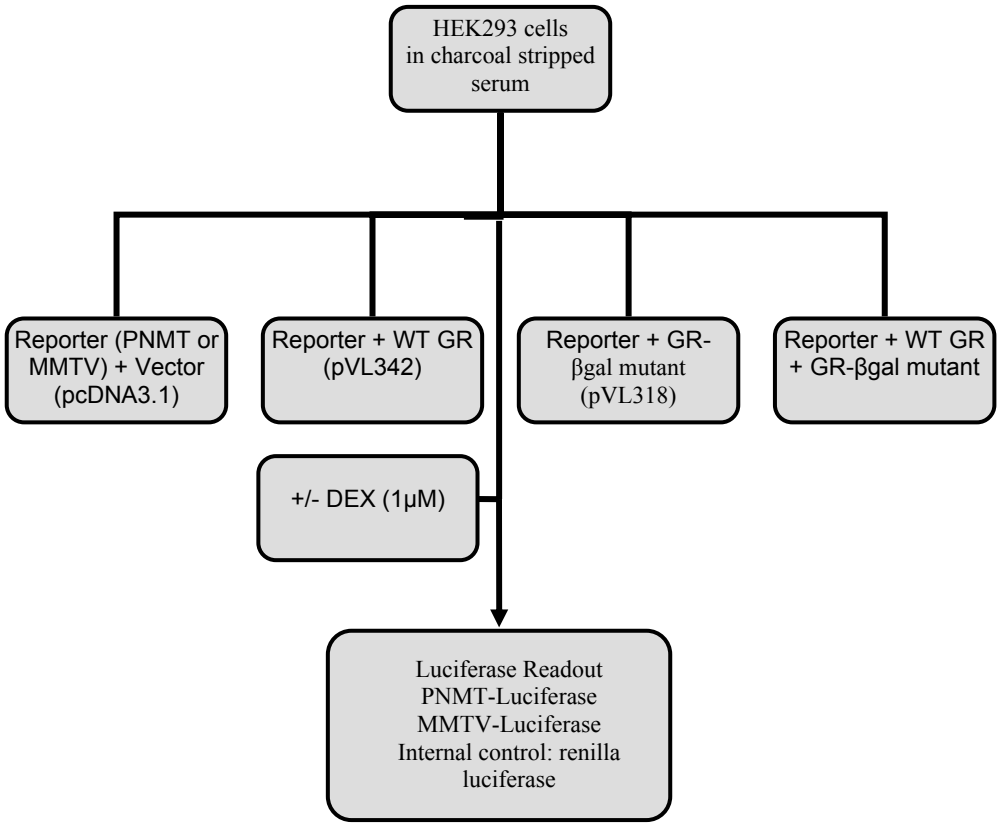

Figure 3.19 Schematic overview of HEK293 transfection experiments to evaluate the nature of GR-βgal allele *in vitro*.

Human embryonic kidney (HEK293) cells were maintained with charcoal stripped serum. Following 24h in culture, cells were transfected with reporter (MMTV-LTR-luciferase or PNMT-luciferase) and either the vector pcDNA3.1(-) alone (used for subcloning the wild type GR and GR-βgal mutant) or wild type (WT) GR or GR-βgal mutant or both the wild type GR and GR-βgal mutant together using lipofectamine 2000. 48h later, 1μM dexamethasone (DEX) was added and cells were lysed and firefly (reporter) and renilla (internal control) luciferase activity assayed. PNMT; phenylethanolamine N-methyltransferase promoter (Adams et al, 2003), MMTV; mouse mammary tumour virus promoter. The PNMT construct was kindly provided by David Pearce. For details on constructs used please refer to appendix A.

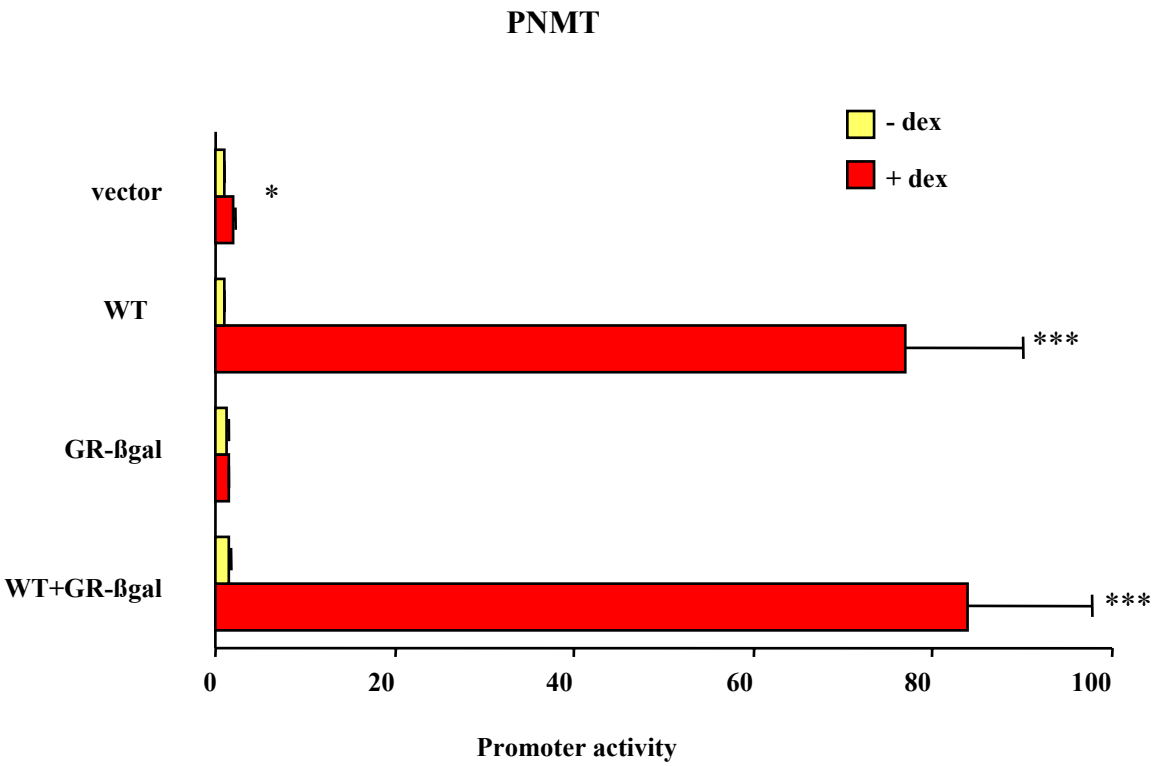

Figure 3.20 WT-GR activates the PNMT promoter in the presence of DEX, but the GR-βgal fusion protein had no effect on PNMT promoter activity.

In the absence of DEX, WT-GR or GR-βgal had no significant effect on promoter activity. DEX treatment increased wild type GR promoter activity but had no effect on the GR-βgal activity. Co-transfection of WT-GR with the mutant GR results in similar to WT-GR promoter activity after DEX treatment, ruling out a dominant negative activity of the GR-βgal fusion protein. Data are mean±SEM of 3 independent experiments, each performed in triplicates. 2-way ANOVA was used to test the construct x DEX interaction, following by post hoc tests. *$p<0.05$, ***$p<0.001$ indicating significant difference between DEX treated and untreated. PNMT; phenylethanolamine N-methyltransferase promoter (PNMT-998/-466-Luc), that does not require GR dimerisation to be activated (Adams et al, 2003). Note that co-transfections used equal amounts of WT-GR and GR-βgal and expression of the latter was verified by βgal activity measurement in transfected cell lysates (data not shown). These data were generated by Kathryn Cockett, an undergraduate student.

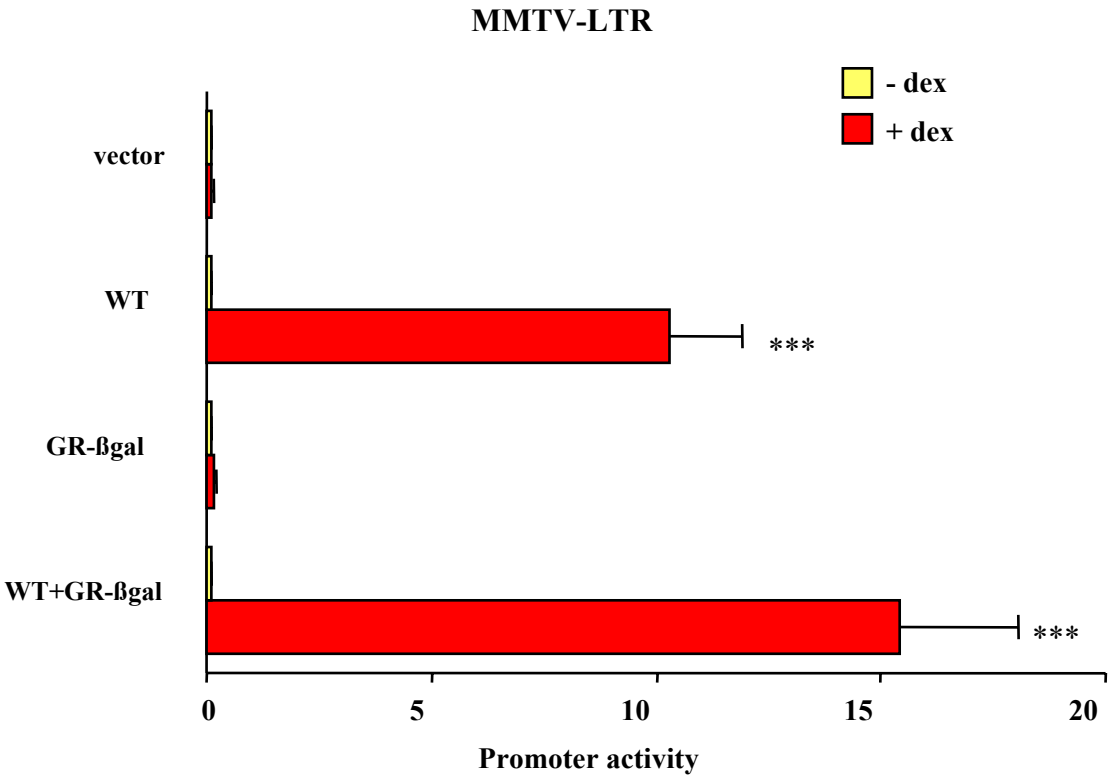

Figure 3.21 WT-GR activates the MMTV-LTR promoter in the presence of DEX, but the GR-βgal fusion protein had no effect on MMTV-LTR promoter activity.

In the absence of DEX, WT-GR or GR-βgal had no significant effect on promoter activity. DEX treatment increased WT-GR promoter activity but had no effect on the GR-βgal activity. Co-transfection of WT-GR with the mutant GR results in similar to WT-GR promoter activity after DEX treatment, ruling out a dominant negative activity of the GR-βgal fusion protein. Data are mean±SEM of 3 independent experiments, each performed in triplicates. 2-way ANOVA was used to test the construct x DEX interaction, following by post hoc tests. *$p<0.05$, ***$p<0.001$ indicating significant difference between DEX treated and untreated. MMTV; mouse mammary tumour virus promoter that requires dimerisation and DNA binding of GR to be activated. Note that co-transfections used equal amounts of WT-GR and GR-βgal and expression of the latter was verified by βgal activity measurement in transfected cell lysates (data not shown). These data were generated by Kathryn Cockett, an undergraduate student.

3.3 Discussion

The ESKN92 cell line identified during a large scale gene trap screen (Sutherland et al, 2001), and had not been extensively characterised. Furthermore, there was some uncertainty regarding the nature of the fusion product, as the preliminary 5'RACE data suggested the absence of all NLS yet it was clearly localized in the nucleus (Sutherland et al., 2001). Therefore, prior to generating the GR mutant mice, it was essential to confirm the insertion site within the GR gene.

FISH performed on ESKN92 metaphase chromosomes confirmed the location of the gene trap cassette at the GR locus on chromosome 18. In addition, FISH revealed that the gene trap is located on both chromatids of only one copy of mouse chromosome 18. This showed that the cassette had integrated at a single genomic location.

5' RACE confirmed that the cassette had inserted into the GR gene and showed that it was located in intron C. This is predicted to generate a "null" allele lacking the second ZF of the DBD and the entire LBD. Both are essential for DNA binding (Picard and Yamamoto, 1987) therefore in theory the mutant GR protein will not be able to bind its target genes. The gene trap also removes the LBD, and therefore the mutant GR-βgal protein presumably will not bind glucocorticoid.

Western blot analysis of ESKN92 cells using a GR antibody directed against the amino-terminus of GR, detected both the intact /wild type GR (95kDa) and an additional protein of 200kDa, the predicted size of the fusion protein, in both differentiated and undifferentiated ESKN92 cells. The intensity of the fusion protein band was weaker in undifferentiated compared to differentiated cells. Because transfer of large proteins maybe inefficient, any differences in GR expression between differentiated and undifferentiated ES cells must be regarded with caution. To confirm whether GR protein levels (intact and fusion) change with differentiation of ES cells and to control for equal protein transfer, future immunoblotting experiments using different GR antibodies and wild type ES cells (for the intact GR) could be informative, but were beyond the scope of this work. As the expressed fusion protein could potentially have residual function or even act as a dominant negative it was essential to characterize the activity of the encoded protein.

Although ESKN92 cells were selected on the basis of the nuclear localization of the βgal fusion protein (Sutherland *et al*., 2001), the 5' RACE showed that the fusion protein was missing both NLS of GR. The nuclear localization of the GR-βgal fusion protein is therefore perplexing. Immunofluorescence, using a β-gal antibody to detect the fusion protein, showed that in both undifferentiated and differentiated ESKN92 cells the fusion protein was diffusely located in both the cytoplasm and nucleus. These observations could reflect a unique property of the undifferentiated ES cells or could be due to other NLS not previously described. To test the former possibility, the cells were differentiated. However, the localisation pattern of the

fusion protein was not affected by differentiation. The fusion protein is too big to passively diffuse into the nucleus, therefore this may reflect the presence of the fusion protein in the nucleus, as originally reported (Sutherland et al, 2001) or may be due to fusion protein immunostaining in the cytoplasm overlying the nucleus. Future examination by confocal microscopy should provide more accurate information regarding the localization of fusion protein. In any case, ESKN92 immunofluorescence experiments suggest that the GR-βgal fusion protein is mis-localised and transfection experiments indicate that it is probably non-functional. To shed further light on the localization of GR in ES cells, expression of intact GR was examined in a parental (WT) ES cell line. Similar to ESKN92, GR immunostaining in WT cells appeared to be also in the nucleus. It still remains puzzling how (a) intact GR in the WT ES cells can be detected in the nucleus in the absence of ligand and (b) a proportion of the fusion protein inserts into the nucleus when both NLSs are missing, since it is widely accepted that GR has two NLSs, one located to the second ZF (NL1) and the other to the LBD (NL2) (Picard and Yamamoto, 1987). One hypothesis could be that a third NLS exists in GR that has not been described previously. Alternatively, GR maybe trans-locates into the nucleus complexed to other NLS-containing proteins, but this will need further investigation. Previous experiments have only examined nuclear translocation of transfected (over-expressed) GR and not expressed at physiological levels. Finally, translocation of GR into the nucleus might happen via an ES cell-specific mechanism.

The intact (WT) GR was located in large punctuate foci in the nucleus in undifferentiated ESKN92 cells, and also diffusely in the cytoplasm, with a few smaller focal patterns and along the cytoskeleton periphery. The same distribution was observed in the parent WT ES cell line. Similar results were obtained using medium containing charcoal-stripped serum, therefore it is unlikely that the nuclear localization was due to residual GC in the serum. These results are surprising, since it is accepted that the unliganded GR is located in the cytoplasm and that receptor translocation into the nucleus occurs after hormone binding (Picard and Yamamoto, 1987; Beato, 1989; Jewell et al, 1995). It has been previously reported that GR accumulates in clusters in the nucleus only after agonist treatment using immunofluorescence on fixed cells representing a number of human and rat cell lines (Van Steensel et al, 1995). This pattern was also observed, using confocal laser scanning microscopy, for a green fluorescent protein (GFP)-tagged GR in living cells after DEX treatment (Htun et al, 1996). However, one study in A549 human alveolar cells reported that GR was located both in the cytoplasm and nucleus, with a stronger signal in the nucleus (Jaffuel et al, 1999). The discrepancies in the above studies could be due to differences in methodology, cell types, transfected *vs* non-transfected and antibodies used.

The experiment designed to investigate the response of GR-βgal fusion and intact/WT GR proteins to DEX showed that the fusion protein (detected with βgal) does not respond to DEX, as predicted. In contrast, there was an increase in the GR signal in the nucleus of undifferentiated and differentiated WT and ESKN92 cells

following DEX. WT cells responded more robustly to DEX by displaying a stronger nuclear signal and a weaker (almost undetectable) cytoplasmic signal compared with untreated cells. ESKN92 cells also seemed to respond to DEX by increasing the intensity of nuclear signal (to a lesser extent than WT cells) but still there was a detectable cytoplasmic signal. This is likely due to the fact that the GR antibody used can detect both the WT GR and GR-βgal fusion protein in ESKN92 cells. However, to confirm the difference between treated and untreated cells it would be better to treat the cells with dexamethasone for longer (30 minutes to an hour) since complete translocation of GR has been observed at 30 minutes (Htun et al, 1996). Also, future immunofluorescence experiments should include a cell line (i.e. A549) as a control to exclude the possibility that the WT GR distribution observed in this study is due to the GR antibody used.

What could be the determinants of the large focal domains (punctate pattern) to which GR localize in the ESKN92 and WT ES cells? From separate examination of the DAPI and FITC channels it is obvious that the GR clusters can not be associated with heterochromatin (round white full spots in DAPI) or nucleoli (seen as holes in DAPI). Splicing speckles, RNA polymerase II (poly II) and coilin are unlikely to form these clusters with GR (Sutherland, personal communication). Splicing speckles usually do not tend to form round clusters, poly II forms smaller foci than the ones observed here and coilin forms only 2-3 focal domains per cell (Sutherland, personal communication). Moreover, van Steensel et al showed that GR clusters (or foci) do not colocalize with newly synthesized pre-mRNA, poly II or splicing factor

SC35 proposing that the observed GR clusters are not involved in transcription activation (Van Steensel et al, 1995). An attractive hypothesis proposes that GR foci may represent receptor storage sites (Van Steensel et al, 1995). A similar hypothesis has also been proposed for splicing speckles based on the observation that accumulation of splicing factors into large foci occurs after transcription inhibition and not when transcription is active (Jimenez-Garcia and Spector, 1993; Wanskink et al 1993; Sutherland et al, 2001).

In the present study, a possible candidate that might co-localize with GR containing foci could be the promyelocytic leukemia (PML) nuclear bodies, which usually appear round but finer bright spots in nucleus (illustrated in fig. 3.22). The average mammalian cell contains 10-30 PML nuclear bodies per nucleus which have been associated with transcription, DNA repair, viral defence, stress, cell cycle regulation, proteolysis and apoptosis (Maul et al, 2000; Borden, 2002; Ching et al., 2005). For the above reasons, future experiments will test this hypothesis by immunofluorescence using dual labeling (an antibody against PML bodies together with the GR antibody).

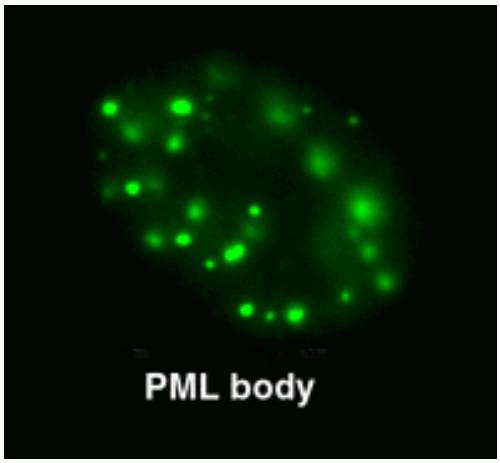

Figure 3.22 PML nuclear bodies in a cell nucleus (taken from http://npd.hgu.mrc.ac.uk/compartments.html).

It is intriguing that the large foci containing GR are not detected following differentiation of ESKN92 or WT cells. The GR signal in differentiated WT cells was detected both in the cytoplasm and nucleus in a diffuse pattern with a stronger signal still observed in the latter. These results are in accordance with the literature (van Steensel et al, 1995; Jaffuel et al, 1999). It can be speculated that differentiated cells are more transcriptionally active, with GR appearing in small diffuse foci, whereas in undifferentiated cells the large GR clusters may represent storage sites. Although it was beyond the scope of this thesis, in the future it will be very interesting to explore the mechanisms behind these pronounced differences.

Finally, the question regarding the nature (null, hypomorphic or dominant negative) of the GR-βgal allele was addressed by recreating it and testing its ability to activate glucocorticoid-responsive reporters (PMNT and MMTV) in transiently transfected HEK293 cells. The GR-βgal fusion protein appears to be transcriptionally inactive.

The possibility of it acting as a dominant negative allele was ruled out since the mutant GR failed to interfere with the WT-GR when co-transfected, and the response of promoter activity to DEX was similar to that of WT-GR alone. Overall, the results suggest that the GR-βgal is a null allele. Therefore, ESKN92 cells were considered suitable to generate GR mutant mice. The β-gal cassette will also provide a valuable reporter of GR promoter activity in vitro which could be explored further in the future.

Chapter 4

B6N92 mouse line generation

4.1 Introduction and Aims

Although lines of mice with reduced or eliminated GR have been generated (described in section 1.6.2), the effect of homozygous or heterozygous disruption of the GR gene upon adiposity and body composition in mice has not previously been described. The disruption of the GR gene with the *β-geo* cassette in ESKN92 cells provides a way to study the effects of altered GR gene dosage on body composition and fat distribution. An additional advantage of the use of ESKN92 cells to generate $GR^{+/\beta geo}$ mice (referred to as $GR^{+/-}$ throughout this Thesis) is that expression of the GR-βgeo (or βgal) fusion protein is under the control of the endogenous GR promoter and therefore acts as a "reporter" of promoter activity, allowing ready detection of expressing cells/tissues. In chapter 3, I showed that the resulting fusion protein lacks part of the DNA binding domain and the entire ligand binding domain and is transcriptionally inactive. In this chapter, the generation and breeding strategy of two mouse lines – on either C57BL/6J or 129Ola genetic backgrounds - from ESKN92 cells (described in chapter 3) is presented. The reason for choosing 2 different genetic backgrounds was because on C57BL/6 mice are prone to develop diet-induced obesity (DIO) whereas on 129Ola are resistant to DIO (http://jaxmice.jax.org/). Unfortunately the generation of $GR^{+/-}$ on 129 Ola background was not successful, thus the mice were bred only onto C57BL/6 background. The MGI nomenclature of the GR-trapped mouse line generated here is *Nr3c1*$^{Gt(ESKN92)mrchgu}$ indicating the gene trap (Gt) allele of the GR gene, in mutant ES cell line ESKN92, made by the MRC Human Genetic Unit, Edinburgh (http://www.informatics.jax.org/mgihome/nomen/gene.shtml#iim). However, for

simplicity reasons here is refered as B6N92 line. Finally, here I validate and quantify the actual GR expression levels in this model.

4.2 Results

4.2.1 Generation and breeding of B6N92 and 129N92 transgenic lines

4.2.1.1 Generation of chimeric mice

$GR^{+/-}$ mutant mice were generated from ESKN92 cells (Sutherland et al, 2001) by blastocyst injection (animal facility staff). C57BL/6J blastocyst recipients at 2.5 d post coitum (dpc) were injected with early passage (passage 4) ESKN92 cells. Five chimeras (identified by a mottled coat colour), four male and one female, designated chimera 1, 2, 3, 4 and 5 respectively, were obtained (Table 4.1). Each chimera was mated with a C57BL/6J mouse. Chimera 3 (male) gave 6 cinchilla offspring (indicating they were derived from the ES cells and not the C57BL/6J host blastocyst), 5 of which produced a PCR product with lacZ primers (figure 4.1 and data not shown), and therefore carried the β-geo cassette. Chimera 1 (male) produced 1 chincilla pup which did not carry the β-geo transgene (data not shown). Chimeras 2, 4 and 5 did not produce any offspring when crossed to C57BL/6 (summarised in Table 4.1).

To establish the line on a 129Ola background (the same as the ESKN92 cells; 129N92), chimeras 1 and 3 (which had already produced offspring with C57BL/6J females) were mated with 129Ola females. Chimera 1 mated with 129Ola produced 44 offspring but none carried the transgene (Table 4.1). Chimera 3 did not produce any offspring (summarised in Table 4.1). Therefore the breeding on 129Ola was stopped.

Table 4.1 Chimeric cross strategy and genotyping of offspring

MOUSE LINE	CHIMERA	SEX	CROSSED TO BACKGROUND	N^{O} OF OFFSPRING	N^{O} OF *LACZ* +VE (+/-)
B6N92 (ESKN92)	1*	♂	C57BL/6	1	0
	2	♂		0	-
	3†	♂		6	5
	4	♂		0	-
	5	♀		0	-
129N92 (ESKN92)	1*	♂	129 Ola	44	0
	3†	♂		NONE	NONE

* and † indicate that is the same chimera 1 and 3 respectively; NONE indicates that there are no offspring born.

4.2.1.2 Genotyping of transgenic mice for LacZ transgene expression

GR heterozygous mice ($GR^{+/-}$) carrying both a wild type allele (*LacZ* negative) and the GR-βgeo allele (*LacZ* positive) were identified by PCR with primers which amplified a 413 bp fragment of the *LacZ* transgene. The primers and amplification programme used are described in section 2.2.1.2.2 (Table 2.4). The *LacZ* genotyping PCR protocol is used throughout this thesis and has previously been used in the Bickmore laboratory, MRC Human Genetics Unit, Edinburgh (Heidi Sutherland, personal communication, details in section 2.2.1.2.2). Heterozygous mice ($GR^{+/-}$) were distinguished from wild type mice ($GR^{+/+}$) by visualisation of the 413 bp band after resolution of PCR products on a 2% agarose gel. A βglobin internal control confirmed the integrity of DNA in all samples. Figure 4.1 shows a typical genotyping PCR of offspring from a heterozygous x wild type cross.

4.2.1.3 Establishment and propagation of B6N92 transgenic mouse line

Offspring of chimeric mice were subsequently backcrossed onto the C57BL/6 genetic background to produce a congenic line (>10 backcrosses, designated B6N92). The genotypes of litters were assayed by *LacZ* PCR (section 4.2.1.2) and analysed for the predicted 1:1 Mendelian ratios of wt:heterozygotes. Table 4.2

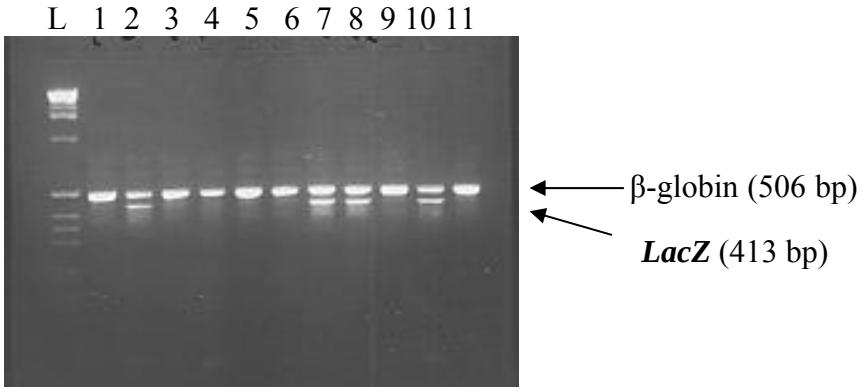

Figure 4.1 Representative gel showing PCR genotyping of $GR^{+/-}$ mice

Heterozygous mice (het) carrying a wt allele (*LacZ* negative) and the ESKN92 GR-βgeo allele (*LacZ* positive) were identified by PCR using primers which amplify a 413 bp fragment of the *LacZ* transgene. A 506 bp PCR product from the β-globin gene serves as a positive control for the presence of DNA and successful PCR. L indicates 1kb DNA ladder, 1-9 are DNA from offspring (from het x wt cross), 10 is a +ve LacZ DNA control and 11 is a –ve LacZ control. Both controls were gifts from Heidi Sutherland. Offspring 2, 7 and 8 all carry the GR-βgeo allele (*LacZ* positive).

Table 4.2 Genotype analysis of $GR^{+/-}$ backcross progeny

GENERATION	C57BL/6 BACKGROUND %	MEAN±SEM LITTER SIZE	GENOTYPES		TOTAL	HETEROZYGOUS %
			+/+	+/-		
N1	75%	7±1	6	8	14	57%
N2	87.5%	7±1	33	21	54	39%
N3	93.7%	8±1	37	42	79	53%
N4	96.9%	6±1	9	10	19	53%
N5	98.5%	6±1	136	115	251	46%
N6	99.3%	5±1	6	10	16	62%
F7	99.7%	6±1	18	16	34	47%
N8	99.9%	6±1	10	8	18	44%
TOTAL		***6±1***	***255***	***220***	***475***	***46.3%***

shows that the ratio wt:heterozygotes approximate to the predicted Mendelian ratio (slightly fewer than 50% heterozygotes; 46.3%). The slight under-representation of heterozygotes from the B6N92 line might suggest that the survival of heterozygotes is compromised. However, genotyping by PCR carries a risk of false negative results, which must be considered when analysing the percentages of heterozygous offspring. The backcrosses were continued and currently the line reached N9 (9 generations of backcross with C57BL/6J meaning this genotype contributed 99.997% of the genome).

4.2.2 Production of homozygous mutant mice

Whilst B6N92 mice are not fully congenic with C57BL/6 before F10, due to time constrains mice from intermediate generations phenotypically characterized. To determine whether the GR-βgeo allele is a "null" allele and therefore predicted to be lethal at birth (Cole et al., 1995) $GR^{+/-}$ mice (F3 or F7) were intercrossed. 146 progeny were generated from these crosses and their genotypes analysed by *LacZ* PCR to identify mice that carry the transgene (Table 4.5). The results for the B6N92 line are consistent with lethality of homozygousity for the GR-βgeo allele , predicted to give a ratio of 2:1 for *LacZ* positive:negative offspring (compared to 3:1 predicted if homozygotes survived).

Of 146 progeny survived to adulthood from 32 litters (~ 4-5 progeny/litter), 60% carried the *LacZ* transgene and 40% did not (*LacZ* negative) and were therefore wt (Table 4.5). In addition, ~7% (10 out of 156 born in total) of which were found dead

at approximately 3 weeks (mean 27.5±1.5 days) after birth. However, it is possible that some heterozygote embryos fail to survive. Thus, C57BL/6 heterozygous mice can breed, but perhaps there are also problems with the heterozygotes during embryonic development.

4.2.2.1 Genotyping of homozygous $GR^{-/-}$ mice by PCR

The site of the gene trap cassette within the itron between exons 3 & 4 was determined. To locate the site and thus identify $GR^{-/-}$ mice, a series of primers was designed to PCR the engrailed gene (en2; primer details in Appendix C) and GR intronic sequences (fig. 4.2). All attempts were unsuccessful (data not shown). It is possible that the splice acceptor (SA) region of *β-geo* has been disrupted in some way during integration. This problem was also encountered in other transgenic lines generated by gene trap approach (Heidi Sutherland, personal communication). Accordingly, an alternate strategy was adopted. Because the cassette is >4kb, integration would disrupt a PCR reaction where the primers spanned the integration. A series of primers (fig. 4.2A, arrows and fig. 4.2B predicted genotype results) were designed to PCR "walk" across the intron between exons 3 & 4. The primer sequences and PCR amplification programme are described in detail in section 2.2.1.2.2 (Table 2.4) and Appendix C. Previous reports predict that the allele would not be embryonic lethal (Cole et al., 1995). Accordingly, to ensure representation of homozygotes, genomic DNA from E18.5 embryos was subject to PCR. All primer pairs except one gave the predicted product from all the DNA samples. For the "red" primer pair (fig.4.2), a 470bp product was produced from 6 of the DNA samples but

not from the other 3 (fig. 4.3). All except samples 2&3&8 yielded a 413bp *LacZ* product (summarized in Table 4.4) indicating they are $GR^{-/-}$. The embryos were also stained with X-gal (fig. 4.4). Embryos 1 & 6, which tested negative for the *LacZ* transgene, did not stain with X-gal confirming the $GR^{+/+}$ genotype. Although non-quantitative, embryos 2 & 3 & 8, which were genotyped as $GR^{-/-}$, showed the strongest stain with X-gal (Table 4.4, fig. 4.4) consistent with expression of the GR-βgeo transgene in these embryos. A total of 60 embryos were genotyped (Table 4.5). The results showed fewer than expected $GR^{+/-}$ (36.7% instead of 50%), close to the expected number of $GR^{-/-}$ (26.6%), but a higher percentage for $GR^{+/+}$ (36.7% instead of 25%). To confirm the homozygous and heterozygous mice as identified by PCR, the generation of a Southern blot assay will be informative. A greater number of adult progeny will need to be assessed in this line to conclude the phenotype of homozygous lethality.

4.3 Adult $GR^{+/-}$ mice show reduced GR expression

All the GR expression analysis data presented here were performed on F5 adult $GR^{+/-}$ mice and littermate controls ($GR^{+/+}$). GR mRNA levels were measured in a variety of tissues while protein levels in a subset.

(A)

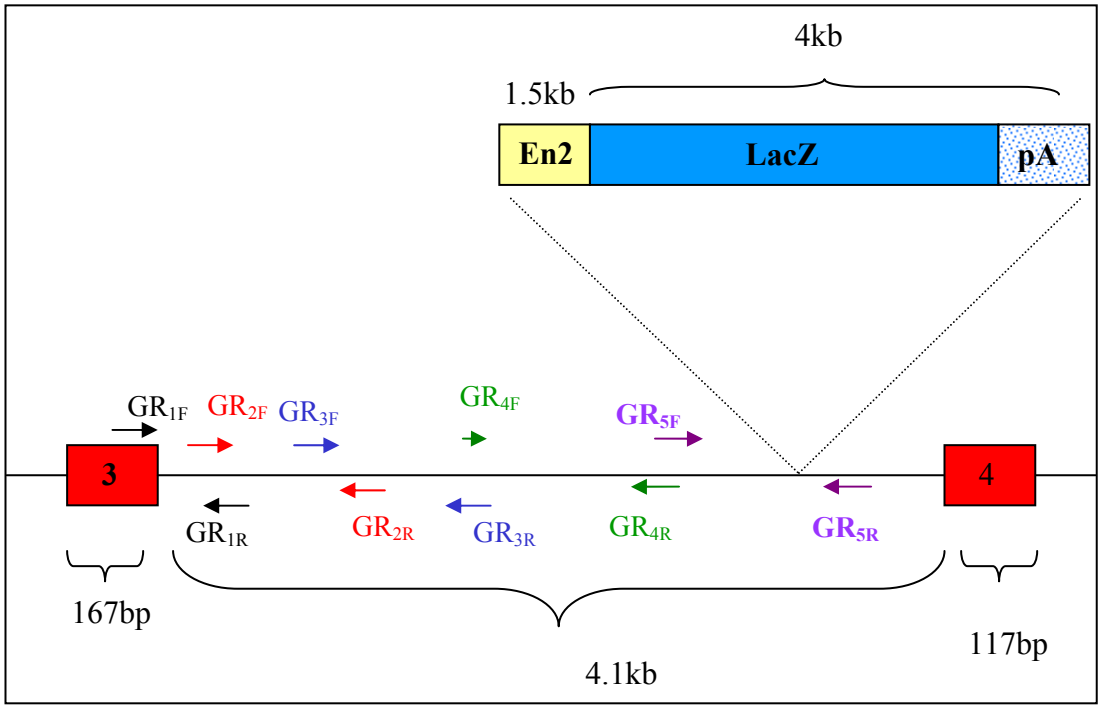

B) Predicted results from LacZ and GR PCR assays

	GENOTYPES		
PCR primers	+/+	+/-	-/-
lacZ (413bp)	-	√	√
GR (470bp)	√	√	-

Figure 4.2 A schematic view of the GR PCR primers designed for the identification of $GR^{-/-}$ mice and predicted results.

(A) 5 sets of GR primers (arrows with same colour represent a set of primers) were designed to amplify sequences within intron C, where 5'RACE results (section 3.2.2, fig. 3.4) showed that the gene trap was integrated. The numbers refer to sizes of exon3 (167bp), intron C (4.1kb), en2 intron (1.5kb) and gene trap cassette (~4kb) and exon4 (117bp) (B) summary of the predicted results to identify wild type (+/+), heterozygous (+/-) and homozygous (+/-) mice. Heterozygotes carry both the wt allele (470 bp band; purple set of primers) and the gene-trap allele (LacZ; 413 bp band). Homozygotes carry the gene-trap allele only (two copies of *LacZ*,) and therefore only the 413 bp band and not the wt allele would be seen on a gel. Wild type mice carry only the GR wt allele.

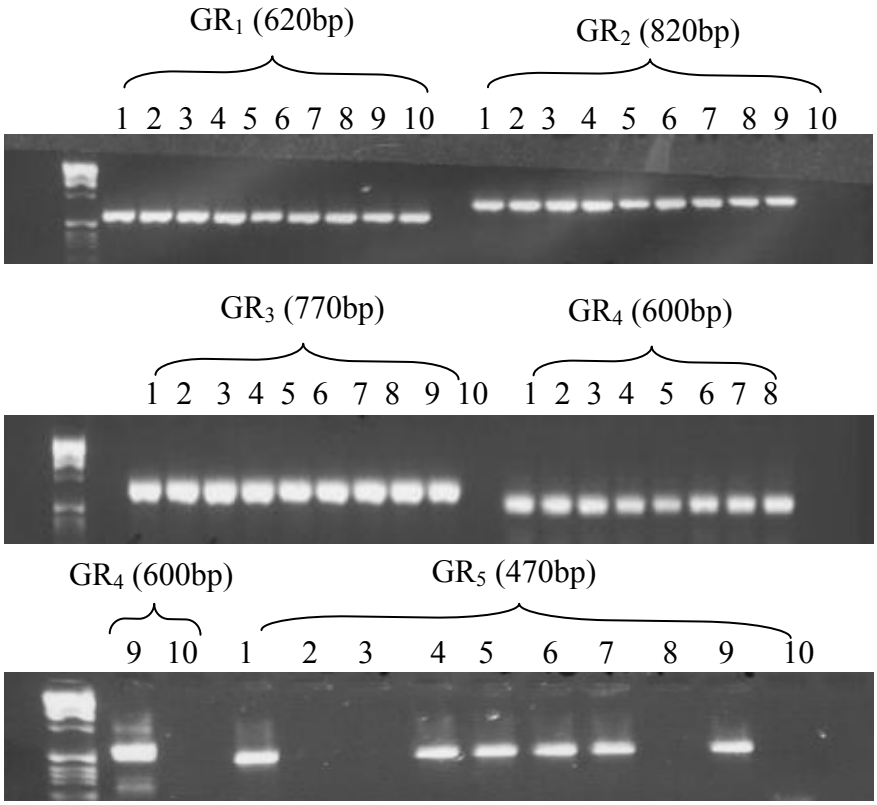

Figure 4.3 PCR of E18.5 DNA from heterozygous intercross using primers from intron C.

A PCR with 5 sets of GR primers (1-5)(amplifying various intronic C sequences; see figure 4.2) was performed using DNA from 9 E18.5 embryos to identify the site of integration and thus the appropriate set of primers to be used for the $GR^{-/-}$ genotyping. PCR products were resolved on a 2% agarose gel. In each case, lanes 1-9 contain DNA from embryos, lane 10 is a negative control (no DNA). GR primers amplifying a 470bp region from intron C were used for the $GR^{-/-}$ genotyping. Embryos 2, 3 and 8 lack the 470 bp band identifying them as homozygous. For details on the primers used refer to Appendix C (Table C.1).

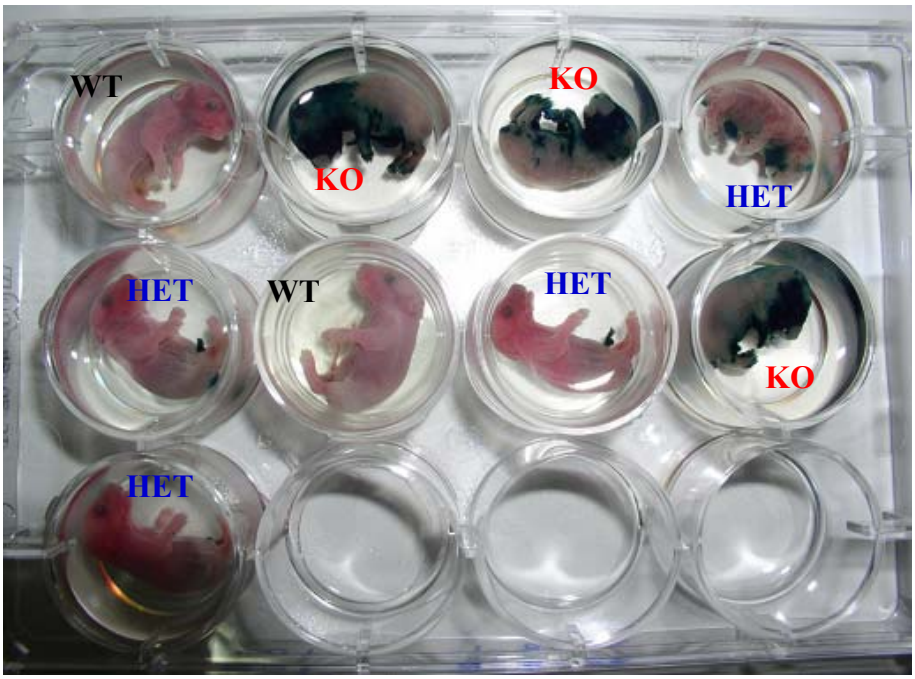

Figure 4.4 X-gal staining of whole E18.5 embryos.

E18.5 embryos from a heterozygous intercross (F7) were harvested, washed briefly in PBS, fixed in LacZ fixative for 3 hours at 4^0C. They were then washed twice with LacZ wash for 15 minutes, stained overnight in LacZ staining buffer at 37^0C and then transferred into PBS. Note intense blue stain in the $GR^{-/-}$ (KO), less stain in $GR^{+/-}$ (HET) and no stain in $GR^{+/+}$ (WT).

Table 4.4 Combined results from LacZ and GR PCR reactions to identify genotypes, and X-gal staining of E18.5 embryos from a heterozygous intercross.

EMBRYO ID	*LACZ* (413BP)	GR (620BP)	GR (820BP)	GR (770BP)	GR (600BP)	GR (470BP)	XGAL STAIN	GENOTYPE
1	-	√	√	√	√	√	-	+/+
2	√	√	√	√	√	-	+++++	-/-
3	√	√	√	√	√	-	+++++	-/-
4	√	√	√	√	√	√	+++	+/-
5	√	√	√	√	√	√	+	+/-
6	-	√	√	√	√	√	-	+/+
7	√	√	√	√	√	√	+	+/-
8	√	√	√	√	√	-	+++++	-/-
9	√	√	√	√	√	√	+	+/-

Embryos 2, 3 and 8 are homozygous (-/-), carrying only the LacZ transgene (note absence of GR470bp band) and stain strongly with X-gal (+++++). Embryos 4, 5, 7 and 9 are heterozygous (+/-), carrying both the LacZ and GR bands and show less X-gal staining (+ to +++). Embryos 1 and 6 are wild type (+/+), carry only the GR band (note absence of LacZ band) and do not stain with X-gal. √ indicates the presence of band (either LacZ or GR or both), - absence of band and + X-gal staining with increasing numbers of + indicating increasing intensity of staining.The *LacZ* (413bp) and GR (470bp) primers could not be combined in the same PCR due to very similar PCR product sizes (data not shown). Therefore two sets of PCRs were performed on all embryos/progeny from a het x het cross.

Table 4.5 Genotype analyses of $GR^{-/-}$ intercross progeny.

GENOTYPES						
Stage	**Generation**	+/+	+/-	-/-	**Total**	***% wt:het:ko***
Adult	F3	60	85	1	146	*~60% hets*
E11.5	F7	3	2	1	6	*36.7% wt*
E14.5	F7	4	2	1	7	*36.7% het*
E15.5	F7	2	2	3	7	*26.6% ko*
E16.5	F7	2	3	5	10	
E17.5 (x2)	F7	5 4	6 3	1 2	21	
E18.5	F7	2	4	3	9	

The expected Mendelian ratio from a heterozygous intercross is 1:2:1 (wt:het:homo).In the adult F3 offspring, the ratio is 60:85:1. If the data are analysed, excluding the one homozygous mouse, the ratio wt:het should be 48:97, however, here it is 60:85 (for a total of 145 mice). A Chi-square analysis with Yates correction gave a value of 3.9, $p<0.05$. This suggests that the heterozygous mice are under-representative in the adult population. If all the pre- and post-natal mice are added up, the ratio is 82(wt):107(het):17(homo). If the homozygous mice are excluded from the analysis, for a total of 189 mice, the expected Mendelian ratio should be 63(wt):126(het). A Chi square analysis gave a value of 8.15, $p<0.05$ suggesting again that het mice are under-representative.

4.3.1 Reduced GR mRNA levels in $GR^{+/-}$ peripheral tissues by real time PCR

To estimate the reduction of GR mRNA levels in $GR^{+/-}$ mice in various peripheral 'metabolic' tissues (adipose, muscle, adrenal, liver), RNA was extracted, reverse transcribed and analysed by real time PCR using a commercial GR primer-probe specific for exons 5-6 (missing from the mRNA encoding GR-βgeo, details in section 2.2.1.1.4.2.). β-actin (for validation see section 2.2.1.1.4.3) was used as an internal standard to correct for RNA concentration. Negative controls omitting reverse transcriptase (Superscript III) or RNA were included in every assay. Table 4.6 shows that loss of one functional GR allele in the $GR^{+/-}$ mice resulted in 45-50% lower levels of GR mRNA in all fat depots examined (epididydymal, inguinal, mesenteric), ~60% lower in muscle (soleus and extensor-longus digitalis; EDL), 30% lower in the liver and 65% lower in the adrenal gland.

4.3.2. *In situ* hybridization showed reduced GR mRNA levels in $GR^{+/-}$ brain.

GR mRNA was localised to all subfields of the hippocampus (CA1, CA2, CA3) and the dentate gyrus (DG), the paraventricular nucleus (PVN) of the hypothalamus and the pituitary gland, in both wild type and heterozygous mice (fig.4.5). Consistent with previous data in brain (Herman *et al.* 1989), expression of GR mRNA was highest in CA2 and DG, with lower levels in CA1, 3 in both genotypes. Nevertheless, $GR^{+/-}$ mice showed a ~50-60% reduction in GR mRNA levels in all fields of the hippocampus (fig. 4.5A-C, Table 4.6), 60% in the pituitary (fig. 4.5D, Table 4.6) and 50% in the PVN (fig. 4.6B, E, F, Table 4.6).

Table 4.6 $GR^{+/-}$ mice have decreased GR mRNA levels in the brain and peripheral tissues.

TISSUES	$GR^{+/+}$	$GR^{+/-}$	REDUCTION %	*P VALUE*
BRAIN	**GR mRNA LEVELS (AU)**			
Hippocampus: CA1	0.4±0.05	0.2±0.03	**50%**	***0.002***
CA2	0.5±0.06	0.2±0.05	**60%**	***0.003***
CA3	0.14±0.01	0.06±0.02	**57%**	***0.002***
DG	0.4±0.03	0.2±0.03	**50%**	***0.002***
PVN	0.4±0.1	0.2±0.05	**50%**	***0.05***
Pituitary	0.5±0.07	0.2±0.04	**60%**	***0.002***
PERIPHERY	**GR mRNA LEVELS (AU)**			
Adrenal	1.7±0.3	0.6±0.08	**65%**	***0.002***
Liver	1.0±0.05	0.7±0.06	**30%**	***0.002***
Epididymal fat	1.3±0.09	0.7±0.05	**46%**	***0.0002***
Inguinal fat	1.1±0.06	0.6±0.1	**45%**	***0.006***
Mesenteric fat	0.6±0.07	0.3±0.08	**50%**	***0.05***
EDL muscle	1.4±0.1	0.6±0.1	**57%**	***0.004***
Soleus muscle	1.0±0.1	0.5±0.04	**50%**	***0.002***

4.3.2.1 X-gal staining of adult brains mirrors GR mRNA expression levels.

$GR^{+/-}$ brain sections were stained with X-gal in order to investigate the GR-βgeo (will be referred as βgal) distribution pattern throughout the brain. The results showed that GR-βgal is present throughout the brain, with strongest staining in the cortex, hippocampus (CA1/2/3, DG) and PVN (fig. 4.6A,C). No staining at all was seen in $GR^{+/+}$ brains (fig. 4.6D) The staining pattern (fig.4.6A) mirrors the distribution of GR mRNA expression seen in $GR^{+/+}$ mice (fig. 4.6B).

4.3.3 GR protein levels in $GR^{+/-}$ mice by western blot analysis

GR protein levels in epididymal fat of $GR^{+/-}$ mice were analysed by western blot. The epitope of the M20 antibody (GR specific; Table 2.5) is located in the N terminus of GR and thus is present in the endogenous and fusion proteins. Figure 4.7 shows reduced levels of the 95kDa functional GR protein in epididymal fat of $GR^{+/-}$ compared to $GR^{+/+}$ littermates. Furthermore, the 191kDa GR-βgal fusion protein was evident in the samples from $GR^{+/-}$ mice (fig. 4.7).

4.4 Unaltered 11β-HSD1 mRNA expression levels in $GR^{+/-}$ mice

To investigate if altered GR density and subsequently compensatory increased corticosterone secretion (described in chapter 5) modulates expression of 11β-HSD1 (the enzyme that converts inactive to active GCs; details in chapetr 1; fig. 1.3), real time PCR was used to measure mRNA levels of the enzyme in the liver and

epididymal adipose tissue of adult $GR^{+/-}$ mice. A commercially available 11β-HSD1 set primer-probe was used (section 2.2.1.1.4.2) and three house keeping genes (β-actin, TATA binding protein; TBP and 18S ribosomal RNA; 18S) were used to correct for variations in RNA concentration between samples. The results showed that hepatic (fig. 4.8A) and epididymal fat (fig. 4.8B) 11β-HSD1 mRNA levels are similar in both $GR^{+/+}$ and $GR^{+/-}$ mice.

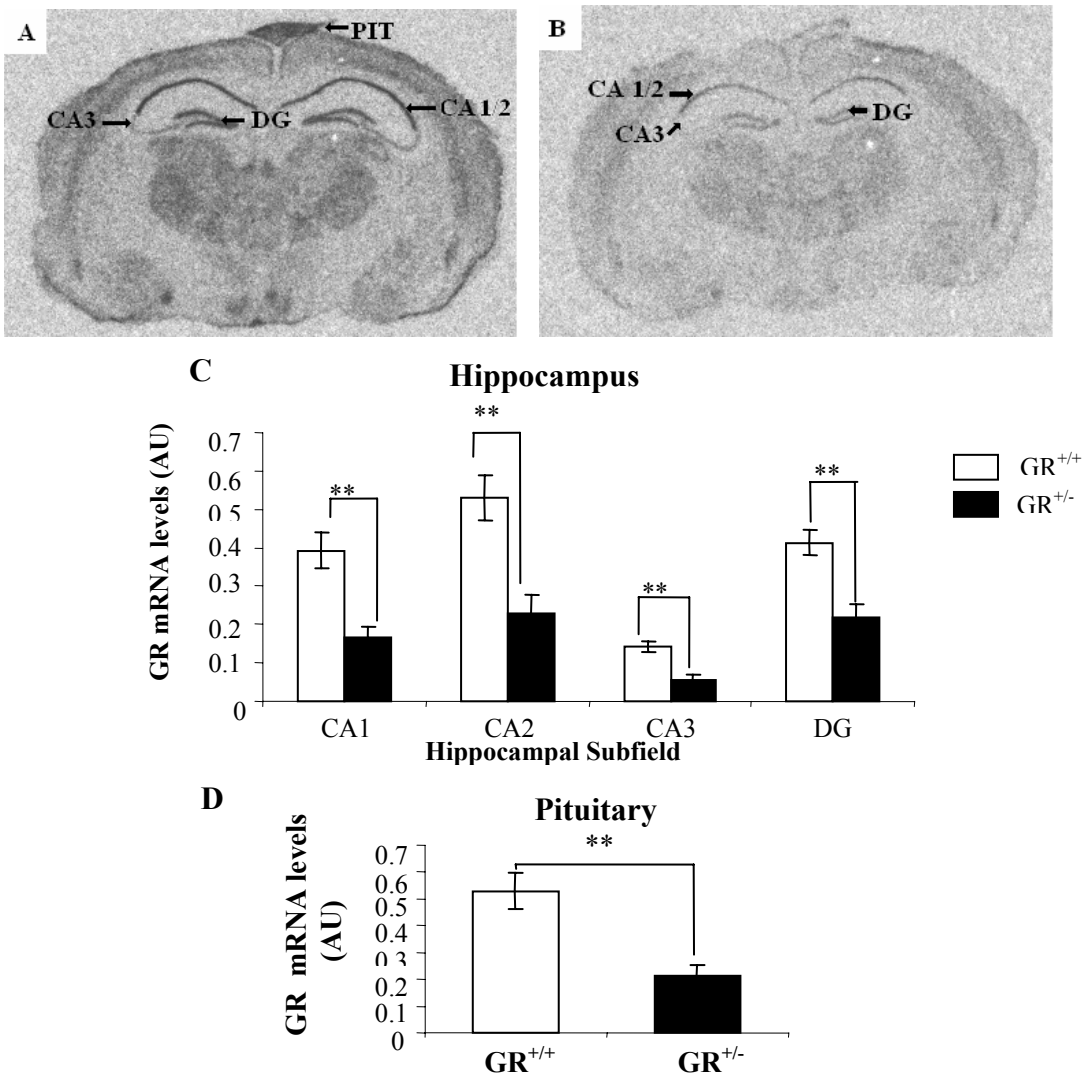

Figure 4.5 GR+/- mice have reduced GR mRNA expression in brain (hippocampus & pituitary).

A&B, Representative photomicrographs of in situ GR mRNA hybridization illustrating higher expression in wild type (A) than in heterozygous mice (B) in the CA1, CA2 and CA3 subfields of the hippocampus and in the DG. Semiquantitative analysis by optical densitometry measurements in the hippocampus (C) and pituitary (D). Two-way analysis of variance revealed a significant effect of genotype and hippocampal subfield and a significant genotype x hippocampal subfield interaction. Post-hoc paired comparisons were performed for differences between subfields. (CA1<CA2, p=0.032; CA1>CA3, p=0.032; CA1=DG, p=0.277; CA2*CA3, p<0.001). n=6/group.** p<0.01. Hippocampal subfields were defined in accordance with the stereotaxic atlas of Paxinos and Watson. Comparison of GR levels in the pituitary by Student's t test. Note that the pituitary has been moved during dissection and placed on the top of the cortex. Data presented here were produced by E. Owen, a MSc project student under my supervision.

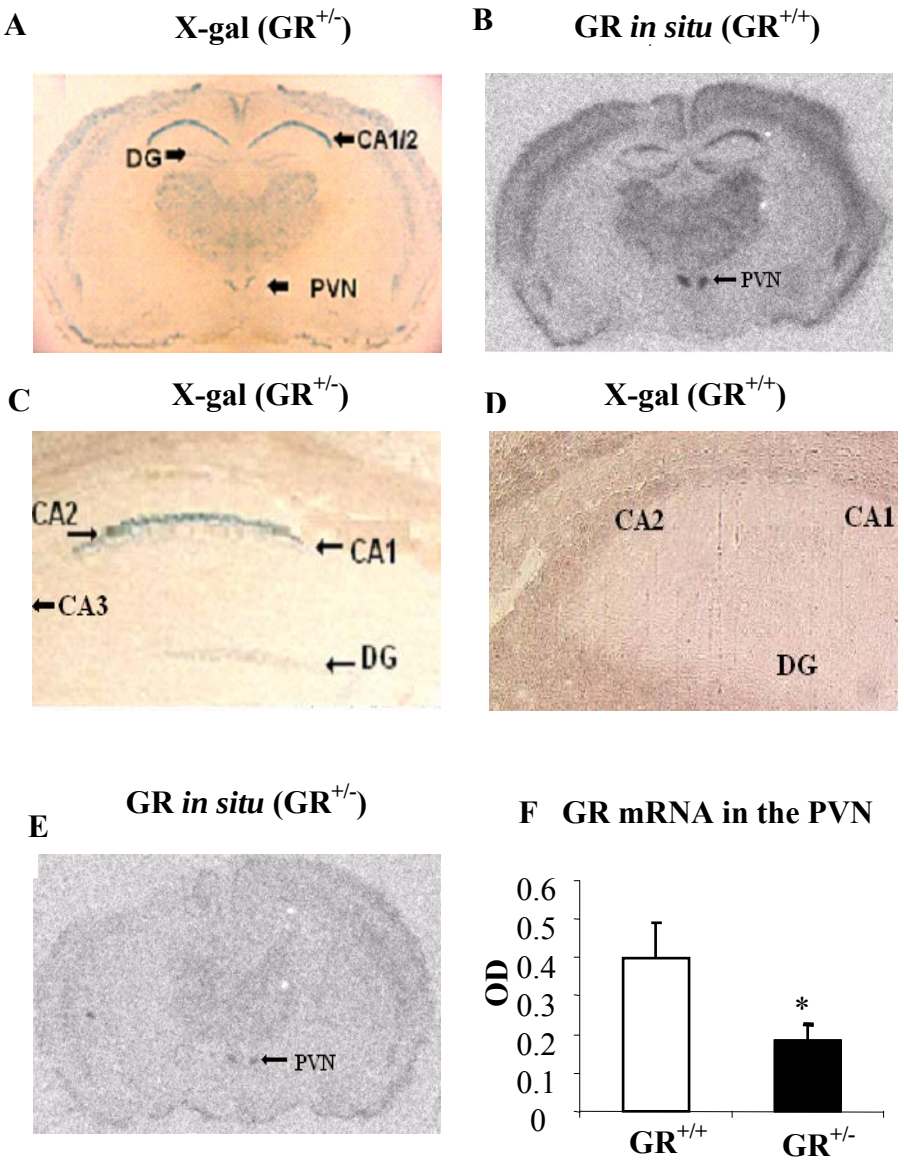

Figure4.6 The pattern of GR-βgal protein distribution mirrors the endogenous GR expression in the brain.

A) Representative brain sections from $GR^{+/-}$ mice stained with X-gal B).Representative autorad images showing *in situ* hybridization (ISH) of $GR^{+/+}$ brain sections (cortex, hippocampus, PVN), (C)-(D) Images showing X-gal staining in hippocampal subfields of $GR^{+/-}$ (C) but not $GR^{+/+}$ (D) mice, E) ISH showing GR expression in the PVN of $GR^{+/-}$ brain and F) Quantification of GR mRNA levels in the PVN of $GR^{+/+}$ (white bar) and $GR^{+/-}$ (black bar) mice showing 50% reduction in the latter. CA1/2/3; hippocampal subfields, DG; dentate gyrus and PVN; paraventricular nucleus. n=6/group, * $p<0.05$. Data presented here were produced by E. Owen, a MSc project student under my supervision.

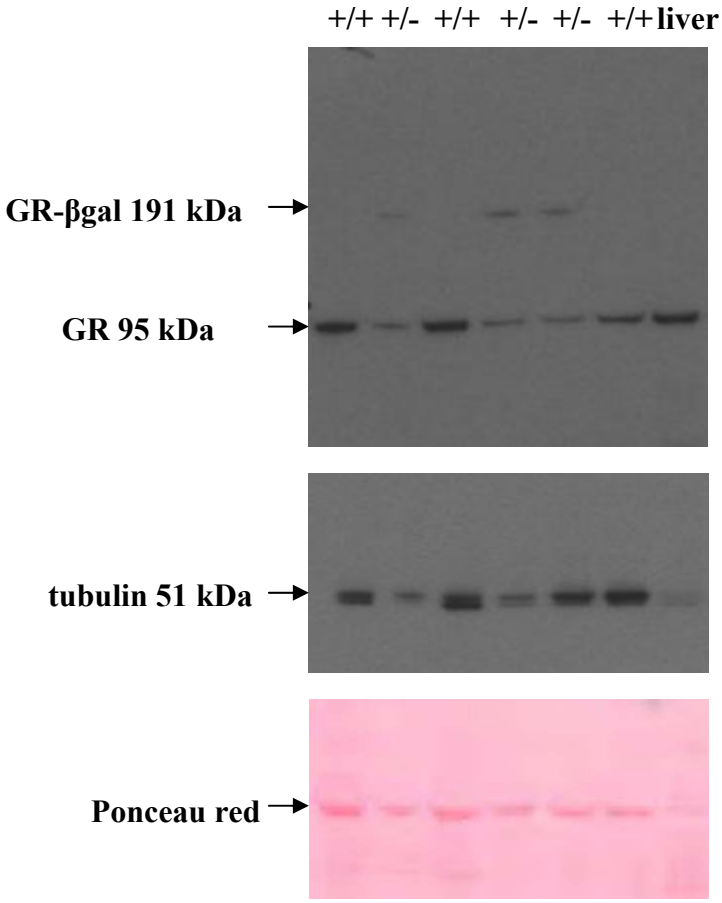

Figure 4.7 GR wild type and fusion protein levels in epididymal adipose tissue.

Representative image of western blot in which wild type (wt) GR and GR-βgal were detected in protein extracts from epididymal fat of adult male $GR^{+/+}$ and $GR^{+/-}$ mice were analysed by western blot (n=6/group). Fusion protein (191 kDa) was apparent only in the $GR^{+/-}$ mice (upper blot). Results showed decreased wt GR protein (95 kDa) levels in $GR^{+/-}$ compared to $GR^{+/+}$ mice. Rat liver protein was included in the analysis as a positive control for the wt GR protein. A tubulin specific antibody and ponceau red were used to check for control for protein loading.

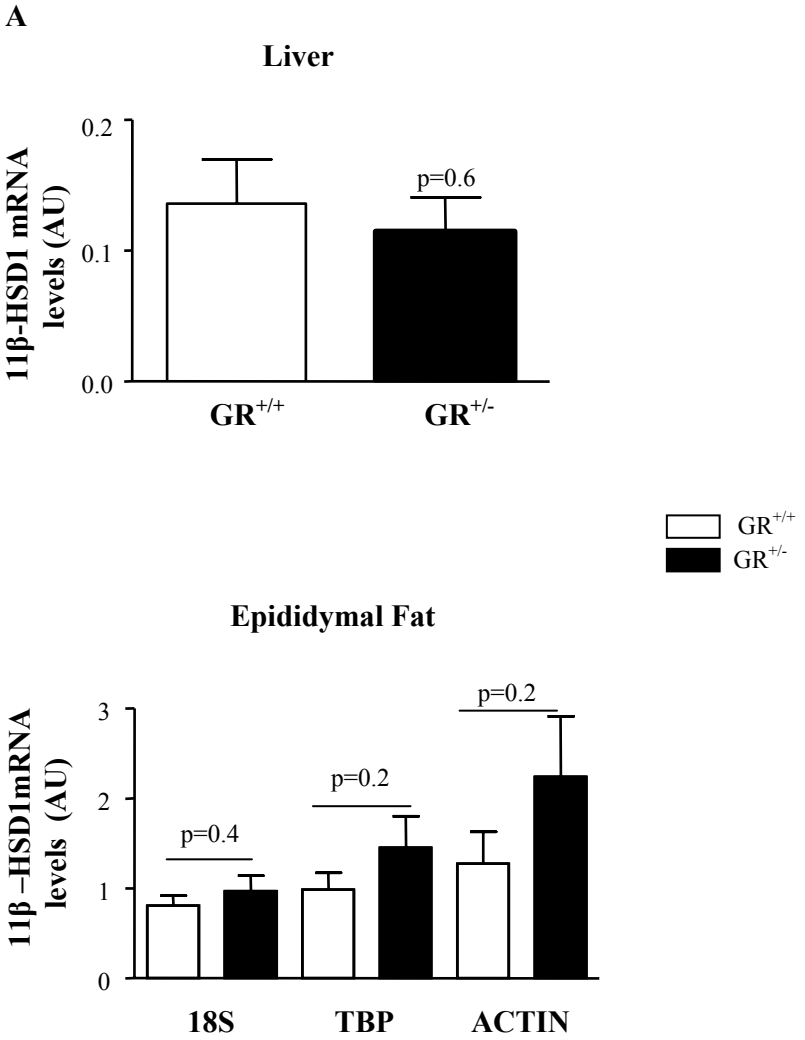

Figure 4. 8 Hepatic and adipose 11β-HSD1 mRNA levels are unaltered in $GR^{+/-}$mice. 11β-HSD1 mRNA levels were measured by real-time PCR using β-actin as an internal control in (A) liver and (B) epididymal fat. Note that in (B) irrespective of the internal control used (18S; ribosomal RNA, TBP; TATA binding protein and β-actin) the results are similar. Student's t test was performed for the comparison of mRNA levels between genotypes.

4.5 Discussion

The approach taken here to generate $GR^{+/-}$ mice has the advantage that the GR-βgal fusion protein is under the control of the endogenous GR promoter and therefore is expressed at physiological levels in the cell. Furthermore, the presence of the β-gal cassette greatly facilitates genotyping of heterozygous mice and provides a dynamic reporter of gene activity, another advantage over existing GR-deficient mice.

The B6N92 line was backcrossed onto the C57BL/6 genetic background for > 9 generations and it is therefore now 'congenic' by current standards (Banbury Conference on Genetic Background in Mice report 1996), though some 129 sequences may remain, especially around the transgene/GR locus if subject to linkage disequilibrium.

The generation of mice homozygous for the GR-βgal allele provided a way to study the potential lethality of the allele. With one exception, all homozygous mice died at birth, consistent with previous models (summarised in Table 1.1). Briefly, 10-20% $GR^{hypo/hypo}$ (hypomorphic allele) mice survived to adulthood (Cole et al., 1995) while $GR^{null/null}$ mice were all died shortly after birth (Finotto et al., 1999). Although, possibility still remains that the GR-βgal might be a hypomorphic allele, it is certainly less "leaky" (incomplete penetrance) compared to $GR^{hypo/hypo}$ since only one homozygote mice survived to adulthood and consistent with lack of transactivation capacity as shown in chapter 3 (section 3.2.5.2). Because a southern blot was not

performed in the model presented here, it still remains a possibility of a genotyping error. In the future, genotyping of offspring from intercrosses of $GR^{+/-}$ mice will be necessary to rule out the possibility of a hypomorphic allele. Interestingly, the fewer number of heterozygotes (46% instead of the expected 50%) from the B6N92 transgenic line could suggest that the survival of heterozygotes may be compromised in this line. Indeed, analysis performed using a Chi-squared test (Table 4.5) suggested that the both homozygous and heterozygous mice are under-representative, with some lost in utero and others post-natally.

Heterozygous mice have only a single intact GR allele and, as predicted, functional levels of mRNA encoding GR were decreased (30-60%) in every tissue analysed in the heterozygous mice. It is interesting that the tissue with the highest down-regulation of GR mRNA expression (65%) was the adrenal gland. Adrenal morphology is completely disorganized in $GR^{hypo/hypo}$ mice (Cole et al., 1995) and is also disrupted in $GR^{+/-}$ mice (chapter 5). Greater than 50% decrease, cannot be simply explained by autoregulation (as in tissues with <50%). It may reflect an altered adrenal morphology with different populations of cells differentially represented (eg higher expressing subset of cells may be under-represented in $GR^{+/-}$ mice). Moreover, the reduction in mRNA expression translated to reduced wild type GR protein consistent with previously reported $GR^{+/-}$ mice (Ridder et al, 2005) and the presence of the GR-βgal fusion protein in the $GR^{+/-}$ mice. Indeed, in brain, X-gal staining faithfully reflected the expected expression pattern of GR. Preliminary data have confirmed expression in both embryonic and adult tissues and highlighted

possible novel sites of expression in the former (unpublished observations). However, detailed analysis is beyond the scope of this Thesis.

The major determinants of tissue GC action, apart from GR density, are the intracellular levels of ligand, the latter determined both by activity of the HPA axis and cellular activity of 11β-HSD enzymes that interconvert active 11-hydroxy (corticosterone, cortisol) and inactive 11-keto (11-dehydrocorticosterone, cortisone) GCs. Here, I showed that 11β-HSD1 mRNA levels in 2 key metabolic tissues (liver and epididymal fat; neither of which express 11β-HSD2) are unaltered in this model of reduced GR density. This suggests that a reduction in the GR *per se* does not appear to regulate the levels of 11β-HSD1 at least in these tissues.

The following chapter describes the use of this model to investigate the effects of reduced GR density in the regulation of HPA axis, body fat distribution and metabolic parameters.

Chapter 5

$GR^{+/-}$ mice phenotyping: A model of HPA axis hyperactivity

5.1 Introduction and aims

In humans, polymorphisms in the GR gene have been linked to altered GC sensitivity and metabolic abnormalities (Rosmond et al., 2000a, 2000b, 2001). GC hypersensitivity has been associated with visceral obesity, insulin resistance, hypertension and increased cardiovascular disease risk (Buemann *et al*. 1997; Rosmond et al., 2000b; Ukkola et al., 2001; Dodson et al., 2001; van Rossum *et al*. 2003 and extensive description in section 1.6.2). However, individuals with substantially reduced GR density are very rare (details in section 1.6.2). The incidence is too low and the underlying variance in humans too great to permit effective study of the effects of GR mutations on body composition.

Given the important associations between GR polymorphisms, fat distribution and hypertension it is perhaps surprising that the effects of globally reduced (transgenic, gene targeted) GR density on body fat distribution (rather than merely whole body fat content) and blood pressure have not previously been described (discussed in section 1.6.2). GC excess (pharmacological) can induce dose-dependent increases in blood pressure and endogenous overproduction of GCs leads to hypertension both in humans and animals (Saruta et al., 1986; Grunfeld, 1990; Sholter and Armstrong, 2000). On the other hand, adrenal insufficiency or GR blockade lowers blood pressure (Gardiner and Bennett, 1983; Udelsman et al., 1986).

Several mouse lines with altered GR expression or function have been generated, and the effects on behaviour and HPA axis regulation have been extensively studied

(reviewed in Gass et al, 2001; Muller et al, 2002; Howell and Muglia 2006, Neigh and Nemeroff, 2006). As described in chapter 1 (section 1.6.1) there is limited exploration on the down-stream effects of altered GR density in peripheral and more metabolically relevant tissues.

In this chapter, the effects of "globally" reduced GR density ($GR^{+/-}$ mice) upon HPA axis function, fat distribution and glucose homeostasis under basal (chow fed) conditions and following a high fat (HF) feeding (that models a high calorie/obesity situation) are described. Furthermore, I tested if reduced GR density affects blood pressure regulation. All the experiments described here were performed on F5 $GR^{+/-}$ and $GR^{+/+}$ littermates. Basal characterization was carried out in both male and female chow-fed mice while the HF experiment was performed on male mice. Figure 5.1 summarizes the two experiments described in this chapter.

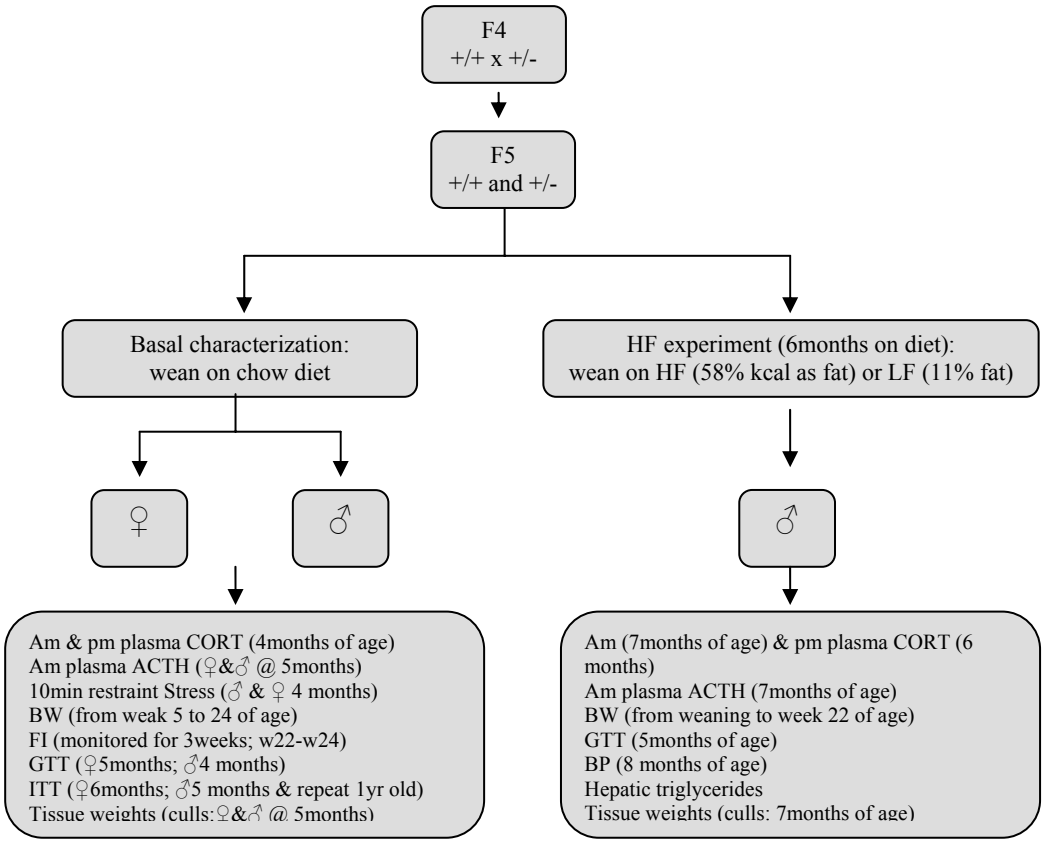

Figure 5.1 Experimental design.

Basal phenotyping was carried out in F5 chow-fed male and female mice. The HPA axis function was studied under basal conditions and acute stress (10 min restraint in a falcon tube) conditions. Briefly, mice were acclimated to single housing and tail nicks performed within 1 minute of disturbing the cage to ensure unstressed plasma corticosterone plasma levels. For corticosterone levels, sampling was performed in the nadir (7am) and peak phase (7pm). For restraint stress, tail tip blood sampling was performed at 20 and 120min after restraint. ACTH secretion was evaluated only in the nadir phase from trunk blood collected by decapitation. Body weight was monitored weekly. Food intake was monitored for 3 weeks when the mice were single caged for individual experiments. At the end of the experiment, mice were culled and tissues were dissected and weighed. To evaluate glucose homeostasis, male and female mice were subjected to glucose tolerance (GTT) and insulin tolerance tests (ITT). Animals were fasted for 6h. For GTT, 2mg/g body weight (BW) of 25% glucose was intraperitoneally (i.p) injected and tail tip blood sampling was performed at time 0 (prior to injection), 15, 30, 60 and 120min after injection. For ITT, 1mU/g BW (females) or 1.5mU/g BW (males) insulin was i.p. injected and blood sampling was performed at time 0, 15, 30 and 60min after injection and plasma glucose was measured. For the diet-induced obesity (DIO) experiment, male mice weaned on high fat (HF) or low fat (LF) control diets and remained for 22 weeks with *ad libitum* access to water and diet. All measurements performed as in basal phenotyping. Systolic blood pressure was measured in conscious warmed mice by tail cuff plethysmography using a tail cuff designed for mice (described in section 2.2.3.5).

5.3. Results

5.3.1. Experiments performed under basal (chow fed) conditions.

5.3.1.1. $GR^{+/-}$ mice show HPA axis hyperactivity and have bigger adrenals.

Nadir (morning) and peak (evening) plasma corticosterone levels as well as morning plasma ACTH levels were measured in order to assess HPA axis function in chow fed adult male and female $GR^{+/-}$ mice. Morning corticosterone levels did not significantly differ between genotypes in either gender (although there was perhaps a trend for higher corticosterone in both male (fig. 5.2A) and female (fig. 5.2C) $GR^{+/-}$ mice. However, evening circulating corticosterone levels were significantly elevated in $GR^{+/-}$ male (fig. 5.2B) and female (fig. 5.2D) mice (male $GR^{+/+}$ *vs* $GR^{+/-}$; 177±28 *vs* 277±17 nM, $p<0.01$; female, 401±35 *vs* 735±56nM, $p<0.001$). Morning plasma ACTH levels were similar in both genotypes in both males (fig. 5.3C) and females (fig. 5.3D). ACTH levels were variable between mice, possibly due to its pulsatile secretion pattern (Lappaluoto et al., 1975; Lopez et al., 1988; Carnes et al., 1989; Goodman et al., 1994 and reviewed in Gudmundsson and Carnes, 1997) and to the fact that blood sampling was performed over a somewhat broad time window (8-10am). All ACTH values measured are presented in figure 5.3A-B. This clearly shows that there are two statistical outliers from the group mean. However, even when the analysis is performed excluding these outliers, the results show that there are no differences between genotypes in either male (fig.5.3C) or female (fig.5.3D) mice, and they are included here to highlight the inherent variability in this parameter. The HPA axis response to an acute restraint stress was assessed in $GR^{+/-}$ mice.

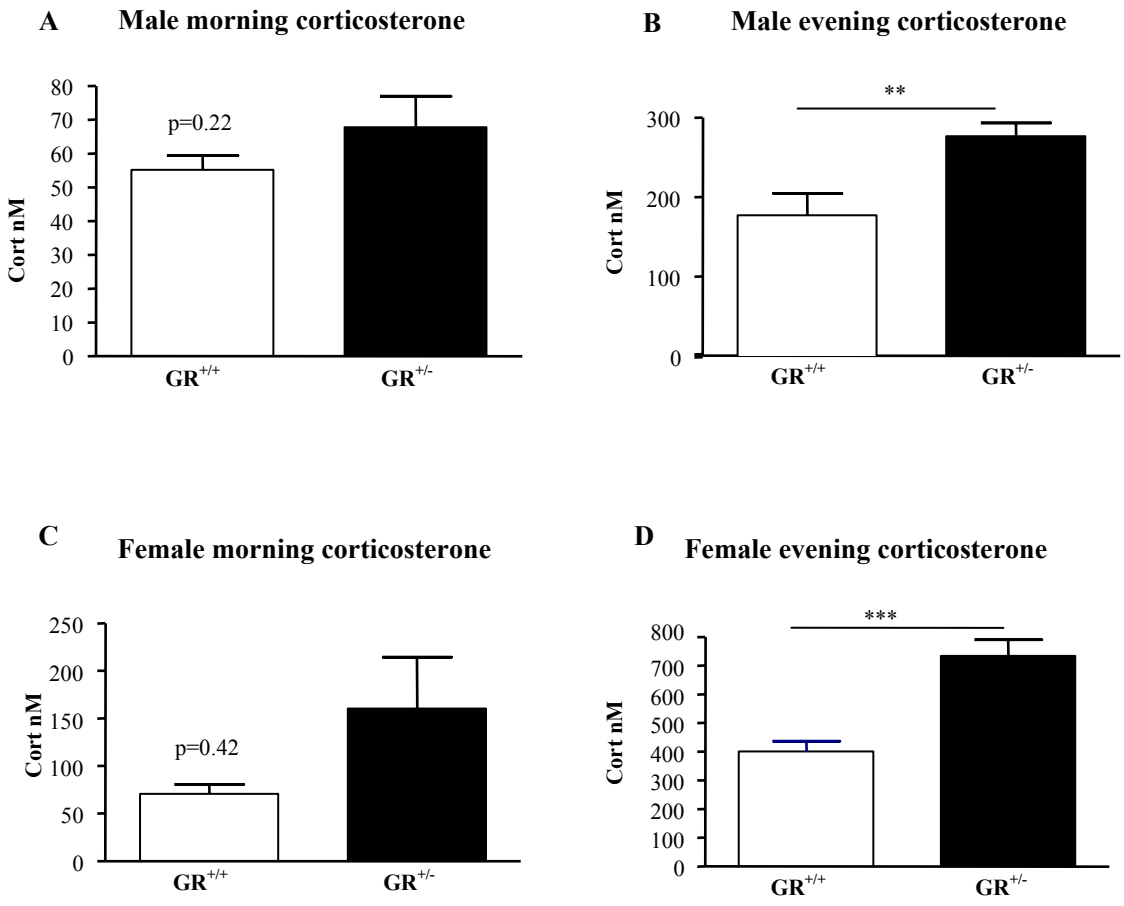

Figure 5.2 $GR^{+/-}$ mice have elavated peak plasma corticosterone levels

(A) Morning (nadir) plasma corticosterone (Cort) levels in male $GR^{+/+}$ and $GR^{+/-}$ mice (n=11/group), (B) Evening (peak) Cort in male $GR^{+/+}$ and $GR^{+/-}$ mice (n=11/group), (C) Morning plasma Cort levels in female $GR^{+/+}$ and $GR^{+/-}$ mice (n=9/group) and (D) Evening Cort in female $GR^{+/+}$ and $GR^{+/-}$ mice (n=9/group). Student t test was performed to identify differences between genotypes. ** $p<0.01$ and *** $p<0.001$.

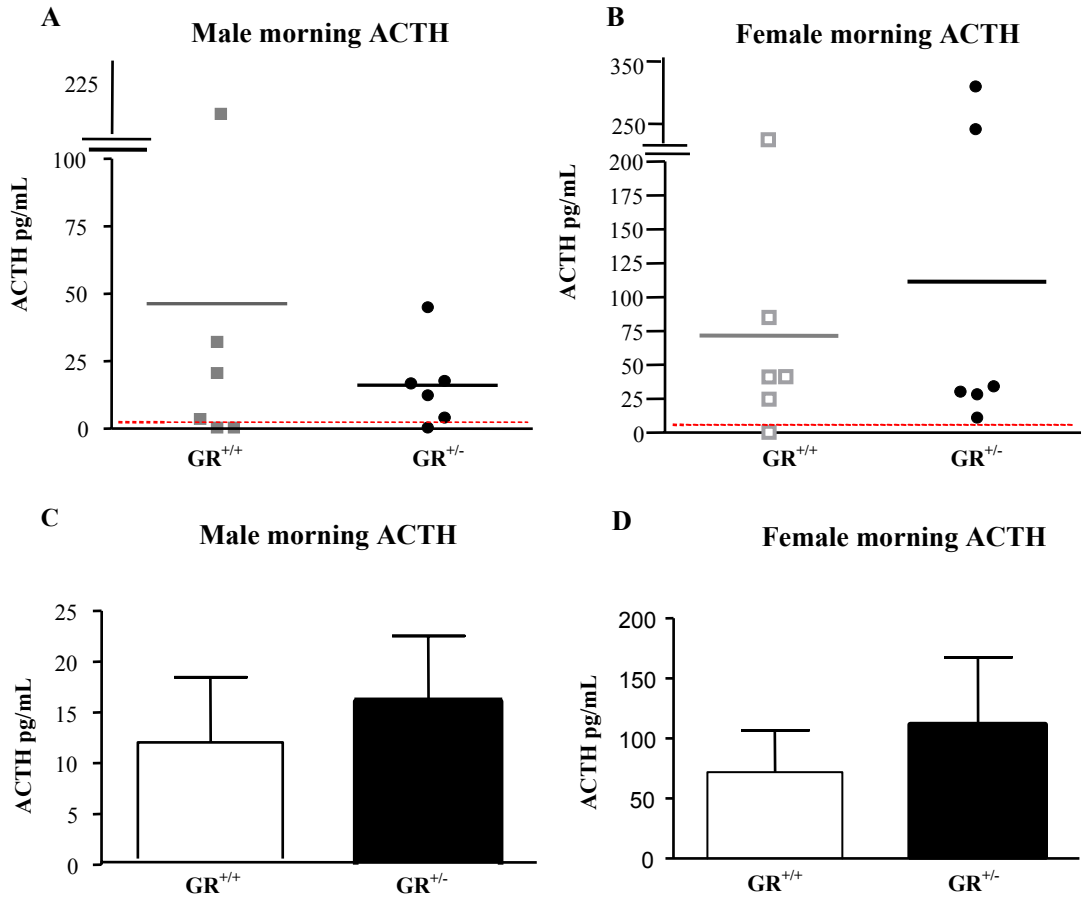

Figure 5.3 $GR^{+/-}$ mice have similar plasma ACTH levels to their $GR^{+/+}$ littermates. Morning plasma ACTH levels in $GR^{+/+}$ and $GR^{+/-}$ male (A and C) and female (B and D) mice. Student t test was performed to identify differences between genotypes (n=6/group). Panels A and B show all the ACTH levels per animal. Panels C and D show the mean±SEM per group. Note that values that "looklike" outliers in panels A and B have been excluded from the analysis after identified as outliers according to the ESD (extreme studentized deviate). Note that in (A) and (B) the red dotted line indicates the sensitivity lower limit of detection in this assay (0.4pg/ml). Because some values were below this sensitivity limit I set them to 0.4 pg/ml to allow comparisons.

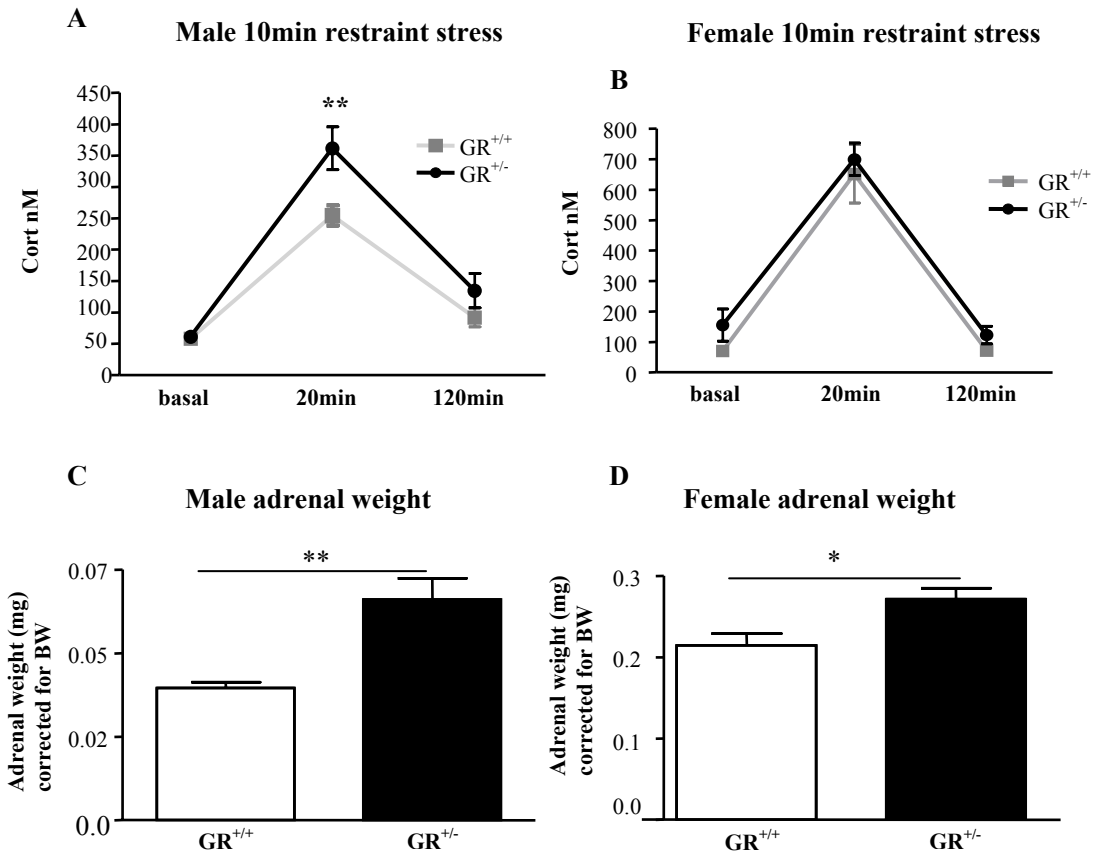

Figure 5.4 Male $GR^{+/-}$ mice have elevated corticosterone response after acute stress. Both male and female $GR^{+/-}$ mice have bigger adrenals.

Plasma corticosterone levels after 10min restrain stress in (A) male (n=9/group) and (B) female (n=7-8/group). Mice were put in a restrain tube (in the morning) for 10min and tail tip blood collected 20 and 120min after restrain. Left adrenal weights corrected for body weight in $GR^{+/+}$ and $GR^{+/-}$ (C) male and (D) female mice. (n=6/group). The reason for male adrenals appear to be smaller than female adrenals is because the former were weighted after their transfer from formalin to 70% ethanol whereas the latter weighted prior to transfer. Student t test was performed to identify differences between genotypes. For restrain stress, repeated measures 2-way ANOVA (factor A being genotype and factor B time) was used to test for differences between genotypes at different time points.* $p<0.05$ and ** $p<0.01$.

Male $GR^{+/-}$ mice showed a higher corticosterone secretion after 10min restraint and a delay in the return to basal levels after 120min compared to $GR^{+/+}$ littermates (fig. 5.4A). In contrast, female $GR^{+/-}$ mice had a similar plasma corticosterone response to restraint stress to $GR^{+/+}$ mice (fig. 5.4B). Moreover, $GR^{+/-}$ male (fig. 5.4C) and female (fig. 5.4D) mice had bigger left adrenal glands.

5.3.1.2. Similar body weight and food intake in $GR^{+/-}$ and $GR^{+/+}$ mice.

There were no differences in body weight in males (fig. 5.5A) or females (fig. 5.6A) between genotypes. Both $GR^{+/-}$ and $GR^{+/+}$ male (fig. 5.5B-C) and female (fig. 5.6B-C) mice showed similar food intake patterns.

5.3.1.3. Similar body composition in $GR^{+/-}$ and $GR^{+/+}$ mice.

To assess whether $GR^{+/-}$ mice have altered body fat distribution or lean mass, fat depots (epididymal, inguinal, mesenteric and brown adipose tissue) and muscle (extensor digitorum longus; EDL and soleus) were weighed. Fat distribution and lean mass were similar in $GR^{+/+}$ and $GR^{+/-}$ male or female mice (Table 5.1). Furthermore, there were no differences in tissue weight apart from the adrenal gland as described above (Table 5.1).

5.3.1.4. Unaltered glucose homeostasis in $GR^{+/-}$ mice.

To investigate the effect of reduced GR density on glucose homeostasis, both glucose and insulin tolerance tests were performed. Analysis of the area under the curve (AUC) showed no differences in GTT responses (fig. 5.7A-B) between genotypes. Both male (fig. 5.6C) and female (fig. 5.6D) $GR^{+/-}$ mice showed similar ITT responses to $GR^{+/+}$ littermates.

Table 5.1 Tissue weights in $GR^{+/-}$ male and female mice.

	MALES			FEMALES		
Tissue weights (mg)	**$GR^{+/+}$**	**$GR^{+/-}$**	**p**	**$GR^{+/+}$**	**$GR^{+/-}$**	**p**
Liver (g)	1.5±0.03	1.4±0.09	NS	nd	nd	
Epididymal fat	445±49	378±78	NS	219±20	219±18	NS
Inguinal fat	297±18	292±42	NS	269±16	250±12	NS
Mesenteric fat	309±31	270±51	NS	182±9	173±12	NS
BAT	94±11	102±10	NS	72±5	82±4	NS
EDL muscle (right)	56±2	145±99	NS	170±17	161±9	NS
Soleus muscle (right)	16±0.7	15±1.5	NS	58±3	71±7	NS
Pancreas	184±7	196±9	NS	nd	nd	
Spleen	81±12	92±5	NS	nd	nd	
Thymus	59±12	47±5	NS	nd	nd	
Adrenal (left)	1.1±0.05	1.9±0.15	**0.0013**	4.8±0.3	6.0±0.3	**0.015**

Student t test was performed to test if there are differences in tissue weights between genotypes (n=6/group). Significance was set at $p<0.05$. NS and nd indicate non significant difference between genotypes and not done respectively. EDL; extensor longus digitalis, BAT; brown adipose tissue.

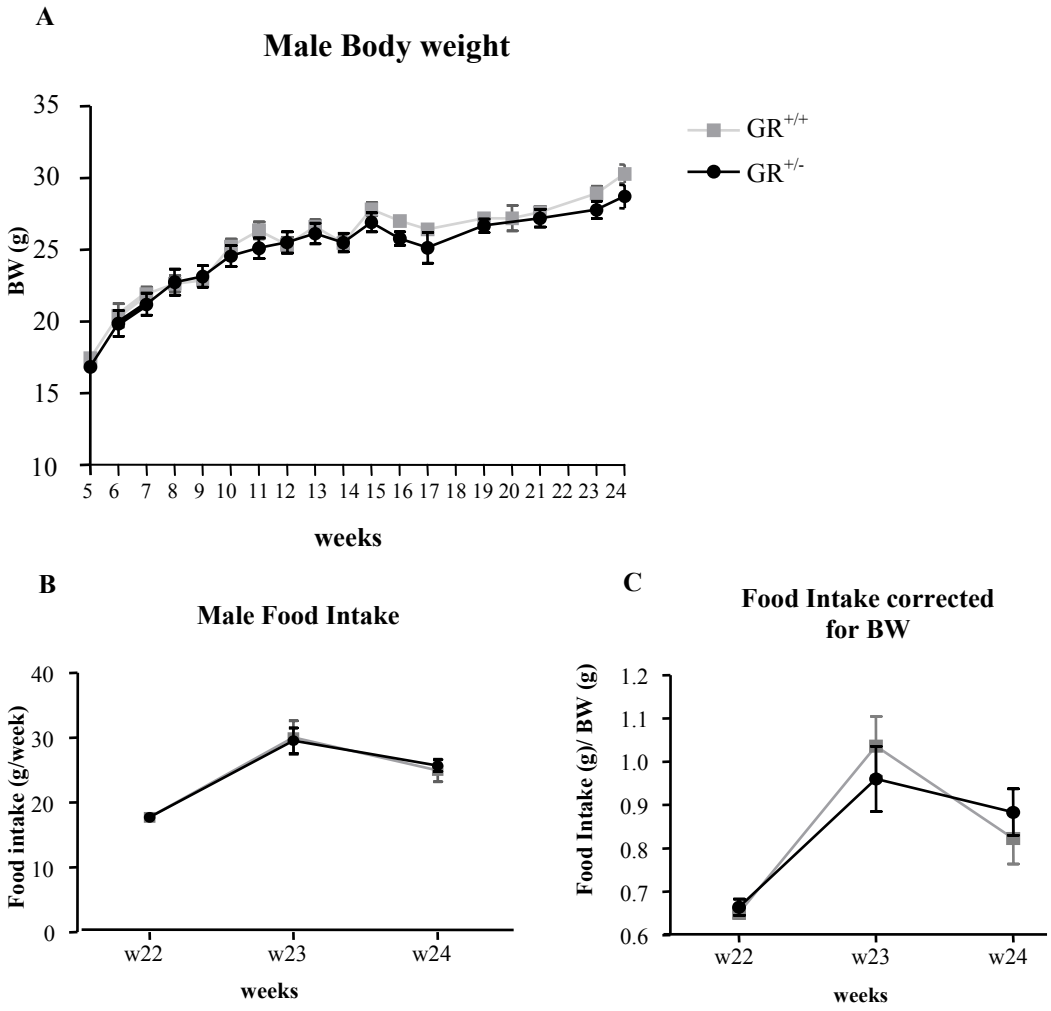

Figure 5.5 Male $GR^{+/-}$ mice have similar body weight and food intake to $GR^{+/+}$ mice. Panels show A) body weights (BW), n=22/group, B) Weekly food intake. Mice were individually caged for 3 weeks for food intake monitoring and C) food intake corrected for body weight in $GR^{+/+}$ and $GR^{+/-}$ mice. n=10/group. Weeks in the x axis indicate age of the animals.

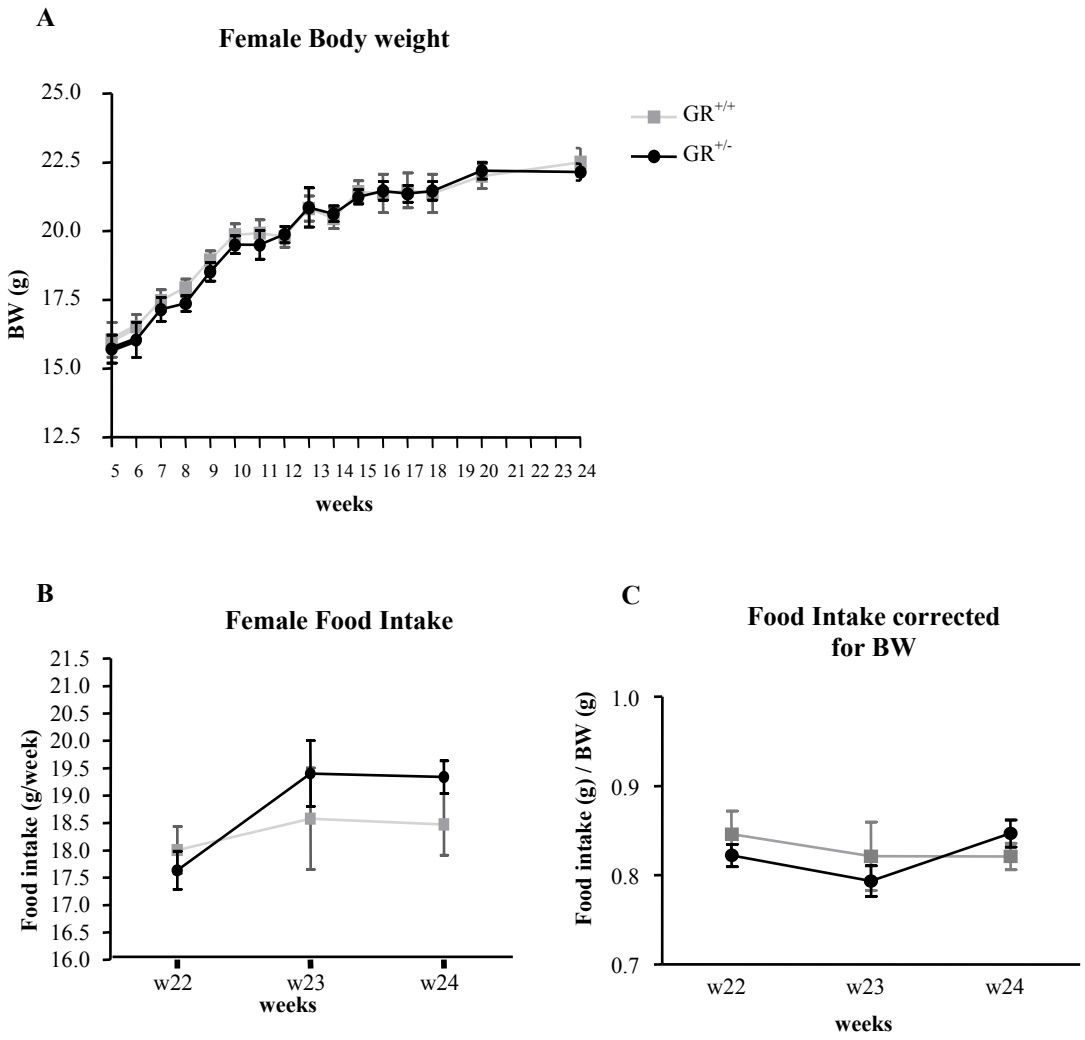

Figure 5.6 Female $GR^{+/-}$ mice have similar body weight and food intake to $GR^{+/+}$ mice.

Panels show A) body weights (BW), n=14/group, B) Weekly food intake. Mice individually caged for 3 weeks for food intake monitoring and C) food intake corrected for body weight in $GR^{+/+}$ and $GR^{+/-}$ mice (n=10/group). Weeks in the x axis indicate age of the animals.

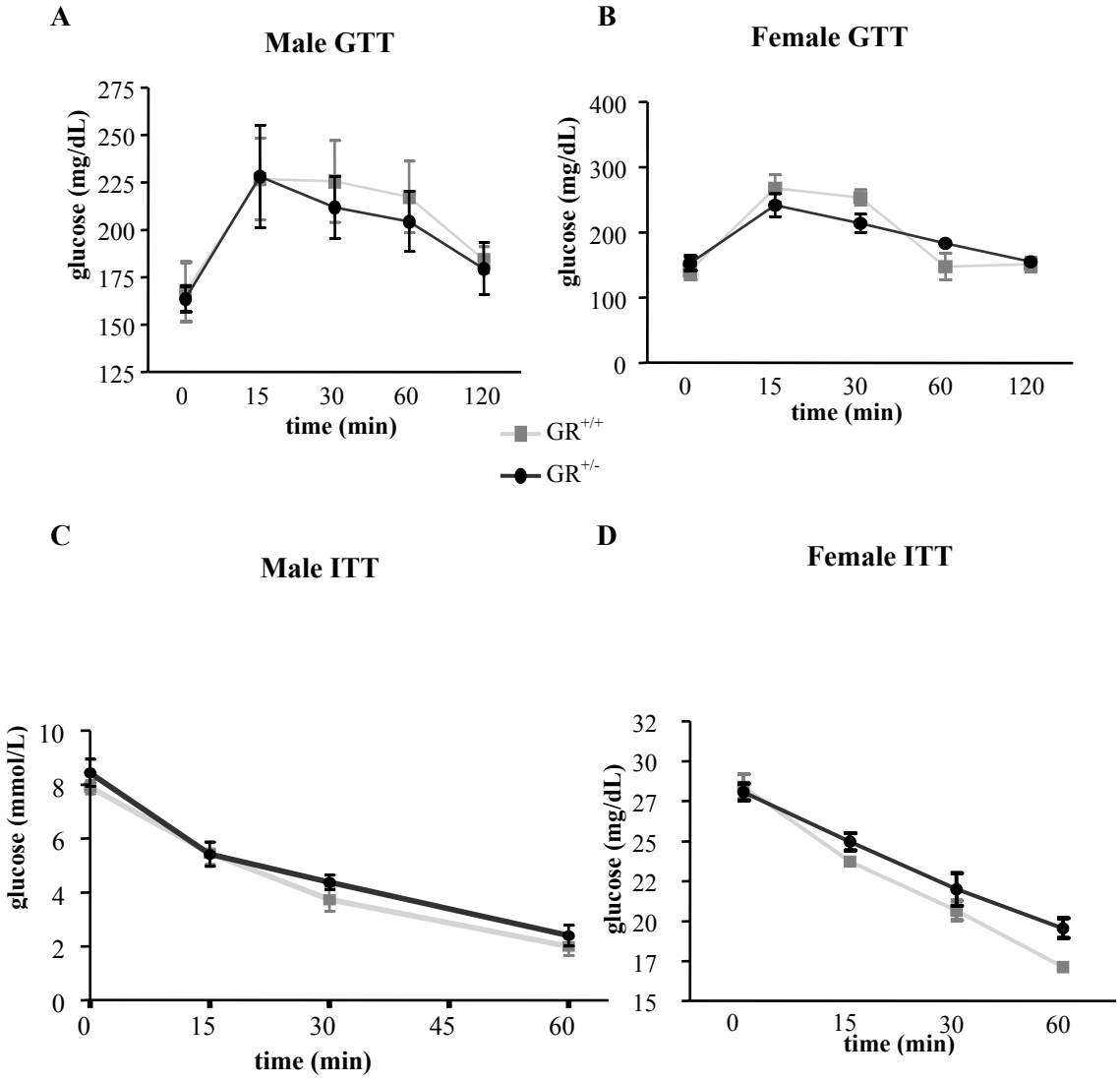

Figure 5.7 Unaltered glucose homeostasis in $GR^{+/-}$ male and female mice.

Glucose tolerance test (GTT) in (A) male and (B) female $GR^{+/+}$ and $GR^{+/-}$ mice. Insulin tolerance test (ITT) in (C) male and (D) female $GR^{+/+}$ and $GR^{+/-}$ mice For GTT and ITT, mice were fasted for 6h. Blood was collected before and after intraperitoneal injection of glucose (2mg/g body weight) or insulin (male; 1.5mU/g BW, female; 1mU/ g BW) at the indicated times. The area under the curve (AUC) per animal was estimated and the mean±SEM AUC per genotype was compared by Student t test (n=6/group). In panels A,B,D, glucose was measured by glucose assay (details in section 2.2.3.4.2). In panel C, glucose measured by a glucose meter (details in section 2.2.3.4.2). GTT: male; $GR^{+/+}$ *vs* $GR^{+/-}$; 25040±1358 AUC *vs* 24010±1741 AUC, p=0.65, female; 21970±1165 AUC *vs* 22500±611 AUC, p=0.7. ITT: male; $GR^{+/+}$ *vs* $GR^{+/-}$; 243±25AUC *vs* 279±17 AUC, p=0.27, female; 12910±192 AUC *vs* 13730±359 AUC, p=0.071.

5.3.2. DIO experiment. Interaction effects of reduced GR and high fat feeding.

To assess if responses to HPA axis regulation, fat distribution, glucose and lipid homeostasis and blood pressure are differentially affected in the $GR^{+/-}$ mice after a high fat challenge (consider as a chronic stressor), male mice were weaned on either high fat (HF) diet (58% kcal as fat) or a control low fat (LF) diet (11% kcal as fat). For the diet-induced obesity (DIO) experiment, mice were kept on the diet for 6 months with *ad libitum* access to water and diet. The experimental design (with the timings of the measurements) is presented in figure 5.1.

5.3.2.1. $GR^{+/-}$ mice have altered HPA axis activity and hypertrophic adrenals.

Nadir (morning) and peak (evening) corticosterone as well as nadir ACTH hormone levels were measured in order to assess HPA axis function in LF and HF fed $GR^{+/-}$ mice. There was a significant increase in both circulating nadir ($GR^{+/+}$ *vs* $GR^{+/-}$; 22±2 *vs* 68±8 nM, $p<0.001$) (fig. 5.8A) and peak corticosterone levels ($GR^{+/+}$ *vs* $GR^{+/-}$; 77±13 vs 179±26 nM, $p<0.001$) in $GR^{+/-}$ mice (fig. 5.8B). HF diet induced a 3-fold ($p<0.01$) increase in morning corticosterone only in the $GR^{+/+}$ mice (fig. 5.8A). Although plasma corticosterone levels were unaffected by HF in $GR^{+/-}$, the peak circulating corticosterone was still higher ($GR^{+/+}$ *vs* $GR^{+/-}$; 100±15 *vs* 174±25 nM, $p<0.01$) compared to $GR^{+/+}$ mice (fig. 5.8B). There were no significant differences in morning circulating ACTH levels between $GR^{+/+}$ and $GR^{+/-}$ mice (fig. 5.8C). However, HF diet increased ACTH levels in both genotypes, 80-fold in $GR^{+/+}$ ($p<0.01$) and 13 fold ($p<0.05$) in $GR^{+/-}$ mice (fig. 5.8C). Moreover, whereas

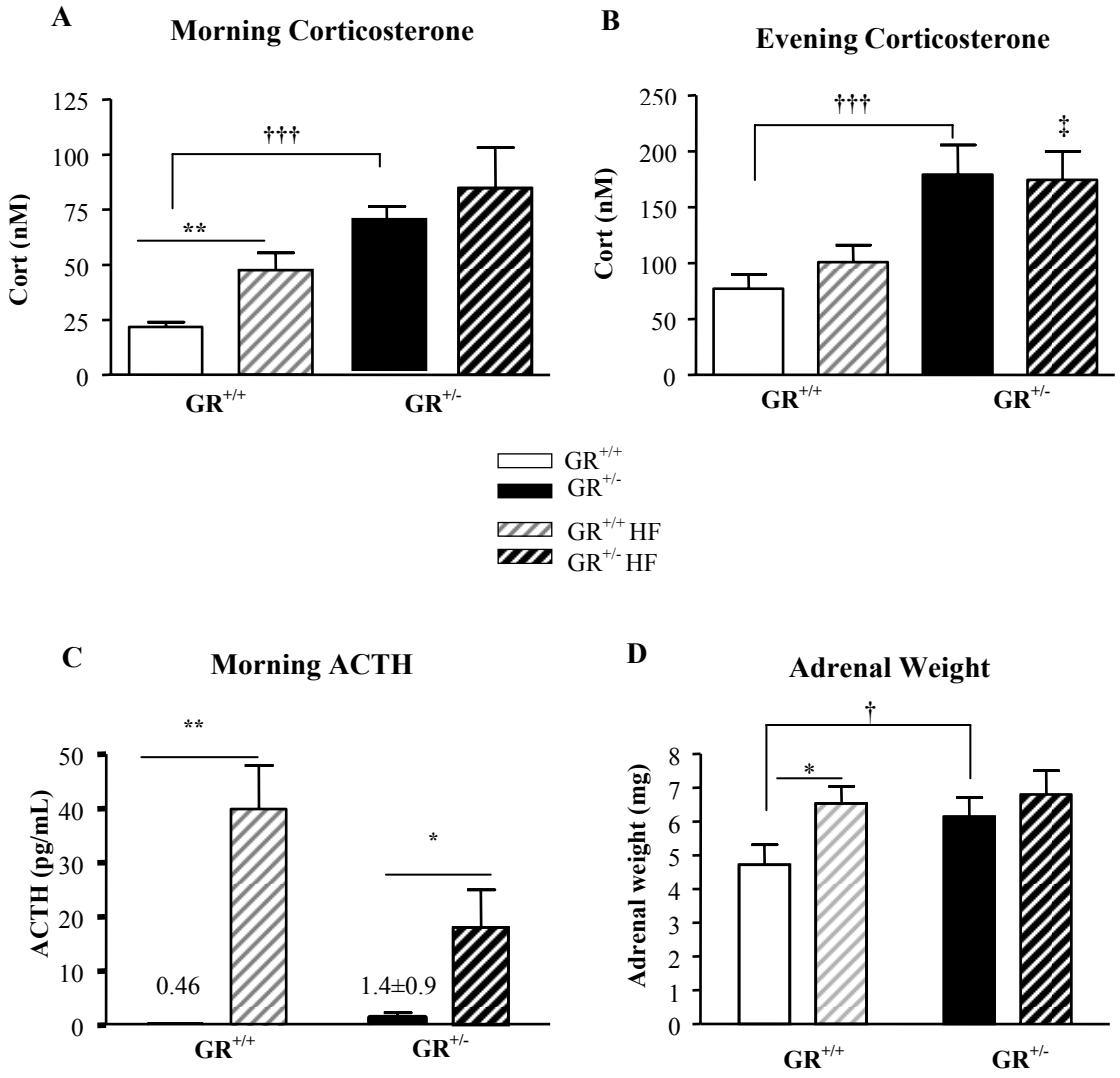

Figure 5.8 $GR^{+/-}$ mice show a hyperactive HPA axis when fed low and high fat diets.
A) Morning plasma corticosterone (Cort) levels in control LF fed $GR^{+/+}$ and $GR^{+/-}$ mice and in HF fed $GR^{+/+}$ and $GR^{+/-}$ mice, B) Evening Cort in control LF fed $GR^{+/+}$ and $GR^{+/-}$ mice and in HF fed $GR^{+/+}$ and $GR^{+/-}$ mice, C) Morning plasma ACTH levels in control LF fed $GR^{+/+}$ and $GR^{+/-}$ mice and in HF fed $GR^{+/+}$ and $GR^{+/-}$ mice and D) Left adrenal weights in control LF fed $GR^{+/+}$ and $GR^{+/-}$ mice and in HF fed $GR^{+/+}$ and $GR^{+/-}$ mice. The effects of genotype and diet interactions were assessed by 2-way ANOVA followed by post-hoc Tukeys' tests for group differences n=8-9/group. * or † $p<0.05$, ** or ‡ $p<0.01$ and *** or ††† $p<0.001$. ‡ indicates statistical significant difference between +/+ and +/- HF-fed mice.
Note that the ACTH levels in $GR^{+/+}$ LF- fed mice are below the assay's sensitivity limit.

HF diet caused adrenal hypertrophy (38% increase in adrenal weight; $p<0.05$) in $GR^{+/+}$ mice, such an effect was not seen in $GR^{+/-}$ mice (fig. 5.8D). As on chow diet (fig. 5.4C), $GR^{+/-}$ mice had larger left adrenal glands ($GR^{+/+}$ *vs* $GR^{+/-}$; 4.7±0.6 *vs* 5.7±0.6mg, $p<0.05$) than $GR^{+/+}$ nice fed LF diet (fig. 5.8D). Adrenal morphology also differed between genotypes (fig. 5.9). In $GR^{+/-}$ adrenals, columns of endocrine cells in the zona fasciculata appeared long, with cells in the columns hypertrophied and with homogenous eosinophilic cytoplasm (fig. 5.9B). The zona glomerulosa appeared thicker than in $GR^{+/+}$ mice, with more glomeruli evident containing hypertrophied epithelium (fig. 5.9A-B). This appearance suggests stimulation of corticosterone and aldosterone producing cells (D. Brownstein, personal communication). This adrenal phenotype was also apparent in $GR^{+/-}$ mice fed HF diet (fig. 5.9C-D). However, while there were no marked differences in adrenal morphology between $GR^{+/-}$ mice fed LF or HF diet, in $GR^{+/+}$ mice columns of endocrine cells in the zona fasciculata appeared longer in HF than in LF fed mice (fig. 5.9A and C).

5.3.2.2. Unaltered fat distribution and glucose homeostasis but elevated liver triglyceride levels in $GR^{+/-}$ mice.

There were no differences in body weight (fig. 5.10A) or food intake (data not shown) between genotypes, on the control LF or HF diet. Fat depot (epididymal, inguinal, mesenteric) and muscle (extensor digitorum longus) weights were similar in $GR^{+/+}$ and $GR^{+/-}$ mice (fig. 5.10B) on either diet. $GR^{+/-}$ mice had smaller livers on the control diet ($GR^{+/+}$ *vs* $GR^{+/-}$; 1.4±0.09 *vs* 1.1±0.07g, $p<0.05$) compared to $GR^{+/+}$

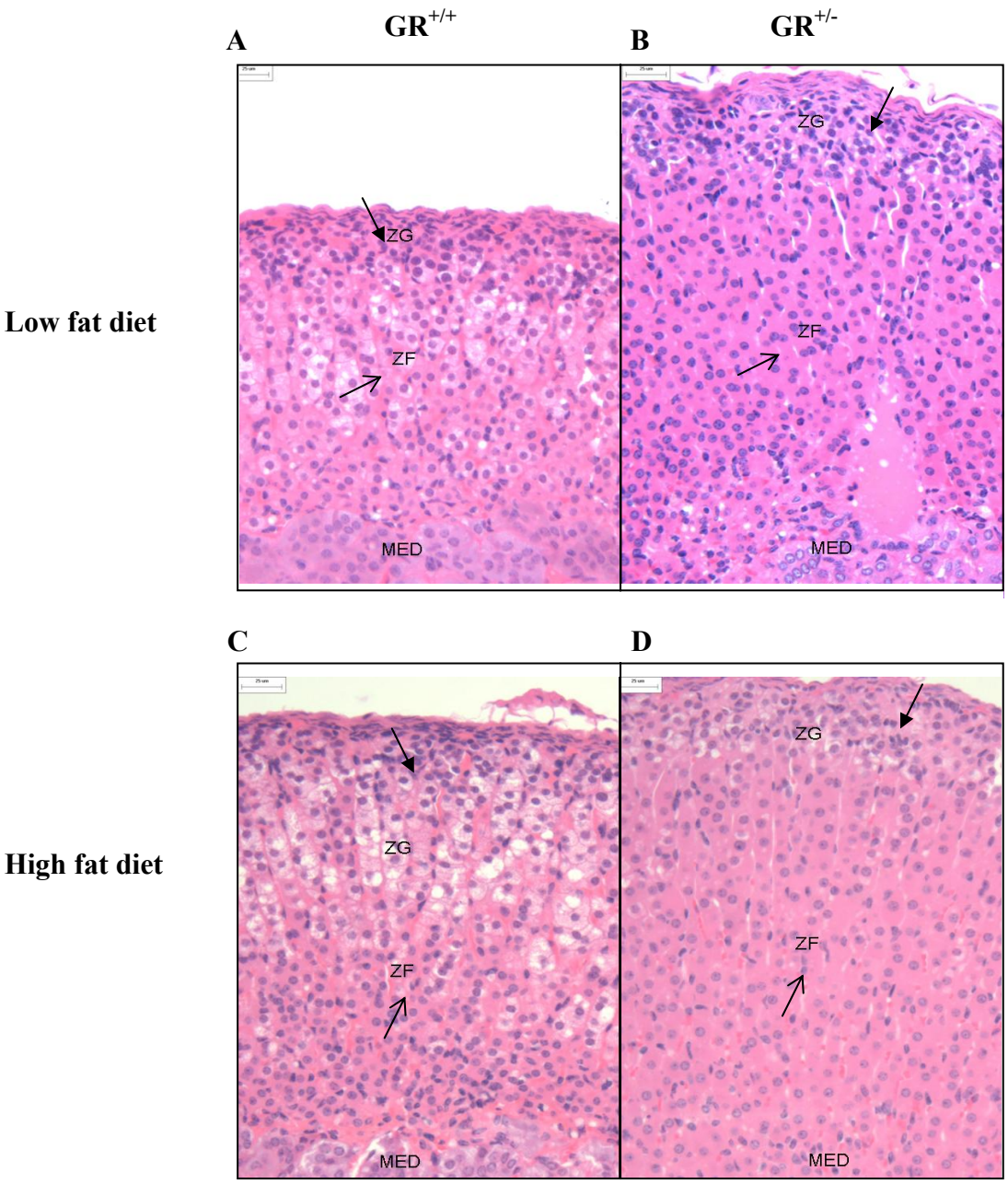

Figure 5.9 Adrenal hypertrophy in $GR^{+/-}$ mice.

Representative images of haematoxylin & eosin (H&E) stained adrenal sections of LF fed (A) $GR^{+/+}$ and (B) $GR^{+/-}$ mice and HF fed (C) $GR^{+/+}$ and (D) $GR^{+/-}$.mice. ZF; zona fasciculate (open arrowheads), ZG; zona glomerulosa (closed arrowheads), MED; medulla. n=8-9/group.scale on top of each image at 25 microns.Images provided by David Brownstein.

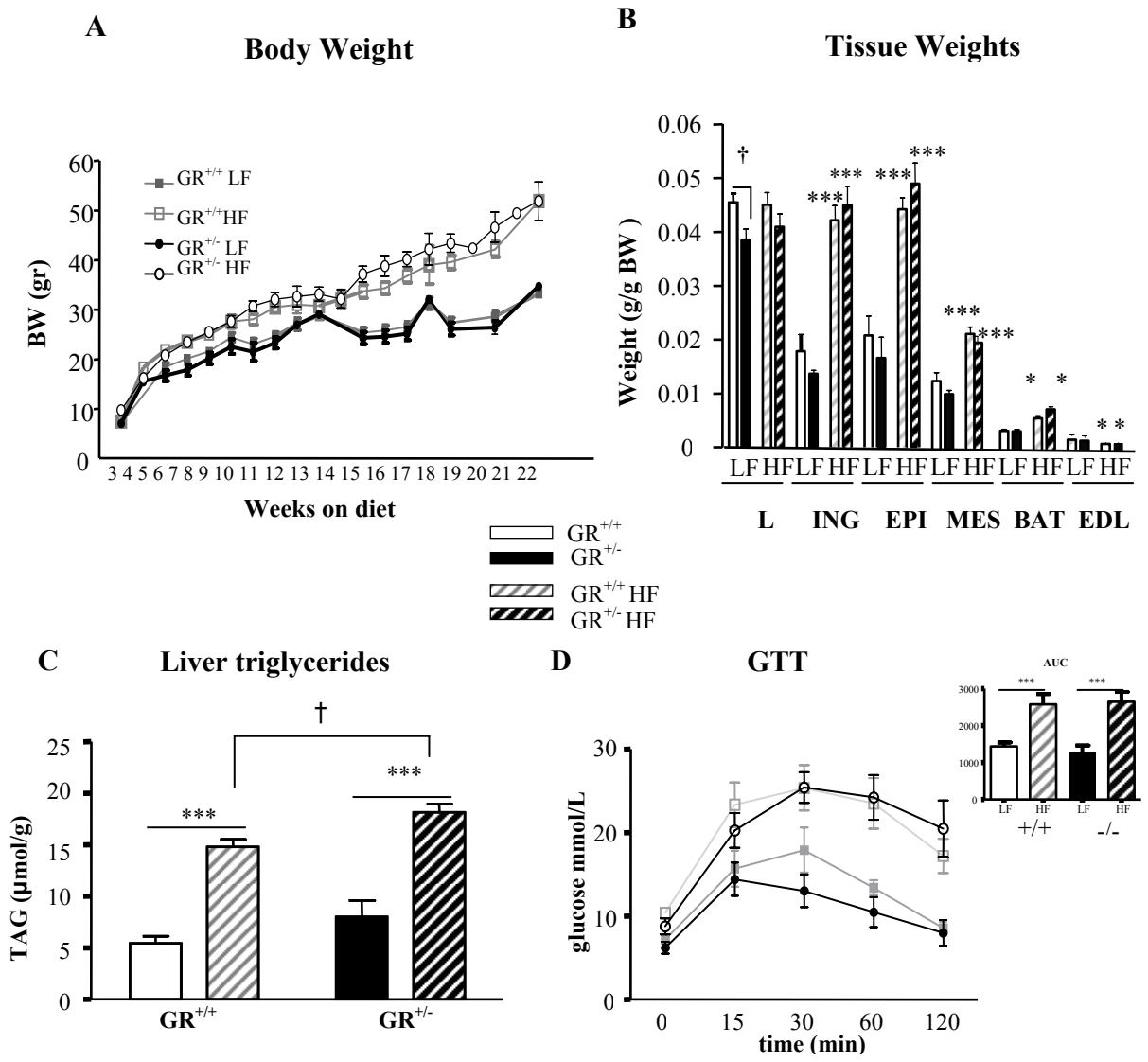

Figure 5.10 Unaltered body composition and glucose homeostasis but higher liver triglycerides in $GR^{+/-}$ mice following HF.

Panels show (A) body weights (BW), (B) tissue weights: liver,adipose tissue (L;liver, epi; epididymal, ing; inguinal, mes; mesenteric) and extensor digitorum longus (EDL) muscle, (C) liver triglyceride (TAGs) levels and (D) glucose tolerance test (GTT) in $GR^{+/+}$ LF, $GR^{+/-}$ LF, $GR^{+/+}$ HF and $GR^{+/-}$ HF fed. Insert showing the area under the curve (AUC) per group. For GTT mice were fasted for 6h. Blood was collected before and after intraperitoneal injection of glucose (2mg/g body weight) at the indicated times. Interactions between genotype and diet were assessed by 2-way ANOVA followed by post-hoc Tukeys' tests for group differences. AUC was calculated per animal and the mean±SEM per group was compared by 2-way ANOVA. LF; low fat diet, HF; high fat diet. n=6/group, † $p<0.05$, ** or †† $p<0.01$, *** $p<0.001$.

littermates (fig. 5.10B). HF diet did not affect liver weight in either genotype. There was a trend for smaller liver in HF fed $GR^{+/-}$ mice (fig. 5.10B). $GR^{+/-}$ mice appeared to have higher hepatic triglyceride levels when fed a HF diet ($GR^{+/+}$ *vs* $GR^{+/-}$; 14.8±0.7 *vs* 18.1±0.8μmol/g, $p<0.001$) compared to $GR^{+/+}$ mice (fig. 5.10C). Glucose tolerance was similar between genotypes on control diet and similarly impaired by HF diet (fig. 5.10D).

5.3.2.3. $GR^{+/-}$ mice have elevated blood pressure due to activation of the renin-angiotensin-aldosterone system (RAAS).

$GR^{+/-}$ mice had 8mmHg higher systolic blood pressure ($GR^{+/+}$ *vs* $GR^{+/-}$; 102±1.3 *vs* 110±1.8mmHg, $p<0.01$) compared to $GR^{+/+}$ mice on control diet (fig. 5.11). Blood pressure in HF fed mice was higher in both genotypes compared to LF diet ($GR^{+/+}$, 14mmHg increase, $p<0.01$ and $GR^{+/-}$, 8mmHg increase, $p<0.05$).

To dissect the potential mechanism involved in the elevated blood pressure in $GR^{+/-}$ mice, systemic or/and tissue (adipose, liver)-specific activation of the renin-angiotensin system (RAS) was investigated. Increased blood pressure in control LF-fed $GR^{+/-}$ mice was associated with a 2-fold increase ($p<0.05$) in plasma renin activity compared to $GR^{+/+}$ mice (fig.5.12A). HF diet did not affect plasma renin activity in either genotype, but sustained higher in the $GR^{+/-}$ mice (fig. 5.12A). In LF-fed mice, plasma angiotensinogen levels were similar in both genotypes but increased 3-fold ($p<0.01$) only in the $GR^{+/-}$ mice after HF feeding (fig. 5.12B). Plasma aldosterone levels were also higher in $GR^{+/-}$ mice (fig. 5.12C) on control diet

($GR^{+/+}$ 20±9 *vs* $GR^{+/-}$ 132±33pmol/L, $p<0.01$). Although unaffected by HF diet, aldosterone levels remained higher in HF-fed $GR^{+/-}$ mice (fig. 5.12C). Moreover, an adipose tissue (epididymal)-specific increase in angiotensinogen mRNA levels (fig. 5.12D) in $GR^{+/-}$ mice (40% higher than $GR^{+/+}$ mice, $p<0.05$), but no change in hepatic angiotensinogen mRNA levels was observed (fig. 5.12E). Despite the increased blood pressure in both genotypes with HF, it is perhaps surprising that HF diet induced a 2.5 and 5 fold *reduction* ($p<0.001$) in epididymal angiotensinogen mRNA levels in $GR^{+/+}$ and $GR^{+/-}$ mice, respectively (fig. 5.12D). In contrast, hepatic angiotensinogen mRNA levels were increased (20%, $p<0.05$) only in the $GR^{+/-}$ mice with HF feeding (fig. 5.12E).

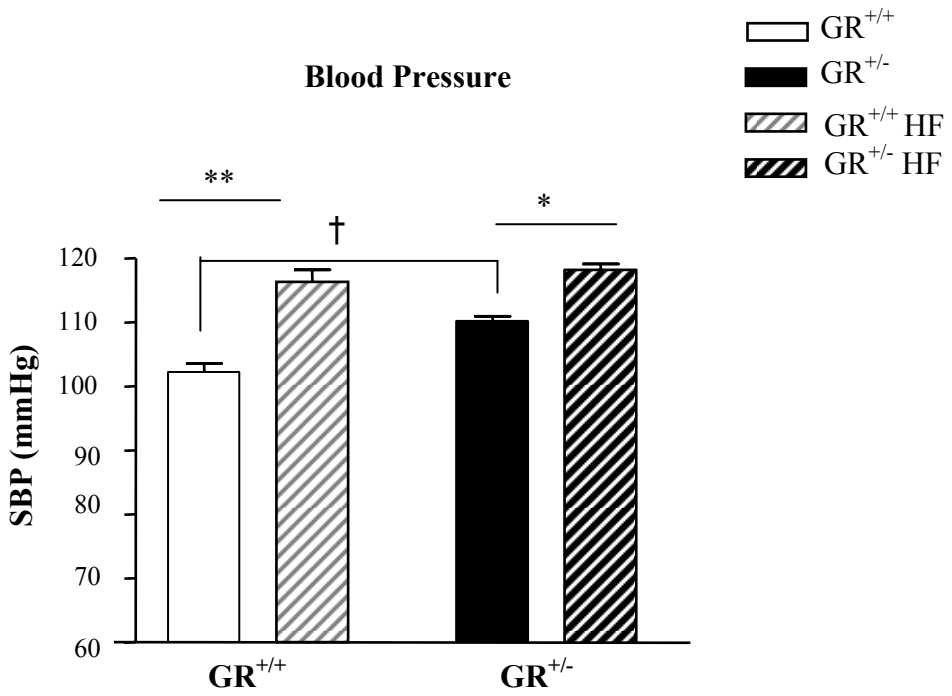

Figure 5.11 $GR^{+/-}$ mice have elevated blood pressure.

Tail cuff plethysmography (performed by Dr Elaine Marshall) was used to measure systolic blood pressure (SBP) in $GR^{+/+}$ LF, $GR^{+/-}$ LF, $GR^{+/+}$ HF and $GR^{+/-}$ HF fed. The effects of genotype and diet interactions were assessed by 2-way ANOVA followed by post-hoc Tukeys' tests for group difference. n=5/group, * or † $p<0.05$, ** $p<0.01$.

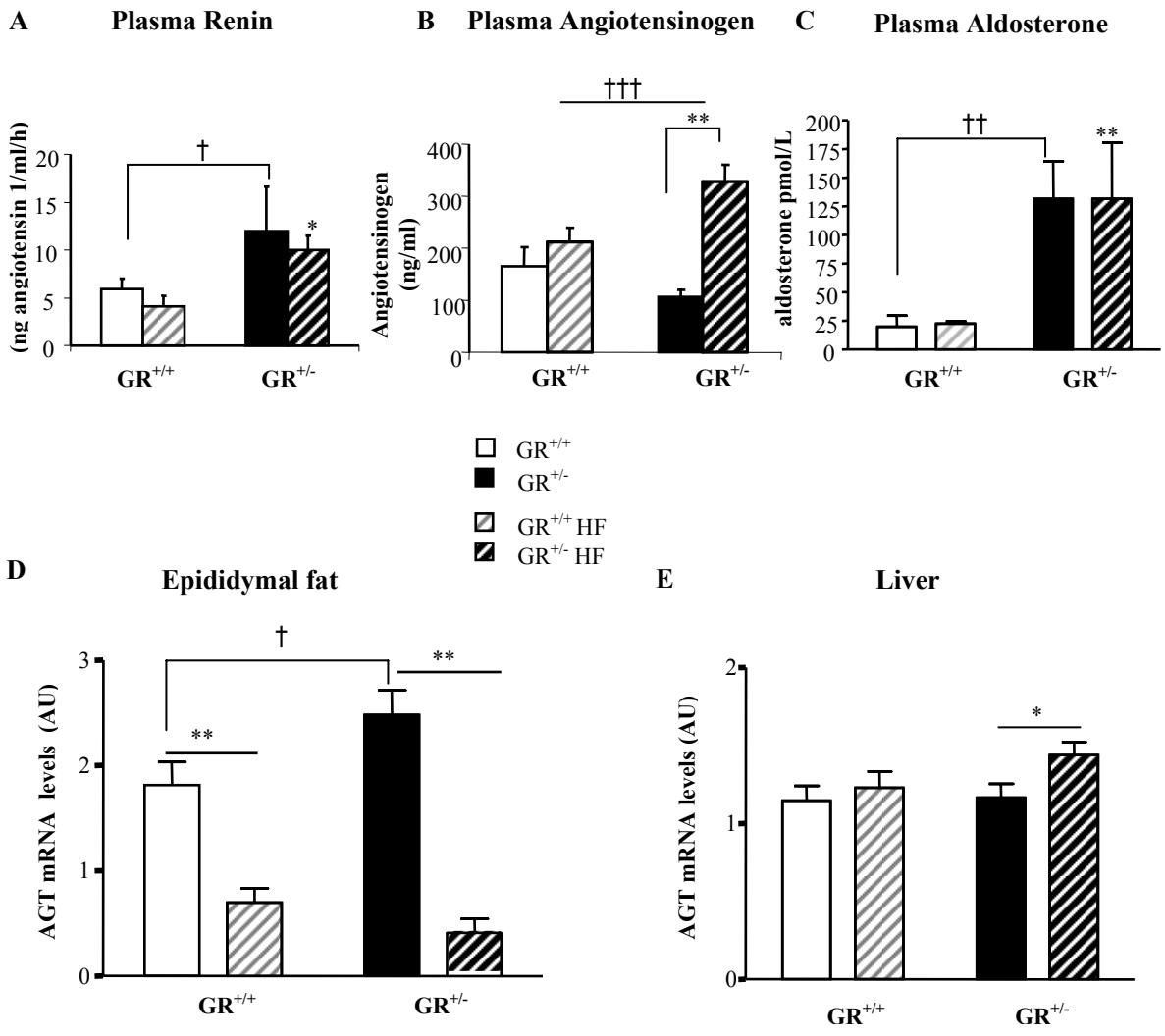

Figure 5.12 Activation of the Renin-Angiotensin-Aldosterone System in $GR^{+/-}$ mice.
Panels show (A) Plasma renin activity, (B) plasma angiotensinogen concentration, (C) plasma aldosterone concentration, (D) epididymal fat angiotensinogen (AGT) mRNA levels and (E) hepatic AGT mRNA levels in $GR^{+/+}$ LF, $GR^{+/-}$ LF, $GR^{+/+}$ HF and $GR^{+/-}$ HF fed mice. For plasma measurements, n=5/group. For mRNA levels, n=8-9/group. AGT mRNA levels were measured by real-time PCR and β-actin was used as an internal control. The ratio of AGT to β-actin mRNA was calculated and the mean ± SEM per group was compared by 2-way ANOVA followed by post-hoc Tukeys' tests for group differences. * or †p<0.05, ** or †† p<0.01, ††† p<0.001.

5. 4. Discussion

In this chapter I demonstrate that global (central and peripheral) reduction in GR density leads to impaired negative feedback inhibition of the HPA axis, unaltered adipose tissue mass and distribution, normal glucose homeostasis, higher hepatic triglyceride accumulation after HF diet challenge and hypertension, the latter perhaps due to systemic activation of the renin-angiotensin-aldosterone system.

An ES cell line, in which a gene-trap cassette had integrated into GR, was exploited to generate $GR^{+/-}$ mice that lack part of the DBD and the entire LBD, to study the effects of reduced GR density on HPA axis regulation under basal and after high fat diet (HF) challenge. Both male and female $GR^{+/-}$ mice under basal (chow-fed) conditions displayed a hyperactive HPA axis phenotype with elevated morning and evening corticosterone levels in accordance with previous GR transgenic lines (Pepin et al., 1992; Tronche et al, 1998; Cole et al., 1995; Reichardt et al, 1998). However, previously described $GR^{+/-}$ mice developed by homologous recombination did not show an HPA axis phenotype under basal (non-stress) conditions, but had higher corticosterone levels following 30 min restraint stress (Ridder et al., 2005). In the model presented here, corticosterone was also higher in male heterozygotes after 10 min restraint stress in accordance with previous data (Ridder et al., 2005) and consistent with their enlarged adrenal glands. These data are consistent with a hyperactive HPA axis in male $GR^{+/-}$ mice under basal and acute stress conditions and suggest reduced negative feedback regulation as a consequence of global reduction in GR density. Indeed, GR expression was ~50-60% decreased in pituitary, PVN and

hippocampus of $GR^{+/-}$ mice compared to $GR^{+/+}$ littermates (chapter 4, section 4.3). It is worth noting that plasma corticosterone levels in female mice were higher than in male at the peak and following restraint stress, as previously described in rodents (Seale et al., 2004; Harizi et al., 2007). Although $GR^{+/-}$ mice displayed higher corticosterone levels basally and under acute stress, morning circulating ACTH levels were unaltered in both male and female $GR^{+/-}$ mice. Due to limitations (time and mice availability), only morning ACTH levels were measured, and although unaltered that does not exclude the possibility that evening ACTH might be elevated in the $GR^{+/-}$ mice. The ACTH data presented here are consistent with one (Reichardt et al., 1998) but in contrast with other GR transgenic models that showed elevated ACTH levels (Pepin et al., 1992; Cole et al., 1995; Schmid et al., 1995; Tronche et al., 1998). However, caution should be taken when comparing different GR models generated by different strategies (especially tissue/cell specific). The $GR^{+/-}$ mice presented here should be better compared with the $GR^{+/null}$ (Finotto et al., 1999), $GR^{+/hypo}$ (Schmid et al., 1995), $GR^{+/dim}$ (Reichardt et al., 1998) and $GR^{+/antisense}$ (Pepin et al., 1992) but unfortunately these data are not available.

Moreover, the effect of chronic HF-feeding, which elevates corticosterone levels and thus can be considered as a chronic "low level" stressor, on HPA axis regulation was investigated in this model. HF diets stimulate ACTH production from the pituitary gland and increase adrenal capacity to secrete corticosterone (Lawson et al, 1981; Tannenbaum et al, 1997; Michel et al, 2004; Lindqvist et al, 2006). For example, elevated free fatty acids have direct effects on (a) increasing (in a dose-related

manner) ACTH and CORT levels after intralipid emulsion administration in rats (Widmaier et al, 1992) and (b) inhibiting ventromedial hypothalamic neuronal firing (Oomura Y., 1976) and thus blunting the inhibitory effect that these neurons have on HPA axis (Dallman, 1984). Indeed, that was apparent in $GR^{+/+}$ mice, in which morning plasma levels of corticosterone and ACTH, and adrenal size were increased by HF. However, in $GR^{+/-}$ mice the HF diet had a lesser effect, increasing morning plasma ACTH levels only 13-fold compared to 80-fold icrease in wild type littermates. Additionally, HF diet did not further increase (already higher) CORT levels and adrenal size in $GR^{+/-}$ mice. It seems as though reduced GR density decreases the ability to adapt to the HF diet. The differences between LF and HF diets were smaller in $GR^{+/-}$ mice such that the $GR^{+/+}$ mice seem to "catch up" on HF diet.

Having confirmed that $GR^{+/-}$ mice have a dysregulated HPA axis, the primary aim was to investigate if reduced GR density and consequently altered GC sensitivity affects body fat distribution, glucose or lipid homeostasis and blood pressure regulation during exposure to an 'obesigenic' diet. Global reduction in GR density did not affect body weight, fat distribution or glucose homeostasis under basal (control low fat diet) or diet-induced obesity (DIO) conditions. GR reduction is therefore likely compensated by activation of the HPA axis. Such compensation might explain why there are no apparent differences between genotypes in body fat distribution or glucose metabolism. The lack of altered glucose homeostasis is not surprising since GR inactivation exclusively in hepatocytes showed that GR is

essential for glucose homeostasis only under prolonged fasting or streptozytocin-induced diabetes (Opherk et al., 2004; described in section 1.6.1 & Table 1.1).

In vitro GCs directly increase hepatic fatty acid (FA) and triglyceride (TG) synthesis (Klausner and Heimberg, 1967; Diamant and Shafrir, 1975; Bartlett and Gibbons, 1988; Brindley, 1988). The effects of GCs on hepatic lipid synthesis in vivo are complex. For example, low dose GCs can restore the impaired hepatic *de novo* fatty acid and TG synthesis, secretion and deposition into lipid stores after adrenalectomy in rats (Kirk et al., 1976; Mantha et al., 1999) and physiological GC levels promote hepatic lipogenesis at least in non-diabetic or not severely stressed rats (Kirk et al., 1976). Although the peripheral effects of GCs on maintaining lipid production and storage are mainly direct, the positive modulation of adipose lipoprotein lipase (LPL; the major enzyme catalyses TG hydrolysis and thus FA release) activity might be indirect and may be "shared" with insulin's actions (Ashby and Robinson, 1980; Fried et al., 1993). $GR^{+/-}$ mice on LF-diet had smaller livers suggesting that reduced GR density could potentially affecting hepatic lipid accumulation and/ or secretion or glycogen storage. Although one might expect that $GR^{+/-}$ mice would have reduced hepatic triglyceride levels that might explain their smaller livers, there was no difference in liver triglyceride levels under basal conditions (control low fat diet) between genotypes. However, the consequences of altered GC status on triglyceride metabolism are strongly dependent on diet (Smith & Romsos, 1985; Kang et al., 1992; Mantha et al., 1999). Corticosterone does not appear to significantly modulate triglyceride metabolism when lipid flux is low, ie when animals are maintained on a low fat diet (Mantha et al., 2000). In contrast, the impact of glucocorticoids on triglyceride metabolism becomes highly significant when animals are fed a HF diet

that induces a high lipid flux (Mantha et al., 2000). Support for this notion comes from adrenalectomy experiments showing that absence of corticosterone significantly reduces hepatic triglyceride accumulation, secretion rate and plasma triglycerides in HF fed animals (Mantha et al., 1999). In this experiment, HF diet increased hepatic triglyceride accumulation in both genotypes, but the effect was more pronounced in $GR^{+/-}$ mice. The enhanced accumulation of hepatic triglycerides could be partly explained by the adrenal cortex hyperfunction and the consequently elevated circulating corticosterone levels observed in both genotypes on HF diet. However, since under basal conditions (LF) the already hypercorticosteronaemic $GR^{+/-}$ mice have unaltered hepatic TG levels (compared to $GR^{+/+}$) it is more likely that there is a synergism of GC and insulin actions promoting hepatic TG synthesis in both genotypes.

Here, the effect of reduced GR density in the control of blood pressure in mice was also investigated. Although the HF diet-dependent increase in blood pressure was apparent in both genotypes, only $GR^{+/-}$ mice under basal conditions had elevated systolic blood pressure. The hypertensive phenotype in $GR^{+/-}$ mice was associated with elevated plasma renin activity and plasma aldosterone concentration as well as an adipose tissue specific up-regulation of angiotensinogen (AGT) mRNA expression indicating both systemic and local activation of RAAS. Despite this induction of the RAAS system components in the $GR^{+/-}$, there was no genotype-dependent increase in blood pressure after HF feeding, indicating that a further adaptation counteracting the RAAS changes had occured. This is noteworthy since it

suggests care should be taken when interpreting tissue specific changes in the RAAS system. Thus, whilst angiotensinogen, the circulating substrate for renin, increased 3-fold in $GR^{+/-}$, this is presumably the end product of secreted angiotensinogen from adipose tissue (where AGT mRNA was more markedly down-regulated in the $GR^{+/-}$ mice) and the liver (where there was a slight increase in AGT mRNA levels). One interpretation would be that liver AGT makes a larger contribution to circulating levels of AGT (Cambell & Habener, 1986; Tamura et al, 1995), nevertheless, even with an increased circulating level, the overall net increase in blood pressure is the same compared to $GR^{+/+}$ which show no change in circulating AGT (coincident with a smaller reduction in AT and unchanged hepatic AGT mRNA levels). Even given the potential for differences in AGT expression and secretion from other organs as well as other fat depots, the lack or exaggerated induction of BP in $GR^{+/-}$ suggests that an alternate adaptive mechanism might be involved.

Adipose tissue is an important source of AGT (Cambell and Habener, 1986; Cassis et al., 1988; Frederic et al., 1992; Engeli et al., 1999) after liver, the major source of AGT production (Cambell and Habener, 1986; Tamura et al., 1995). Adipose AGT can reach the bloodstream and potentially regulate blood pressure (Massiera et al., 2001). Plasma and liver AGT levels were unaltered under basal conditions but increased by HF feeding in line with observations that AGT protein concentration in plasma parallels mRNA levels in the liver (Lu et al., 2007). Moreover, adrenal histopathology in $GR^{+/-}$ mice suggested stimulation of aldosterone-producing cells in

the zona glomerulosa that may contribute to the hypertensive phenotype, with elevated circulating aldosterone levels.

Although DIO was associated with up-regulation of adipose AGT expression levels (Massiera et al., 2001; Boustany et al., 2004), intriguingly a down-regulation of AGT with HF feeding was observed in both genotypes. Another study also failed to show an increase in adipose AGT mRNA with obesity in rats (Gabrieli et al., 2001). At present is unclear what underlies these discrepancies. Liver cells are targets for various hormones that regulate AGT, including the major pertinent metabolic hormones insulin and GC. In contrast, adipocytes appear to be responsive only to the effects of GCs in the regulation of AGT (Aubert et al., 1997). However, data from *in vitro* studies suggested that insulin may act as a negative regulator of AGT mRNA expression in adipose tissue (Aubert et al., 1998; Aihaud, 1999), which would be consistent with the observation of a greater down-regulation in the hypercorticosteronaemic $GR^{+/-}$ mice. Additionally, *in vivo* studies showed that mild hyperinsulinemia decreased fat AGT expression (Gabriely et al., 2001), and in streptozotocin-diabetic rats, hyperinsulineamia induced a down-regulation of renin and adipose AGT mRNA levels (Cassis, 1992). It is possible that in the experiments reported in the current study, the HF-induced hyperinsulinemia overrided the GC effect, thus adipose AGT expression appeared decreased (Aubert et al., 1998). Since data on the regulation of AGT by insulin are inconsistent, measurement of plasma insulin levels in this study will be informative. Figure 5.13 illustrates the

mechanisms that might be involved in the activation of RAS and thus contributing to the hypertensive phenotype in $GR^{+/-}$ mice.

Finally, it will be of great interest to distinguish the effects of reduced GR density from the possibly confounding effects of increased GC secretion on blood pressure in the $GR^{+/-}$ mice. Future adrenalectomy experiments with fixed CORT- replacement levels will be informative. Additionally, alterations in the GC clearance rates by A-ring reductases (etc) in this model will be important to be addressed in the future studies. Differences in local (adipose or liver) GC amplification (by altered 11β-HSD1) in this model can probably be ruled out since $GR^{+/-}$ mice had similar 11β-HSD1 mRNA levels in adipose and liver to $GR^{+/+}$ littermates.

In conclusion, mice heterozygous for a null mutation in the GR gene have a hyperactive HPA axis with adrenal hypertrophy, elevated hepatic triglyceride levels and a novel hypertensive phenotype. Altered tissue GC sensitivity, mediated through altered GR density, can differentially result in a variety of phenotypic changes. These may not lead to a disease state *per se* but may explain, in part, an individual's susceptibility to a favourable or unfavourable metabolic and cardiovascular profile as seen in humans carrying polymorphisms in the GR gene (described in section 1.6.2).

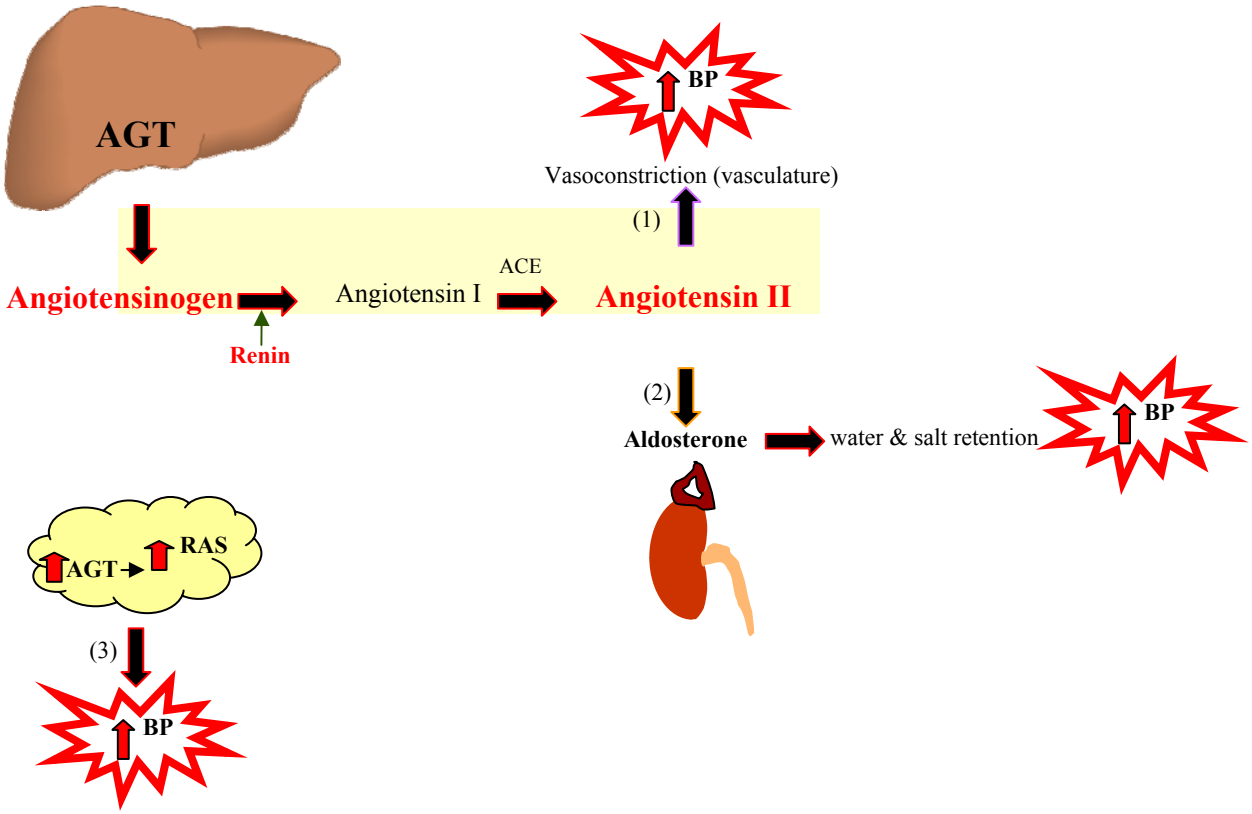

5.13 The circulating and adipose-specific activation of the renin-angiotensin system (RAS) in $GR^{+/-}$ mice and its potential involvement in their hypertensive phenotype.

The classical RAS pathway is shaded in yellow. The major source of angiotensinogen (AGT) production is the *liver*. Renin secreted by the kidney, cleaves angiotensin I (inactive) from angiotensinogen. Angiotensin I is then converted to angiotensin II by the angiotensin converting enzyme (ACE). In GR $^{+/-}$ mice, plasma renin activity is elevated. This might lead to subsequent increased angiotensin II production which in turn affects downstream systems by inducing (1) vasoconstriction in the vasculature and affects blood pressure (BP) or (2) aldosterone secretion by the adrenal cortex and thus water and salt retention that might lead to increased BP. Alternatively, since $GR^{+/-}$ adrenals appear hypertrophied with signs of increased aldosterone producing cells, and indeed elevated plasma aldosterone levels which would be predicted to have a direct effect on the renovasculature and thus BP regulation. Finally, $GR^{+/-}$ mice exhibit increased AGT mRNA levels specifically in adipose tissue (3), directly implicating adipose-induced activation of RAS and its involvement in the hypertensive phenotype (this is less likely since AGT is significantly reduced in HF-fed hypertensive $GR^{+/-}$ and $GR^{+/+}$ mice) .

Chapter 6

Pomc$^{-/-}$ mice: A model of HPA axis hypoactivity and peripheral glucocorticoid hypersensitivity

6.1 Introduction

In the previous chapter, the role of reduced GR levels on obesity, metabolic parameters and blood pressure was examined using a model of HPA axis hyperactivity and GC resistance ($GR^{+/-}$ mice). In this chapter, a model of rodent obesity with dysregulated GC action, the *Pomc*$^{-/-}$ mice, was investigated as a model of HPA axis hypoactivity and increased GC sensitivity.

Inactivating mutations of the gene encoding POMC in humans and mice cause obesity (Yaswen et al., 1996; Krude et al., 1998; Challis et al., 2004). POMC is the polypeptide precursor to a number of bioactive peptides including α-, β- and γ-melanocyte-stimulating hormone (MSH) – the melanocortins – which, in the hypothalamus play critical roles in the regulation of appetite and energy expenditure (Schwartz, 2000). Lack of melanocortin signalling in the hypothalamus drives hyperphagia and obesity in both humans and mice (reviewed in Coll., 2007) POMC is also the precursor to ACTH, sectreted by the anterior pituitary and is essential for adrenal gland steroidogenesis (reviewed in Pritchard and White, 2007). Because of the lack of ACTH, POMC-deficient humans and mice have adrenal insufficiency and low or absent circulating glucocorticoids (Yaswen et al., 1996; Krude et al., 1998; Challis et al., 2004).

Pomc$^{-/-}$ mice are unusual because most rodent models of obesity are characterised by hypercorticosteronemia, with weight gain normalised following adrenalectomy and reinstated by GC replacement (Debons et al., 1982; Freedman et al., 1986; Sainsbury

et al., 1997; Makimura et al., 2000). Additionally, some rodent models of obesity have increased levels of 11β-HSD1 selectively in their adipose tissue (Masuzaki et al., 2001; Livingstone et al., 2000) as is found in human obesity (see chapter 7). The potentially causative role of higher adipose 11β-HSD1 levels in metabolic disease is exemplified by the phenotype of mice with transgenic over-expression of 11β-HSD1 in adipocytes (aP2-HSD1 mice). aP2-HSD1 mice have hyperphagia, visceral obesity, insulin resistance and hypertension despite unchanged systemic GC levels (Masuzaki et al., 2001; Masuzaki et al., 2003). Hepatic over-expression of 11β-HSD1 has no effect on adiposity, but causes hypertension and insulin resistance (Paterson et al., 2004). *Pomc*$^{-/-}$ mice are therefore unusual amongst rodent models in that obesity develops in the absence of high circulating or tissue GCs (Challis et al., 2004). Indeed the obesity and metabolic disease would appear to be entirely secondary to central loss of the appetite suppressant melanocortins which tonically inhibit food intake (reviewed in Coll, 2007; Lee and Wadlow, 2007; Lam et al., 2007). However, treatment of adult *Pomc*$^{-/-}$ mice with corticosterone for 10 days exacerbated their hyperphagia and obesity (Coll et al., 2005). CORT treated *Pomc*$^{-/-}$ mice showed a significant increase in weight (38.7$\pm$0.6 *vs*. 34.9$\pm$1.1 g, CORT *vs*. vehicle, $P<0.05$), total fat mass (12.8$\pm$0.4 *vs*. 9.0$\pm$0.5, $P<0.001$) and daily food intake (6.4$\pm$0.2 *vs*. 4.9$\pm$0.1 g, $P<0.001$). Plasma leptin levels increased 4-fold and insulin levels more than 50-fold in CORT *vs* vehicle treated *Pomc* null mice (Coll et al., 2005). Thus, glucocorticoid deficiency seen in *Pomc* null mice ameliorates the severe adverse metabolic consequences of the lack of melanocortin peptides (Coll et al., 2005). Here I investigated whether altered adipose GR levels or/and GC reactivation contributed to the severity of the metabolic abnormalities.

The effects of GC treatment on obesity and the worsening of the metabolic profile in *Pomc*$^{-/-}$ mice was of considerable interest, one reason being that therapeutic strategies aim to directly affect tissue-specific GC action rather than the HPA axis. Therefore, the work presented in this chapter was designed to study the peripheral mechanisms involved in GC hypersensitivity in corticosterone treated *Pomc*$^{-/-}$ mice. It has been hypothesised that corticosterone treated *Pomc*$^{-/-}$ mice would have increased GC action in peripheral tissues (liver or/and adipose tissue) and that this would underlie their apparent GC-hypersensitivity and exaggerated metabolic syndrome-like phenotype. The experimental design of the study is outlined in Figure 6.1.

6.2 Results

6.2.1 *Pomc*$^{-/-}$ mice have reduced basal intra-adipose GC action but exaggerated GC-amplification responses when CORT treated.

Corticosterone-treated (CORT) *Pomc*$^{-/-}$ and wild type mice had similar plasma CORT levels and hypothalamic CRH mRNA levels (Coll *et al*. 2005). CORT treated *Pomc*$^{-/-}$ mice showed a significant increase in weight (38.7$\pm$0.6 *vs*. 34.9$\pm$1.1 g, CORT *vs*. untreated, $P<0.05$), total fat mass (12.8$\pm$0.4 *vs*. 9.0$\pm$0.5, $P<0.001$) and daily food intake (6.4$\pm$0.2 *vs*. 4.9$\pm$0.1 g, $P<0.001$) (Coll *et al*. 2006). To examine potential mechanisms of CORT hypersensitivity in *Pomc*$^{-/-}$ mice, 11β-HSD1 and GR mRNA levels were measured in epididymal, inguinal and retroperitoneal adipose depots. Adipose 11β-HSD1 mRNA expression was lower in all untreated *Pomc*$^{-/-}$ compared to wild type mice (fig. 6.2A,B) and was dramatically increased by CORT in both genotypes (fig. 6.2A,B), with larger increases (2 to 4-fold greater) in *Pomc*$^{-/-}$

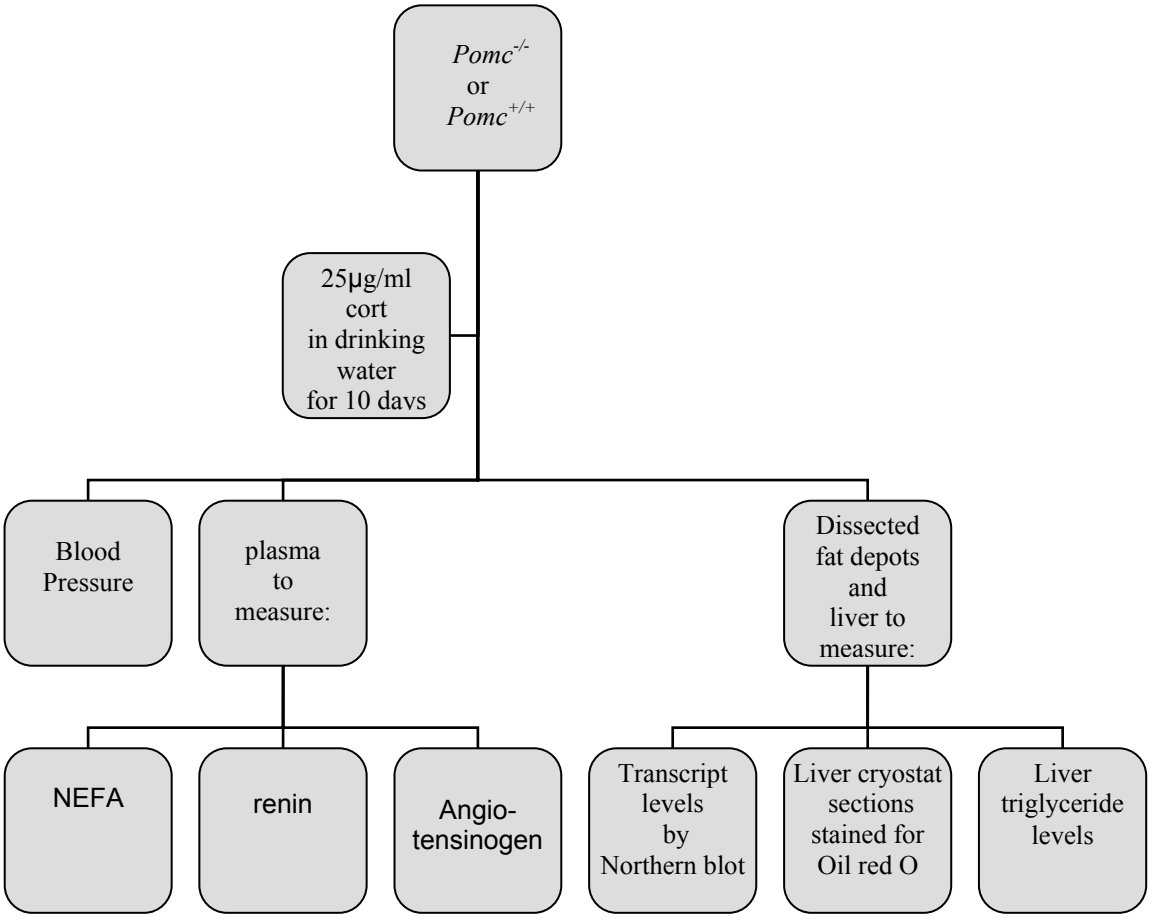

Figure 6.1 Experimental design.

Eight week-old male mice (n=5/group) were treated with corticosterone (25µg/ml) in their drinking water, a dose that results in similar plasma glucocorticoid levels and hypothalamic CRH mRNA levels in *Pomc*$^{-/-}$ and wild type mice (Coll *et al*. 2005). All mice had *ad libitum* access to water and chow diet. Systolic blood pressure was measured photoelectrically in the tail of restrained conscious mice. Animals were killed between 0800 and 0900h by cervical dislocation. Plasma from trunk blood samples was used to assay non-esterified fatty acid (NEFA), triglyceride levels renin and angiotensinogen concentrations. RNA from liver and adipose tissues (inguinal, retroperitoneal and epididymal) was denatured, northern blotted and hybridized to ^{32}P-labelled cDNA probes for mouse 11β-HSD1, GR, angiotensinogen, phosphoenolpyruvate carboxykinase (PEPCK), lipoprotein lipase (LPL) and 18S. Specific mRNAs were quantified using a phosphorimager and Aida image analysis software and are expressed in arbitrary units (A.U.) relative to 18S. Neutral lipids, cholesterol and fatty acids were identified by light microscopy in liver sections (30µm) stained with Oil red O and counter-stained with haematoxylin. Hepatic triglycerides were extracted and measured spectrophotometrically. For details please refer to methods (chapter 2). The corticosterone-replacement experiment, blood pressure, plasma NEFA and triglyceride measurements were performed by Tony Coll (Cambridge).

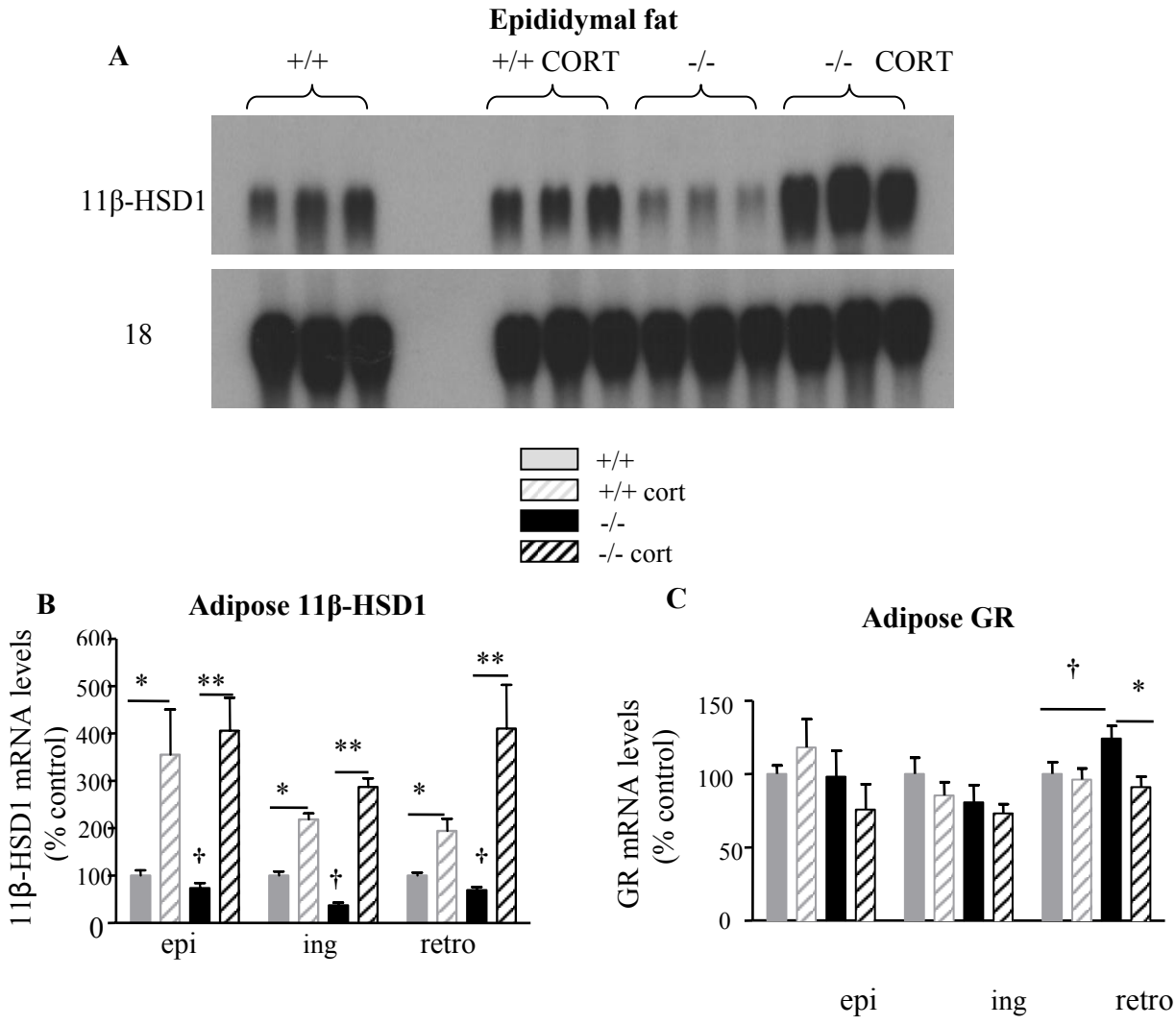

Figure 6.2 Mediators of GC action in adipose tissue of Pomc$^{-/-}$ mice.

(A) Representative northern blot showing levels of 11β-HSD1 mRNA and 18S RNA in epididymal adipose tissue of *Pomc*$^{-/-}$ (-/-) and wild type (+/+) mice, either untreated or treated for 10 days with corticosterone (cort). (B-C) Quantitation of adipose tissue-specific 11β-HSD1 (B), GR (C) in experimental mice. Data are presented as % of the value in untreated wild type mice (100%) and are the means ± SEM; n=5/group. Data analysed by 2-way ANOVA for the effect of genotype and treatment followed by post-hoc Tukeys' tests for group differences. Significance, †P<0.05, **P<0.01 and ***P<0.001.epi; epididymal, ing; inguinal, retro; retroperitoneal fat depots. † and * showing differences between genotypes and treatment respectively.

mice. Adipose expression of GR mRNA was higher in the retroperitoneal fat of *Pomc*$^{-/-}$ mice and was restored to wild type levels after CORT treatment (fig. 6.2C). GR mRNA levels did not differ in inguinal and epididymal fat between *Pomc*$^{-/-}$ and wild type mice, and were unaffected by CORT treatment in either genotype (fig. 6.2C).

To investigate mechanisms downstream of 11β-HSD1/GR by which CORT-treatment selectively increases fat mass in *Pomc*$^{-/-}$ mice, adipose levels of mRNA encoding lipoprotein lipase (LPL), a GC-regulated gene (Fried *et al*., 1993), were measured. Although LPL mRNA levels were the same in untreated *Pomc*$^{-/-}$ and wild type mice in all depots, adipose LPL expression in *Pomc*$^{-/-}$ mice was markedly increased by CORT-treatment (fig. 6.3A) consistent with increased triglyceride uptake, and fat mass in *Pomc*$^{-/-}$ mice. In wild type mice, CORT-treatment increased LPL mRNA only in the inguinal depot, and to a lesser extent than in *Pomc*$^{-/-}$ mice (fig. 6.3A), suggesting adipose depot-dependent regulation of LPL by GCs in non-obese mice, consistent with previous data in rats (Freedman *et al*. 1986).

Phosphoenolpyruvate carboxykinase (PEPCK) is essential for gluconeogenesis in liver and for glycerol synthesis in adipose tissue (Pilkis & Granner 1992; Reshef *et al*. 2003). PEPCK is a classical GC-target gene which is positively regulated by glucocorticoids in hepatocytes and negatively regulated in adipocytes (Sasaki *et al*.1984; Nechushtan *et al*. 1987). Consistent with this, adipose PEPCK mRNA levels were decreased in epididymal and retroperitoneal fat by CORT-treatment in wild

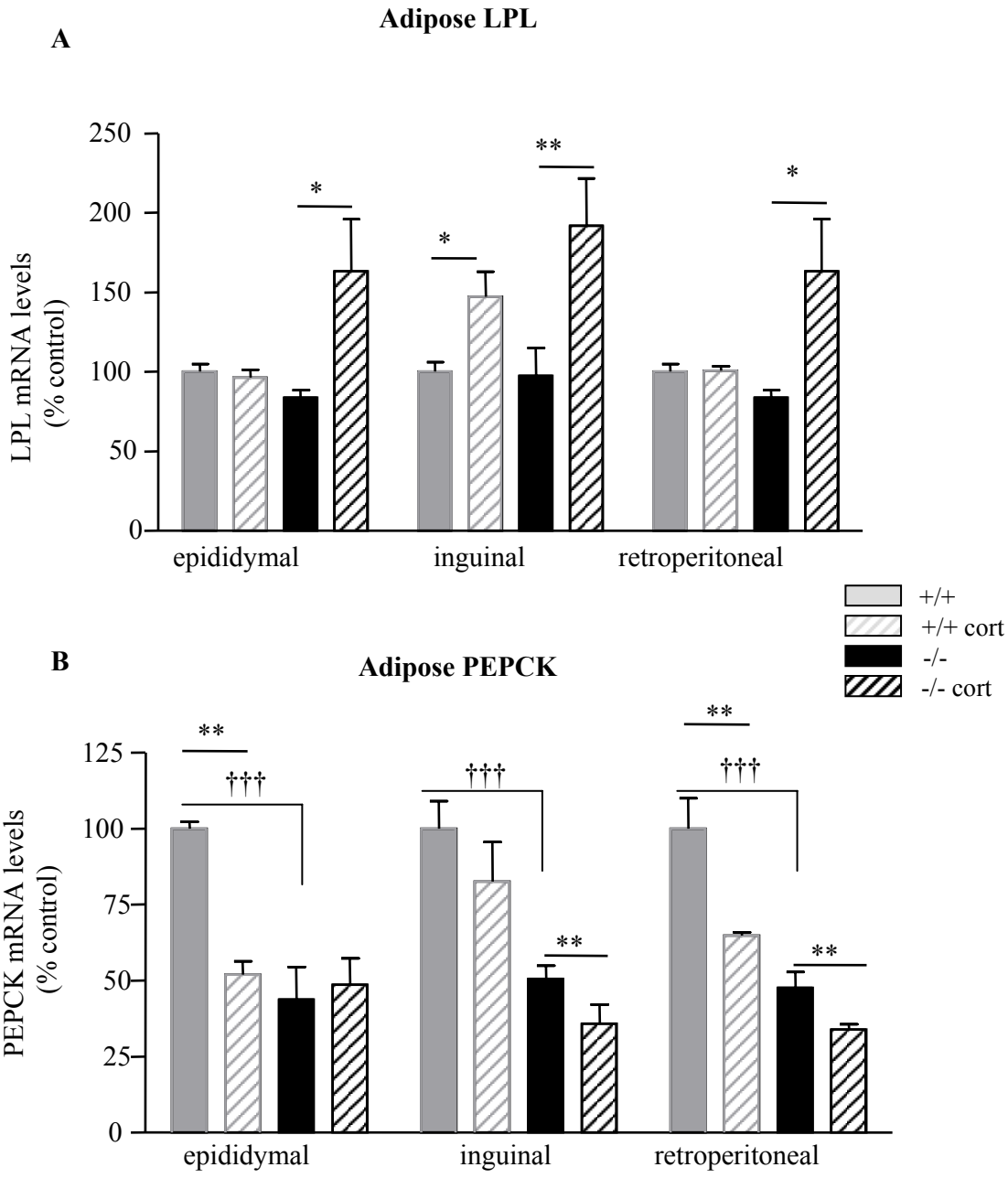

Figure 6.3 Effects of CORT-treatment on GC target genes in adipose tissue

Quantitation of data from northern blots showing levels of mRNA encoding LPL (A) and PEPCK (B) in adipose tissues of *Pomc*$^{-/-}$ and wild type mice, either untreated or treated for 10 days with corticosterone (cort). Data are presented as % of the value in untreated wild type mice (100%) and are the means ± SEM; n=5/group. Data analysed by 2-way ANOVA for the effect of genotype and treatment followed by post-hoc Tukeys' tests for group differences. Significance, **P*<0.05, ***P*<0.01 and †††*P*<0.001. † and * showing differences between genotypes and treatment respectively.

type mice (Fig. 6.3B). Surprisingly, given their GC deficiency, *Pomc*$^{-/-}$ mice had lower levels of PEPCK mRNA in adipose tissue than wild type (Fig. 6.3B). However, although CORT treatment decreased PEPCK expression in inguinal and retroperitoneal adipose tissue in *Pomc*$^{-/-}$ mice (significantly lower than in CORT-treated wild type mice; p=0.01), it had no effect on PEPCK mRNA levels in epididymal adipose tissue, suggesting that other regulatory factors dominate PEPCK expression in adipose tissue of *Pomc*$^{-/-}$ mice (Fig. 6.3B).

6.2.2 *Pomc*$^{-/-}$ mice have unaltered hepatic 11β-HSD1 but higher GR mRNA levels.

Hepatic 11β-HSD1 mRNA levels were similar between the two genotypes (fig. 6.4A) and unaffected by CORT (fig. 6.4A). Hepatic GR mRNA levels were higher in *Pomc*$^{-/-}$ compared to wild type mice (fig. 6.4B), but again CORT had no effect on GR mRNA levels (fig. 6.4B). Hepatic PEPCK expression was lower in *Pomc*$^{-/-}$ than in wild type mice (fig. 6.4C) and was increased by CORT treatment to levels equivalent to untreated wild type mice. In contrast, CORT decreased hepatic PEPCK mRNA levels in wild type mice (fig.6.4C).

6.2.3 *Pomc*$^{-/-}$ mice are dyslipidaemic.

Pomc$^{-/-}$ mice showed markedly higher circulating triglyceride levels (fig. 6.5A) and hepatic lipid accumulation than wild type mice (fig. 6.5B), with 6-fold higher levels of hepatic triglyceride (P<0.001) (fig. 6.5C). However, CORT had no effect on plasma triglyceride levels in either genotype (fig. 6.5A), nor did it worsen the liver

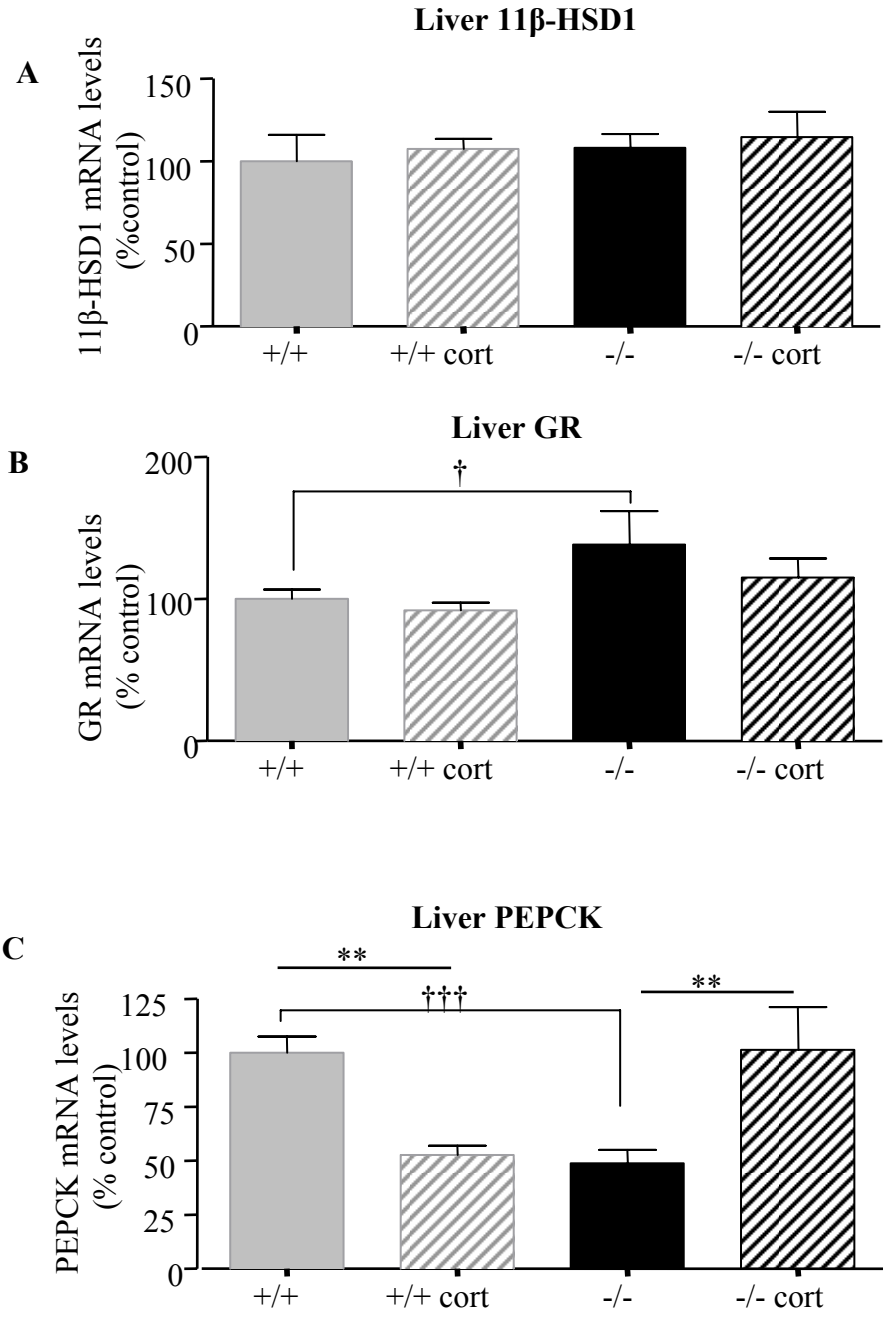

Figure 6.4 Mediators of GC action in liver of Pomc$^{-/-}$ mice and effects of CORT-treatment on PEPCK mRNA levels.

Liver expression of (A) 11β-HSD1, (B) GR and (C) PEPCK mRNA in *Pomc*$^{-/-}$ (-/-) and wild type (+/+) mice, either untreated or treated for 10d with corticosterone (cort). Data are presented as % of the value in untreated control mice (100%) and are the means ± SEM; n=5/group. Data analysed by 2-way ANOVA for the effect of genotype and treatment followed by post-hoc Tukeys' tests for group differences. Significance, †P <0.05, **P<0.01 and †††P<0.001. † and * showing differences between genotypes and treatment, respectively.

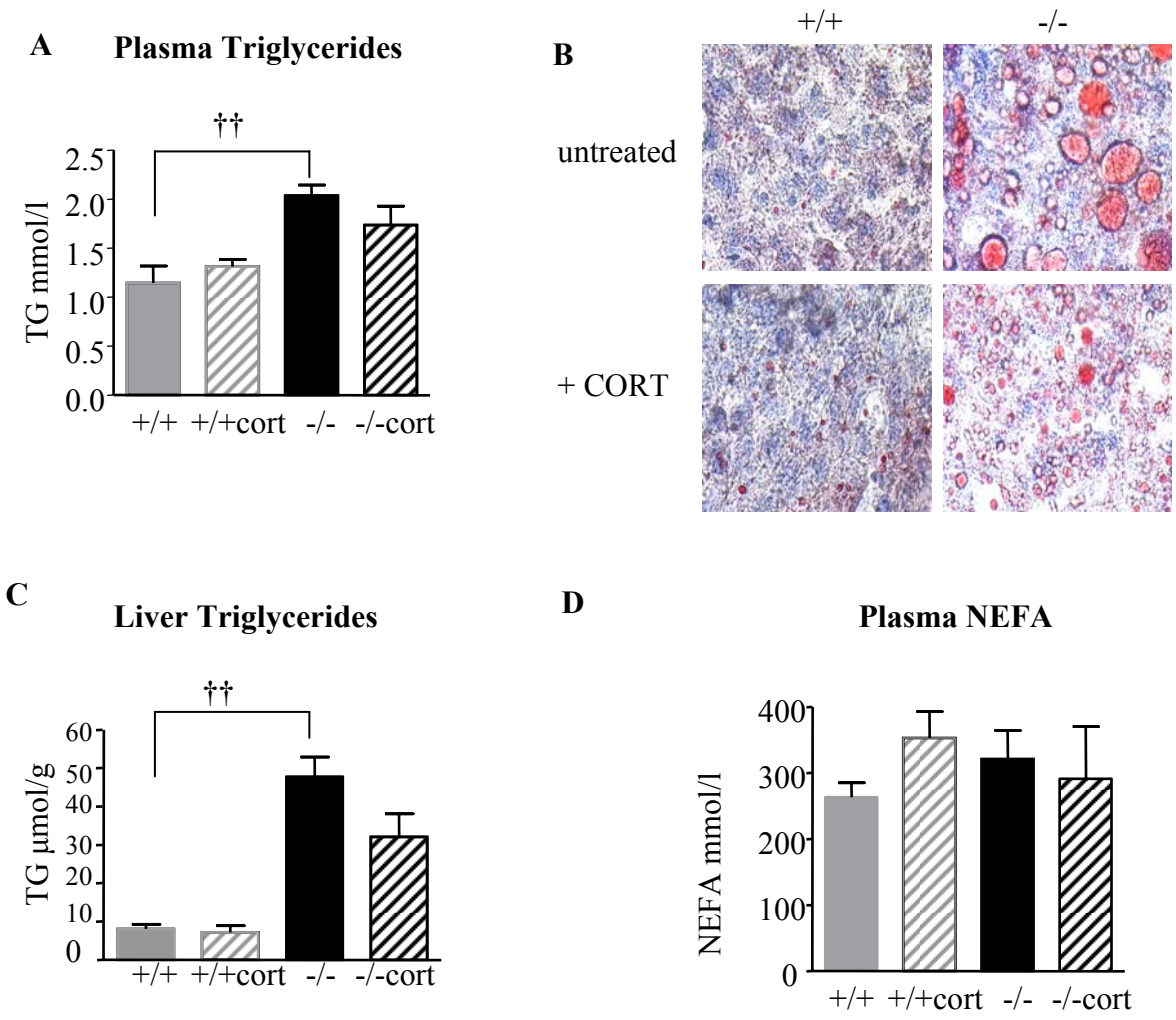

Figure 6.5 Dyslipideamia and fatty liver in Pomc$^{-/-}$ mice.

(A) Plasma triglyceride (TG) levels in *Pomc*$^{-/-}$ (-/-) and wild type (+/+) mice, either untreated or treated for 10d with corticosterone (cort). (B) Oil Red O staining of neutral lipid in liver sections of wild type mice (+/+, left upper panel), CORT-treated wild type mice (+/+, left bottom panel), *Pomc*$^{-/-}$ (-/-, right upper panel) and CORT-treated *Pomc*$^{-/-}$ (-/-, right bottom panel). Magnification x40; red=Oil red O, blue =haematoxylin (nuclei). (C) hepatic triglyceride content in *Pomc*$^{-/-}$ (-/-) and wild type (+/+) mice, either untreated or treated for 10 days with corticosterone (cort). (D) plasma levels of non esterified fatty acids (NEFA) in *Pomc*$^{-/-}$ (-/-) and wild type (+/+) mice, either untreated or treated for 10 days with corticosterone (cort). Data are means ± SEM; (n=6/group). Data analysed by 2-way ANOVA for the effect of genotype and treatment followed by post-hoc Tukeys' tests for group differences. Significance, ††P<0.01. The data on plasma triglycerides (A) and NEFA (D) have been provided by Tony Coll (Cambridge).

phenotype (fig. 6.5C). *Pomc*$^{-/-}$ and wild type mice had similar plasma NEFA levels which were unaffected by CORT (fig. 6.5D).

6.2.4 CORT drives hypertension in *Pomc*$^{-/-}$ mice independently of adipose and liver renin-angiotensin system (RAS) activation.

Pomc$^{-/-}$ mice had similar blood pressure to wild type mice (fig. 6.6). CORT markedly increased blood pressure only in *Pomc*$^{-/-}$ mice (fig. 6.6). Since hypertension following transgenic expression of 11β-HSD1 in adipose or liver is associated with increased levels of angiotensinogen in each of these tissues, respectively (Masuzaki *et al*. 2001; Paterson *et al*. 2004), it was feasible that a similar mechanism may drive CORT-mediated hypertension in *Pomc*$^{-/-}$ mice. Therefore, key components of the renin-angiotensin system (Guyton, 1991) were examined. *Pomc*$^{-/-}$ mice had higher hepatic angiotensinogen mRNA levels than controls (fig. 6.7A). However, CORT did not alter hepatic angiotensinogen mRNA levels in either genotype (fig. 6.7A).

Consistent with lower intra-adipose GC action, adipose angiotensinogen mRNA levels were lower in *Pomc*$^{-/-}$ mice in all adipose depots (fig. 6.7B). CORT increased angiotensinogen mRNA levels specifically in epididymal adipose tissue of both genotypes (2 fold increase; $P<0.001$) (fig. 6.7B) but had no effect on angiotensinogen mRNA levels in inguinal or retroperitoneal adipose tissue of either genotype (fig. 6.7B). Plasma angiotensinogen concentrations did not differ with genotype or CORT (fig. 6.7C). As has been found in another model of GC deficient

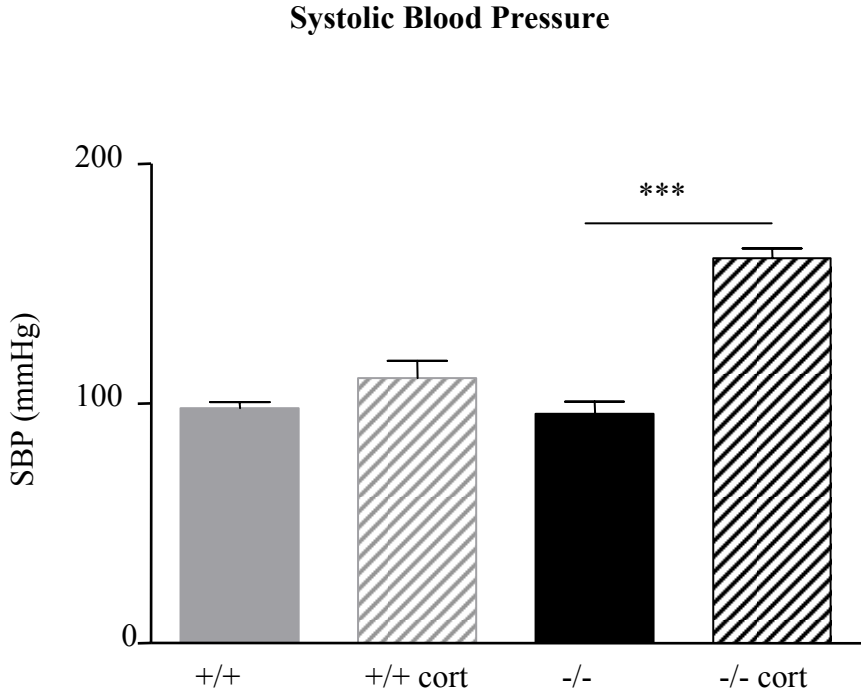

Figure 6.6 Corticosterone treatment increases blood pressure in Pomc$^{-/-}$ mice

Effect of 10d corticosterone treatment (cort) on systolic blood pressure in wild type (+/+) and *Pomc*$^{-/-}$ (-/-) mice. Systolic blood pressure was measured photoelectrically in the tail of restrained conscious mice using an IITC model 179 analyser (Woodland Hills, California, USA). Prior to recording measurements, all mice underwent 3 periods of training to accustom them to the procedure. Mice were warmed at 32^{o}C for 30 min before taking 10 consecutive readings. The first 5 were discounted and a mean value of systolic blood pressure was calculated from the last 5 readings. Five mice from each treatment group were measured. All analog recordings were analysed by an independent observer who was blinded to the genotype of the mice and any treatment they had received. Data are the means ± SEM; Significance; ***P<0.001. Data analysed by 2-way ANOVA for the effect of genotype and treatment followed by post-hoc Tukeys' tests for group differences. Data provided by Tony Coll (Cambridge).

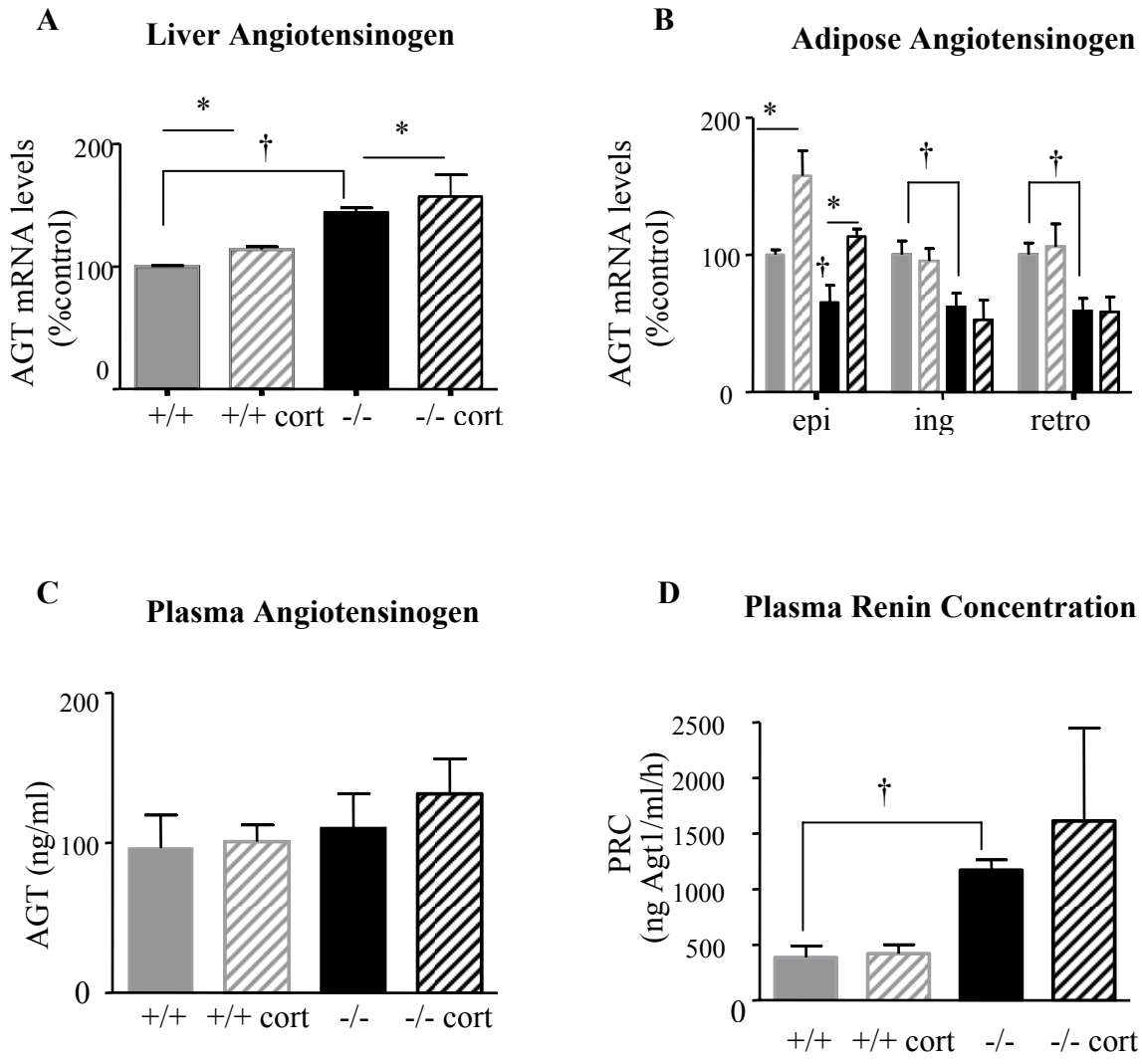

Figure 6.7 Effect of CORT-treatment on the renin-angiotensin system

Effect of 10d corticosterone treatment (cort) on (A) angiotensinogen (AGT) mRNA levels in liver, (B) angiotensinogen (AGT) mRNA in adipose tissue, (C) plasma angiotensinogen and (D) plasma renin concentration in wild type (+/+) and *Pomc*$^{-/-}$ (-/-) mice. Epi, epididymal fat; ing, inguinal fat; retro, retroperitoneal fat. Data are the means ± SEM, and for transcript levels are expressed relative to levels in untreated wild type mice (100%); n=5/group. Data analysed by 2-way ANOVA for the effect of genotype and treatment followed by post-hoc Tukeys' tests for group differences. Significance; * or †P<0.05. † and * showing differences between genotypes and treatment respectively. Note that -/- cort renin level show high variability but outliers cannot be excluded since small number of animals was analysed .

obesity (Fat mice; Morton *et al*. 2005), plasma renin concentration was markedly higher in *Pomc*$^{-/-}$ mice (fig. 6.7D) but this was unaffected by CORT (fig. 6.7D).

6.3 Discussion

Increased GC action specifically in adipose (Masuzaki et al., 2001) or liver (Paterson et al., 2004) produce distinct metabolic syndromes with hypertension. Increased GR sensitivity is also associated with altered fat distribution, hypertension and cardiometabolic disease (Buemann et al., 1997; Rosmond et al., 2000; Ukkola et al., 2001; Dodson et al., 2001; van Rossum et al., 2003). Here, it was hypothesized that altered tissue regeneration of active GC and/or peripheral tissue sensitivity to GCs underlay, in part, the exaggerated fat accumulation, insulin resistance (Coll et al., 2005) and the hypertension (work presented here) observed in *Pomc*$^{-/-}$ mice with GC replacement.

With fixed circulating GC levels such as that achieved with CORT treatment in the current studies, 11β-HSD1 and GR expression levels are the key determinants of GC action. *Pomc*$^{-/-}$ mice had lower adipose but similar hepatic levels of 11β-HSD1 mRNA levels to wild type mice. CORT-treatment dramatically and more markedly increased 11β-HSD1 expression in the adipose tissue of *Pomc*$^{-/-}$ mice. This was accompanied by a marked increase in LPL expression, a GC-inducible gene (Fried et al., 1993), consistent with the exaggerated accumulation of fat in these mice. Intriguingly, these data suggest that, at least in adipose tissue, 11β-HSD1 itself is a

GC target gene. This finding is consistent with most (Jamieson et al., 1995; Voice et al., 1996; Hammami & Siteri 1991; Bujalska et al., 1999), but not all (Napolitano et al., 1998) previous reports of GC induction of 11β-HSD1 in a variety of cell types. Although not specifically measured here, increased adipose 11β-HSD1 activity is predicted to selectively amplify intra-adipose GC concentrations, particularly when circulating levels of substrate are high (eg with HPA axis hyperactivity). On the other hand, the present data suggest that congenital GC deficiency has little impact upon hepatic 11β-HSD1 levels *in vivo* and hepatic 11β-HSD1 levels are not regulated by corticosterone. In contrast, 11β-HSD1 mRNA levels are highly and positively regulated by GCs in adipose tissue.

GR levels are another major determinant of cellular GC sensitivity (Vanderbilt et al., 1987; Geley et al., 1996). Small differences in GR mRNA levels can markedly alter glucocorticoid responsiveness (Geley et al., 1996; Reichardt et al., 2000). *Pomc*$^{-/-}$ mice had elevated GR mRNA levels in liver and retroperitoneal adipose tissue, suggesting increased GC sensitivity selectively in these depots. Following CORT replacement in *Pomc*$^{-/-}$ mice, GR mRNA levels were restored to wild type levels in retroperitoneal adipose tissue but not in liver, consistent with tissue- and time-specific differences in GR autoregulation (Reichardt et al., 2000; Sheppard et al., 1990; Holmes et al., 1990; Holmes et al., 1995; Holmes et al., 1997; Kalinyak *et al*. 1987; Dong et al., 1988).

CORT had no additional effects on the hypertriglyceridaemia and fatty liver of the *Pomc*$^{-/-}$ mice, and did not affect plasma NEFAs, which were normal in *Pomc*$^{-/-}$ mice. The CORT-driven caloric excess in *Pomc*$^{-/-}$ mice may drive a further increase in the flux of triglycerides from the liver, that, coupled with increased adipose fatty acid uptake via LPL, maintains the circulating and liver triglyceride levels constant and is consistent with increased adipose tissue mass in CORT treated *Pomc*$^{-/-}$ mice (Coll et al., 2005).

Adipose PEPCK is critical for glyceroneogenesis and is thus a key regulator of the level of fatty acid re-esterification (reviewed in Reshef et al., 2003). Unexpectedly, since GCs reduce adipose PEPCK, GC-deficient *Pomc*$^{-/-}$ mice had lower levels of PEPCK mRNA in all adipose depots. This was further decreased by CORT treatment. The lower level of PEPCK mRNA in untreated *Pomc*$^{-/-}$ mice may be due to their higher fed blood glucose levels, thus reducing the need for glyceroneogenesis to generate glycerol-phosphate for fatty acid re-esterification (Nechushtan et al., 1987; Opherk et al., 2004). *Pomc*$^{-/-}$ mice have lower hepatic expression of PEPCK. This may not be due to lack of GC signalling in liver, as mice with a liver-specific knock-out of GR have normal levels of PEPCK in liver (Opherk et al., 2004), but may be related to the higher circulating levels of insulin in *Pomc*$^{-/-}$ mice compared to wild type (Coll et al., 2005). Insulin dominantly and negatively suppresses hepatic PEPCK in the fed state (Pilkis & Granner 1992). In CORT-treated wild type mice, the repressive effect of insulin predominated. Indeed, the decreased levels of PEPCK in these mice compared to untreated wild type mice may reflect the increase in

insulin levels following CORT treatment (Coll et al., 2005). In contrast, hepatic PEPCK mRNA levels doubled following CORT treatment in *Pomc*$^{-/-}$ mice, consistent with hepatic insulin resistance and marked hyperinsulinaemia (Coll et al., 2005).

Blood pressure in *Pomc*$^{-/-}$ mice is normal despite their hypoadrenal state. This implies that secondary mechanisms are invoked to maintain cardiovascular function when circulating aldosterone and corticosterone concentrations are chronically reduced (Coll et al., 2004). It seems likely that the increased renin activity which observed in *Pomc*$^{-/-}$ mice is part of this adaptive process. However, corticosterone replacement did not normalise renin activity and selectively increased blood pressure in *Pomc*$^{-/-}$ mice. This was not attributed to a further activation of the circulating renin-angiotensin system, since neither renin nor its substrate angiotensinogen were increased. Indeed expression of angiotensinogen mRNA in liver and adipose tissues did not correlate with blood pressure. It seems likely that corticosterone augmented existing mechanisms that were already sustaining vascular function. Apart from renin, these secondary processes are likely to involve the hyperinsulinaemic (Sowers 2004) state of *Pomc*$^{-/-}$ mice (which is exacerbated by corticosterone treatment) (Coll et al., 2005), the sympathetic nervous system (Rascher et al., 1979) (which is thought to explain glucocorticoid-induced hypertension in normal mice) or structural adaptation of the vasculature (Wallerath et al., 2004).

Although *Pomc*$^{-/-}$ mice represent a mouse model of congenital lack of GCs, it will be interesting and more informative to address the effects of GC replacement on blood pressure and metabolic parameters in adrenalectomized wild type and *Pomc*$^{-/-}$ mice to avoid a) any possible residual GCs that were undetectable by the corticosterone assay and b) the inevitable supraphysiological levels of corticosterone replacement.

In summary, the data presented here show that increased adipose tissue-specific sensitivity to GCs in *Pomc*$^{-/-}$ mice may result in part from exaggerated induction of 11β-HSD1 in adipose tissue with CORT administration. Whilst acknowledging that mRNA changes do not always translate to altered protein (or enzyme activity) levels, these data nevertheless suggest that 11β-HSD1 might be a more potent mediator of intra-adipose GC action than the GR levels whereas in liver, higher GR levels contribute to the diabetogenic phenotype of the *Pomc*$^{-/-}$ mice.

Chapter 7

Glucocorticoid action in multiple adipose depots in human obesity

7.1 Introduction

In the previous 2 chapters, the effects of altered GC sensitivity on obesity and parameters of the Metabolic Syndrome were studied in 2 distinct animal models ($GR^{+/-}$ and *Pomc*$^{-/-}$ mice) with altered peripheral GC sensitivity and dysfunctional HPA axis. In this chapter alterations in GC action in multiple adipose tissue compartments in human obesity are explored.

Exposure to high circulating GC levels, as found in Cushing's syndrome, causes a metabolic disease that resembles features of idiopathic metabolic syndrome including pronounced visceral obesity (reviewed in Seckl et al, 2004). However, idiopathic obesity is not associated with high circulating GC levels in humans (Marin et al., 1992). Rather, it appears that intra-cellular regeneration of active GCs by the enzyme 11β-HSD1 is aberrantly elevated in adipose tissue of obese individuals (reviewed in Walker and Andrew, 2006). Visceral (omental) obesity is associated with an increased risk for type 2 diabetes, hyperlipidemia and hypertension (Fujioka et al., 1987; Despres et al., 1989). In contrast, comparable amounts of fat stored preferentially in gluteal or femoral depots (lower body obesity) were associated with lower risk of morbidity and mortality from metabolic abnormalities (Kennel et al., 1991). Given the key association of intra-abdominal (visceral) adipose tissue with metabolic and cardiovascular risk, it has been hypothesized that increased 11β-HSD1 in the visceral, rather than subcutaneous, adipose depot causes the adverse metabolic consequences of idiopathic obesity and the Metabolic Syndrome - so called 'Cushings disease of the omentum' (Bujalska et al., 1997). Data from human studies

have engendered some confusion as to whether visceral as well as subcutaneous 11β-HSD1 is elevated in human obesity (section 1.6.3).

Mechanistically, GCs induce adipose tissue expansion by stimulating preadipocyte differentiation (Xu and Bjorntorp, 1990). A key factor in this process, are levels of the GRα. In contrast to the plethora of studies (section 1.6.3) of 11β-HSD1 in adipose tissue and metabolic parameters, curiously few studies have examined associations between GR and such parameters. Higher levels of GR are found in omental compared to subcutaneous fat (Rebuffe-Scrive et al., 1990), therefore it could be expected that GR levels will have a more pronounced effect on GC action in the omental depot. Here, the hypothesis that altered GR, as well as 11β-HSD1 mRNA levels are associated with obesity in human visceral (omental) and subcutaneous (abdominal, thigh, gluteal) adipose tissue was tested.

Specifically the objective of this study was to determine the association between 11β-HSD1 and GRα mRNA levels in 4 distinct adipose depots and measures of obesity and the Metabolic Syndrome. Therefore, adipose tissue biopsies from subcutaneous (sc; abdominal, thigh, gluteal) and intra-abdominal (omental) adipose depots from 21 women were analysed for 11β-HSD1 and GRα mRNA levels by real time PCR. Body composition, fat distribution, fat cell size and blood lipid, glucose and insulin levels were correlated with the transcript levels.

7.2 Results

7.2.1 Subject characteristics

Volunteers were recruited to the Mayo Clinic (Rochester, USA) and were Caucasian females undergoing tubal ligation surgery, carried out in the follicular phase of the menstrual cycle to reduce the risk of pregnancy. The mean age was 35 ± 1 year with mean BMI 32.7±1.5 kg/m^2 (Table 7.1), indicating an obese group. Median± IQR fasting plasma insulin levels were 15.6±19.6 μU/ml and HOMA-IR was 3.3±4.6 (range 0.42-47). Median fasting plasma glucose levels and mean triglyceride concentrations averaged 4.9 ±0.44 mmol/L and 148± 19 mg/dl, respectively (Table 7.1).

7.2.2 11β-HSD1 mRNA levels are highest in abdominal sc and omental adipose tissues whereas GRα mRNA is highest in the omental fat.

11β-HSD1 mRNA levels were greater in abdominal subcutaneous and omental than in gluteal or thigh subcutaneous adipose depots (fig 7.1A). 11β-HSD1 mRNA levels were positively correlated in the 3 sc depots: abdominal vs thigh; R=0.83, P<0.005 and abdominal vs gluteal; R=0.86, P<0.005. There were no associations between abdominal sc and omental 11β-HSD1 mRNA levels. GRα mRNA levels were highest in omental and lowest in thigh sc adipose tissue (fig 7.1B) but were not correlated between any depots. No correlation was found between 11β-HSD1 and GRα mRNA levels in any depot (fig 7.1C).

Table 7.1 Anthropometric and metabolic characteristics of study participants

CHARACTERISTICS	FEMALES (N=21)
Anthropometry	
Age (years)	35.3±1.4 (20-44)
BMI (kg/m^2)	32.7±1.5 (20-42)
Body Fat (%)	46 ± 2 (23-56)
VAT area (cm^2)	96±163 (23-236)
SAT area (cm^2)	326±35 (59-577)
VAT/SAT	0.28±0.03 (0.11-0.64)
Plasma Biochemistry	
Fasting Glucose (mmol/L)	4.9±0.44 (4.1-7.0)
Fasting Insulin (μU/ml)	15.6±19.6 (2.2-167)
Fasting Triglyceride (mg/dl)	146.7±18.7 (38-278)

Prior to surgery, body composition was assessed by measuring weight, height, body fatness (% fat) using dual x-ray absorptiometry (DEXA;DPX-IQ; Lunar Radiation, Madison, WI) and abdomial fat distribution using a single sliced computerized tomography scan at the L_{2-3} level. Visceral and subcutaneous adipose tissue areas were calculated as previously described (Jensen et al, 1993). Data are presented as mean ± SEM. For glucose and insulin, data are presented as median ± IQR. Range of values in parenthesis. BMI; body mass index, VAT; visceral adipose tissue, SAT; subcutaneous adipose tissue. These data were kindly provided by Prof Michael D Jensen (Mayo Clinic, Rochester).

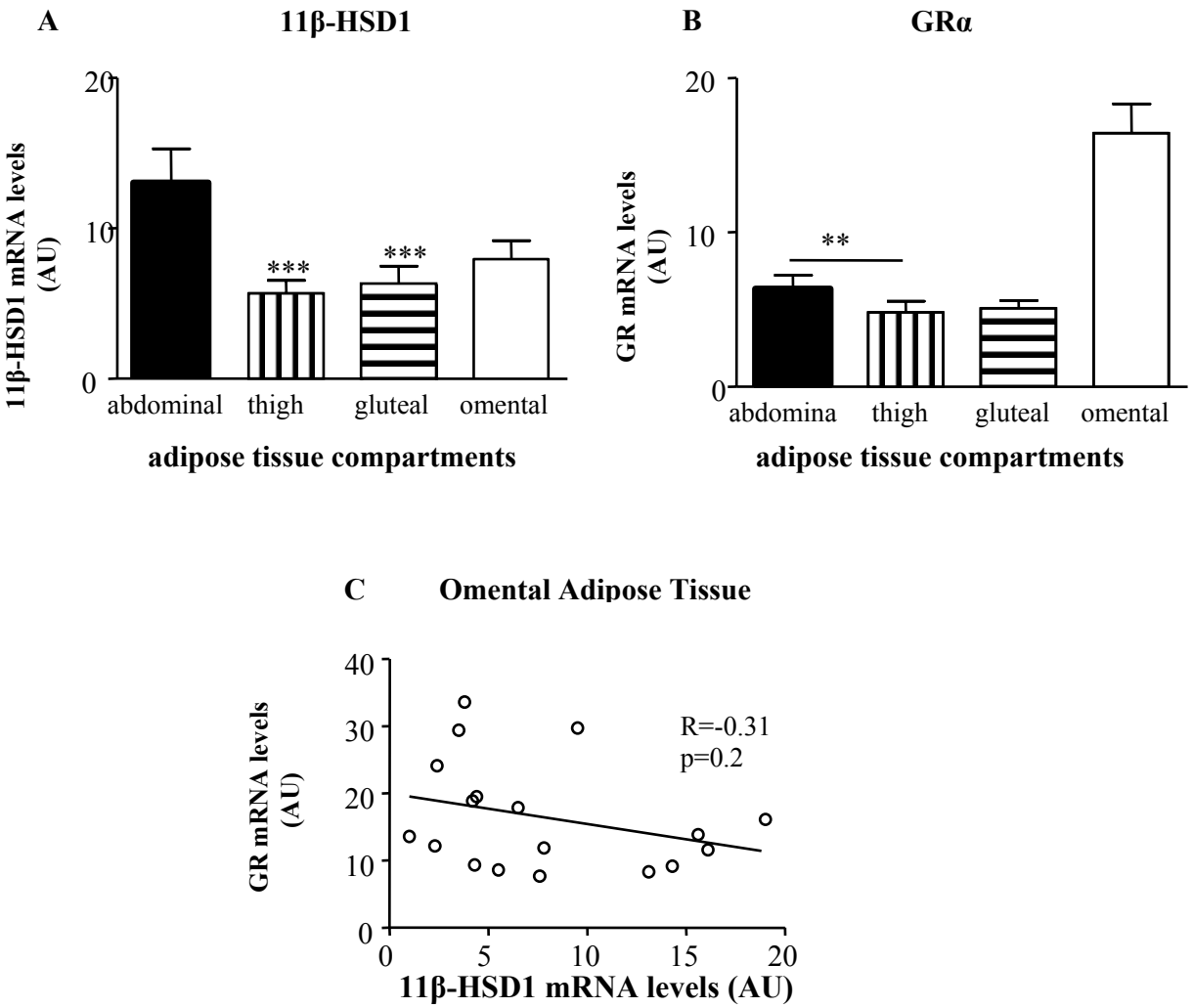

Figure 7.1 11β-HSD1 and GRα mRNA levels in multiple human adipose tissue compartments.

A) 11β-HSD1 mRNA levels were higher in abdominal and omental compared to thigh and gluteal adipose tissues. B) GRα mRNA levels were higher in omental and lower in thigh compared to the other adipose tissue compartments. C) 11β-HSD1 and GRα mRNA levels are not correlated in omental adipose tissue. Real time PCR analysis was performed to measure mRNA levels in multiple adipose compartments. Internal control was cyclophilin a. One way ANOVA was used to compare differences in mRNA levels between depots. Data are presented as mean ± SEM. Pearson correlation was performed to determine an association between 11βHSD1 and GRα mRNA levels. ** $p<0.01$ and *** $p<0.001$. For primer-probe details please refer to Table 2.1.

7.2.3 Parameters of GC action in the omentum

7.2.3.1 Obesity is associated with elevated 11β-HSD1 but reduced GRα mRNA in omental adipose tissue.

A strong positive association between BMI and omental adipose 11β-HSD1 mRNA levels was observed: R=0.570, P<0.01 (fig 7.2A, Table 7.2). Moreover, visceral fat area determined by CT (VAT) correlated with increased 11β-HSD1 mRNA levels in the omentum (fig 7.2B, Table 7.2). Omental 11β-HSD1 mRNA levels were consistently and positively associated with general adiposity (defined by % of body fat; R=0.462, P<0.05) and with subcutaneous/peripheral (SAT) adiposity (Table 7.2). In contrast, obesity was associated with decreased GRα mRNA levels in the omental depot (R=-0.627, P<0.001) (fig 7.2D, Table 7.2). Visceral adiposity (fig 7.2E) was negatively correlated with omental GRα mRNA levels (VAT; R= - 0.507, P<0.05).

7.2.3.2 Omental fat cell hypertrophy is associated with increased 11β-HSD1 but reduced GRα transcript levels.

Fat cells were smaller in the omental depot than in subcutaneous adipose tissue (omental; 84 ± 4 μm; *vs* abdominal sc, thigh, gluteal 104 ± 3 μm, 109 ± 3 μm, 106 ± 2 μm $P<0.0001$). Omental fat cell size was positively correlated with 11β-HSD1 mRNA levels (R=0.72, $P<0.001$) (fig 7.2C, Table 7.2). In contrast, GRα transcript levels were negatively correlated with omental fat cell size (fig 7.2F, Table 7.2). In order to test for independent effects, multiple regression analyses was performed to understand the effects of obesity (BMI) and fat cell size on 11β-HSD1 or GRα mRNA levels. Omental fat cell size was strongly and independently correlated with 11β-HSD1 (standardized β coefficient 1.2; $P<0.05$), whereas GRα was not associated with fat cell size independently of obesity.

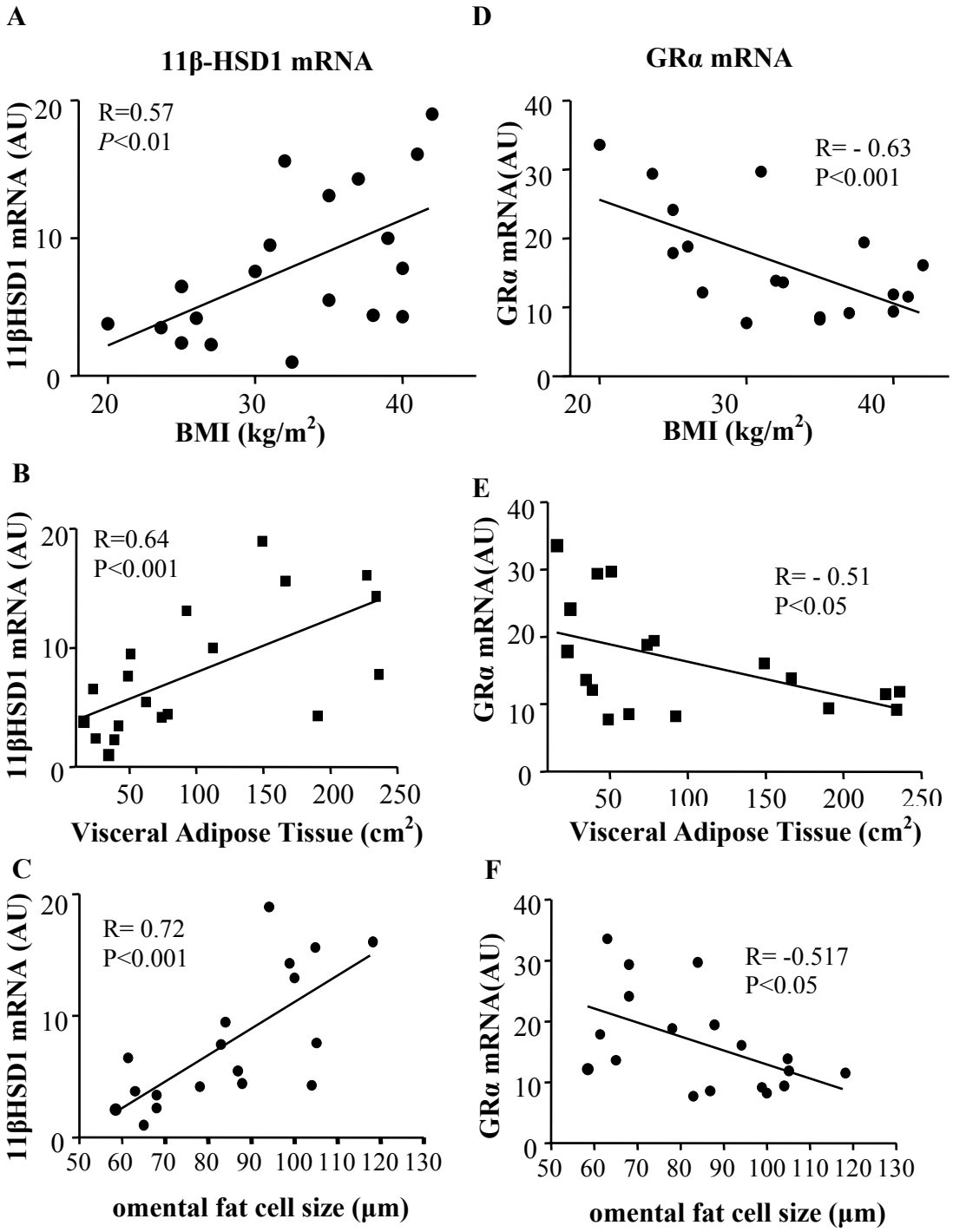

Figure 7.2 Correlation of 11β-HSD1 and GRα mRNA levels with anthropometric parameters and fat cell size in the omental adipose compartment.

Correlation of (A) BMI with 11βHSD1, (B) Visceral adiposity (VAT) with 11β-HSD1, (C) Fat cell size with 11βHSD1, (D) BMI with GRα , (E) VAT with GRα and (F) Fat cell size with GRα mRNA levels. Pearson correlation between transcript levels and anthropometric parameters. Regression lines, R and *P* values are indicated in each graph.

Table 7.2 Pearson correlation of 11β-HSD1 and GR mRNA levels in multiple adipose tissue depots with body composition, metabolic parameters and fat cell size.

	11B-HSD1 MRNA				**GRA MRNA**			
	Abdominal	Thigh	Gluteal	Omental	Abdominal	Thigh	Gluteal	Omental
BMI	0.58*	0.53*	0.54*	0.57**	-0.59*	-0.24	-0.20	-0.63***
% Body fat	0.22	0.41	0.44	0.46*	-0.50	-0.24	-0.01	-0.41
VAT	0.55*	0.73***	0.71***	0.64***	-0.30	-0.05	-0.32	-0.51*
SAT	0.36	0.55**	0.40	0.63***	-0.57	-0.15	-0.13	-0.60***
Log fasting glucose	0.20	-0.29	-0.32	-0.18	0.14	-0.41	-0.04	-0.27
Log fasting insulin	0.13	0.04	0.33	0.31	-0.1	-0.47	0.01	-0.48
Fasting triglycerides	0.21	0.57**	0.46	0.46 *	-0.44	0.01	0.2	-0.50*
Log FSC abdominal	0.19				-0.80**			
FSC thigh		0.28				-0.51*		
FSC gluteal			0.40				0.03	
FSC omental				0.72***				-0.52**

% Body fat was measured using DEXA.VAT and SAT are visceral and subcutaneous adipose tissue areas respectively, measured by CT scan. Fat cell sizes (FCS) was determined by measuring the mean adipocyte diameter. Plasma insulin and glucose values, abdominal fat cell size and 11β-HSD1 mRNA levels in thigh and gluteal regions and GR mRNA levels in thigh showed inhomogeneity of variance, therefore were log transformed prior to analysis. * $p<0.05$, ** $p<0.01$ and *** $p<0.001$.

7.2.4 Parameters of GC action in abdominal sc depot

7.2.4.1 Obesity is associated with increased 11β-HSD1 mRNA levels in all sc depots but reduced GRα mRNA in the abdominal sc.

Since reporting on GC action has been largely in the abdominal sc depot, studies described in this chapter are extended beyond this to gluteal and thigh in order to test whether the expected relationships held in these anatomically and metabolically distinct compartments. Positive associations with BMI and 11β-HSD1 mRNA levels were detected in all sc adipose compartments examined (eg. abdominal subcutaneous adipose: R=0.584, $P<0.05$) (Table 7.2). Thigh adipose 11β-HSD1 mRNA levels correlated positively with SAT and this relationship showed a consistent trend in the other depots (Table 7.2). In contrast, abdominal sc GRα mRNA levels were inversely correlated with BMI (R=-0.589, $P<0.05$) (Table 7.2). No significant associations were observed between SAT and abdominal sc GRα mRNA levels (fig 7.3B) or GRα mRNA levels in any other sc depot (Table 7.2).

7.2.4.2 Abdominal sc hypertrophy is associated with reduced GRα mRNA levels.

Although multiple regression analysis with small numbers of abdominal sc biopsies should be interpreted cautiously, the data presented here nevertheless indicate the following. Surprisingly, in abdominal sc adipose tissue 11β-HSD1 mRNA levels were not associated with fat cell size (fig 7.3C). In contrast, GRα transcript levels were negatively correlated with fat cell size (fig 7.3D). Multiple regression analysis confirmed that GRα mRNA levels were independently and negatively correlated with abdominal sc fat cell size (standardized β coefficient -0.014; $P<0.05$). Although GRα

mRNA levels were negatively correlated with fat cell size in the thigh, this relationship did not hold when tested by multiple regression analysis.

7.2.5 Associations of depot-specific glucocorticoid action with metabolic parameters.

Pearson correlation was used to examine interrelationships between transcript levels and metabolic parameters (Table 7.2). Omental and thigh 11β-HSD1 mRNA levels were associated with increased plasma triglyceride levels (omental; R=0.46, $P<0.05$ and thigh; R=0.57, $P<0.01$). This effect was not independent of obesity as confirmed by multiple linear regression analysis. There were no significant associations between fasting glucose, insulin or HOMA-IR and 11β-HSD1 transcript levels. In contrast, there was a negative correlation between GRα mRNA levels and plasma triglyceride levels selectively in the omental compartment (R=-0.50, $P<0.05$). Moreover, there was a trend for an inverse association between omental GRα mRNA levels and fasting plasma insulin levels (R=-0.48, $P=0.052$).

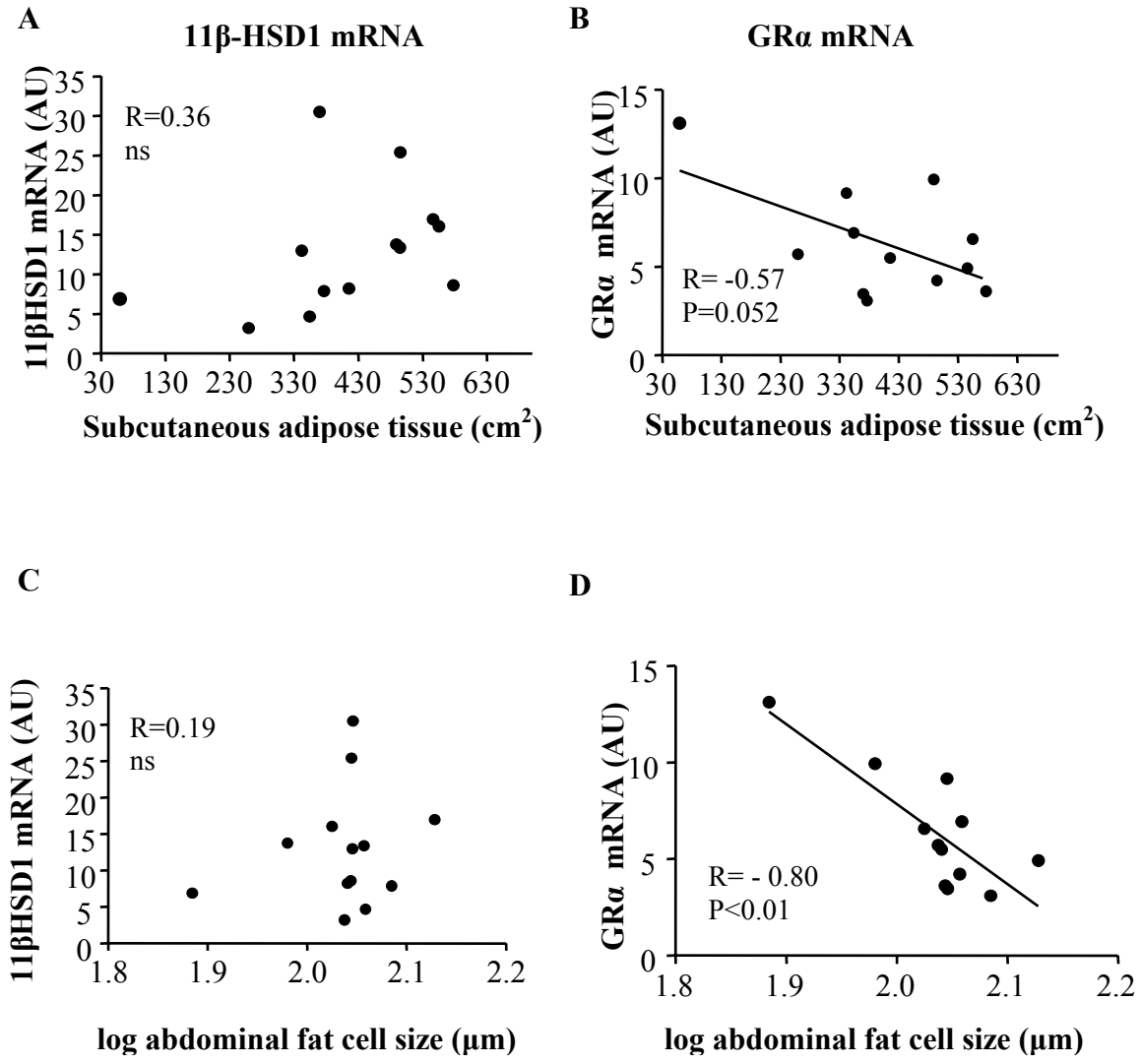

Figure 7.3 Correlation of 11β-HSD1 and GRα transcript levels with peripheral adiposity and fat cell size in abdominal sc compartment.

Pearson correlation of (A) subcutaneous adipose tissue area (SAT) with 11βHSD1 mRNA levels, (B) SAT with GRα mRNA levels, (C) Fat cell size (FCS) with 11βHSD1 mRNA levels and (D) FCS with GRα mRNA levels. Regression lines, R and *P* values are indicated in each graph. NS indicates non-significant correlation

7.3 Discussion

This study examined relationships between two major determinants of tissue GC action in multiple adipose tissue depots in lean and obese women. The key findings were (i) 11β-HSD1 mRNA is most highly expressed in sc abdominal and omental, whereas GRα mRNA is highest in omental adipose tissue; (ii) within individuals, there are positive associations between 11β-HSD1 mRNA levels in sc adipose depots but not omental fat, whereas GRα mRNA levels do not correlate between depots; (iii) between individuals, 11β-HSD1 mRNA levels in all adipose depots including omentum are positively associated with BMI and local fat mass, whereas for GRα mRNA the main relationships (with BMI, VAT, triglycerides) were negative associations in the omentum; (iv) increased fat cell size strongly associates with increased 11β-HSD1 but reduced GRα in the omentum.

Here I extend previous observations form our group (Rask et al., 2002; Lindsay et al., 2003; Wake et al., 2004) and others (Paulimyer-Lacroix et al., 2002; Engeli et al., 2004; Kannisto et al., 2004) on abdominal sc adipose to show a positive relationship between BMI and 11β-HSD1 mRNA levels in all 4 adipose compartments examined. This implies an upregulation of GC reganarating capacity in multiple adipose tissue compartments, including the visceral fat depot. Increased visceral fat is a better predictor of metabolic abnormalities compared to upper-body subcutaneous fat (Fujioka et al., 1987; Despres et al., 1989), and is independently correlated with increased morbidity and mortality (Kuk et al., 2006). In contrast, lower-body obesity may even confer a protective effect with respect to metabolic abnormalities (Snijder

et al., 2006). In this cohort, omental 11β-HSD1 mRNA levels were most strongly associated with increased general adiposity (% body fat). Kannisto et al., 2004 previously reported a positive association between % body fat and 11β-HSD1 mRNA levels in sc fat in obese male and female monozygotic twins. In the present study, subcutaneous adipose expression of 11β-HSD1 mRNA did not correlate with % body fat. Differences between these studies may be due to the distinct populations studied and/or our limited power to detect this interaction since 11β-HSD1 did correlate with other markers of generalised obesity such as BMI. Although in the present study 11β-HSD1 activity levels were not measured due to limited sizes of biopsies, it is expected, based on previous studies (Lindsay et al., 2003; Wake et al., 2003), that activity and mRNA levels will be correlated in abdominal sc adipose tissue biopsies.

GRα transcript levels were highest in omental (visceral) fat, as previously reported in humans (Rebuffe-Scrive et al., 1990) and mice (Masuzaki et al., 2001). The major new finding is that in omental, as well as abdominal sc adipose, GRα mRNA levels are inversely associated with adiposity and fat cell size. A previous study has also reported lower GRα mRNA levels in sc adipose tissue in morbidly obese women (Boullu-Ciocca et al., 2003). Omental GRα mRNA levels were negatively associated with plasma triglyceride and, albeit as a trend, insulin levels. This finding is perhaps counterintuitive since GR polymorphisms associated with increased GC sensitivity and increased visceral fat accumulation (Trembley et al., 2003). The data in the present study suggest that reduction of GR levels to the degree observed in

obesity, does not sufficiently compensate for the hypertrophy caused by increased ligand regeneration (via 11β-HSD1). This notion is supported by data from transgenic animal models. Thus, fat-specific 11β-HSD1 overexpressing mice (Masuzaki et al., 2001) have increased visceral adiposity and 11βHSD1-deficient mice have reduced visceral adiposity (Morton et al., 2004) despite unaltered GR levels. In contrast in humans, this is the first study describing a consistent opposing change in 11β-HSD1 and GRα mRNAs in multiple adipose compartments with obesity. However, since the two transcripts were not correlated in any depot, consistent with previous observations in sc adipose tissue (Kannisto et al., 2004), it appears unlikely that GRα and 11β-HSD1 directly regulate each other. Naturally, there are clearly limitations with association studies, which do not test causality and further direct investigation is needed to elucidate possible mechanisms involved.

The volunteers who participated in this study had normal glucose and triglyceride levels but impaired insulin sensitivity. Increased plasma triglycerides were associated with increased 11β-HSD1 mRNA levels in both thigh and omental regions but with reduced GRα mRNA levels selectively in the omental compartment. Neither 11β-HSD1 nor GRα mRNA levels were associated with fasting glucose, which is consistent with a previous report (Lindsay et al., 2003). However, there appeared to be a trend for a negative association of omental and thigh GRα mRNA levels with fasting insulin levels that would be interesting to confirm in larger cohorts.

Visceral fat adipocytes are more resistant to insulin's antilipolytic effects compared to sc adipocytes (Richelsen et al., 1991). Transgenic mice overexpressing 11β-HSD1 in fat develop central obesity attributed to adipocyte hypertrophy particularly in the mesenteric depot (Masuzaki et al, 2001). To my knowledge, this is the first study that addressed the relationship of 11βHSD1 or GRα mRNA levels with regional fat cell size in humans. Consistent with previous studies (Ostman et al., 1976; Rebuffe-Scrive et al., 1990b; Tchernof et al., 2006), abdominal sc adipocytes were larger compared to omental, indicating higher fat storage in this depot in women. Furthermore, a strong positive correlation between 11β-HSD1 and adipocyte size in the omental depot, independent of obesity was apparent. Despite the negative association of GRα mRNA with omental fat cell size, this was not independent of obesity. Although 11β–HSD1 was also highest in the abdominal sc depot, there was not an association between 11β–HSD1 mRNA levels and abdominal fat cell size, despite the strong positive correlation with BMI. This may appear counterintuitive. The reasons for this might be either the limited power to detect a possible correlation since there were fewer abdominal sc than omental adipose biopsies. Alternatively, 11β–HSD1 may not be a strong predictor of *subcutaneous* hypertrophy in this cohort. This is supported by the lack of correlation between 11β–HSD1 and fat cell size in the thigh and gluteal sc depots. In contrast to findings in the omental depot, GRα mRNA levels were negatively associated with fat cell size in the abdominal sc depot, independent of obesity. It would appear that obesity is associated with a down-regulation of GRα that may limit the hypertrophic effects of GCs in adipose tissue (Cigolini and Smith, 1979; Xu and Bjormtrop, 1990; Fried et al., 1993). However, the data in the present study suggest that this GR down-regulation cannot entirely

counteract increased ligand levels particularly in the omental depot. It will be important to determine whether and how altered GR levels can indeed reach a functionally limiting state with respect to adipose hypetrophy in obesity.

In conclusion, 11β–HSD1 mRNA is a strong predictor of omental fat hypertrophy whereas GR mRNA is negatively associated with obesity in humans.

Chapter 8

A unified model of altered glucocorticoid sensitivity

8. Discussion

In this Thesis I investigated the peripheral effects of altered glucocorticoid sensitivity and showed that the downstream consequences of either glucocorticoid hypersensitivity or resistance are complex and notably involve modulation of blood pressure regulation. Specifically, a model of GC resistance, with widespread/globally reduced GR density, was generated ($GR^{+/-}$ mice) and phenotyped with respect to HPA axis function, glucose, lipid and blood pressure homeostasis. Secondly, a model of GC hypersensitivity (POMC-null) was used to study whether altered peripheral tissue glucocorticoid reactivation and GR levels contributed to the severity of the metabolic abnormalities and blood pressure regulation. The effects of altered GR on the HPA axis found in the $GR^{+/-}$ model is in agreement with other published models (Pepin et al., 1992; Tronche et al., 1999; Reichardt et al., 1998; Finotto et al., 1999; Ridder et al., 2005), whereas, in contrast to earlier reports (Pepin et al., 1992; Richard et al., 1993; Cole et al., 1995; Tronche et al., 1998; Tronche et al., 1999; Kellendonk et al., 2002).Reduced GR density had negligible effects on fat distribution and nutrient homeostasis in the GR model studied here in contrast with previous observations (Pepin et al., 1992; Kellendonk et al., 2002). Therefore, in the following paragraphs I compare and contrast the 2 models ($GR^{+/-}$ and $Pomc^{-/-}$ mice), focusing mainly on the pronounced and novel effects that altered GC sensitivity had on blood pressure (BP). Finally, alterations in GC sensitivity mediated by alterations in peripheral (adipose and liver) 11β-HSD1 and GR expression levels, in the 2 models and in human obesity are discussed.

8.1 Scenario A: Glucocorticoid hypersecretion and reduced GR density

Figure 8.1 illustrates the metabolic and blood pressure effects in the $GR^{+/-}$ mice under normal conditions (fig. 8.1A) and after a chronic HF challenge (fig. 8.1B). Overall,a'global' reduction of GR levels have no effect on body composition or metabolic parameters (glucose and lipid homeostasis) under basal or DIO (HF feeding) conditions. However, reduction of GR density leads to hypertension. Although it is difficult to dissect if the increased BP in $GR^{+/-}$ mice is due to GR reduction or increased circulating GC levels *per se*, it appears to be driven by the hyperactive HPA axis. Hypertension develops, in part, through an activation of the systemic RAAS components. Possibly, impaired negative feedback leads to elevated ACTH levels (although unaltered morning levels, still remains to be tested if evening levels are higher in $GR^{+/-}$ mice), adrenal hypertrophy (zona fasciculate) and concequently elevated plasma GCs. There are a couple of possibilities that might explain the activation of the RAAS system in this model. It could be speculated that elevated ACTH could affect the aldosterone producing cells in the zona reticularis (ZR) of the adrenal gland (evidence in this model that ZR is hypertrophied) thus producing (preliminary data showing increased aldosterone synthase immunoreactivity) and secreting increased aldosterone in accordance with previous studies (Takeda et al., 1996; Honda et al., 1977; Hautanena et al., 1998). Additionally, observations in a ACTH-induced hypertension model showed up-regulation of renin mRNA expression in the adrenal and elevated plasma aldosterone (Chris Kenyon, personal communication). Alternatively, hypercorticosteroneamia could stimulate the non-selective MR in aldosterone target organs such as the kidney and could potentially lead to renal sodium retention, blood volume expansion and

increased blood pressure (reviewed in Ferrari, 2003). However, this is less likely since in a state of MR overstimulation by GC excess, plasma renin is suppressed and aldosterone levels are either normal or decreased (Ferrari, 2003), which does not appear to be the case in the model presented here. The GR+/- mice had increased renin (secreted by the kidney) activity, which subsequently cleaves angiotensinogen, secreted mainly from the liver (Cambell & Habener, 1986; Tamura et al, 1995) in the plasma to form angiotensin I which is further converted to angiotensin II by ACE. Consequently, increased angiotensin II levels (although not directly measured here) can increase aldosterone secretion directly from the adrenal cortex, indeed the case here. Aldosterone increases blood pressure through direct modulation of vascular tone and elevation of blood volume by increasing sodium and water retention in the kidney. It can be speculated that the $GR^{+/-}$ mice probably exhibit a renovascular hypertension, although further investigation (eg kidney morphology, 11β-HSD2 activity in the kidney and also see 8.4) is required to confirm it. Local renin-angiotensin system (RAS) activation can contribute to altered blood pressure (Engeli et al., 2003; Goossens et al., 2007). However, it is unlikely the primary player in the hypertension phenotype of $GR^{+/-}$ phenotype because, although adipose angiotensionogen (AGT) mRNA levels appeared to be elevated, liver AGT levels (main sourse) were unchanged. It is possible that local RAS activation contributes to the already established hypertension in the $GR^{+/-}$ mice and further exaggerates the blood pressure phenotype upon chronic HF feeding, through increased hepatic angiotensinogen mRNA expression and, consequently, increased production and secretion of angiotensinogen with the downstream consequences mentioned above. Hypercorticosteroneamia is also likely a trigger for the hypertension phenotype

observed in HF-fed wild type littermates (fig. 8.2). However, in this case there is no apparent RAAS activation (neither elevation of plasma renin activity or angiotensinogen or aldosterone nor hepatic AGT mRNA leves). A number of parameters might contribute to the elevated BP, either direct effects of GCs on for example cardiac output and increases in total or regional peripheral resistance (Montero and Boscaro, 1992; Whitworth et al., 1995; Kelly et al., 1998) or alternatively, in DIO- mediated hypertension it is likely that synergistic effects of hypercorticosteroneamia (see above), hyperinsulineamia (Sowers, 2004) and hyperleptineamia (as occurs with increased fat mass; Rahmouni et al., 2005) may activate the sympathetic nervous system and thus lead to elevated BP (Racher et al., 1979).

Furthermore, there may be developmental effects programming hypertension in $GR^{+/-}$ mice. It has been shown that GC-overexposure in utero reduces nephron number and consequently leads to late onset hypertension (Celsi et al., 1998; Langley-Evans, 2001; Ortiz et al., 2001; Vehaskari et al., 2001). One could presume that the $GR^{+/-}$ mice might be exposed to high GCs in utero (if $GR^{+/-}$ mums are used for breeding). Whether or not they are "protected" from high GC exposure by lower GR density is unknown but would be very interesting to address by studies of renal structure, nephron number, 11β-HSD2 and MR levels..

When interpreting the current data, a disadvantage of the $GR^{+/-}$ model needs to be considered. The global reduction GR density makes it difficult to dissect the net

effects on specific organ/cellular systems. Because global reduction of the receptor leads to HPA axis hyperactivity and consequently elevated circulating levels of corticosterone, this confounds interpretation of downstream tissue-specific effects and should be addressed in the future. Critically, adrenalectomy (adx) experiments followed by replacement of CORT to fixed levels will help to dissect the confounding responses caused by high systemic CORT levels. Furthermore, it would be informative to address whether reduced GR density is compensated by increased MR expression (in MR expressing tissues, such as the heart), which will presumably be further activated (full receptor occupancy due to lower levels) by elevated CORT (if the levels exceed the capacity of MR protecting 11β-HSD2 to inactivate CORT) and target aldosrerone sensitive tissues/organs (like kidney) or the heart causing renal/cardiac hyperthrophy and consequently affecting BP. However, preliminary observations (Michailidou, Brownstein, Chapman, unpublished) in adult male $GR^{+/-}$ hearts do not indicate any cardiac hypertrophy.

Another important issue with respect to GC metabolism is the clearance of glucocorticoids by hepatic A-ring reductases. Therefore it will be interesting to investigate if $GR^{+/-}$ mice have altered GC-clearance rates by measuring the ratio of urinary or fecal glucocorticoid metabolites.

Of course, tissue-specific models of GR knock down (with cre-lox) or overexpression (with tissue specific promoters) proved to be informative. As discussed in chapter 1, this has illuminated the effects of GR reduction in the liver

(Kellendonk et al., 2000; Orpherk et al., 2004) and overexpression in the pancreas (Delaunay et al., 1997; Davani et al., 2004). With respect to the effects of altered GR on adipose tissue dysregulation, adipose-tissue specific up- and down-regulation GR models (recently generated in Edinburgh) will also be informative, although they also have their limitations when it comes to relate/translate findings in mice to human pathologies, since polymorphisms in humans are "globally" acting.

Fig. 8.1 Model of HPA axis Hyperactivity ($GR^{+/-}$): ↓GR & ↑↑ CORT

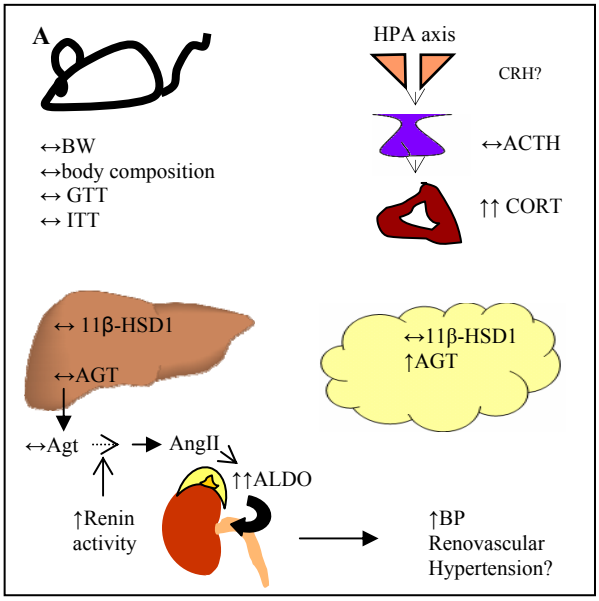

↓ GR levels

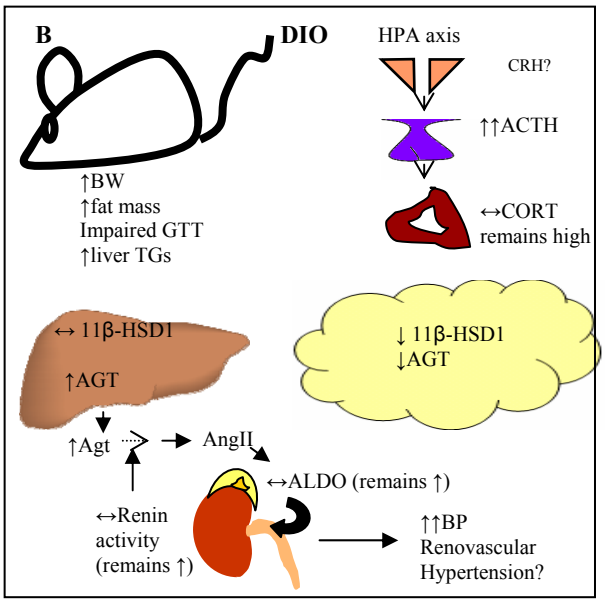

Figure 8.1 $GR^{+/-}$ mice: a Model of GC-resistance

A schematic view of the effects of reduced GR density on the HPA axis, metabolic parameters and blood pressure homeostasis (A) under basal conditions (low fat diet) and (B) after HF feeding. Under basal conditions (A), $GR^{+/-}$ mice, with globally reduced GR levels, displayed higher plasma CORT levels, unaltered ACTH levels, body weight and glucose homeostasis compared to wild type littermates. $GR^{+/-}$ were hypertensive, with elevated renin activity and plasma aldosterone concentration and hypertrophic adrenals (zona fasciculate and glomeruloza). The hypertension is probably due to activation of RAAS, with elevated ALDO levels predicted to directly affect the kidney and cause salt and water retention (however still remains to evaluate kidney histology). The mRNA levels of 11β-HSD1 in liver or adipose tissue were unaffected by reduced GR density or hypercorticosteroneamia. After chronic HF feeding (B) plasma CORT remained elevated but ACTH increased. Although all the phenotyping changes with DIO were observed (obesity, hepatic increased TGs, impaired glucose tolerance), they were identical to the wild type mice responses (fig. 8.2). The BP was further increased with the systemic RAAS components remaining still higher than in the $GR^{+/+}$ mice but not further increased by HF diet. Conversely, an up-regulation of hepatic AGT mRNA levels was observed in HF-fed $GR^{+/-}$ mice possibly further attributing to the increased BP. BW; body weight, CORT; corticosterone, AGT; angiotensinogen mRNA,Agt; plasma angiotensinogen concentration, ALDO; aldosterone; AngII; angiotensin II, BP; blood pressure ,GTT; glucose tolerance test, TGs; triglycerides, RAS; renin-angiotensin-aldosterone system, DIO; diet induced obesity, ? indicates that measurements (eg CRH) have not been performed.

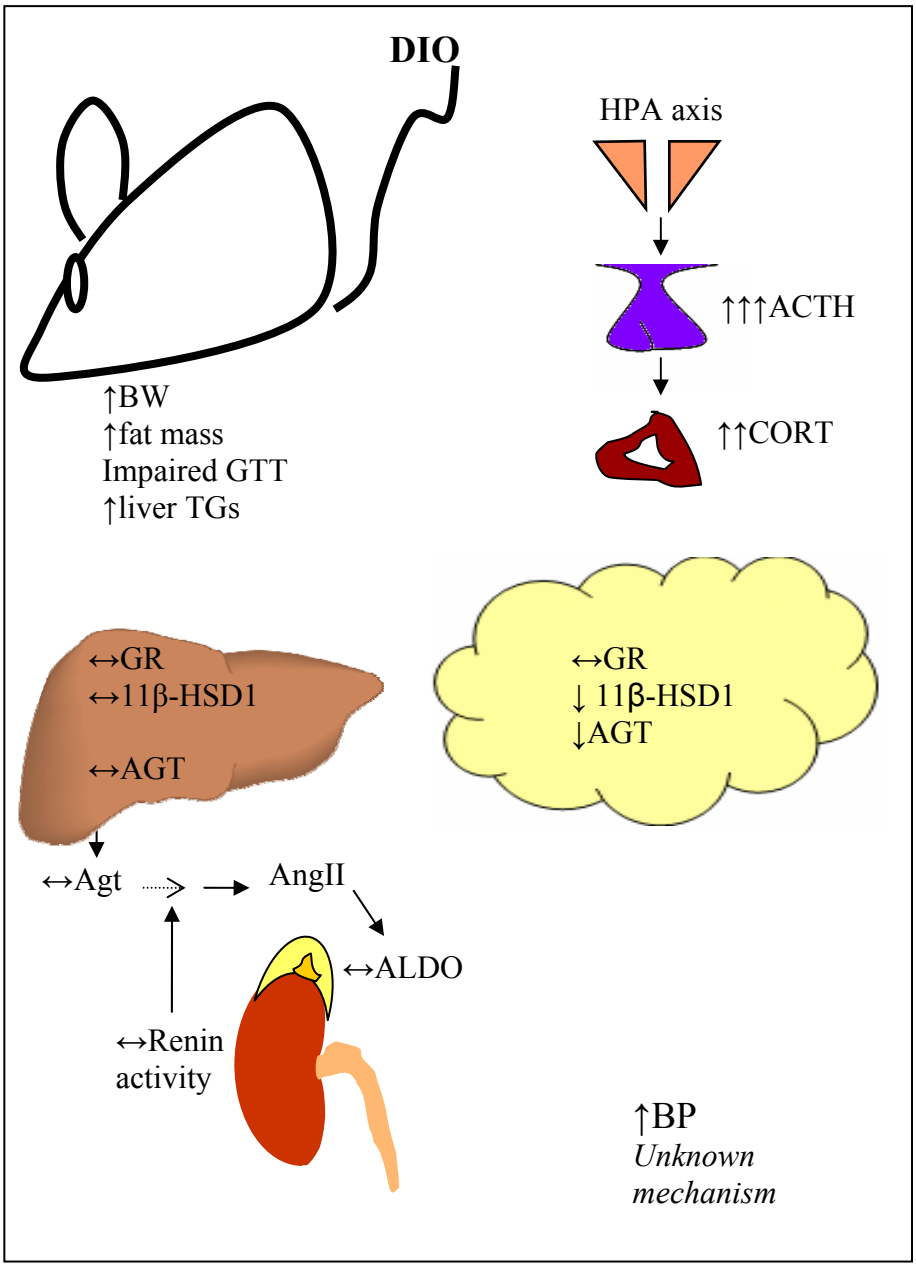

Figure 8.2 Responses of chronically HF-fed wild type mice.

Chronic HF feeding increased circulating CORT and ACTH levels and led to hypertension but without any alterations in any of the renin-angiotensin-aldosterone system components.

8.2 Scenario B: Fixed glucocorticoid levels and "normal" GR density

Figure 8.3 illustrates the metabolic and blood pressure effects in the *Pomc*$^{-/-}$ mice in the "absence" of CORT (fig. 8.3A) and after CORT-replacement (fig. 8.3B). Lack of all POMC-derived peptides (including ACTH) leads to obesity due to central hyperphagia (loss of the appetite suppressing MSH signal), a variety of metabolic abnormalities, undetectable plasma CORT but normal BP in *Pomc*$^{-/-}$ mice (Challis et al., 2004; Coll et al., 2005; Michailidou et al., 2007). CORT-replacement augments the

obesity phenotype and the metabolic abnormalities (Coll et al., 2005) and also induces hypertension (Michailidou et al., 2007) in *Pomc*$^{-/-}$ mice. In contrast to hypercorticosteroneamic GR$^{+/-}$ mice, the hypertensive phenotype in *Pomc*$^{-/-}$ mice, with supraphysiological GC levels (Coll et al., 2005), cannot be attributed to systemic RAAS activation since none of the RAAS components are affected in the latter (although insufficient plasma was available for aldosterone assay). Moreover, the lack of renal morphological changes (Kenyon, Michailidou, Chapman, unpublished observations) in *Pomc*$^{-/-}$ mice, that might be explained by low aldosterone levels, rule out a renovascular BP phenotype. Renovascular hypertension is typically attributed to RAS activation, with consequently severe angiotensin-mediated vasoconstriction, elevated aldosterone release and renal ischemia (Bettmann et al., 2004; Arruda et al., 2005; Heo et al., 2007). Renal impairment is prominent when plasma aldosterone levels are increased, as observed in aP2-11HSD1 mice (Masuzaki et al., 2003) and Zucker rats (Claphman and Turner, 1997; Villarreal et al., 1998) and is absent when aldosterone is low, as in *Pomc*$^{-/-}$

(Coll et al., 2004) and Fat mice (Morton et al., 2005). Conversely, in the CORT-treated wild type mice, it is difficult to evaluate the net circulating CORT levels (amount of endogenously produced *vs* exogenously provided in the drinking water) since the mice had intact adrenals. There are 2 possibilities; circulating CORT is (a) reduced after CORT-treatment (due to reduced hypothalamic CRH expression, Coll et al., 2005) or (b) unaltered and the exogenous CORT suppressed the HPA axis. In any case exogenous CORT treatment in wild type mice did not affect BP or any of the systemic RAS components (fig. 8.4). It seems likely that in *Pomc*$^{-/-}$ mice corticosterone augmented existing mechanisms that were already sustaining vascular function. The elavated renin concentration observed in the untreated *Pomc*$^{-/-}$ mice might be due to renal compensation of the very low aldosterone levels in this model. Apart from renin, these secondary processes are likely to involve the hyperinsulinaemic state (Sowers, 2004) of *Pomc*$^{-/-}$ mice (which is profoundly exacerbated by corticosterone treatment) (Coll et al., 2005), the sympathetic nervous system (Rascher et al., 1979) (which is thought to explain GC-induced hypertension in normal mice) or structural adaptation or the vasculature (Wallerathetal., 2004). Finally, developmental effects could be contributing to the hypertensive phenotype in *Pomc*$^{-/-}$mice.

Fig. 8.3 Model of HPA axis Hypoactivity: POMC-null: ↑GR & negligible CORT

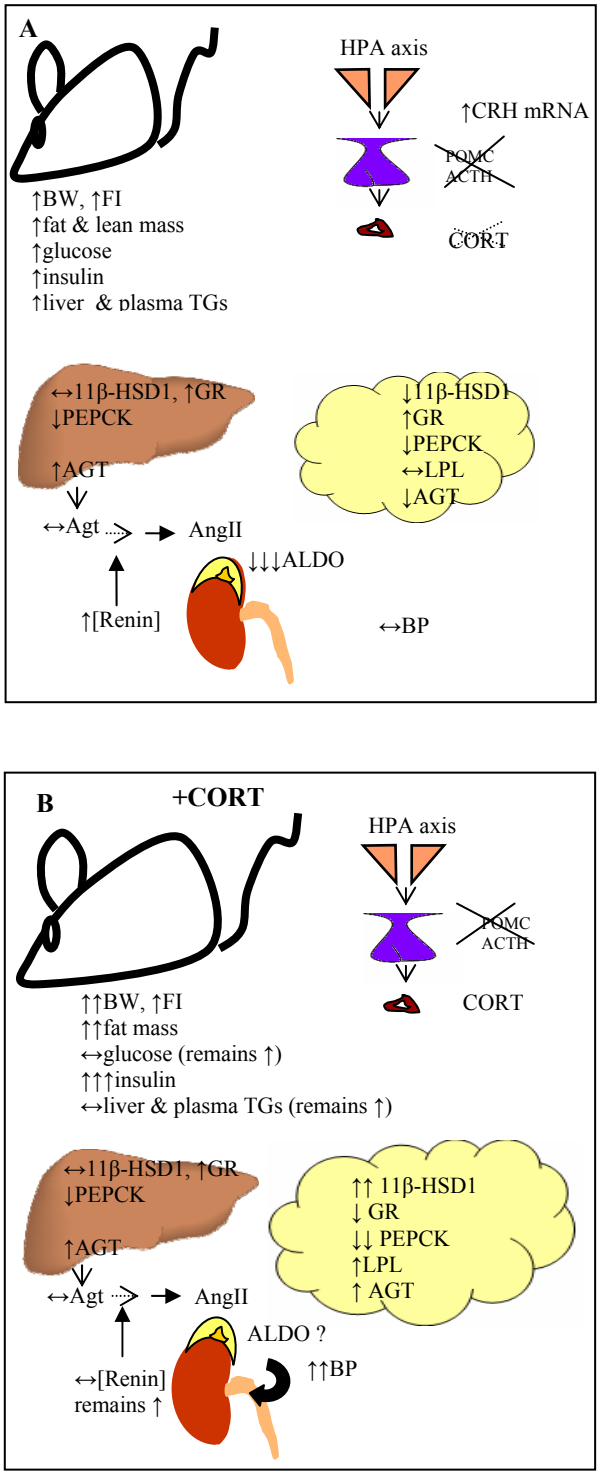

Figure 8.3 POMC-null mice: A model of GC hypersensitivity

Pomc-null mice responses (A) under basal conditions and (B) after CORT-replacement. Under basal conditions, Poomc-null mice had undetectable CORT and reduced ALDO levels (Coll et al., 2005) and displayed alterations in GC sensitivity (reduced adipose 11β-HSD1 but elevated hepatic and retroperitoneal GR levels) but unaltered BP compared to wild type mice. After CORT treatment, they developed hypertension (together with exaggerated obesity and insulin resistance, Coll et al., 2005). The BP phenotype in the Pomc-null mice cannot be attributed to systemic RAAS activation, since none of the components were elevated. The cause of the elevated BP appears to be complex and possibly the consequence of multi-parameters dysregulation (eg profound hyperinsulineamia, hypeleptineamia). Additionally, Pomc-null mice showed an increased sensitivity to CORT treatment with elevated 11β-HSD1 Mrna levels specifically in adipose tissue and up-regulation of GC-target genes such as LPL and AGT (Michailidou et al., 2007)

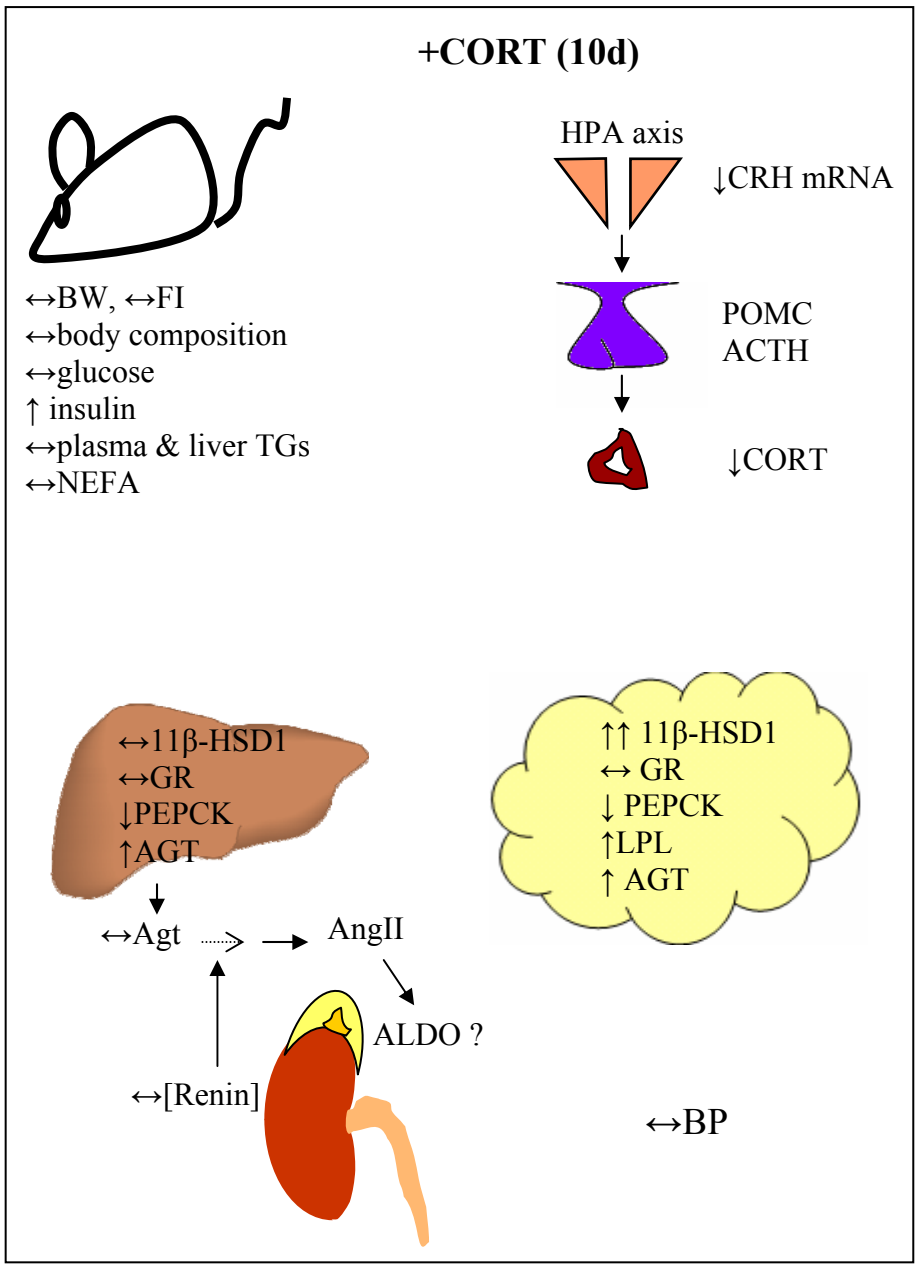

Figure 8.4 CORT treatment in wild type mice does not affect blood pressure.

8.3 Peripheral Interplay: CORT, GR and 11β-HSD1 levels

An interesting finding from the *Pomc*$^{-/-}$ study was the apparent regulation of 11β-HSD1 mRNA levels by CORT in adipose tissue but not in liver. The data presented in this study provide further evidence that 11β-HSD1 mRNA levels are differentially regulated by GCs in adipose and hepatic tissues. In the absence of circulating CORT, the GR is up-regulated in both liver and retroperitoneal fat, while 11β-HSD1 is specifically down-regulated in adipose in *Pomc*$^{-/-}$. CORT-replacement suggested that glucocorticoid regulation of 11β-HSD1 in liver *in vivo* is minimal, at least at "physiological" levels of corticosterone and GR, but that 11β-HSD1 mRNA levels are highly regulated by glucocorticoids in adipose tissue (fig. 8.3). This is predicted to selectively amplify intra-adipose glucocorticoid concentrations, particularly when circulating levels of 11β-HSD1 substrate are high – for example, following HPA activation (Harris et al., 2001). In contrast, the elevated CORT levels in GR$^{+/-}$ mice with reduced GR levels, did not affect 11β-HSD1 mRNA levels in either liver or adipose tissue (fig. 8.1). Moreover, when GR$^{+/-}$ mice develop obesity (DIO experiment) they still exhibit high circulating CORT, but 11β-HSD1 mRNA levels are significantly down-regulated, as previously published (Morton et al., 2004). More interestingly, in a human population (chapter 7), although no cortisol measurements are available (but unlikely to be high in indiopathic obesity, see section 1.6.4), there are clearly differences in both GR and 11β-HSD1 mRNA expression levels between normal weight and obese individuals. Specifically, obese women have significantly higher 11β-HSD1 but lower GR mRNA levels in all depots compared to normal weight females (fig. 8.5). It seems that there is a fine tuning of GR and 11β-HSD1 and modulations seem to occur reciprocally to compensate for local GC-

amplification in peripheral (abdominal sc) but not in visceral (omental) adipose tissue (fig. 8.5). In the latter GR remains equally high as do 11β-HSD1 levels. Thus it could be predicted that a series of "abnormalities" such as (a) unfavourable deposition of fat in the omentum (because of the anatomical position; drains to the portal vein) (b) consequently, elevated 11β-HSD1 levels (positively correlate with visceral adipose mass increase) and local amplification of cortisol, and finally (c) failure to compensate by reducing the levels of GR, may lead to increased fat deposition, adipose insulin resistance (therefore increased portal delivery of free fatty acids), altered adipokine expression and consequent metabolic abnormalities. These, observations are very interesting but require further investigation in a larger human cohort in which cortisol (circulating, portal vein and tissue levels) will be measured.

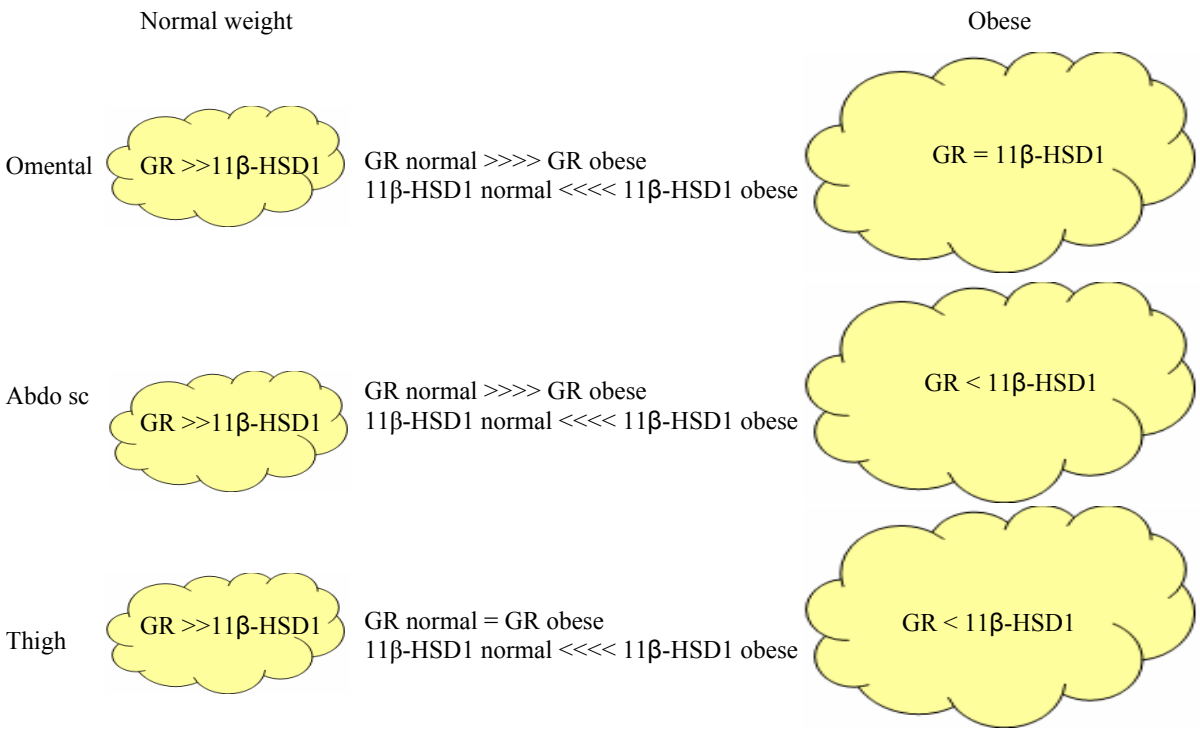

Figure 8.5 Comparison of adipose GR and 11β-HSD1 levels in normal weight and obese females.

In normal weight (BMI: 24.8±0.9) GR mRNA levels are higher while 11β-HSD1 mRNA levels are lower compared to obese (BMI: 36.6±1) females. In all depots, apart from omental, it seems that elevated 11β-HSD1 mRNA levels and thus local glucocorticoid regeneration with obesity are compensated by reduced GR levels.

8.4 Future perspectives in the use of $GR^{+/-}$ model

Overall, the $GR^{+/-}$ model proved to be informative regarding the role of reduced GR density on body composition, metabolic parameters and blood pressure homeostasis. It is clear that GR haploinsufficiency does not have a permissive effect on the development of glucose or lipid abnormalities and does not play an essential role in modulating body composition, even when the model is challenged with a chronic HF feeding. However, the novel finding of increased blood pressure provides new perspectives of the role of GR in the regulation of blood pressure. Future experiments could address the net effect (by adx) of reduced GR on, for example, salt-induced hypertension.

Additionally, the effects of reduced GR can be studied in a number of systems. For example, preliminary data on embryonic heart development (not presented in this Thesis) suggest an essential role in a critical "window" (time dependent) of GR in cardiac remodelling and will be very exciting to follow up. Furthermore, the presence of the LacZ reporter makes it a very useful tool to follow the receptor function and regulation in specific cell types (eg of the immune system).

APPENDIX A: PLASMIDS

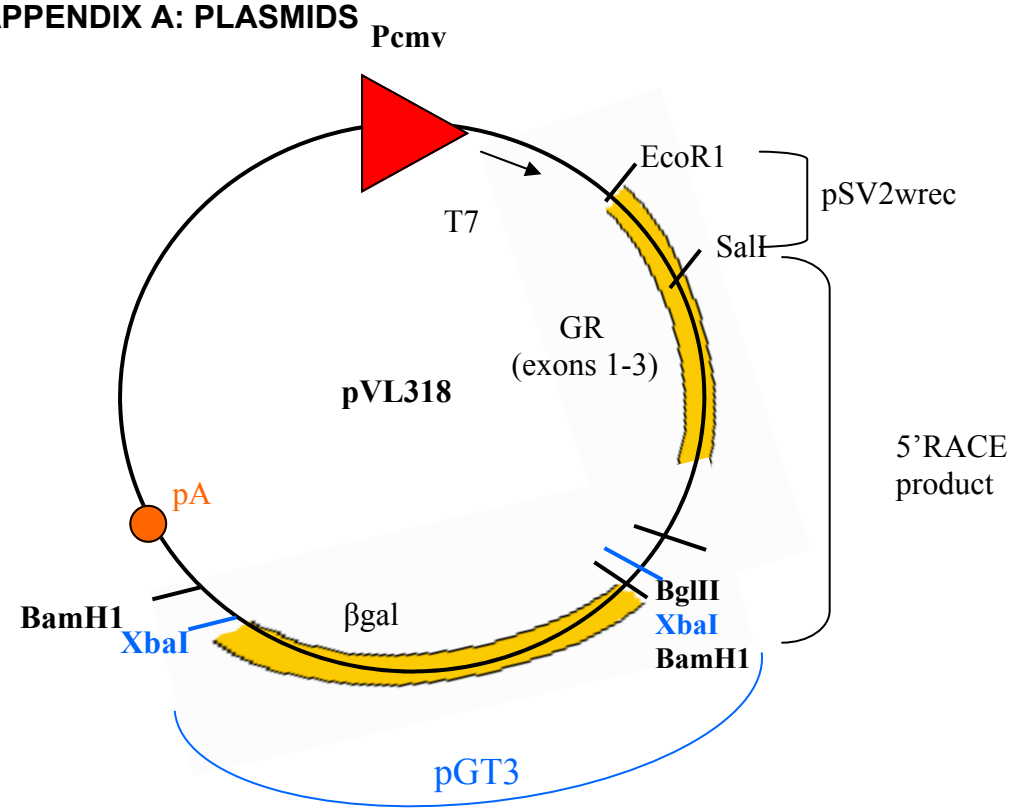

Figure A1. Construct pVL318 encodes the GR-ßgal fusion protein (ESKN92).

pVL318 was constructed by Val Lyons. It is in a pcDNA3.1 vector (Invitrogen) and was assembled using the following plasmids/DNAs: pSV2wrec (Danielsen et al., 1986), 5'-RACE product from ESKN92 and pGT3 (the gene trap vector).pSV2wrec (shown in fig. A3) encodes the WT mouse GR cDNA (accession number X04435) and was kindly provided by Mark Danielsen. An EcoRI site is present at the extreme 5' end of the GR cDNA in pSV2wrec (Danielsen et al., 1986). GR cDNA also has a unique SalI site within exon 2 (nucleotide 438). During the course of the subcloning, sequencing revealed that the 129Ola derived DNA from ESKN92, as well as C57BL6/J DNA differed at a single nucleotide in exon 3 from the pSV2wrec encoded cDNA (derived from the mouse lymphoma cell line, W7.2). This results in a Val437 (in pSV2wrec) to Gly437 (in 129Ola and C57BL6/J) polymorphism. Although this polymorphism is reported not to influence the activity of GR (Kasai, 1990), site-directed mutagenesis was used to change the pSV2wrec sequence to that of 129Ola/C57BL6J (generating pSV2wrecG437). The following fragments were ligated together to generate an intermediate plasmid (pVL336): pcDNA3.1(-) cut with EcoRI and BamHI, a 440bp EcoRI-SalI fragment comprising the 5' portion of mouse GR cDNA from pSV2wrec and an ~1kb SalI (GR exon 2 site)-BamHI (site in the linker of the pGT3 vector immediately preceding ß-gal) fragment from the 5'-RACE PCR product. The pVL336 intermediate plasmid was linearised with XbaI (cutting within the pGT3 linker sequence, next to BamHI) and ligated to an XbaI fragment from pGT3 encoding the ßgeo cassette. The correct plasmids were identified by restriction digests and confirmed by DNA sequencing (Wellcome Clinical Research Fascility, Western General Hospital) using appropriate primers.

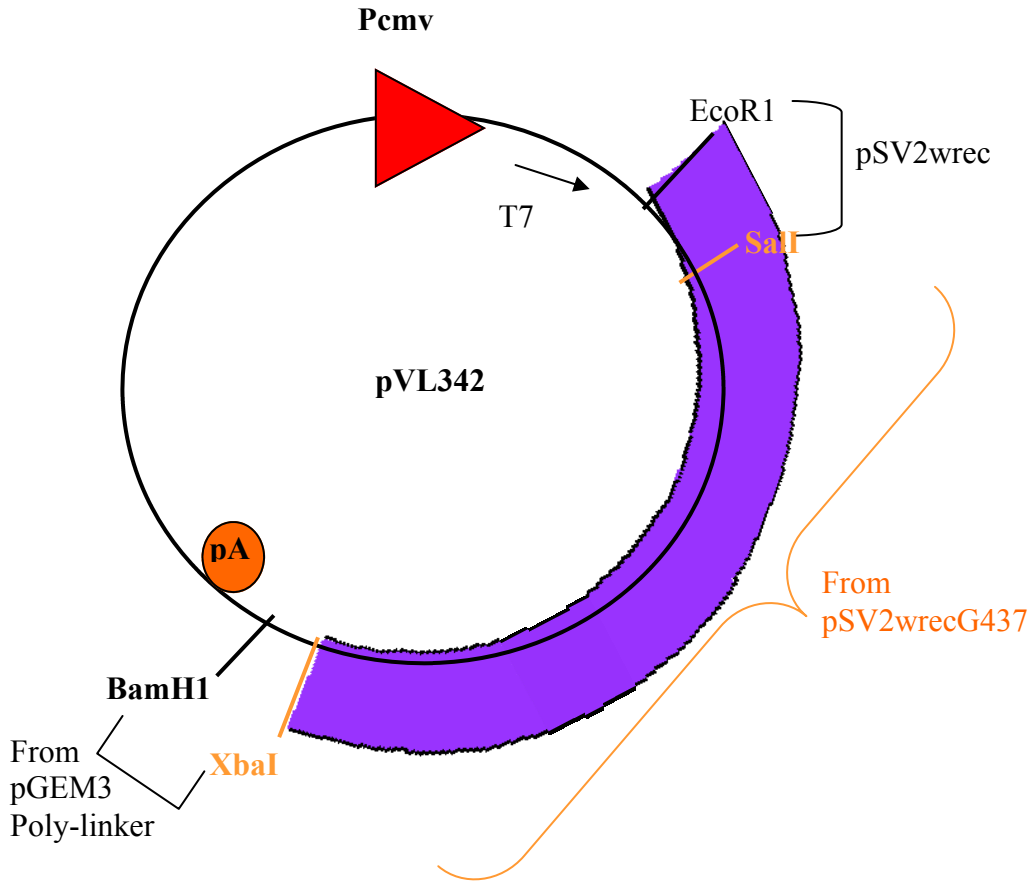

Figure A2. pVL342 encodes the WT mouse GR

pVL342 was also constructed by Val Lyons. It is in a pcDNA3.1 vector (Invitrogen) and was assembled using the following plasmids/DNAs: pSV2wrec (Danielsen et al., 1986) and pGem3 (Promega). An intermediate cloning step in which a 2050bp SalI-XbaI fragment from pSV2wrecG437 (see legent fig.A1) was subcloned into pGem3. This placed a BamHI site immediately 3' to the XbaI site. The 2060bp SalI-BamHI fragment from this intermediate plasmid, together with the 440bp EcoRI-SalI fragment from pSV2wrec were ligated into pcDNA3.1(-) cut with EcoRI and BamHI. Correctly ligated plasmids were identified by restriction digest and confirmed by DNA sequencing.

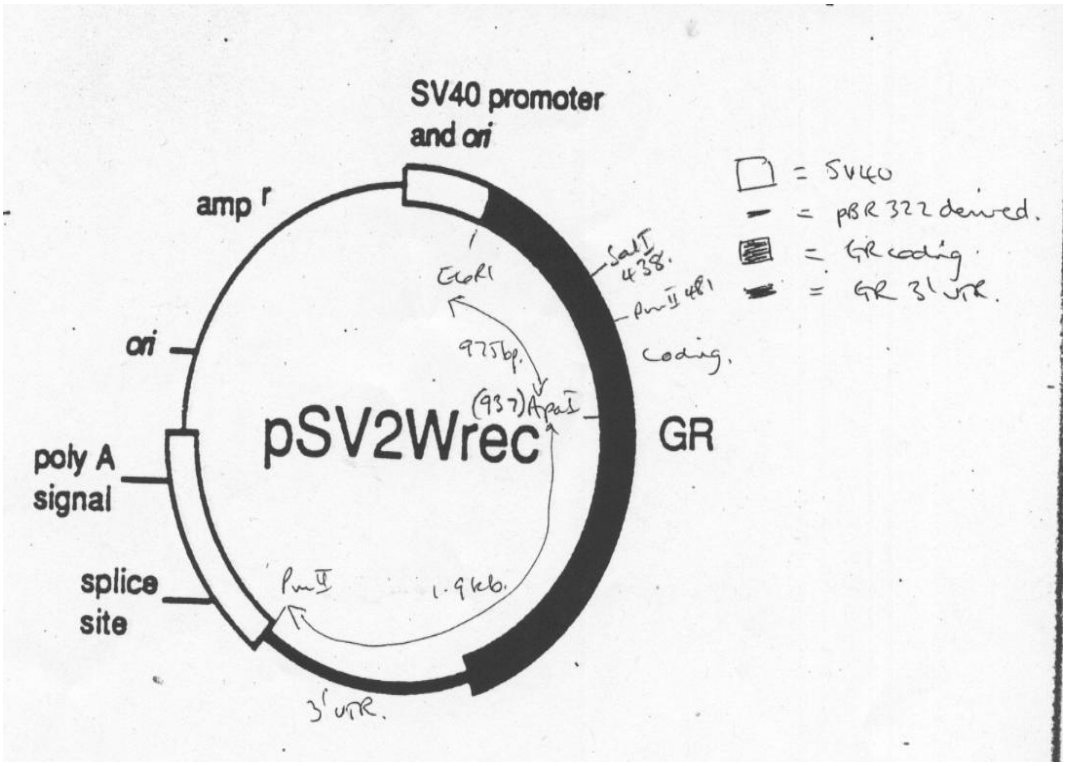

Figure A3 The pSV2wrec plasmid (Danielsen et al., 1986)

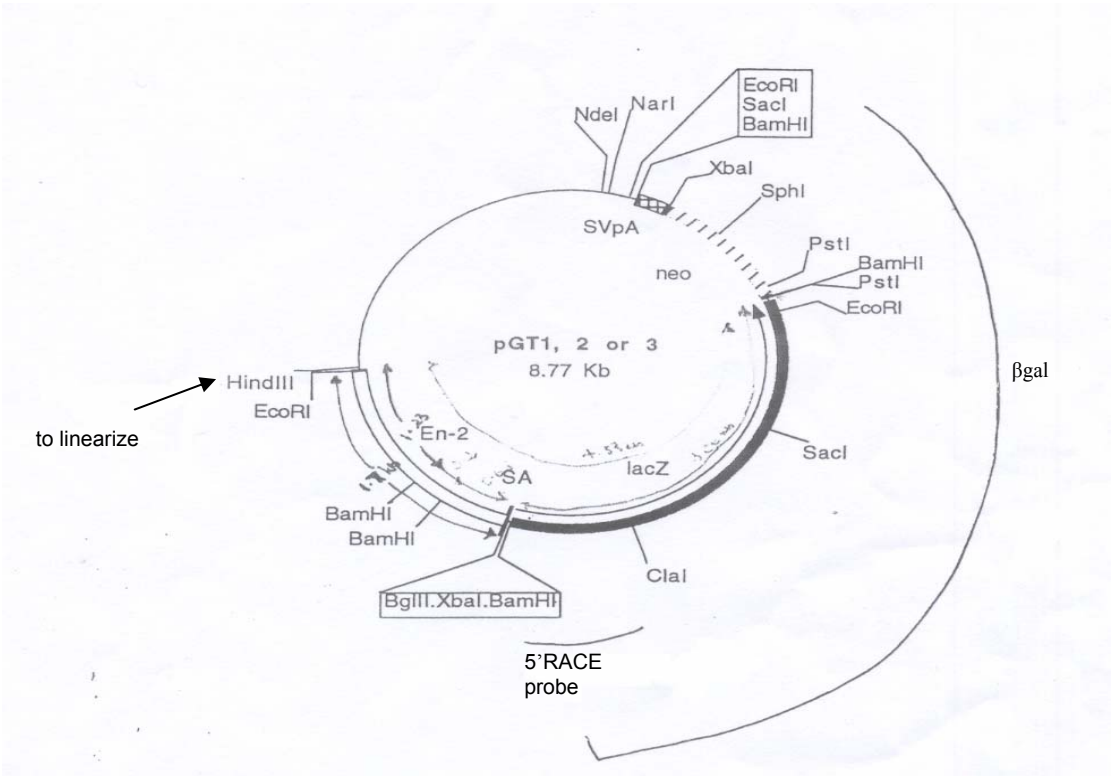

Figure A4. The pGT1-3 gene trap vector

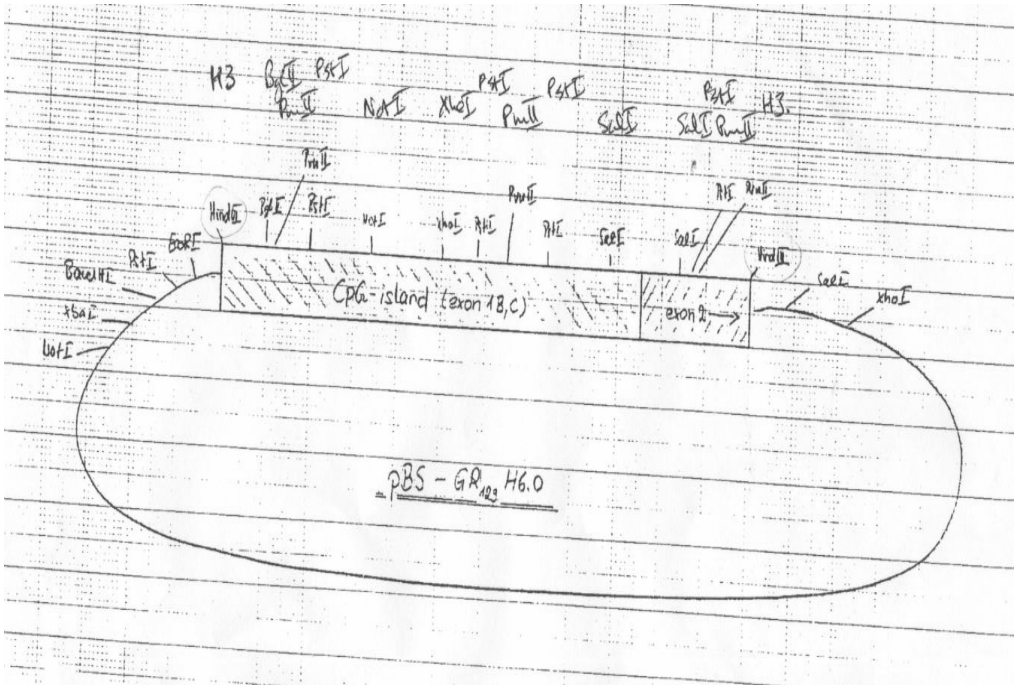

Figure A5 The pBS-GR129H6.0 plasmid was used for the generation of GR probe in FISH (section 2.2.2.3.2.3.2)

Briefly, the pBS-GR129H6.0 plasmid (gift from H. Reichardt) was digested with HindIII in a 25µl digest (5µl DNA, 2.5µl 10xbuffer B, 1µl HindIII and 16.5µl dH_2O) at 37oC for 2h. The digest was run on a 0.8% low melting point agarose gel and the ~6kb fragment was cut out, purified and eluted in 24µl (final concentration 100ng/µl) for further use in FISH.

APPENDIX B: Sequences

B1. Gene trap vector (pGT1) sequence

AAGCTTCGCGAAGGGGTTCGAGCTTGGAATTCATGGGAAGAGGAACCGAAAGTATGTTTT
TCAGATGTTCTTTCTCAGAAATAGGAGTTTGCGGAGGTTGGAGTGTGTGTTGTAGGACAC
GAACCCCAGGGTGGAGGAGACTGGAGGACAGAGCCCTCTTTCCCAGGGAGGGAAGGAGGA
GAGTTTGAGATCCGCTCCGGAAGTCGGGGTTCAGGTTTGAGCAGGCCAGGCCTCTCCCGT
GGTCTCGCCCTCTTGTCCTAGAAGCCTCACTGGCCAGGTGTAAGCCAGGTCGTGGGTGCC
GAGCCCTGCTCCCTCATCCTCAGCATGGATGTGAAGAGGACTGTATGGCGTGCGGGTGTG
TGTGACCGTGGGTACACTTAAAACACCGGGTTTTGGATCTGCACTGTCCCGGATGTCCTC
TGGTGCTCAAAGACCCTTTTGGGTTTGCCCTTTGGTAAGAGCGCCGGGATCTACTTGTCT
GGAGGCCAGGGAGTCCTCAGCCGAGGCTTGCCGCCCCTGACTGCACTGCACTGAGTAGTG
GATGGGAGAGTCTGGTACCGCACTGCCGGTTTCCTCCACCATCCCCGCAGCGCAGGGCAG
TGCATTCCGTCCTGGCTGCGAAGGGGGATGGTCGGGCCTTCTCCAGCCTCTTCCGCTTCT
AGCGAAGGGGCCTTGATGGAAGGGCCCGCATGTCTCCAAAGTTGATTCATGCTTCTTGCA
CAGAGAAAGACCAGAAAGAAGGTCTCAAGTTTTAGCCGGTAGCCCGGATGGCCTTTTCCT
GCACGGCACCATATGAACCTTGTGACCCTGACTTTGAGACCCCTCTAACCCAAGGCCCCT
ACCACTTTACCCTTTCCCTTTGAAGGCTTTCCCACACCACCCTCCACACTTNCCCCAAAC
ACTGCCAACTATGTAGGAGGAAGGGGTTGGGACTAACAGAAGAACCCGTTGTGGGGAAGC
TGTTGGGAGGGTCACTTTATGTTCTTGCCCAAGGTCAGTTGGGTGGCCTGCTTCTGATGA
GGTGGTCCCAAGGTCTGGGGTAGAAGGTGAGAGGGACAGGCCACCAAGGTCAGCCCCCCC
CCCCTATCCCATAGGAGCCAGGTCCCTCTCCTGGACAGGAAGACTGAAGGGGAGATGCCA
GAGACTCAGTGAAGCCTGGGGTACCCTATTGGAGTCCTTCAAGGAAACAAACTTGGCCTC
ACCAGGCCTCAGCCTTGGCTCCTCCTGGGAACTCTACTGCCCTTGGGATCCCTTGTAGTT
GTGGGTTACATAGGAAGGGGACGGATTCCCCTTGACTGGCTAGCCTACTCTTTTCTTCAG
TCTTCTCCATCTCCTCTCACCGTTCTCTCGACCCTTTCCCTAGGATAGACTTGGAAAAAG
ATAAGGGGAGAAAAACAAATGCAAACGAGGCCAGAAAGATTTTGGCTGGGCATTCCTTCC
GCTAGCTTTTATTGGGATCCCCTAGTTTGTGATAGGCCTTTTAGCTACATCTGCCAATCC
ATCTCATTTTCACACACACACACACCACTTTCCTTCTGGTCAGTGGGCACATGTCCAGCC
CCCAACACTTGTATGGCCTTGGCGGGGTCATCCCCCCCCCACCCCCAGTATCTGCAACCT
CAAGCTAGCTTGGGTGCGTTGGTTGTGGATAAGTAGCTAGACTCCAGCAACCAGTAACCT
CTGCCCTTTCTCCTCCATGACAACCAGGTCCCAGGTCCCGAAAACCAAAGAAGAAGAACC
CTAACAAAGAGGACAAGCGGCCTCGCACAGCCTTCACTGCTGAGCAGCTCCAGAGGCTCA
AGGCTGAGTTTCAGACCAACAGGTACCTGACAGAGCAGCGGCGCCAGAGTCTGGCACAGG
AGCTCGGTACCCGGAAGATCTGGACTCTAGAGGATCCCGTCGTTTTACAACGTCGTGACT

GGGAAAACCCTGGCGTTACCCAACTTAATCGCCTTGCAGCACATCCCCCTTTCGCCAGCT
GGCGTAATAGCGAAGAGGCCCGCACCGATCGCCCTTCCCAACAGTTGCGCAGCCTGAATG
GCGAATGGCGCTTTGCCTGGTTTCCGGCACCAGAAGCGGTGCCGGAAAGCTGGCTGGAGT
GCGATCTTCCTGAGGCCGATACTGTCGTCGTCCCCTCAAACTGGCAGATGCACGGTTACG
ATGCGCCCATCTACACCAACGTAACCTATCCCATTACGGTCAATCCGCCGTTTGTTCCCA
CGGAGAATCCGACGGGTTGTTACTCGCTCACATTTAATGTTGATGAAAGCTGGCTACAGG
AAGGCCAGACGCGAATTATTTTTGATGGCGTTAACTCGGCGTTTCATCTGTGGTGCAACG
GGCGCTGGGTCGGTTACGGCCAGGACAGTCGTTTGCCGTCTGAATTTGACCTGAGCGCAT
TTTTACGCGCCGGAGAAAACCGCCTCGCGGTGATGGTGCTGCGTTGGAGTGACGGCAGTT
ATCTGGAAGATCAGGATATGTGGCGGATGAGCGGCATTTTCCGTGACGTCTCGTTGCTGC
ATAAACCGACTACACAAATCAGCGATTTCCATGTTGCCACTCGCTTTAATGATGATTTCA
GCCGCGCTGTACTGGAGGCTGAAGTTCAGATGTGCGGCGAGTTGCGTGACTACCTACGGG
TAACAGTTTCTTTATGGCAGGGTGAAACGCAGGTCGCCAGCGGCACCGCGCCTTTCGGCG
GTGAAATTATCGATGAGCGTGGTGGTTATGCCGATCGCGTCACACTACGTCTGAACGTCG
AAAACCCGAAACTGTGGAGCGCCGAAATCCCGAATCTCTATCGTGCGGTGGTTGAACTGC
ACACCGCCGACGGCACGCTGATTGAAGCAGAAGCCTGCGATGTCGGTTTCCGCGAGGTGC
GGATTGAAAATGGTCTGCTGCTGCTGAACGGCAAGCCGTTGCTGATTCGAGGCGTTAACC
GTCACGAGCATCATCCTCTGCATGGTCAGGTCATGGATGAGCAGACGATGGTGCAGGATA
TCCTGCTGATGAAGCAGAACAACTTTAACGCCGTGCGCTGTTCGCATTATCCGAACCATC
CGCTGTGGTACACGCTGTGCGACCGCTACGGCCTGTATGTGGTGGATGAAGCCAATATTG
AAACCCACGGCATGGTGCCAATGAATCGTCTGACCGATGATCCGCGCTGGCTACCGGCGA
TGAGCGAACGCGTAACGCGAATGGTGCAGCGCGATCGTAATCACCCGAGTGTGATCATCT
GGTCGCTGGGGAATGAATCAGGCCACGGCGCTAATCACGACGCGCTGTATCGCTGGATCA
AATCTGTCGATCCTTCCCGCCCGGTGCAGTATGAAGGCGGCGGAGCCGACACCACGGCCA
CCGATATTATTTGCCCGATGTACGCGCGCGTGGATGAAGACCAGCCCTTCCCGGCTGTGC
CGAAATGGTCCATCAAAAAATGGCTTTCGCTACCTGGAGAGACGCGCCCGCTGATCCTTT
GCGAATACGCCCACGCGATGGGTAACAGTCTTGGCGGTTTCGCTAAATACTGGCAGGCGT
TTCGTCAGTATCCCCGTTTACAGGGCGGCTTCGTCTGGGACTGGGTGGATCAGTCGCTGA
TTAAATATGATGAAAACGGCAACCCGTGGTCGGCTTACGGCGGTGATTTTGGCGATACGC
CGAACGATCGCCAGTTCTGTATGAACGGTCTGGTCTTTGCCGACCGCACGCCGCATCCAG
CGCTGACGGAAGCAAAACACCAGCAGCAGTTTTTCCAGTTCCGTTTATCCGGGCAAACCA
TCGAAGTGACCAGCGAATACCTGTTCCGTCATAGCGATAACGAGCTCCTGCACTGGATGG
TGGCGCTGGATGGTAAGCCGCTGGCAAGCGGTGAAGTGCCTCTGGATGTCGCTCCACAAG
GTAAACAGTTGATTGAACTGCCTGAACTACCGCAGCCGGAGAGCGCCGGGCAACTCTGGC
TCACAGTACGCGTAGTGCAACCGAACGCGACCGCATGGTCAGAAGCCGGGCACATCAGCG
CCTGGCAGCAGTGGCGTCTGGCGGAAAACCTCAGTGTGACGCTCCCCGCCGCGTCCCACG
CCATCCCGCATCTGACCACCAGCGAAATGGATTTTTGCATCGAGCTGGGTAATAAGCGTT
GGCAATTTAACCGCCAGTCAGGCTTTCTTTCACAGATGTGGATTGGCGATAAAAAACAAC
TGCTGACGCCGCTGCGCGATCAGTTCACCCGTGCACCGCTGGATAACGACATTGGCGTAA

GTGAAGCGACCCGCATTGACCCTAACGCCTGGGTCGAACGCTGGAAGGCGGCGGGCCATT
ACCAGGCCGAAGCAGCGTTGTTGCAGTGCACGGCAGATACACTTGCTGATGCGGTGCTGA
TTACGACCGCTCACGCGTGGCAGCATCAGGGGAAAACCTTATTTATCAGCCGGAAAACCT
ACCGGATTGATGGTAGTGGTCAAATGGCGATTACCGTTGATGTTGAAGTGGCGAGCGATA
CACCGCATCCGGCGCGGATTGGCCTGAACTGCCAGCTGGCGCAGGTAGCAGAGCGGGTAA
ACTGGCTCGGATTAGGGCCGCAAGAAAACTATCCCGACCGCCTTACTGCCGCCTGTTTTG
ACCGCTGGGATCTGCCATTGTCAGACATGTATACCCCGTACGTCTTCCCGAGCGAAAACG
GTCTGCGCTGCGGGACGCGCGAATTGAATTATGGCCCACACCAGTGGCGCGGCGACTTCC
AGTTCAACATCAGCCGCTACAGTCAACAGCAACTGATGGAAACCAGCCATCGCCATCTGC
TGCACGCGGAAGAAGGCACATGGCTGAATATCGACGGTTTCCATATGGGGATTGGTGGCG
ACGACTCCTGGAGCCCGTCAGTATCGGCGGAATTCCAGCTGAGCGCCGGTCGCTACCATT
ACCAGTTGGTCTGGTGTCAGGGGATCCCCCGGGCTGCAGCCAATATGGGATCGGCCATTG
AACAAGATGGATTGCACGCAGGTTCTCCGGCCGCTTGGGTGGAGAGGCTATTCGGCTATG
ACTGGGCACAACAGACAATCGGCTGCTCTGATGCCGCCGTGTTCCGGCTGTCAGCGCAGG
GGCGCCCGGTTCTTTTTGTCAAGACCGACCTGTCCGGTGCCCTGAATGAACTGCAGGACG
AGGCAGCGCGGCTATCGTGGCTGGCCACGACGGGCGTTCCTTGCGCAGCTGTGCTCGACG
TTGTCACTGAAGCGGGAAGGGACTGGCTGCTATTGGGCGAAGTGCCGGGGCAGGATCTCC
TGTCATCTCACCTTGCTCCTGCCGAGAAAGTATCCATCATGGCTGATGCAATGCGGCGGC
TGCATACGCTTGATCCGGCTACCTGCCCATTCGACCACCAAGCGAAACATCGCATCGAGC
GAGCACGTACTCGGATGGAAGCCGGTCTTGTCGATCAGGATGATCTGGACGAAGAGCATC
AGGGGCTCGCGCCAGCCGAACTGTTCGCCAGGCTCAAGGCGCGCATGCCCGACGGCGAGG
ATCTCGTCGTGACCCATGGCGATGCCTGCTTGCCGAATATCATGGTGGAAAATGGCCGCT
TTTCTGGATTCATCGACTGTGGCCGGCTGGGTGTGGCGGACCGCTATCAGGACATAGCGT
TGGCTACCCGTGATATTGCTGAAGAGCTTGGCGGCGAATGGGCTGACCGCTTCCTCGTGC
TTTACGGTATCGCCGCTCCCGATTCGCAGCGCATCGCCTTCTATCGCCTTCTTGACGAGT
TCTTCTGAGCGGGACTCTGGGGTTCGAAATGACCGACCAAGCGACGCCCAACCTGCCATC
ACGAGATTTCGATTCCACCGCCGCCTTCTATGAAAGGTTGGGCTTCGGAATCGTTTTCCG
GGACGCCGGCTGGATGATCCTCCAGCGCGGGGATCTCATGCTGGAGTTCTTCGCCCACCC
CCCGGATCTAAGCTCTAGATAAGTAATGATCATAATCAGCCATACCACATTTGTAGAGGT
TTTACTTGCTTTAAAAAACCTCCCACACCTCCCCCTGAACCTGAAACATAAAATGAATGC
AATTGTTGTTGTTAACTTGTTTATTGCAGCTTATAATGGTTACAAATAAAGCAATAGCAT
CACAAATTTCACAAATAAAGCATTTTTTTCACTGCATTCTAGTTGTGGTTTGTCCAAACT
CATCAATGTATCTTATCATGTCTGGATCCGGGGGTACCGCGAGCTCGCGTCGAATTC

B2. 5'-RACE sequence of "trapped" GR

Sequence in green corresponds to exon 2 of GR, sequence in red corresponds to exon 3 of GR and blue is the lacZ sequence encoding βgal. The β-geo cassette is spliced onto the 3'-end of exon 3.

TCAGCAGCAGGATCAGAAGCCTGTTTTTAATGTCATTCCNCCAATTCCTG
TTGGTTCTGAAAACTGGAATAGGTGCCAAGGGTCTGGAGAGGACAACCTG
ACTTCCTTGGGGGCTATGAACTTCGCAGGCCGCTCAGTGTTTTCTAATGG
ATATTCAAGCCCTGGAATGAGACCAGATGTGAGTTCTCCTCCGTCCAGCT
CCTCCACAGCAACGGGACCNCCTCCCAAACTCTGCCTGGTGTGCTCCGAT
GAAGCTTCGGGATGCCATTATGGGGTGCTGANGTGTGGAAGCTGTAAAGT
CTTCTTTAAAAGAGCAGTGGAAGGTCCCAGGTCCCGAAAACGAAAGAAGA
AACGCAGATCGCAGATCNNAGATCTGGACTCTAGAGGTCCCNCTTNCC…

B3. Mouse GR cDNA sequense (accession X04435; length: 2575)

```
   1  GGAAGTTAAT ATTTGCCAAT GGACTCCAAA GAATCCTTAG CTCCCCCTGG
  51  TAGAGACGAA GTCCCCAGCA GTTTGCTTGG CCGGGGGAGG GGAAGCGTGA
 101  TGGACTTGTA TAAAACCCTG AGGGGTGGAG CTACAGTCAA GGTTTCTGCG
 151  TCTTCACCCT CAGTGGCTGC TGCTTCTCAG GCAGATTCCA AGCAGCAGAG
 201  GATTCTCCTT GATTTTTCAA AAGGCTCAGC AAGCAATGCA CAGCAGCAGC
 251  AGCAGCAGCA GCAGCCGCAG CCAGATTTAT CCAAAGCCGT TTCACTGTCC
 301  ATGGGACTGT ATATGGGAGA GACCGAAACA AAAGTGATGG GGAATGACTT
 351  GGGCTACCCA CAGCAGGGCC AGCTTGGCCT CTCCTCTGGG GAAACAGACT
 401  TTCGGCTTCT GGAAGAAAGC ATTGCAAACC TCAATAGGTC GACCAGCCGT
 451  CCAGAGAATC CCAAGAGTTC AACACCTGCA GCTGGGTGTG CTACCCCGAC
 501  AGAGAAGGAG TTTCCCCAGA CTCACTCTGA TCCATCTTCA GAACAGCAAA
 551  ATAGAAAAAG CCAGCCTGGC ACCAACGGTG GCAGTGTGAA ATTGTATACC
 601  ACAGACCAAA GCACCTTTGA CATCTTGCAG GATTTGGAGT TTTCTGCCGG
 651  GTCCCCAGGT AAAGAGACAA ACGAGAGTCC TTGGAGGTCA GACCTGTTGA
 701  TAGATGAAAA CTTGCTTTCT CCTTTGGCGG GAGAAGATGA TCCATTCCTT
 751  CTGGAAGGGG ACGTGAATGA GGATTGCAAG CCTCTTATTT TACCGGACAC
```

```
 801  TAAACCTAAA ATTCAGGATA CTGGAGATAC AATCTTATCA AGCCCCAGCA
 851  GTGTGGCACT GCCCCAAGTG AAAACAGAGA AAGATGATTT CATTGAGCTT
 901  TGCACCCCTG GGGTAATTAA GCAAGAGAAA CTGGGCCCGG TTTATTGCCA
 951  GGCAAGCTTT TCTGGGACAA ATATAATTGG GAATAAAATG TCTGCCATTT
1001  CTGTTCATGG CGTGAGTACC TCTGGAGGAC AGATGTACCA CTATGACATG
1051  AATACAGCAT CCCTTTCTCA GCAGCAGGAT CAGAAGCCTG TTTTTAATGT
1101  CATTCCACCA ATTCCTGTTG GTTCTGAAAA CTGGAATAGG TGCCAAGGGT
1151  CTGGAGAGGA CAACCTGACT TCCTTGGGGG CTATGAACTT CGCAGGCCGC
1201  TCAGTGTTTT CTAATGGATA TTCAAGCCCT GGAATGAGAC CAGATGTGAG
1251  TTCTCCTCCG TCCAGCTCCT CCACAGCAAC GGGACCACCT CCCAAACTCT
1301  GCCTGGTGTG CTCCGATGAA GCTTCGGTAT GCCATTATGG GGTGCTGACG
1351  TGTGGAAGCT GTAAAGTCTT CTTTAAAAGA GCAGTGGAAG GACAGCACAA
1401  TTACCTTTGT GCTGGAAGAA ATGATTGCAT CATTGATAAA ATTCGAAGAA
1451  AAAACTGTCC AGCATGCCGC TATCGAAAAT GTCTTCAAGC TGGAATGAAC
1501  CTGGAAGCTC GAAAAACGAA GAAAAAAATT AAAGGAATTC AGCAAGCCAC
1551  TGCAGGAGTC TCACAAGACA CTTCTGAAAA CGCTAACAAA ACAATAGTTC
1601  CTGCCGCGCT GCCACAGCTT ACCCCTACCC TGGTGTCACT GCTGGAGGTG
1651  ATCGAGCCTG AGGTGTTATA TGCAGGATAT GACAGCTCTG TTCCAGACTC
1701  AGCATGGAGA ATTATGACCA CGCTCAACAT GTTAGGTGGG CGCCAAGTGA
1751  TTGCCGCAGT GAAATGGGCA AAGGCGATAC CAGGATTCAG AAACTTACAC
1801  CTGGATGACC AAATGACCCT TCTACAGTAC TCATGGATGT TTCTCATGGC
1851  ATTTGCCCTG GGTTGGAGAT CATACAGACA AGCAAGTGGA AACCTGCTAT
1901  GCTTTGCTCC TGATCTGATT ATTAATGAGC AGAGAATGAC TCTACCCTGC
1951  ATGTATGACC AATGTAAACA CATGCTGTTT ATCTCCACTG AATTACAAAG
2001  ATTGCAGGTA TCCTATGAAG AGTATCTCTG TATGAAAACC TTACTGCTTC
2051  TCTCCTCAGT TCCTAAGGAA GGTCTGAAGA GCCAAGAGTT ATTTGATGAG
2101  ATTCGAATGA CTTATATCAA AGAGCTAGGA AAAGCCATTG TCAAAAGGGA
2151  AGGAAACTCC AGTCAGAATT GGCAGCGGTT TTATCAACTG ACAAAACTTT
2201  TGGACTCCAT GCATGATGTG GTTGAAAATC TCCTTAGCTA CTGCTTCCAA
```

2251 ACATTTTTGG ATAAGTCCAT GAGTATTGAA TTCCCAGAGA TGTTAGCTGA

2301 AATCATCACT AATCAGATAC CAAAATACTC AAATGGAAAT ATCAAAAAGC

2351 TTCTGTTTCA TCAGAAATGA CTGCCTTACT AAGAAAGGCT GCCTTAAAGA

2401 AAGTTGAATT TATAGCTTTT ACTGTACAAA CTTATCAACT TGTCTTGTAG

2451 ATGTTTTGTC GTTCTTTTTG TTTGTCTTGT TTGTTTTCTA TACGCACTAC

2501 ATGTGGTCTC TAGAGGGCCA AGACTTGGCA ACAGAAGCAG ATGAGCCATC

2551 ACTTTTCAGT GACAGGAAAG CAGAC

B4. GR Fasta format (2575 bases)

GGAAGTTAATATTTGCCAATGGACTCCAAAGAATCCTTAGCTCCCCCTGG

TAGAGACGAAGTCCCCAGCAGTTTGCTTGGCCGGGGGAGGGGAAGCGTGA

TGGACTTGTATAAAACCCTGAGGGGTGGAGCTACAGTCAAGGTTTCTGCG

TCTTCACCCTCAGTGGCTGCTGCTTCTCAGGCAGATTCCAAGCAGCAGAG

GATTCTCCTTGATTTTTCAAAAGGCTCAGCAAGCAATGCACAGCAGCAGC

AGCAGCAGCAGCAGCCGCAGCCAGATTTATCCAAAGCCGTTTCACTGTCC

ATGGGACTGTATATGGGAGAGACCGAAACAAAAGTGATGGGGAATGACTT

GGGCTACCCACAGCAGGGCCAGCTTGGCCTCTCCTCTGGGGAAACAGACT

TTCGGCTTCTGGAAGAAAGCATTGCAAACCTCAATAGGTCGACCAGCCGT

CCAGAGAATCCCAAGAGTTCAACACCTGCAGCTGGGTGTGCTACCCCGAC

AGAGAAGGAGTTTCCCCAGACTCACTCTGATCCATCTTCAGAACAGCAAA

ATAGAAAAAGCCAGCCTGGCACCAACGGTGGCAGTGTGAAATTGTATACC

ACAGACCAAAGCACCTTTGACATCTTGCAGGATTTGGAGTTTTCTGCCGG

GTCCCCAGGTAAAGAGACAAACGAGAGTCCTTGGAGGTCAGACCTGTTGA

TAGATGAAAACTTGCTTTCTCCTTTGGCGGGAGAAGATGATCCATTCCTT

CTGGAAGGGGACGTGAATGAGGATTGCAAGCCTCTTATTTTACCGGACAC

TAAACCTAAAATTCAGGATACTGGAGATACAATCTTATCAAGCCCCAGCA

GTGTGGCACTGCCCCAAGTGAAAACAGAGAAAGATGATTTCATTGAGCTT

TGCACCCCTGGGGTAATTAAGCAAGAGAAACTGGGCCCGGTTTATTGCCA

GGCAAGCTTTTCTGGGACAAATATAATTGGGAATAAAATGTCTGCCATTT

CTGTTCATGGCGTGAGTACCTCTGGAGGACAGATGTACCACTATGACATG

AATACAGCATCCCTTTCTCAGCAGCAGGATCAGAAGCCTGTTTTTAATGT

CATTCCACCAATTCCTGTTGGTTCTGAAAACTGGAATAGGTGCCAAGGGT

CTGGAGAGGACAACCTGACTTCCTTGGGGGCTATGAACTTCGCAGGCCGC

TCAGTGTTTTCTAATGGATATTCAAGCCCTGGAATGAGACCAGATGTGAG

TTCTCCTCCGTCCAGCTCCTCCACAGCAACGGGACCACCTCCCAAACTCT

GCCTGGTGTGCTCCGATGAAGCTTCGGTATGCCATTATGGGGTGCTGACG

TGTGGAAGCTGTAAAGTCTTCTTTAAAAGAGCAGTGGAAGGACAGCACAA

TTACCTTTGTGCTGGAAGAAATGATTGCATCATTGATAAAATTCGAAGAA

AAAACTGTCCAGCATGCCGCTATCGAAAATGTCTTCAAGCTGGAATGAAC

CTGGAAGCTCGAAAAACGAAGAAAAAAATTAAAGGAATTCAGCAAGCCAC

TGCAGGAGTCTCACAAGACACTTCTGAAAACGCTAACAAAACAATAGTTC

CTGCCGCGCTGCCACAGCTTACCCCTACCCTGGTGTCACTGCTGGAGGTG

ATCGAGCCTGAGGTGTTATATGCAGGATATGACAGCTCTGTTCCAGACTC

AGCATGGAGAATTATGACCACGCTCAACATGTTAGGTGGGCGCCAAGTGA

TTGCCGCAGTGAAATGGGCAAAGGCGATACCAGGATTCAGAAACTTACAC

CTGGATGACCAAATGACCCTTCTACAGTACTCATGGATGTTTCTCATGGC

ATTTGCCCTGGGTTGGAGATCATACAGACAAGCAAGTGGAAACCTGCTAT

GCTTTGCTCCTGATCTGATTATTAATGAGCAGAGAATGACTCTACCCTGC

ATGTATGACCAATGTAAACACATGCTGTTTATCTCCACTGAATTACAAAG

ATTGCAGGTATCCTATGAAGAGTATCTCTGTATGAAAACCTTACTGCTTC

TCTCCTCAGTTCCTAAGGAAGGTCTGAAGAGCCAAGAGTTATTTGATGAG

ATTCGAATGACTTATATCAAAGAGCTAGGAAAAGCCATTGTCAAAAGGGA

AGGAAACTCCAGTCAGAATTGGCAGCGGTTTTATCAACTGACAAAACTTT

TGGACTCCATGCATGATGTGGTTGAAAATCTCCTTAGCTACTGCTTCCAA

ACATTTTTGGATAAGTCCATGAGTATTGAATTCCCAGAGATGTTAGCTGA

AATCATCACTAATCAGATACCAAAATACTCAAATGGAAATATCAAAAAGC

TTCTGTTTCATCAGAAATGACTGCCTTACTAAGAAAGGCTGCCTTAAAGA

AAGTTGAATTTATAGCTTTTACTGTACAAACTTATCAACTTGTCTTGTAG

ATGTTTTGTCGTTCTTTTTGTTTGTCTTGTTTGTTTTCTATACGCACTAC

ATGTGGTCTCTAGAGGGCCAAGACTTGGCAACAGAAGCAGATGAGCCATC
ACTTTTCAGTGACAGGAAAGCAGAC

APPENDIX C: OTHER PRIMERS USED IN THIS THESIS

Table C1: Primer sequences used to identify $GR^{-/-}$ mice (details in section 4.2.2.1)

Gene	Forward (5'-3')	Reverse (5'-3')
GR1	GAAGCTTCGGGATGCCATTATGG	GGAATGTGAACCCGTCAACACATG
GR2	GTTTGAAAGAAGATGACTGCAAGG	GGGCCACTAATTGATTTTGGATG
GR3	GTTCTCCATGTCCTTATGCCCAG	GCCAGCTTACAGGATAGCCAGTG
GR4	GGCATCTGGTTCCCTAGAATTGG	GTAACAGTCAGTTCACCAGTTGG
GR5	TGTTCCAACTGGTGAACTGACTG	TGTTACCAACTTCTAGCCACTGG
En-2 & GR	Any of the above GR forward primers	CTGGGGTTCGTGTCCTACAACAC
En-2 & GR	Any of the above GR forward primers	TCTGTCCTCCAGTCTCCTCCAC
En-2 & GR	Any of the above GR forward primers	GAACATCTGAAAAACATACTTTCGG
En-2 & GR	Any of the above GR forward primers	GTCCTCTTCACATCCATGCTGAGG

Combinations of (a) GR forward and reverse primers (described in section 4.2.2 figures 4.2 and 4.3 (indicating relavant PCR product sizes and (b) GR forward and engrailed 2 (en-2) reverse primers were used to identify $GR^{-/-}$ mice. Note that all attempts with GR forward and en-2 reverse were not successful.

Appendix D: Addresses of Suppliers

Amersham Pharmacia Biotech UK Ltd., Little Chalfont, Bucks., HP7 9NA, U.K.

Beckman Coulter (U.K.) Ltd., Oakley Court, Kingsmead Business Park, London Road, High Wycombe, Bucks., HP11 1JU, U.K.

Berthold Technologies (U.K.) Ltd., The Priory, High Street, Redbourn, Herts., AL3 7LZ, U.K.

BD UK Ltd, Between Towns Road, Cowley, Oxford, Oxon., OX4 3LY, U.K.

Bio-Rad Laboratories Ltd., Bio-Rad House, Maylands Avenue, Hemel Hempstead, Herts., HP2 7TD, U.K.

Cambrex Bio Science Wokingham Ltd., 1 Ashville Way, Wokingham, Berks., RG41 2PL, U.K.

Eppendorf AG, Barkhausenweg 1, 22331 Hamburg, Germany

Greiner Bio-One Ltd., Brunel Way, Stroudwater Business Park, Stonehouse, Glos., GL10 3SX, U.K.

IKA Labortechnik, IKA-Werke GmbH & Co. KG, Janke & Kunkel-Str. 10, D-79219 Staufen, Germany

Invitrogen, Ichinnan Business Park, 3 Fountain Drive, Paisley, PA4 9RF, U.K.

Kendro Laboratory Products Plc., Stortford Hall Park, Bishhop's Stortford, Herts., CM23 5GZ, U.K.

Nalgene Labware, Unit 1a, Thorn Business Park, Hereford, HR2 6JS, U.K.

Oswel DNA service, Medical & Biological Sciences Building, University of Southampton, Boldrewood, Bassett Crescent East, Southampton, SO16 7PX, UK.

Promega Ltd., Delta house, Chilworth Research Centre, Southampton, SO1 7NS, U.K.

Qbiogene-Alexis Ltd., P.O. Box 6757, Bingham, Nottingham, NG13 8LS, U.K.

Quantum Appligene, Parc d'Innovation, BP 72, Illkirch 67402, France

Roche Diagnostics Ltd., Bell Lane, Lewes, East Sussex, BN7 1LG, U.K.

Sarstedt Ltd., 68 Boston Road, Beaumont Leys, Leicester, LE4 1AW, U.K.

Shimadzu Europa U.K., Mill Court, Featherstone Road, Wolverton Mill South, Milton Keynes, Bucks., MK12 5RE, U.K.

Sigma-Aldrich Company Ltd., Fancy Road, Poole, Dorset, BH12 4OH, U.K.

Stratagene Europe, Gebouw California, Hogehilweg 15, 1101 CB Amsterdam Zuidoost, The Netherlands

Techne, Duxford, Cambridge, CB2 4P2, U.K.

Tropix Ltd., 47 Wiggins Avenue, Bedford, MA, U.S.A.

Worthington Biochemicals, Lorne Laboratories Ltd., 7 Tavistock Estate, Ruscombe Business Park, Ruscombe Lane, Twyford, Reading, Berks., RG10 9NJ, U.K.

VWR International Ltd., Hunter Boulevard, Magna Park, Lutterworth, Leics., LE17 4XN, U.K.

Reference List

Abernathy, R. S., and Spink, W. W. (1957). Resistance to endotoxin after protection against initial lethal challenge with adrenocorticosteroids or chlorpromazine. Proc Soc Exp Biol Med *95*, 580-581.

Adams, M., Meijer, O. C., Wang, J., Bhargava, A., and Pearce, D. (2003). Homodimerization of the glucocorticoid receptor is not essential for response element binding: activation of the phenylethanolamine N-methyltransferase gene by dimerization-defective mutants. Mol Endocrinol *17*, 2583-2592.

Ailhaud, G. (1999). Cross talk between adipocytes and their precursors: relationships with adipose tissue development and blood pressure. Ann N Y Acad Sci *892*, 127-133.

Aizawa-Abe, M., Ogawa, Y., Masuzaki, H., Ebihara, K., Satoh, N., Iwai, H., Matsuoka, N., Hayashi, T., Hosoda, K., Inoue, G.*, et al.* (2000). Pathophysiological role of leptin in obesity-related hypertension. J Clin Invest *105*, 1243-1252.

Akner, G., Wikstrom, A. C., and Gustafsson, J. A. (1995). Subcellular distribution of the glucocorticoid receptor and evidence for its association with microtubules. J Steroid Biochem Mol Biol *52*, 1-16.

Akner, G., Wikstrom, A. C., Mossberg, K., Sundqvist, K. G., and Gustafsson, J. A. (1994). Morphometric studies of the localization of the glucocorticoid receptor in mammalian cells and of glucocorticoid hormone-induced effects. J Histochem Cytochem *42*, 645-657.

Aldhahi, W., Mun, E., and Goldfine, A. B. (2004). Portal and peripheral cortisol levels in obese humans. Diabetologia *47*, 833-836.

Almlof, T., Wright, A. P., and Gustafsson, J. A. (1995). Role of acidic and phosphorylated residues in gene activation by the glucocorticoid receptor. J Biol Chem *270*, 17535-17540.

Anderson, D. J. (1993). Molecular control of cell fate in the neural crest: the sympathoadrenal lineage. Annu Rev Neurosci *16*, 129-158.

Andersson, S., Berman, D. M., Jenkins, E. P., and Russell, D. W. (1991). Deletion of steroid 5 alpha-reductase 2 gene in male pseudohermaphroditism. Nature *354*, 159-161.

Andrews, R. C., and Walker, B. R. (1999). Glucocorticoids and insulin resistance: old hormones, new targets. Clin Sci (Lond) *96*, 513-523.

Anzick, S. L., Kononen, J., Walker, R. L., Azorsa, D. O., Tanner, M. M., Guan, X. Y., Sauter, G., Kallioniemi, O. P., Trent, J. M., and Meltzer, P. S. (1997). AIB1, a steroid receptor coactivator amplified in breast and ovarian cancer. Science *277*, 965-968.

Arriza, J. L., Simerly, R. B., Swanson, L. W., and Evans, R. M. (1988). The neuronal mineralocorticoid receptor as a mediator of glucocorticoid response. Neuron *1*, 887-900.

Arriza, J. L., Weinberger, C., Cerelli, G., Glaser, T. M., Handelin, B. L., Housman, D. E., and Evans, R. M. (1987). Cloning of human mineralocorticoid receptor complementary DNA: structural and functional kinship with the glucocorticoid receptor. Science *237*, 268-275.

Arruda, R. M., Peotta, V. A., Meyrelles, S. S., and Vasquez, E. C. (2005). Evaluation of vascular function in apolipoprotein E knockout mice with angiotensin-dependent renovascular hypertension. Hypertension *46*, 932-936.

Ashby, P., and Robinson, D. S. (1980). Effects of insulin, glucocorticoids and adrenaline on the activity of rat adipose-tissue lipoprotein lipids. Biochem J *188*, 185-192.

Ashraf, J., and Thompson, E. B. (1993a). Glucocorticoid receptors in leukemias, lymphomas and myelomas of young and old. Adv Exp Med Biol *330*, 241-269.

Ashraf, J., and Thompson, E. B. (1993b). Identification of the activation-labile gene: a single point mutation in the human glucocorticoid receptor presents as two distinct receptor phenotypes. Mol Endocrinol *7*, 631-642.

Ashwell, J. D., Lu, F. W., and Vacchio, M. S. (2000). Glucocorticoids in T cell development and function*. Annu Rev Immunol *18*, 309-345.

Aubert, J., Darimont, C., Safonova, I., Ailhaud, G., and Negrel, R. (1997). Regulation by glucocorticoids of angiotensinogen gene expression and secretion in adipose cells. Biochem J *328*, 701-706.

Aubert, J., Safonova, I., Negrel, R., and Ailhaud, G. (1998). Insulin down-regulates angiotensinogen gene expression and angiotensinogen secretion in cultured adipose cells. Biochem Biophys Res Commun *250*, 77-82.

Baid, S., and Nieman, L. K. (2004). Glucocorticoid excess and hypertension. Curr Hypertens Rep *6*, 493-499.

Ballard, P. L., Baxter, J. D., Higgins, S. J., Rousseau, G. G., and Tomkins, G. M. (1974). General presence of glucocorticoid receptors in mammalian tissues. Endocrinology *94*, 998-1002.

Bamberger, C. M., Bamberger, A. M., de Castro, M., and Chrousos, G. P. (1995). Glucocorticoid receptor beta, a potential endogenous inhibitor of glucocorticoid action in humans. J Clin Invest *95*, 2435-2441.

Bamberger, C. M., Schulte, H. M., and Chrousos, G. P. (1996). Molecular determinants of glucocorticoid receptor function and tissue sensitivity to glucocorticoids. Endocr Rev *17*, 245-261.

Barratt, K., and Mackay, J. F. (2002). Improving real-time PCR genotyping assays by asymmetric amplification. J Clin Microbiol *40*, 1571-1572.

Bartlett, S. M., and Gibbons, G. F. (1988). Short- and longer-term regulation of very-low-density lipoprotein secretion by insulin, dexamethasone and lipogenic substrates in cultured hepatocytes. A biphasic effect of insulin. Biochem J *249*, 37-43.

Basu, R., Singh, R. J., Basu, A., Chittilapilly, E. G., Johnson, M. C., Toffolo, G., Cobelli, C., and Rizza, R. A. (2005). Obesity and Type 2 Diabetes Do Not Alter Splanchnic Cortisol Production in Humans. J Clin Endocrinol Metab.

Beato, M., Chalepakis, G., Schauer, M., and Slater, E. P. (1989). DNA regulatory elements for steroid hormones. J Steroid Biochem *32*, 737-748.

Beato, M., Chavez, S., and Truss, M. (1996). Transcriptional regulation by steroid hormones. Steroids *61*, 240-251.

Bertini, R., Bianchi, M., and Ghezzi, P. (1988). Adrenalectomy sensitizes mice to the lethal effects of interleukin 1 and tumor necrosis factor. J Exp Med *167*, 1708-1712.

Bettmann, M. A., Dake, M. D., Hopkins, L. N., Katzen, B. T., White, C. J., Eisenhauer, A. C., Pearce, W. H., Rosenfield, K. A., Smalling, R. W., Sos, T. A., and Venbrux, A. C. (2004). Atherosclerotic Vascular Disease Conference: Writing Group VI: revascularization. Circulation *109*, 2643-2650.

Bhattacharyya, S., Brown, D. E., Brewer, J. A., Vogt, S. K., and Muglia, L. J. (2007). Macrophage glucocorticoid receptors regulate Toll-like receptor 4-mediated inflammatory responses by selective inhibition of p38 MAP kinase. Blood *109*, 4313-4319.

Bhopal, R., Unwin, N., White, M., Yallop, J., Walker, L., Alberti, K. G., Harland, J., Patel, S., Ahmad, N., Turner, C.*, et al.* (1999). Heterogeneity of coronary heart disease risk factors in Indian, Pakistani, Bangladeshi, and European origin populations: cross sectional study. Bmj *319*, 215-220.

Björntorp, P., and Rosmond, R. (2000). Obesity and cortisol. Nutrition *16*, 924-936.

Bledsoe, R. K., Montana, V. G., Stanley, T. B., Delves, C. J., Apolito, C. J., McKee, D. D., Consler, T. G., Parks, D. J., Stewart, E. L., Willson, T. M.*, et al.* (2002). Crystal structure of the glucocorticoid receptor ligand binding domain reveals a novel mode of receptor dimerization and coactivator recognition. Cell *110*, 93-105.

Borden, K. L. (2002). Pondering the promyelocytic leukemia protein (PML) puzzle: possible functions for PML nuclear bodies. Mol Cell Biol *22*, 5259-5269.

Boullu-Ciocca, S., Paulmyer-Lacroix, O., Fina, F., Ouafik, L., Alessi, M. C., Oliver, C., and Grino, M. (2003). Expression of the mRNAs coding for the glucocorticoid receptor isoforms in obesity. Obes Res *11*, 925-929.

Boustany, C. M., Bharadwaj, K., Daugherty, A., Brown, D. R., Randall, D. C., and Cassis, L. A. (2004). Activation of the systemic and adipose renin-angiotensin system in rats with diet-induced obesity and hypertension. Am J Physiol Regul Integr Comp Physiol *287*, R943-949.

Boyle, M. P., Brewer, J. A., Funatsu, M., Wozniak, D. F., Tsien, J. Z., Izumi, Y., and Muglia, L. J. (2005). Acquired deficit of forebrain glucocorticoid receptor produces depression-like changes in adrenal axis regulation and behavior. Proc Natl Acad Sci U S A *102*, 473-478.

Brasier, A. R., Ron, D., Tate, J. E., and Habener, J. F. (1990). Synergistic enhansons located within an acute phase responsive enhancer modulate glucocorticoid induction of angiotensinogen gene transcription. Mol Endocrinol *4*, 1921-1933.

Brewer, J. A., Khor, B., Vogt, S. K., Muglia, L. M., Fujiwara, H., Haegele, K. E., Sleckman, B. P., and Muglia, L. J. (2003). T-cell glucocorticoid receptor is required to suppress COX-2-mediated lethal immune activation. Nat Med *9*, 1318-1322.

Brilla, C. G., and Weber, K. T. (1992). Mineralocorticoid excess, dietary sodium, and myocardial fibrosis. J Lab Clin Med *120*, 893-901.

Brindley, D. N., Akester, H., Derrick, G. P., Irvine, C. D., Patmore, R. D., Spencer, H., Yule-Smith, A., Finnerty, C., Saxton, J., Macdonald, I. A., and et al. (1988). Effects of chronic administration of benfluorex to rats on the metabolism of corticosterone, glucose, triacylglycerols, glycerol and fatty acid. Biochem Pharmacol *37*, 695-705.

Brindley, G. S. (1988). The Ferrier lecture, 1986. The actions of parasympathetic and sympathetic nerves in human micturition, erection and seminal emission, and their restoration in paraplegic patients by implanted electrical stimulators. Proc R Soc Lond B Biol Sci *235*, 111-120.

Brönnegard, M., Reynisdottir, S., Marcus, C., Stierna, P., and Arner, P. (1995). Effect of glucocorticosteroid treatment on glucocorticoid receptor expression in human adipocytes. J Clin Endocrinol Metab *80*, 3608-3612.

Brook, C., Marshall, NJ (2001). Endocrinology, 4th edn: Blackwell).

Brotman, D. J., Girod, J. P., Garcia, M. J., Patel, J. V., Gupta, M., Posch, A., Saunders, S., Lip, G. Y., Worley, S., and Reddy, S. (2005). Effects of short-term glucocorticoids on cardiovascular biomarkers. J Clin Endocrinol Metab *90*, 3202-3208.

Brown, R., Seckl, J R, (2005). Glucocorticoid action in development. Current Opinion in Endocrinology and Diabetes *12*, 224-232.

Bruley, C., Lyons, V., Worsley, A. G., Wilde, M. D., Darlington, G. D., Morton, N. M., Seckl, J. R., and Chapman, K. E. (2006). A novel promoter for the 11beta-hydroxysteroid dehydrogenase type 1 gene is active in lung and is C/EBPalpha independent. Endocrinology *147*, 2879-2885.

Buckingham, J. C. (2006). Glucocorticoids: exemplars of multi-tasking. Br J Pharmacol *147 Suppl 1*, S258-268.

Buemann, B., Vohl, M. C., Chagnon, M., Chagnon, Y. C., Gagnon, J., Perusse, L., Dionne, F., Despres, J. P., Tremblay, A., Nadeau, A., and Bouchard, C. (1997). Abdominal visceral fat is associated with a BclI restriction fragment length polymorphism at the glucocorticoid receptor gene locus. Obes Res *5*, 186-192.

Bujalska, I. J., Draper, N., Michailidou, Z., Tomlinson, J. W., White, P. C., Chapman, K. E., Walker, E. A., and Stewart, P. M. (2005). Hexose-6-phosphate dehydrogenase confers oxo-reductase activity upon 11 beta-hydroxysteroid dehydrogenase type 1. J Mol Endocrinol *34*, 675-684.

Bujalska, I. J., Kumar, S., Hewison, M., and Stewart, P. M. (1999). Differentiation of adipose stromal cells: the roles of glucocorticoids and 11®-hydroxysteroid dehydrogenase. Endocrinology *140*, 3188-3196.

Bujalska, I. J., Kumar, S., and Stewart, P. M. (1997). Does central obesity reflect "Cushing's disease of the omentum"? Lancet *349*, 1210-1213.

Burnstein, K. L., Jewell, C. M., Sar, M., and Cidlowski, J. A. (1994). Intragenic Sequences of the Human Glucocorticoid Receptor Complementary DNA Mediate Hormone-Inducible Receptor Messenger-Rna Down-Regulation Through Multiple Mechanisms. Mol Endocrinol *8*, 1764-1773.

Campbell, D. J., and Habener, J. F. (1986). Angiotensinogen gene is expressed and differentially regulated in multiple tissues of the rat. J Clin Invest *78*, 31-39.

Carnes, M., Lent, S., Feyzi, J., and Hazel, D. (1989). Plasma adrenocorticotropic hormone in the rat demonstrates three different rhythms within 24 h. Neuroendocrinology *50*, 17-25.

Cassis, L. A. (1992). Downregulation of the renin-angiotensin system in streptozotocin-diabetic rats. Am J Physiol *262*, E105-109.

Cassis, L. A., Saye, J., and Peach, M. J. (1988). Location and regulation of rat angiotensinogen messenger RNA. Hypertension *11*, 591-596.

Celsi, G., Kistner, A., Aizman, R., Eklof, A. C., Ceccatelli, S., de Santiago, A., and Jacobson, S. H. (1998). Prenatal dexamethasone causes oligonephronia, sodium retention, and higher blood pressure in the offspring. Pediatr Res *44*, 317-322.

Chakravarty, K., Cassuto, H., Reshef, L., and Hanson, R. W. (2005). Factors that control the tissue-specific transcription of the gene for phosphoenolpyruvate carboxykinase-C. Crit Rev Biochem Mol Biol *40*, 129-154.

Challis, B. G., Coll, A. P., Yeo, G. S., Pinnock, S. B., Dickson, S. L., Thresher, R. R., Dixon, J., Zahn, D., Rochford, J. J., White, A.*, et al.* (2004). Mice lacking pro-opiomelanocortin are sensitive to high-fat feeding but respond normally to the acute anorectic effects of peptide-YY(3-36). Proc Natl Acad Sci U S A *101*, 4695-4700.

Chandran, U. R., Warren, B. S., Baumann, C. T., Hager, G. L., and DeFranco, D. B. (1999). The glucocorticoid receptor is tethered to DNA-bound Oct-1 at the mouse gonadotropin-releasing hormone distal negative glucocorticoid response element. J Biol Chem *274*, 2372-2378.

Ching, R. W., Dellaire, G., Eskiw, C. H., and Bazett-Jones, D. P. (2005). PML bodies: a meeting place for genomic loci? J Cell Sci *118*, 847-854.

Cidlowski, J. A., Bellingham, D. L., Powell-Oliver, F. E., Lubahn, D. B., and Sar, M. (1990). Novel antipeptide antibodies to the human glucocorticoid receptor: recognition of multiple receptor forms in vitro and distinct localization of cytoplasmic and nuclear receptors. Mol Endocrinol *4*, 1427-1437.

Cigolini, M., and Smith, U. (1979). Human adipose tissue in culture. VIII. Studies on the insulin-antagonistic effect of glucocorticoids. Metabolism *28*, 502-510.

Cittadini, A., Mantzoros, C. S., Hampton, T. G., Travers, K. E., Katz, S. E., Morgan, J. P., Flier, J. S., and Douglas, P. S. (1999). Cardiovascular abnormalities in transgenic mice with reduced brown fat: an animal model of human obesity. Circulation *100*, 2177-2183.

Clapham, J. C., and Turner, N. C. (1997). Effects of the glucocorticoid II receptor antagonist mifepristone on hypertension in the obese Zucker rat. J Pharmacol Exp Ther *282*, 1503-1508.

Cleasby, M. E., Kelly, P. A., Walker, B. R., and Seckl, J. R. (2003). Programming of rat muscle and fat metabolism by *in utero* overexposure to glucocorticoids. Endocrinology *144*, 999-1007.

Cole, T. J., Blendy, J. A., Monaghan, A. P., Krieglstein, K., Schmid, W., Aguzzi, A., Fantuzzi, G., Hummler, E., Unsicker, K., and Schutz, G. (1995). Targeted disruption of the glucocorticoid receptor gene blocks adrenergic chromaffin cell development and severely retards lung maturation. Genes Dev *9*, 1608-1621.

Cole, T. J., Harris, H. J., Hoong, I., Solomon, N., Smith, R., Krozowski, Z., and Fullerton, M. J. (1999). The glucocorticoid receptor is essential for maintaining basal and dexamethasone-induced repression of the murine corticosteroid-binding globulin gene. Mol Cell Endocrinol *154*, 29-36.

Cole, T. J., Myles, K., Purton, J. F., Brereton, P. S., Solomon, N. M., Godfrey, D. I., and Funder, J. W. (2001). GRKO mice express an aberrant dexamethasone-binding glucocorticoid receptor, but are profoundly glucocorticoid resistant. Mol Cell Endocrinol *173*, 193-202.

Coll, A. P. (2007). Effects of pro-opiomelanocortin (POMC) on food intake and body weight: mechanisms and therapeutic potential? Clin Sci (Lond) *113*, 171-182.

Coll, A. P., Challis, B. G., Lopez, M., Piper, S., Yeo, G. S., and O'Rahilly, S. (2005). Proopiomelanocortin-Deficient Mice Are Hypersensitive to the Adverse Metabolic Effects of Glucocorticoids. Diabetes *54*, 2269-2276.

Coll, A. P., Challis, B. G., Yeo, G. S., Snell, K., Piper, S. J., Halsall, D., Thresher, R. R., and O'Rahilly, S. (2004). The effects of proopiomelanocortin deficiency on murine adrenal development and responsiveness to adrenocorticotropin. Endocrinology *145*, 4721-4727.

Coll, A. P., Fassnacht, M., Klammer, S., Hahner, S., Schulte, D. M., Piper, S., Tung, Y. C., Challis, B. G., Weinstein, Y., Allolio, B*., et al.* (2006). Peripheral administration of the N-terminal pro-opiomelanocortin fragment 1-28 to Pomc-/- mice reduces food intake and weight but does not affect adrenal growth or corticosterone production. J Endocrinol *190*, 515-525.

Comuzzie, A. G., Hixson, J. E., Almasy, L., Mitchell, B. D., Mahaney, M. C., Dyer, T. D., Stern, M. P., MacCluer, J. W., and Blangero, J. (1997). A major quantitative trait locus determining serum leptin levels and fat mass is located on human chromosome 2. Nat Genet *15*, 273-276.

Dahlman-Wright, K., Grandien, K., Nilsson, S., Gustafsson, J. A., and Carlstedt-Duke, J. (1993). Protein-protein interactions between the DNA-binding domains of nuclear receptors: influence on DNA-binding. J Steroid Biochem Mol Biol *45*, 239-250.

Dahlman-Wright, K., Wright, A., Carlstedt-Duke, J., and Gustafsson, J. A. (1992a). DNA-binding by the glucocorticoid receptor: a structural and functional analysis. J Steroid Biochem Mol Biol *41*, 249-272.

Dahlman-Wright, K., Wright, A., Gustafsson, J. A., and Carlstedt-Duke, J. (1991). Interaction of the glucocorticoid receptor DNA-binding domain with DNA as a dimer is mediated by a short segment of five amino acids. J Biol Chem *266*, 3107-3112.

Dahlman-Wright, K., Wright, A. P., and Gustafsson, J. A. (1992b). Determinants of high-affinity DNA binding by the glucocorticoid receptor: evaluation of receptor domains outside the DNA-binding domain. Biochemistry *31*, 9040-9044.

Dallman, M. F. (1984). Viewing the ventromedial hypothalamus from the adrenal gland. Am J Physiol *246*, R1-12.

Dallman, M. F., Strack, A. M., Akana, S. F., Bradbury, M. J., Hanson, E. S., Scribner, K. A., and Smith, M. (1993). Feast and Famine - Critical Role of Glucocorticoids With Insulin in Daily Energy-Flow. Frontiers in Neuroendocrinology *14*, 303-347.

Dalman, F. C., Scherrer, L. C., Taylor, L. P., Akil, H., and Pratt, W. B. (1991). Localization of the 90-kDa heat shock protein-binding site within the hormone-binding domain of the glucocorticoid receptor by peptide competition. J Biol Chem *266*, 3482-3490.

Danielsen, M., Northrop, J. P., and Ringold, G. M. (1986). The mouse glucocorticoid receptor: mapping of functional domains by cloning, sequencing and expression of wild-type and mutant receptor proteins. Embo J *5*, 2513-2522.

Davani, B., Portwood, N., Bryzgalova, G., Reimer, M. K., Heiden, T., Ostenson, C. G., Okret, S., Ahren, B., Efendic, S., and Khan, A. (2004). Aged transgenic mice with increased glucocorticoid sensitivity in pancreatic beta-cells develop diabetes. Diabetes *53 Suppl 1*, S51-59.

de Castro, M., Elliot, S., Kino, T., Bamberger, C., Karl, M., Webster, E., and Chrousos, G. P. (1996). The non-ligand binding beta-isoform of the human glucocorticoid receptor (hGR beta): tissue levels, mechanism of action, and potential physiologic role. Mol Med *2*, 597-607.

De Kloet, E. R. (2004). Hormones and the stressed brain. Ann N Y Acad Sci *1018*, 1-15.

De Kloet, E. R., Vreugdenhil, E., Oitzl, M. S., and Joels, M. (1998). Brain corticosteroid receptor balance in health and disease. Endocr Rev *19*, 269-301.

Debons, A. F., Siclari, E., Das, K. C., and Fuhr, B. (1982). Gold thioglucose-induced hypothalamic damage, hyperphagia, and obesity: dependence on the adrenal gland. Endocrinology *110*, 2024-2029.

DeCastro, R., Zhang, Y., Guo, H., Kataoka, H., Gordon, M. K., Toole, B., and Biswas, G. (1996). Human keratinocytes express EMMPRIN, an extracellular matrix metalloproteinase inducer. J Invest Dermatol *106*, 1260-1265.

Delaunay, F., Khan, A., Cintra, A., Davani, B., Ling, Z. C., Andersson, A., Ostenson, C. G., Gustafsson, J., Efendic, S., and Okret, S. (1997). Pancreatic beta cells are important targets for the diabetogenic effects of glucocorticoids. J Clin Invest *100*, 2094-2098.

Denton, R. R., Eisen, L. P., Elsasser, M. S., and Harmon, J. M. (1993). Differential autoregulation of glucocorticoid receptor expression in human T- and B-cell lines. Endocrinology *133*, 248-256.

DeRijk, R. H., Schaaf, M., and de Kloet, E. R. (2002). Glucocorticoid receptor variants: clinical implications. J Steroid Biochem Mol Biol *81*, 103-122.

Despres, J. P., Nadeau, A., Tremblay, A., Ferland, M., Moorjani, S., Lupien, P. J., Theriault, G., Pinault, S., and Bouchard, C. (1989). Role of deep abdominal fat in the association between regional adipose tissue distribution and glucose tolerance in obese women. Diabetes *38*, 304-309.

Dhawan, J., Bray, C. L., Warburton, R., Ghambhir, D. S., and Morris, J. (1994). Insulin resistance, high prevalence of diabetes, and cardiovascular risk in immigrant Asians. Genetic or environmental effect? Br Heart J *72*, 413-421.

Di Blasio, A. M., van Rossum, E. F., Maestrini, S., Berselli, M. E., Tagliaferri, M., Podesta, F., Koper, J. W., Liuzzi, A., and Lamberts, S. W. (2003). The relation between two polymorphisms in the glucocorticoid receptor gene and body mass index, blood pressure and cholesterol in obese patients. Clin Endocrinol (Oxf) *59*, 68-74.

Diamant, S., and Shafrir, E. (1975). Modulation of the activity of insulin-dependent enzymes of lipogenesis by glucocorticoids. Eur J Biochem *53*, 541-546.

Dobrian, A. D., Davies, M. J., Prewitt, R. L., and Lauterio, T. J. (2000). Development of hypertension in a rat model of diet-induced obesity. Hypertension *35*, 1009-1015.

Dobson, M. G., Redfern, C. P., Unwin, N., and Weaver, J. U. (2001). The N363S polymorphism of the glucocorticoid receptor: potential contribution to central obesity in men and lack of association with other risk factors for coronary heart disease and diabetes mellitus. J Clin Endocrinol Metab *86*, 2270-2274.

Dong, Y., Poellinger, L., Gustafsson, J.-Å., and Okret, S. (1988). Regulation of glucocorticoid receptor expression: evidence for transcriptional and posttranslational mechanisms. Mol Endocrinol *2*, 1256-1264.

Dunn, J. F., Nisula, B. C., and Rodbard, D. (1981). Transport of steroid hormones: binding of 21 endogenous steroids to both testosterone-binding globulin and corticosteroid-binding globulin in human plasma. J Clin Endocrinol Metab *53*, 58-68.

Durtschi, J. D., Stevenson, J., Hymas, W., and Voelkerding, K. V. (2007). Evaluation of quantification methods for real-time PCR minor groove binding hybridization probe assays. Anal Biochem *361*, 55-64.

Eisen, L. P., Elsasser, M. S., and Harmon, J. M. (1988). Positive regulation of the glucocorticoid receptor in human T-cells sensitive to the cytolytic effects of glucocorticoids. J Biol Chem *263*, 12044-12048.

Elbi, C., Walker, D. A., Romero, G., Sullivan, W. P., Toft, D. O., Hager, G. L., and DeFranco, D. B. (2004). Molecular chaperones function as steroid receptor nuclear mobility factors. Proc Natl Acad Sci U S A *101*, 2876-2881.

Encio, I. J., and Detera-Wadleigh, S. D. (1991). The genomic structure of the human glucocorticoid receptor. J Biol Chem *266*, 7182-7188.

Engeli, S., Bohnke, J., Feldpausch, M., Gorzelniak, K., Heintze, U., Janke, J., Luft, F. C., and Sharma, A. M. (2004). Regulation of 11beta-HSD genes in human adipose tissue: influence of central obesity and weight loss. Obes Res *12*, 9-17.

Engeli, S., Gorzelniak, K., Kreutz, R., Runkel, N., Distler, A., and Sharma, A. M. (1999). Co-expression of renin-angiotensin system genes in human adipose tissue. J Hypertens *17*, 555-560.

Engeli, S., Schling, P., Gorzelniak, K., Boschmann, M., Janke, J., Ailhaud, G., Teboul, M., Massiera, F., and Sharma, A. M. (2003). The adipose-tissue renin-angiotensin-aldosterone system: role in the metabolic syndrome? Int J Biochem Cell Biol *35*, 807-825.

Feldmer, M., Kaling, M., Takahashi, S., Mullins, J. J., and Ganten, D. (1991). Glucocorticoid- and estrogen-responsive elements in the 5'-flanking region of the rat angiotensinogen gene. J Hypertens *9*, 1005-1012.

Ferrari, P. (2003). Cortisol and the renal handling of electrolytes: role in glucocorticoid-induced hypertension and bone disease. Best Pract Res Clin Endocrinol Metab *17*, 575-589.

Finotto, S., Krieglstein, K., Schober, A., Deimling, F., Lindner, K., Bruhl, B., Beier, K., Metz, J., GarciaArraras, J. E., RoigLopez, J. L.*, et al.* (1999). Analysis of mice carrying targeted mutations of the glucocorticoid receptor gene argues against an essential role of glucocorticoid signalling for generating adrenal chromaffin cells. Development *126*, 2935-2944.

Fleury, I., Beaulieu, P., Primeau, M., Labuda, D., Sinnett, D., and Krajinovic, M. (2003). Characterization of the BclI polymorphism in the glucocorticoid receptor gene. Clin Chem *49*, 1528-1531.

Flier, J. S. (2004). Obesity wars: molecular progress confronts an expanding epidemic. Cell *116*, 337-350.

Franchimont, D., Galon, J., Vacchio, M. S., Fan, S., Visconti, R., Frucht, D. M., Geenen, V., Chrousos, G. P., Ashwell, J. D., and O'Shea, J. J. (2002). Positive effects of glucocorticoids on T cell function by up-regulation of IL-7 receptor alpha. J Immunol *168*, 2212-2218.

Frederich, R. C., Jr., Kahn, B. B., Peach, M. J., and Flier, J. S. (1992). Tissue-specific nutritional regulation of angiotensinogen in adipose tissue. Hypertension *19*, 339-344.

Freedman, L. P. (1999). Increasing the complexity of coactivation in nuclear receptor signaling. Cell *97*, 5-8.

Freedman, M. R., Horwitz, B. A., and Stern, J. S. (1986). Effect of adrenalectomy and glucocorticoid replacement on development of obesity. Am J Physiol *250*, R595-607.

Fried, S. K., Russell, C. D., Grauso, N. L., and Brolin, R. E. (1993). Lipoprotein lipase regulation by insulin and glucocorticoid in subcutaneous and omental adipose tissues of obese women and men. J Clin Invest *92*, 2191-2198.

Fujioka, S., Matsuzawa, Y., Tokunaga, K., and Tarui, S. (1987). Contribution of intra-abdominal fat accumulation to the impairment of glucose and lipid metabolism in human obesity. Metabolism *36*, 54-59.

Funder, J. (1992). Acth, Cortisol and 11-Beta-Ohsd - Quis Custodet Custodes. Clinical Endocrinology *37*, 481-482.

Gaillard, D., Wabitsch, M., Pipy, B., and Negrel, R. (1991). Control of terminal differentiation of adipose precursor cells by glucocorticoids. J Lipid Res *32*, 569-579.

Gardiner, S. M., and Bennett, T. (1983). Post-adrenalectomy hypotension in rats; absence of baroreflex resetting or effect of naloxone. Clin Sci (Lond) *64*, 371-376.

Garland, R. C. (1986). Induction of glucose 6-phosphatase in cultured hepatoma cells by dexamethasone. Biochem Biophys Res Comm *139*, 1130-1134.

Gass, P., Reichardt, H. M., Strekalova, T., Henn, F., and Tronche, F. (2001). Mice with targeted mutations of glucocorticoid and mineralocorticoid receptors: models for depression and anxiety? Physiol Behav *73*, 811-825.

Gehring, U., Segnitz, B., Foellmer, B., and Francke, U. (1985). Assignment of the human gene for the glucocorticoid receptor to chromosome 5. Proc Natl Acad Sci USA *82*, 3751-3755.

Geley, S., Hartmann, B. L., Hala, M., Strasser-Wozak, E. M., Kapelari, K., and Kofler, R. (1996). Resistance to glucocorticoid-induced apoptosis in human T-cell acute lymphoblastic leukemia CEM-C1 cells is due to insufficient glucocorticoid receptor expression. Cancer Res *56*, 5033-5038.

Giguere, V., Hollenberg, S. M., Rosenfeld, M. G., and Evans, R. M. (1986). Functional domains of the human glucocorticoid receptor. Cell *46*, 645-652.

Giguere, V., Yang, N., Segui, P., and Evans, R. M. (1988). Identification of a new class of steroid hormone receptors. Nature *331*, 91-94.

Godfrey, D. I., Purton, J. F., Boyd, R. L., and Cole, T. J. (2000). Stress-free T-cell development: glucocorticoids are not obligatory. Immunol Today *21*, 606-611.

Godowski, P. J., Rusconi, S., Miesfeld, R., and Yamamoto, K. R. (1987). Glucocorticoid Receptor Mutants That Are Constitutive Activators of Transcriptional Enhancement. Nature *325*, 365-368.

Gomi, M., Moriwaki, K., Katagiri, S., Kurata, Y., and Thompson, E. B. (1990). Glucocorticoid effects on myeloma cells in culture: correlation of growth inhibition with induction of glucocorticoid receptor messenger RNA. Cancer Res *50*, 1873-1878.

Goodman, B. M., Carnes, M., and Lent, S. J. (1994). Model simulations of ACTH pulsatility. Life Sci *54*, 1659-1669.

Goossens, G. H., Jocken, J. W., Blaak, E. E., Schiffers, P. M., Saris, W. H., and van Baak, M. A. (2007). Endocrine role of the renin-angiotensin system in human adipose tissue and muscle: effect of beta-adrenergic stimulation. Hypertension *49*, 542-547.

Grunfeld, J. P. (1990). Glucocorticoids in blood pressure regulation. Horm Res *34*, 111-113.

Gruol, D. J., Rajah, F. M., and Bourgeois, S. (1989). Cyclic AMP-dependent protein kinase modulation of the glucocorticoid-induced cytolytic response in murine T-lymphoma cells. Mol Endocrinol *3*, 2119-2127.

Gudmundsson, A., and Carnes, M. (1997). Pulsatile adrenocorticotropic hormone: an overview. Biol Psychiatry *41*, 342-365.

Gunn, J. M., Hanson, R. W., Meyuhas, O., Reshef, L., and Ballard, F. J. (1975). Glucocorticoids and the regulation of phosphoenolpyruvate carboxykinase (guanosine triphosphate) in the rat. Biochem J *150*, 195-203.

Hache, R. J., Tse, R., Reich, T., Savory, J. G., and Lefebvre, Y. A. (1999). Nucleocytoplasmic trafficking of steroid-free glucocorticoid receptor. J Biol Chem *274*, 1432-1439.

Hager, G. L., Fletcher, T. M., Xiao, N., Baumann, C. T., Muller, W. G., and McNally, J. G. (2000). Dynamics of gene targeting and chromatin remodelling by nuclear receptors. Biochem Soc Trans *28*, 405-410.

Hager, J., Dina, C., Francke, S., Dubois, S., Houari, M., Vatin, V., Vaillant, E., Lorentz, N., Basdevant, A., Clement, K.*, et al.* (1998). A genome-wide scan for human obesity genes reveals a major susceptibility locus on chromosome 10. Nat Genet *20*, 304-308.

Hajduch, E., Balendran, A., Batty, I. H., Litherland, G. J., Blair, A. S., Downes, C. P., and Hundal, H. S. (2001). Ceramide impairs the insulin-dependent membrane recruitment of protein kinase B leading to a loss in downstream signalling in L6 skeletal muscle cells. Diabetologia *44*, 173-183.

Hall, J. E., Kuo, J. J., da Silva, A. A., de Paula, R. B., Liu, J., and Tallam, L. (2003). Obesity-associated hypertension and kidney disease. Curr Opin Nephrol Hypertens *12*, 195-200.

Halliday, H. L. (2004). Postnatal steroids and chronic lung disease in the newborn. Paediatr Respir Rev *5 Suppl A*, S245-248.

Hammami, M. M., and Siiteri, P. K. (1991). Regulation of 11®-hydroxysteroid dehydrogenase activity in human skin fibroblasts: enzymatic modulation of glucocorticoid action. J Clin Endocrinol Metab *73*, 326-334.

Hammer, F., and Stewart, P. M. (2006). Cortisol metabolism in hypertension. Best Pract Res Clin Endocrinol Metab *20*, 337-353.

Hammond, G. L. (1988). Molecular analyses of human corticosteroid-binding globulin. Expression and gene structure. Ann N Y Acad Sci *538*, 25-29.

Hanson, R. W., and Reshef, L. (1997). Regulation of phosphoenolpyruvate carboxykinase (GTP) gene expression. Annu Rev Biochem *66*, 581-611.

Harizi, H., Homo-Delarche, F., Amrani, A., Coulaud, J., and Mormede, P. (2007). Marked genetic differences in the regulation of blood glucose under immune and restraint stress in mice reveals a wide range of corticosensitivity. J Neuroimmunol *189*, 59-68.

Harris, H. J., Kotelevtsev, Y., Mullins, J. J., Seckl, J. R., and Holmes, M. C. (2001). Intracellular regeneration of glucocorticoids by 11β-hydroxysteroid dehydrogenase (11β-HSD)-1 plays a key role in regulation of the hypothalamic-pituitary-adrenal axis: analysis of 11β-HSD-1 deficient mice. Endocrinology *142*, 114-120.

Hautanena, A., Lankinen, L., Kupari, M., Janne, O. A., Adlercreutz, H., Nikkila, H., and White, P. C. (1998). Associations between aldosterone synthase gene polymorphism and the adrenocortical function in males. J Intern Med *244*, 11-18.

Hebbar, P. B., and Archer, T. K. (2003). Chromatin remodeling by nuclear receptors. Chromosoma *111*, 495-504.

Heo, H. J., Yun, M. R., Jung, K. H., Lee, J. Y., Park, J. Y., Lee, S. J., Bae, S. S., Lee, W. S., and Kim, C. D. (2007). Endogenous angiotensin II enhances atherogenesis in apoprotein E-deficient mice with renovascular hypertension through activation of vascular smooth muscle cells. Life Sci *80*, 1057-1063.

Herman, J. P., Patel, P. D., Akil, H., and Watson, S. J. (1989). Localization and regulation of glucocorticoid and mineralocorticoid receptor messenger RNAs in the hippocampal formation of the rat. Mol Endocrinol *3*, 1886-1894.

Herman, J. P., and Spencer, R. (1998). Regulation of hippocampal glucocorticoid receptor gene transcription and protein expression in vivo. J Neurosci *18*, 7462-7473.

Hochgeschwender, U., Costa, J. L., Reed, P., Bui, S., and Brennan, M. B. (2003). Altered glucose homeostasis in proopiomelanocortin-null mouse mutants lacking central and peripheral melanocortin. Endocrinology *144*, 5194-5202.

Hoeck, W., Rusconi, S., and Groner, B. (1989). Down-regulation and phosphorylation of glucocorticoid receptors in cultured cells. Investigations with a monospecific antiserum against a bacterially expressed receptor fragment. J Biol Chem *264*, 14396-14402.

Holland, W. L., Knotts, T. A., Chavez, J. A., Wang, L. P., Hoehn, K. L., and Summers, S. A. (2007). Lipid mediators of insulin resistance. Nutr Rev *65*, S39-46.

Hollenberg, S. M., and Evans, R. M. (1988). Multiple and cooperative *trans*-activation domains of the human glucocorticoid receptor. Cell *55*, 899-906.

Hollenberg, S. M., Giguere, V., Segui, P., and Evans, R. M. (1987). Colocalization of DNA-binding and transcriptional activation functions in the human glucocorticoid receptor. Cell *49*, 39-46.

Hollenberg, S. M., Weinberger, C., Ong, E. S., Cerelli, G., Oro, A., Lebo, R., Thompson, E. B., Rosenfeld, M. G., and Evans, R. M. (1985). Primary structure and expression of a functional human glucocorticoid receptor cDNA. Nature *318*, 635-641.

Holmes, M. C., Abrahamsen, C. T., French, K. L., Paterson, J. M., Mullins, J. J., and Seckl, J. R. (2006). The mother or the fetus? 11beta-hydroxysteroid dehydrogenase type 2 null mice provide evidence for direct fetal programming of behavior by endogenous glucocorticoids. J Neurosci *26*, 3840-3844.

Holmes, M. C., French, K. L., and Seckl, J. R. (1997). Dysregulation of diurnal rhythms of serotonin 5-HT2C and corticosteroid receptor gene expression in the hippocampus with food restriction and glucocorticoids. J Neurosci *17*, 4056-4065.

Holmes, M. C., Yau, J. L., French, K. L., and Seckl, J. R. (1995). The effect of adrenalectomy on 5-hydroxytryptamine and corticosteroid receptor subtype messenger RNA expression in rat hippocampus. Neuroscience *64*, 327-337.

Holmes, M. C., Yau, J. L., Kotelevtsev, Y., Mullins, J. J., and Seckl, J. R. (2003). 11 Beta-hydroxysteroid dehydrogenases in the brain: two enzymes two roles. Ann N Y Acad Sci *1007*, 357-366.

Holmes, M.C. and Seckl, J.R. (2006). The role of 11beta-hydroxysteroid dehydrogenases in the brain.Mol Cell Endocrinol *248*(1-2):9-14.

Homma, M., Tanaka, A., Hino, K., Takamura, H., Hirano, T., Oka, K., Kanazawa, M., Miwa, T., Notoya, Y., Niitsuma, T., and Hayashi, T. (2001). Assessing systemic 11beta-hydroxysteroid dehydrogenase with serum cortisone/cortisol ratios in healthy subjects and patients with diabetes mellitus and chronic renal failure. Metabolism *50*, 801-804.

Honda, M., Nowaczynski, W., Guthrie, G. P., Jr., Messerli, F. H., Tolis, G., Kuchel, O., and Genest, J. (1977). Response of several adrenal steroids to ACTH stimulation in essential hypertension. J Clin Endocrinol Metab *44*, 264-272.

Hong, H., Kohli, K., Trivedi, A., Johnson, D. L., and Stallcup, M. R. (1996). GRIP1, a novel mouse protein that serves as a transcriptional coactivator in yeast for the hormone binding domains of steroid receptors. Proceedings of the National Academy of Sciences of the United States of America *93*, 4948-4952.

Horner, H. C., Munck, A., and Lienhard, G. E. (1987). Dexamethasone causes translocation of glucose transporters from the plasma membrane to an intracellular site in human fibroblasts. J Biol Chem *262*, 17696-17702.

Howell, M. P., and Muglia, L. J. (2006). Effects of genetically altered brain glucocorticoid receptor action on behavior and adrenal axis regulation in mice. Front Neuroendocrinol *27*, 275-284.

Htun, H., Barsony, J., Renyi, I., Gould, D. L., and Hager, G. L. (1996). Visualization of glucocorticoid receptor translocation and intranuclear organization in living cells with a green fluorescent protein chimera. Proc Natl Acad Sci USA *93*, 4845-4850.

Huizenga, N. A., Koper, J. W., de Lange, P., Pols, H. A., Stolk, R. P., Grobbee, D. E., de Jong, F. H., and Lamberts, S. W. (1998). Interperson variability but

intraperson stability of baseline plasma cortisol concentrations, and its relation to feedback sensitivity of the hypothalamo-pituitary-adrenal axis to a low dose of dexamethasone in elderly individuals. J Clin Endocrinol Metab *83*, 47-54.

Hundertmark, S., Buhler, H., Ragosch, V., Dinkelborg, L., Arabin, B., and Weitzel, H. K. (1995). Correlation of surfactant phosphatidylcholine synthesis and 11 beta-hydroxysteroid dehydrogenase in the fetal lung. Endocrinology *136*, 2573-2578.

Hurley, D. M., Accili, D., Stratakis, C. A., Karl, M., Vamvakopoulos, N., Rorer, E., Constantine, K., Taylor, S. I., and Chrousos, G. P. (1991). Point mutation causing a single amino acid substitution in the hormone binding domain of the glucocorticoid receptor in familial glucocorticoid resistance. J Clin Invest *87*, 680-686.

Hutchison, K. A., Dittmar, K. D., and Pratt, W. B. (1994). All of the factors required for assembly of the glucocorticoid receptor into a functional heterocomplex with heat shock protein 90 are preassociated in a self-sufficient protein folding structure, a "foldosome". J Biol Chem *269*, 27894-27899.

Hutchison, K. A., Scherrer, L. C., Czar, M. J., Stancato, L. F., Chow, Y. H., Jove, R., and Pratt, W. B. (1993). Regulation of glucocorticoid receptor function through assembly of a receptor-heat shock protein complex. Ann N Y Acad Sci *684*, 35-48.

Iida, S., Nakamura, Y., Fujii, H., Nishimura, J., Tsugawa, M., Gomi, M., Fukata, J., Tarui, S., Moriwaki, K., and Kitani, T. (1990). A patient with hypocortisolism and Cushing's syndrome-like manifestations: cortisol hyperreactive syndrome. J Clin Endocrinol Metab *70*, 729-737.

Jamieson, P. M., Chapman, K. E., Edwards, C. R. W., and Seckl, J. R. (1995). 11®-hydroxysteroid dehydrogenase is an exclusive 11®-reductase in primary cultures of rat hepatocytes: effect of physicochemical and hormonal manipulations. Endocrinology *136*, 4754-4761.

Jamieson, P. M., Chapman, K. E., and Seckl, J. R. (1999). Tissue- and temporal-specific regulation of 11®-hydroxysteroid dehydrogenase type 1 by glucocorticoids in vivo. J Steroid Biochem Mol Biol *68*, 245-250.

Jamieson, P. M., Walker, B. R., Chapman, K. E., Andrew, R., Rossiter, S., and Seckl, J. R. (2000). 11 beta-hydroxysteroid dehydrogenase type 1 is a predominant 11 beta-reductase in the intact perfused rat liver. J Endocrinol *165*, 685-692.

Jensen, M. D., Kanaley, J. A., Reed, J. E., and Sheedy, P. F. (1995). Measurement of abdominal and visceral fat with computed tomography and dual-energy x-ray absorptiometry. Am J Clin Nutr *61*, 274-278.

Jensen, M. D., Kanaley, J. A., Roust, L. R., O'Brien, P. C., Braun, J. S., Dunn, W. L., and Wahner, H. W. (1993). Assessment of body composition with use of dual-energy x-ray absorptiometry: evaluation and comparison with other methods. Mayo Clin Proc *68*, 867-873.

Jensen, M. D., Sarr, M. G., Dumesic, D. A., Southorn, P. A., and Levine, J. A. (2003). Regional uptake of meal fatty acids in humans. Am J Physiol Endocrinol Metab *285*, E1282-1288.

Jewell, C. M., and Cidlowski, J. A. (2007). Molecular evidence for a link between the N363S glucocorticoid receptor polymorphism and altered gene expression. J Clin Endocrinol Metab *92*, 3268-3277.

Jimenez-Garcia, L. F., and Spector, D. L. (1993). In vivo evidence that transcription and splicing are coordinated by a recruiting mechanism. Cell *73*, 47-59.

Jones, M. T., and Gillham, B. (1988). Factors involved in the regulation of adrenocorticotropic hormone/beta-lipotropic hormone. Physiol Rev *68*, 743-818.

Kalinyak, J. E., Dorin, R. I., Hoffman, A. R., and Perlman, A. J. (1987). Tissue-specific regulation of glucocorticoid receptor mRNA by dexamethasone. J Biol Chem *262*, 10441-10444.

Kang, J. S., Pilkington, J. D., Ferguson, D., Kim, H. K., and Romsos, D. R. (1992). Dietary glucose and fat attenuate effects of adrenalectomy on energy balance in ob/ob mice. J Nutr *122*, 895-905.

Kannisto, K., Pietilainen, K. H., Ehrenborg, E., Rissanen, A., Kaprio, J., Hamsten, A., and Yki-Jarvinen, H. (2004). Overexpression of 11beta-hydroxysteroid dehydrogenase-1 in adipose tissue is associated with acquired obesity and features of insulin resistance: studies in young adult monozygotic twins. J Clin Endocrinol Metab *89*, 4414-4421.

Kaul, S., Murphy, P. J., Chen, J., Brown, L., Pratt, W. B., and Simons, S. S., Jr. (2002). Mutations at positions 547-553 of rat glucocorticoid receptors reveal that hsp90 binding requires the presence, but not defined composition, of a seven-amino acid sequence at the amino terminus of the ligand binding domain. J Biol Chem *277*, 36223-36232.

Kellendonk, C., Eiden, S., Kretz, O., Schutz, G., Schmidt, I., Tronche, F., and Simon, E. (2002). Inactivation of the GR in the nervous system affects energy accumulation. Endocrinology *143*, 2333-2340.

Kellendonk, C., Opherk, C., Anlag, K., Schutz, G., and Tronche, F. (2000). Hepatocyte-specific expression of Cre recombinase. Genesis *26*, 151-153.

Keller-Wood, M. E., and Dallman, M. F. (1984). Corticosteroid inhibition of ACTH secretion. Endocr Rev *5*, 1-24.

Kelly, J. J., Mangos, G., Williamson, P. M., and Whitworth, J. A. (1998). Cortisol and hypertension. Clin Exp Pharmacol Physiol Suppl *25*, S51-56.

Kelly, J. J., Martin, A., and Whitworth, J. A. (2000). Role of erythropoietin in cortisol-induced hypertension. J Hum Hypertens *14*, 195-198.

Kennelly, P. J., and Krebs, E. G. (1991). Consensus Sequences As Substrate-Specificity Determinants For Protein-Kinases and Protein Phosphatases. Journal of Biological Chemistry *266*, 15555-15558.

Kim, J. J., and Haller, J. (2007). Glucocorticoid hyper- and hypofunction: stress effects on cognition and aggression. Ann N Y Acad Sci *1113*, 291-303.

Kirk, C. J., Verrinder, T. R., and Hems, D. A. (1976). Fatty acid synthesis in the perfused liver of adrenalectomized rats. Biochem J *156*, 593-602.

Klausner, H., and Heimberg, M. (1967). Effect of adrenalcortical hormones on release of triglycerides and glucose by liver. Am J Physiol *212*, 1236-1246.

Koeijvoets, K. C., van Rossum, E. F., Dallinga-Thie, G. M., Steyerberg, E. W., Defesche, J. C., Kastelein, J. J., Lamberts, S. W., and Sijbrands, E. J. (2006). A functional polymorphism in the glucocorticoid receptor gene and its relation to cardiovascular disease risk in familial hypercholesterolemia. J Clin Endocrinol Metab *91*, 4131-4136.

Koper, J. W., Stolk, R. P., de Lange, P., Huizenga, N. A., Molijn, G. J., Pols, H. A., Grobbee, D. E., Karl, M., de Jong, F. H., Brinkmann, A. O., and Lamberts, S. W. (1997). Lack of association between five polymorphisms in the human glucocorticoid receptor gene and glucocorticoid resistance. Hum Genet *99*, 663-668.

Kotelevtsev, Y., Holmes, M. C., Burchell, A., Houston, P. M., Schmoll, D., Jamieson, P., Best, R., Brown, R., Edwards, C. R. W., Seckl, J. R., and Mullins, J. J. (1997). 11β-hydroxysteroid dehydrogenase type 1 knockout mice show attenuated glucocorticoid inducible responses and resist hyperglycaemia on obesity or stress. Proc Natl Acad Sci USA *94*, 14924-14929.

Krozowski, Z., Albiston, A. L., Obeyesekere, V. R., Andrews, R. K., and Smith, R. E. (1995a). The human 11 beta-hydroxysteroid dehydrogenase type II enzyme: comparisons with other species and localization to the distal nephron. J Steroid Biochem Mol Biol *55*, 457-464.

Krozowski, Z., Baker, E., Obeyesekere, V., and Callen, D. F. (1995b). Localization of the gene for human 11 beta-hydroxysteroid dehydrogenase type 2 (HSD11B2) to chromosome band 16q22. Cytogenet Cell Genet *71*, 124-125.

Krozowski, Z., MaGuire, J. A., Stein-Oakley, A. N., Dowling, J., Smith, R. E., and Andrews, R. K. (1995c). Immunohistochemical localization of the 11 beta-hydroxysteroid dehydrogenase type II enzyme in human kidney and placenta. J Clin Endocrinol Metab *80*, 2203-2209.

Krude, H., Biebermann, H., Luck, W., Horn, R., Brabant, G., and Gruters, A. (1998). Severe early-onset obesity, adrenal insufficiency and red hair pigmentation caused by POMC mutations in humans. Nat Genet *19*, 155-157.

Kuk, J. L., Katzmarzyk, P. T., Nichaman, M. Z., Church, T. S., Blair, S. N., and Ross, R. (2006). Visceral fat is an independent predictor of all-cause mortality in men. Obesity (Silver Spring) *14*, 336-341.

Kurihara, I., Shibata, H., Suzuki, T., Ando, T., Kobayashi, S., Hayashi, M., Saito, I., and Saruta, T. (2000). Transcriptional regulation of steroid receptor coactivator-1 (SRC-1) in glucocorticoid action. Endocr Res *26*, 1033-1038.

Lam, D. D., Farooqi, I. S., and Heisler, L. K. (2007). Melanocortin receptors as targets in the treatment of obesity. Curr Top Med Chem *7*, 1085-1097.

Langley-Evans, S. C. (2001). Fetal programming of cardiovascular function through exposure to maternal undernutrition. Proc Nutr Soc *60*, 505-513.

Laplante, M., Sell, H., MacNaul, K. L., Richard, D., Berger, J. P., and Deshaies, Y. (2003). PPAR-gamma activation mediates adipose depot-specific effects on gene

expression and lipoprotein lipase activity: mechanisms for modulation of postprandial lipemia and differential adipose accretion. Diabetes *52*, 291-299.

Laurent, V., Kimble, A., Peng, B., Zhu, P., Pintar, J. E., Steiner, D. F., and Lindberg, I. (2002). Mortality in 7B2 null mice can be rescued by adrenalectomy: involvement of dopamine in ACTH hypersecretion. Proc Natl Acad Sci U S A *99*, 3087-3092.

Lawson, N., Jennings, R. J., Pollard, A. D., Sturton, R. G., Ralph, S. J., Marsden, C. A., Fears, R., and Brindley, D. N. (1981). Effects of chronic modification of dietary fat and carbohydrate in rats. Biochem J *200*, 265-273.

Lee, M., and Wardlaw, S. L. (2007). The central melanocortin system and the regulation of energy balance. Front Biosci *12*, 3994-4010.

Lefebvre, P., Barard, D. S., Cordingley, M. G., and Hager, G. L. (1991). Two regions of the mouse mammary tumor virus long terminal repeat regulate the activity of its promoter in mammary cell lines. Mol Cell Biol *11*, 2529-2537.

Lefstin, J. A., Thomas, J. R., and Yamamoto, K. R. (1994). Influence of a Steroid-Receptor Dna-Binding Domain On Transcriptional Regulatory Functions. Genes & Development *8*, 2842-2856.

Leppaluoto, J., Laisi, U., Lybeck, H., Partanen, J., Ranta, T., and Virkkunen (1975). Pulsatile secretion of ACTH, GH, LH and TSH in man. Acta Physiol Scand *95*, 470-476.

Leung, K., and Munck, A. (1975). Peripheral actions of glucocorticoids. Annu Rev Physiol *37*, 245-272.

Levitt, N. S., Lindsay, R. S., Holmes, M. C., and Seckl, J. R. (1996). Dexamethasone in the last week of pregnancy attenuates hippocampal glucocorticoid receptor gene expression and elevates blood pressure in the adult offspring in the rat. Neuroendocrinology *64*, 412-418.

Lin, R. C., Wang, W. Y., and Morris, B. J. (1999). High penetrance, overweight, and glucocorticoid receptor variant: case-control study. Bmj *319*, 1337-1338.

Lin, R. C., Wang, X. L., and Morris, B. J. (2003). Association of coronary artery disease with glucocorticoid receptor N363S variant. Hypertension *41*, 404-407.

Lind, U., Greenidge, P., Gillner, M., Koehler, K. F., Wright, A., and Carlstedt-Duke, J. (2000). Functional probing of the human glucocorticoid receptor steroid-interacting surface by site-directed mutagenesis. Gln-642 plays an important role in steroid recognition and binding. J Biol Chem *275*, 19041-19049.

Lindqvist, A., Mohapel, P., Bouter, B., Frielingsdorf, H., Pizzo, D., Brundin, P., and Erlanson-Albertsson, C. (2006). High-fat diet impairs hippocampal neurogenesis in male rats. Eur J Neurol *13*, 1385-1388.

Lindsay, R. S., Wake, D. J., Nair, S., Bunt, J., Livingstone, D. E., Permana, P. A., Tataranni, P. A., and Walker, B. R. (2003). Subcutaneous adipose 11 beta-hydroxysteroid dehydrogenase type 1 activity and messenger ribonucleic acid levels are associated with adiposity and insulinemia in Pima Indians and Caucasians. J Clin Endocrinol Metab *88*, 2738-2744.

Livingstone, D. E. W., Jones, G. C., Smith, K., Jamieson, P. M., Andrew, R., Kenyon, C. J., and Walker, B. R. (2000). Understanding the role of glucocorticoids in obesity: Tissue-specific alterations of corticosterone metabolism in obese Zucker rats. Endocrinology *141*, 560-563.

Lopez, F. J., and Negro-Vilar, A. (1988). Estimation of endogenous adrenocorticotropin half-life using pulsatility patterns: a physiological approach to the evaluation of secretory episodes. Endocrinology *123*, 740-746.

Low, S. C., Chapman, K. E., Edwards, C. R. W., and Seckl, J. R. (1994). 'Liver-type' 11β-hydroxysteroid dehydrogenase cDNA encodes reductase not dehydrogenase activity in intact mammalian COS-7 cells. J Mol Endocrinol *13*, 167-174.

Lu, H., Boustany-Kari, C. M., Daugherty, A., and Cassis, L. A. (2007). Angiotensin II increases adipose angiotensinogen expression. Am J Physiol Endocrinol Metab *292*, E1280-1287.

Luisi, B. F., Xu, W. X., Otwinowski, Z., Freedman, L. P., Yamamoto, K. R., and Sigler, P. B. (1991). Crystallographic Analysis of the Interaction of the Glucocorticoid Receptor With Dna. Nature *352*, 497-505.

Lukola, A., Akerman, K., and Pessa, T. (1985). Human lymphocyte glucocorticoid receptors reside mainly in the cytoplasm. Biochem Biophys Res Commun *131*, 877-882.

Luu-The, V., Paquet, N., Calvo, E., and Cumps, J. (2005). Improved real-time RT-PCR method for high-throughput measurements using second derivative calculation and double correction. Biotechniques *38*, 287-293.

Madan, A. P., and DeFranco, D. B. (1993). Bidirectional transport of glucocorticoid receptors across the nuclear envelope. Proc Natl Acad Sci U S A *90*, 3588-3592.

Magiakou, M. A., Smyrnaki, P., and Chrousos, G. P. (2006). Hypertension in Cushing's syndrome. Best Pract Res Clin Endocrinol Metab *20*, 467-482.

Makimura, H., Mizuno, T. M., Roberts, J., Silverstein, J., Beasley, J., and Mobbs, C. V. (2000). Adrenalectomy reverses obese phenotype and restores hypothalamic melanocortin tone in leptin-deficient ob/ob mice. Diabetes *49*, 1917-1923.

Mantha, L., and Deshaies, Y. (2000). Energy intake-independent modulation of triglyceride metabolism by glucocorticoids in the rat. Am J Physiol Regul Integr Comp Physiol *278*, R1424-1432.

Mantha, L., Palacios, E., and Deshaies, Y. (1999). Modulation of triglyceride metabolism by glucocorticoids in diet-induced obesity. Am J Physiol *277*, R455-464.

Marin, P., Darin, N., Amemiya, T., Andersson, B., Jern, S., and Bjorntorp, P. (1992). Cortisol secretion in relation to body fat distribution in obese premenopausal women. Metabolism *41*, 882-886.

Martens, P. R., Calle, P., Van den Poel, B., and Lewi, P. (1995). Further prospective evidence of a circadian variation in the frequency of call for sudden cardiac death. Belgian Cardiopulmonary Cerebral Resuscitation Study Group. Intensive Care Med *21*, 45-49.

Marti, A., Ochoa, M. C., Sanchez-Villegas, A., Martinez, J. A., Martinez-Gonzalez, M. A., Hebebrand, J., Hinney, A., and Vedder, H. (2006). Meta-analysis on the effect of the N363S polymorphism of the glucocorticoid receptor gene (GRL) on human obesity. BMC Med Genet *7*, 50.

Martins, V. R., Pratt, W. B., Terracio, L., Hirst, M. A., Ringold, G. M., and Housley, P. R. (1991). Demonstration By Confocal Microscopy That Unliganded Overexpressed Glucocorticoid Receptors Are Distributed in a Nonrandom Manner Throughout All Planes of the Nucleus. Molecular Endocrinology *5*, 217-225.

Mason, S. A., and Housley, P. R. (1993). Site-Directed Mutagenesis of the Phosphorylation Sites in the Mouse Glucocorticoid Receptor. Journal of Biological Chemistry *268*, 21501-21504.

Massiéra, F., Bloch-Faure, M., Ceiler, D., Murakami, K., Fukamizu, A., Gasc, J.-M., Quignard-Boulangé, A., Negrel, R., Ailhaud, G., Seydoux, J.*, et al.* (2001). Adipose angiotensinogen is involved in adipose tissue growth and blood pressure regulation. FASEB J *15*, 2727-2729.

Masuzaki, H., Paterson, J., Shinyama, H., Morton, N. M., Mullins, J. J., Seckl, J. R., and Flier, J. S. (2001). A transgenic model of visceral obesity and the metabolic syndrome. Science *294*, 2166-2170.

Masuzaki, H., Yamamoto, H., Kenyon, C. J., Elmquist, J. K., Morton, N. M., Paterson, J. M., Shinyama, H., Sharp, M. G., Fleming, S., Mullins, J. J.*, et al.* (2003). Transgenic amplification of glucocorticoid action in adipose tissue causes high blood pressure in mice. J Clin Invest *112*, 83-90.

Matthews, D. R., Hosker, J. P., Rudenski, A. S., Naylor, B. A., Treacher, D. F., and Turner, R. C. (1985). Homeostasis model assessment: insulin resistance and beta-cell function from fasting plasma glucose and insulin concentrations in man. Diabetologia *28*, 412-419.

Mattsson, C., and Olsson, T. (2007). Estrogens and glucocorticoid hormones in adipose tissue metabolism. Curr Med Chem *14*, 2918-2924.

Maul, G. G., Negorev, D., Bell, P., and Ishov, A. M. (2000). Review: properties and assembly mechanisms of ND10, PML bodies, or PODs. J Struct Biol *129*, 278-287.

McEwan, I. J., Wright, A. P. H., and Gustafsson, J. A. (1997). Mechanism of gene expression by the glucocorticoid receptor: Role of protein-protein interactions. Bioessays *19*, 153-160.

McEwen, B. S. (1999). Stress and the aging hippocampus. Frontiers in Neuroendocrinology *20*, 49-70.

McEwen, B. S. (2005). Glucocorticoids, depression, and mood disorders: structural remodeling in the brain. Metabolism *54*, 20-23.

McEwen, B. S., Biron, C. A., Brunson, K. W., Bulloch, K., Chambers, W. H., Dhabhar, F. S., Goldfarb, R. H., Kitson, R. P., Miller, A. H., Spencer, R. L., and Weiss, J. M. (1997). The role of adrenocorticoids as modulators of immune function in health and disease: neural, endocrine and immune interactions. Brain Res Rev *23*, 79-133.

McIntyre, W. R., and Samuels, H. H. (1985). Triamcinolone acetonide regulates glucocorticoid-receptor levels by decreasing the half-life of the activated nuclear-receptor form. J Biol Chem *260*, 418-427.

Meaney, M. J., Aitken, D. H., van Berkel, C., Bhatnagar, S., and Sapolsky, R. M. (1988). Effect of neonatal handling on age-related impairments associated with the hippocampus. Science *239*, 766-768.

Meaney, M. J., Diorio, J., Francis, D., Weaver, S., Yau, J., Chapman, K., and Seckl, J. R. (2000). Postnatal handling increases the expression of cAMP-inducible transcription factors in the rat hippocampus: the effects of thyroid hormones and serotonin. J Neurosci *20*, 3926-3935.

Meyre, D., Lecoeur, C., Delplanque, J., Francke, S., Vatin, V., Durand, E., Weill, J., Dina, C., and Froguel, P. (2004). A genome-wide scan for childhood obesity-associated traits in French families shows significant linkage on chromosome 6q22.31-q23.2. Diabetes *53*, 803-811.

Meyuhas, O., Reshef, L., Gunn, J. M., Hanson, R. W., and Ballard, F. J. (1976). Regulation of phosphoenolpyruvate carboxykinase (GTP) in adipose tissue in vivo by glucocorticoids and insulin. Biochem J *158*, 1-7.

Michailidou, Z., Coll, A. P., Kenyon, C. J., Morton, N. M., O'Rahilly, S., Seckl, J. R., and Chapman, K. E. (2007). Peripheral mechanisms contributing to the glucocorticoid hypersensitivity in proopiomelanocortin null mice treated with corticosterone. J Endocrinol *194*, 161-170.

Miesfeld, R., Okret, S., Wikstrom, A. C., Wrange, O., Gustafsson, J. A., and Yamamoto, K. R. (1984). Characterization of a steroid hormone receptor gene and mRNA in wild-type and mutant cells. Nature *312*, 779-781.

Miller, A. H., Spencer, R. L., Stein, M., and McEwen, B. S. (1990). Adrenal steroid receptor binding in spleen and thymus after stress or dexamethasone. Am J Physiol *259*, E405-412.

Morton, N. M., Densmore, V., Wamil, M., Ramage, L., Nichol, K., Bunger, L., Seckl, J. R., and Kenyon, C. J. (2005). A Polygenic Model of the Metabolic Syndrome With Reduced Circulating and Intra-Adipose Glucocorticoid Action. Diabetes *54*, 3371-3378.

Morton, N. M., Holmes, M. C., Fiévet, C., Staels, B., Tailleux, A., Mullins, J. J., and Seckl, J. R. (2001). Improved lipid and lipoprotein profile, hepatic insulin sensitivity, and glucose tolerance in 11®-hydroxysteroid dehydrogenase type 1 null mice. J Biol Chem *276*, 41293-41300.

Morton, N. M., Paterson, J. M., Masuzaki, H., Holmes, M. C., Staels, B., Fievet, C., Walker, B. R., Flier, J. S., Mullins, J. J., and Seckl, J. R. (2004a). Novel adipose tissue-mediated resistance to diet-induced visceral obesity in 11®-hydroxysteroid dehydrogenase type 1-deficient mice. Diabetes *53*, 931-938.

Morton, N. M., Ramage, L., and Seckl, J. R. (2004b). Down-regulation of adipose 11®-hydroxysteroid dehydrogenase type 1 by high-fat feeding in mice: a potential

adaptive mechanism counteracting metabolic disease. Endocrinology *145*, 2707-2712.

Muglia, L., Jacobson, L., Dikkes, P., and Majzoub, J. A. (1995). Corticotropin-Releasing Hormone Deficiency Reveals Major Fetal But Not Adult Glucocorticoid Need. Nature *373*, 427-432.

Murray, J. C., Smith, R. F., Ardinger, H. A., and Weinberger, C. (1987). RFLP for the glucocorticoid receptor (GRL) located at 5q11-5q13. Nucleic Acids Res *15*, 6765.

Napolitano, A., Voice, M. W., Edwards, C. R. W., Seckl, J. R., and Chapman, K. E. (1998). 11®-hydroxysteroid dehydrogenase 1 in adipocytes: expression is differentiation-dependent and hormonally regulated. J Steroid Biochem Molec Biol *64*, 251-260.

Nechushtan, H., Benvenisty, N., Brandeis, R., and Reshef, L. (1987). Glucocorticoids control phosphoenolpyruvate carboxykinase gene expression in a tissue specific manner. Nuc Acids Res *15*, 6405-6417.

Neigh, G. N., and Nemeroff, C. B. (2006). Reduced glucocorticoid receptors: consequence or cause of depression? Trends Endocrinol Metab *17*, 124-125.

Newfield, R. S., Kalaitzoglou, G., Licholai, T., Chilton, D., Ashraf, J., Thompson, E. B., and New, M. I. (2000). Normocortisolemic Cushing's syndrome initially presenting with increased glucocorticoid receptor numbers. J Clin Endocrinol Metab *85*, 14-21.

Newton, R., and Holden, N. S. (2007). Separating transrepression and transactivation: a distressing divorce for the glucocorticoid receptor? Mol Pharmacol *72*, 799-809.

Ni, X. P., Pearce, D., Butler, A. A., Cone, R. D., and Humphreys, M. H. (2003). Genetic disruption of ©-melanocyte-stimulating hormone signaling leads to salt-sensitive hypertension in the mouse. J Clin Invest *111*, 1251-1258.

Nieman, L. K., Chrousos, G. P., Kellner, C., Spitz, I. M., Nisula, B. C., Cutler, G. B., Merriam, G. R., Bardin, C. W., and Loriaux, D. L. (1985). Successful treatment of Cushing's syndrome with the glucocorticoid antagonist RU 486. J Clin Endocrinol Metab *61*, 536-540.

Nishi, M., and Kawata, M. (2007). Dynamics of glucocorticoid receptor and mineralocorticoid receptor: implications from live cell imaging studies. Neuroendocrinology *85*, 186-192.

Nobukuni, Y., Smith, C. L., Hager, G. L., and Detera-Wadleigh, S. D. (1995). Characterization of the human glucocorticoid receptor promoter. Biochemistry *34*, 8207-8214.

Normington, K., and Russell, D. W. (1992). Tissue distribution and kinetic characteristics of rat steroid 5 alpha-reductase isozymes. Evidence for distinct physiological functions. J Biol Chem *267*, 19548-19554.

Nyirenda, M. J., Lindsay, R. S., Kenyon, C. J., Burchell, A., and Seckl, J. R. (1998). Glucocorticoid exposure in late gestation permanently programs rat hepatic phosphoenolpyruvate carboxykinase and glucocorticoid receptor expression and causes glucose intolerance in adult offspring. J Clin Invest *101*, 2174-2181.

Oakley, R. H., Jewell, C. M., Yudt, M. R., Bofetiado, D. M., and Cidlowski, J. A. (1999). The dominant negative activity of the human glucocorticoid receptor beta isoform - Specificity and mechanisms of action. Journal of Biological Chemistry *274*, 27857-27866.

Oakley, R. H., Sar, M., and Cidlowski, J. A. (1996). The human glucocorticoid receptor beta isoform. Expression, biochemical properties, and putative function. J Biol Chem *271*, 9550-9559.

Oakley, R. H., Webster, J. C., Sar, M., Parker, R., and Cidlowski, J. A. (1997). Expression and subcellular distribution of the beta-isoform of the human glucocorticoid receptor. Endocrinology *138*, 5028-5038.

Odermatt, A., Atanasov, A. G., Balazs, Z., Schweizer, R. A., Nashev, L. G., Schuster, D., and Langer, T. (2006). Why is 11beta-hydroxysteroid dehydrogenase type 1 facing the endoplasmic reticulum lumen? Physiological relevance of the membrane topology of 11beta-HSD1. Mol Cell Endocrinol *248*, 15-23.

Okret, S., Poellinger, L., Dong, Y., and Gustafsson, J. A. (1986). Down-Regulation of Glucocorticoid Receptor Messenger-Rna By Glucocorticoid Hormones and Recognition By the Receptor of a Specific Binding Sequence Within a Receptor Cdna Clone. Proceedings of the National Academy of Sciences of the United States of America *83*, 5899-5903.

Olswang, Y., Blum, B., Cassuto, H., Cohen, H., Biberman, Y., Hanson, R. W., and Reshef, L. (2003). Glucocorticoids repress transcription of phosphoenolpyruvate carboxykinase (GTP) gene in adipocytes by inhibiting its C/EBP-mediated activation. J Biol Chem *278*, 12929-12936.

Onate, S. A., Tsai, S. Y., Tsai, M. J., and O'Malley, B. W. (1995). Sequence and characterization of a coactivator for the steroid hormone receptor superfamily. Science *270*, 1354-1357.

Ong, J. M., Kirchgessner, T. G., Schotz, M. C., and Kern, P. A. (1988). Insulin increases the synthetic rate and messenger RNA level of lipoprotein lipase in isolated rat adipocytes. J Biol Chem *263*, 12933-12938.

Oomura, Y., Ono, T., and Sugimori, M. (1976). Acetylcholine, an inhibitory transmitter in the rat lateral hypothalamus. Brain Res Bull *1*, 151-153.

Opherk, C., Tronche, F., Kellendonk, C., Kohlmuller, D., Schulze, A., Schmid, W., and Schutz, G. (2004). Inactivation of the glucocorticoid receptor in hepatocytes leads to fasting hypoglycemia and ameliorates hyperglycemia in streptozotocin-induced diabetes mellitus. Mol Endocrinol *18*, 1346-1353.

Orth, D. (1992). The adrenal cortex, Vol 8th edition by Wilson JD and Foster DW).

Orti, E., Bodwell, J. E., and Munck, A. (1992). Phosphorylation of steroid hormone receptors. Endocrine Rev *13*, 105-128.

Ortiz, L. A., Quan, A., Weinberg, A., and Baum, M. (2001). Effect of prenatal dexamethasone on rat renal development. Kidney Int *59*, 1663-1669.

Ortlepp, J. R., Kluge, R., Giesen, K., Plum, L., Radke, P., Hanrath, P., and Joost, H. G. (2000). A metabolic syndrome of hypertension, hyperinsulinaemia and hypercholesterolaemia in the New Zealand obese mouse. Eur J Clin Invest *30*, 195-202.

Ostman, I., and Nyback, H. (1976). Adaptive changes in central and peripheral noradrenergic neurons in rats following chronic exercise. Neuroscience *1*, 41-47.

Ottosson, U. B., Carlstrom, K., Damber, J. E., and von Schoultz, B. (1984). Conversion of oral progesterone into deoxycorticosterone during postmenopausal replacement therapy. Acta Obstet Gynecol Scand *63*, 577-579.

Pardridge, W. M. (1987). Plasma protein-mediated transport of steroid and thyroid hormones. Am J Physiol *252*, E157-164.

Paterson, J. M., Morton, N. M., Fiévet, C., Kenyon, C. J., Holmes, M. C., Staels, B., Seckl, J. R., and Mullins, J. J. (2004). Metabolic syndrome without obesity: Hepatic overexpression of 11β-hydroxysteroid dehydrogenase type 1 in transgenic mice. Proc Natl Acad Sci USA *101*, 7088-7093.

Paulmyer-Lacroix, O., Boullu, S., Oliver, C., Alessi, M. C., and Grino, M. (2002). Expression of the mRNA coding for 11ß-hydroxysteroid dehydrogenase type 1 in adipose tissue from obese patients: an *in situ* hybridization study. J Clin Endocrinol Metab *87*, 2701-2705.

Pedersen, K. B., Geng, C. D., and Vedeckis, W. V. (2004). Three mechanisms are involved in glucocorticoid receptor autoregulation in a human T-lymphoblast cell line. Biochemistry *43*, 10851-10858.

Penefsky, Z. J., and Kahn, M. (1971). Inotropic effects of dexamethasone in mammalian heart muscle. Eur J Pharmacol *15*, 259-266.

Pepin, M.-C., Pothier, F., and Barden, N. (1992). Impaired type II glucocorticoid receptor function in mice bearing antisense RNA transgene. Nature *355*, 725-728.

Petersen, H. H., Andreassen, T. K., Breiderhoff, T., Brasen, J. H., Schulz, H., Gross, V., Grone, H. J., Nykjaer, A., and Willnow, T. E. (2006). Hyporesponsiveness to glucocorticoids in mice genetically deficient for the corticosteroid binding globulin. Mol Cell Biol *26*, 7236-7245.

Pfahl, M., Kelleher, R. J., Jr., and Bourgeois, S. (1978). General features of steroid resistance on lymphoid cell lines. Mol Cell Endocrinol *10*, 193-207.

Pfeffer, J. M., Pfeffer, M. A., and Frohlich, E. D. (1971). Validity of an indirect tail-cuff method for determining systolic arterial pressure in unanesthetized normotensive and spontaneously hypertensive rats. J Lab Clin Med *78*, 957-962.

Picard, D., and Yamamoto, K. R. (1987). Two signals mediate hormone-dependent nuclear localization of the glucocorticoid receptor. EMBO J *6*, 3333-3340.

Piemonti, L., Monti, P., Allavena, P., Sironi, M., Soldini, L., Leone, B. E., Socci, C., and Di Carlo, V. (1999). Glucocorticoids affect human dendritic cell differentiation and maturation. J Immunol *162*, 6473-6481.

Pilkis, S. J., and Granner, D. K. (1992). Molecular Physiology of the Regulation of Hepatic Gluconeogenesis and Glycolysis. Annual Review of Physiology *54*, 885-909.

Powell, D. J., Hajduch, E., Kular, G., and Hundal, H. S. (2003). Ceramide disables 3-phosphoinositide binding to the pleckstrin homology domain of protein kinase B (PKB)/Akt by a PKCzeta-dependent mechanism. Mol Cell Biol *23*, 7794-7808.

Pratt, W. B. (1993). The Role of Heat-Shock Proteins in Regulating the Function, Folding, and Trafficking of the Glucocorticoid Receptor. Journal of Biological Chemistry *268*, 21455-21458.

Pratt, W. B. (1998). The hsp90-based chaperone system: involvement in signal transduction from a variety of hormone and growth factor receptors. Proc Soc Exp Biol Med *217*, 420-434.

Pratt, W. B., and Toft, D. O. (1997). Steroid receptor interactions with heat shock protein and immunophilin chaperones. Endocr Rev *18*, 306-360.

Purton, J. F., Boyd, R. L., Cole, T. J., and Godfrey, D. I. (2000). Intrathymic T cell development and selection proceeds normally in the absence of glucocorticoid receptor signaling. Immunity *13*, 179-186.

Rahmouni, K., Morgan, D. A., Morgan, G. M., Mark, A. L., and Haynes, W. G. (2005). Role of selective leptin resistance in diet-induced obesity hypertension. Diabetes *54*, 2012-2018.

Rajan, V., Chapman, K. E., Lyons, V., Jamieson, P., Mullins, J. J., Edwards, C. R., and Seckl, J. R. (1995). Cloning, sequencing and tissue-distribution of mouse 11 beta-hydroxysteroid dehydrogenase-1 cDNA. J Steroid Biochem Mol Biol *52*, 141-147.

Ramirez, F., Fowell, D. J., Puklavec, M., Simmonds, S., and Mason, D. (1996). Glucocorticoids promote a TH2 cytokine response by CD4+ T cells in vitro. J Immunol *156*, 2406-2412.

Rascher, W., Dietz, R., Schomig, A., Burkart, G., Luth, J. B., Mann, J. F., and Weber, J. (1979). Modulation of sympathetic vascular tone by prostaglandins in corticosterone-induced hypertension in rats. Clin Sci (Lond) *57 Suppl 5*, 235s-237s.

Rask, E., Walker, B. R., Soderberg, S., Livingstone, D. E., Eliasson, M., Johnson, O., Andrew, R., and Olsson, T. (2002). Tissue-specific changes in peripheral cortisol metabolism in obese women: increased adipose 11beta-hydroxysteroid dehydrogenase type 1 activity. J Clin Endocrinol Metab *87*, 3330-3336.

Rasmussen, T., Knudsen, L. M., and Johnsen, H. E. (2001). Frequency and prognostic relevance of cyclin D1 dysregulation in multiple myeloma. Eur J Haematol *67*, 296-301.

Reaven, G. M. (2005). The metabolic syndrome: requiescat in pace. Clin Chem *51*, 931-938.

Reaven, G. M. (2006). The metabolic syndrome: is this diagnosis necessary? Am J Clin Nutr *83*, 1237-1247.

Rebuffe-Scrive, M., Anderson, B., Olbe, L., and Bjorntorp, P. (1990a). Metabolism of adipose tissue in intraabdominal depots in severely obese men and women. Metabolism *39*, 1021-1025.

Rebuffe-Scrive, M., Bronnegard, M., Nilsson, A., Eldh, J., Gustafsson, J. A., and Bjorntorp, P. (1990b). Steroid hormone receptors in human adipose tissues. J Clin Endocrinol Metab *71*, 1215-1219.

Reichardt, H. M., Kaestner, K. H., Tuckermann, J., Kretz, O., Wessely, O., Bock, R., Gass, P., Schmid, W., Herrlich, P., Angel, P., and Schütz, G. (1998). DNA binding of the glucocorticoid receptor is not essential for survival. Cell *93*, 531-541.

Reichardt, H. M., Umland, T., Bauer, A., Kretz, O., and Schütz, G. (2000). Mice with an increased glucocorticoid receptor gene dosage show enhanced resistance to stress and endotoxic shock. Mol Cell Biol *20*, 9009-9017.

Reshef, L., Olswang, Y., Cassuto, H., Blum, B., Croniger, C. M., Kalhan, S. C., Tilghman, S. M., and Hanson, R. W. (2003). Glyceroneogenesis and the triglyceride/fatty acid cycle. J Biol Chem *278*, 30413-31416.

Reul, J. M., and de Kloet, E. R. (1985). Two receptor systems for corticosterone in rat brain: microdistribution and differential occupation. Endocrinology *117*, 2505-2511.

Richard, D., Chapdelaine, S., Deshaies, Y., Pepin, M. C., and Barden, N. (1993). Energy balance and lipid metabolism in transgenic mice bearing an antisense GCR gene construct. Am J Physiol *265*, R146-R150.

Richelsen, B., Pedersen, S. B., Moller-Pedersen, T., and Bak, J. F. (1991). Regional differences in triglyceride breakdown in human adipose tissue: effects of catecholamines, insulin, and prostaglandin E2. Metabolism *40*, 990-996.

Ridder, S., Chourbaji, S., Hellweg, R., Urani, A., Zacher, C., Schmid, W., Zink, M., Hortnagl, H., Flor, H., Henn, F. A.*, et al.* (2005). Mice with genetically altered glucocorticoid receptor expression show altered sensitivity for stress-induced depressive reactions. J Neurosci *25*, 6243-6250.

Rivers, C., Levy, A., Hancock, J., Lightman, S., and Norman, M. (1999). Insertion of an amino acid in the DNA-binding domain of the glucocorticoid receptor as a result of alternative splicing. J Clin Endocrinol Metab *84*, 4283-4286.

Robyr, D., Wolffe, A. P., and Wahli, W. (2000). Nuclear hormone receptor coregulators in action: diversity for shared tasks. Mol Endocrinol *14*, 329-347.

Rosewicz, S., McDonald, A. R., Maddux, B. A., Goldfine, I. D., Miesfeld, R. L., and Logsdon, C. D. (1988). Mechanism of glucocorticoid receptor down-regulation by glucocorticoids. Journal Of Biological Chemistry *263*, 2581-2584.

Rosmond, R., and Björntorp, P. (2000). The hypothalamic-pituitary-adrenal axis activity as a predictor of cardiovascular disease, type 2 diabetes and stroke. J Intern Med *247*, 188-197.

Rosmond, R., Bouchard, C., and Bjorntorp, P. (2001). Tsp509I polymorphism in exon 2 of the glucocorticoid receptor gene in relation to obesity and cortisol secretion: cohort study. Bmj *322*, 652-653.

Rosmond, R., Chagnon, Y. C., Chagnon, M., Perusse, L., Bouchard, C., and Björntorp, P. (2000a). A polymorphism of the 5'-flanking region of the glucocorticoid receptor gene locus is associated with basal cortisol secretion in men. Metabolism *49*, 1197-1199.

Rosmond, R., Chagnon, Y. C., Holm, G., Chagnon, M., Pérusse, L., Lindell, K., Carlsson, B., Bouchard, C., and Björntorp, P. (2000b). A glucocorticoid receptor gene marker is associated with abdominal obesity, leptin, and dysregulation of the hypothalamic-pituitary- adrenal axis. Obes Res *8*, 211-218.

Rupprecht, R., Reul, J. M., van Steensel, B., Spengler, D., Soder, M., Berning, B., Holsboer, F., and Damm, K. (1993). Pharmacological and functional characterization of human mineralocorticoid and glucocorticoid receptor ligands. Eur J Pharmacol *247*, 145-154.

Russcher, H., Smit, P., van den Akker, E. L., van Rossum, E. F., Brinkmann, A. O., de Jong, F. H., Lamberts, S. W., and Koper, J. W. (2005a). Two polymorphisms in the glucocorticoid receptor gene directly affect glucocorticoid-regulated gene expression. J Clin Endocrinol Metab *90*, 5804-5810.

Russcher, H., van Rossum, E. F., de Jong, F. H., Brinkmann, A. O., Lamberts, S. W., and Koper, J. W. (2005b). Increased expression of the glucocorticoid receptor-A translational isoform as a result of the ER22/23EK polymorphism. Mol Endocrinol *19*, 1687-1696.

Sainsbury, A., Cusin, I., Rohner-Jeanrenaud, F., and Jeanrenaud, B. (1997). Adrenalectomy prevents the obesity syndrome produced by chronic central neuropeptide Y infusion in normal rats. Diabetes *46*, 209-214.

Sainte-Marie, Y., Nguyen Dinh Cat, A., Perrier, R., Mangin, L., Soukaseum, C., Peuchmaur, M., Tronche, F., Farman, N., Escoubet, B., Benitah, J. P., and Jaisser, F. (2007). Conditional glucocorticoid receptor expression in the heart induces atrio-ventricular block. Faseb J *21*, 3133-3141.

Sambhi, M. P., Venning, E. H., and Beck, J. C. (1964). Aldosterone Secretion Rate and Electrolyte Balance Studies on Three Patients with Hypertension. Influence of Guanethidine, Hydralazine and Methyclothiazide. Metabolism *13*, 212-220.

Samra, J. S., Clark, M. L., Humphreys, S. M., MacDonald, I. A., Bannister, P. A., and Frayn, K. N. (1998). Effects of physiological hypercortisolemia on the regulation of lipolysis in subcutaneous adipose tissue. J Clin Endocrinol Metab *83*, 626-631.

Sanchez, E. R., Hirst, M., Scherrer, L. C., Tang, H. Y., Welsh, M. J., Harmon, J. M., Simons, S. S., Jr., Ringold, G. M., and Pratt, W. B. (1990). Hormone-free mouse glucocorticoid receptors overexpressed in Chinese hamster ovary cells are localized to the nucleus and are associated with both hsp70 and hsp90. J Biol Chem *265*, 20123-20130.

Sandeep, T. C., Andrew, R., Homer, N. Z., Andrews, R. C., Smith, K., and Walker, B. R. (2005). Increased in vivo regeneration of cortisol in adipose tissue in human obesity and effects of the 11beta-hydroxysteroid dehydrogenase type 1 inhibitor carbenoxolone. Diabetes *54*, 872-879.

Saruta, T., Suzuki, H., Handa, M., Igarashi, Y., Kondo, K., and Senba, S. (1986). Multiple factors contribute to the pathogenesis of hypertension in Cushing's syndrome. J Clin Endocrinol Metab *62*, 275-279.

Sasaki, K., Cripe, T. P., Koch, S. R., Andreone, T. L., Petersen, D. D., Beale, E. G., and Granner, D. K. (1984). Multihormonal regulation of phosphoenolpyruvate carboxykinase gene transcription. The dominant role of insulin. J Biol Chem *259*, 15242-15251.

Schmid, W., Cole, T. J., Blendy, J. A., and Schutz, G. (1995). Molecular genetic analysis of glucocorticoid signalling in development. J Steroid Biochem Mol Biol *53*, 33-35.

Schwartz, M. W., Woods, S. C., Porte, D., Jr., Seeley, R. J., and Baskin, D. G. (2000). Central nervous system control of food intake. Nature *404*, 661-671.

Seale, J. V., Wood, S. A., Atkinson, H. C., Harbuz, M. S., and Lightman, S. L. (2004). Gonadal steroid replacement reverses gonadectomy-induced changes in the corticosterone pulse profile and stress-induced hypothalamic-pituitary-adrenal axis activity of male and female rats. J Neuroendocrinol *16*, 989-998.

Seckl, J. R., Dickson, K. L., and Fink, G. (1990). Central 5,7-dihydroxytryptamine lesions decrease hippocampal glucocorticoid and mineralocorticoid receptor messenger ribonucleic acid expression. J Neuroendocrinol *2*, 911-916.

Seckl, J. R., Morton, N. M., Chapman, K. E., and Walker, B. R. (2004). Glucocorticoids and 11®-hydroxysteroid dehydrogenase in adipose tissue. Recent Prog Horm Res *59*, 359-393.

Seckl, J. R., and Walker, B. R. (2001). Minireview: 11®-hydroxysteroid dehydrogenase type 1- a tissue-specific amplifier of glucocorticoid action. Endocrinology *142*, 1371-1376.

Seckl, J. R., and Walker, B. R. (2004). 11beta-hydroxysteroid dehydrogenase type 1 as a modulator of glucocorticoid action: from metabolism to memory. Trends Endocrinol Metab *15*, 418-424.

Sheppard, K. E., Roberts, J. L., and Blum, M. (1990). Differential regulation of type II corticosteroid receptor messenger ribonucleic acid expression in the rat anterior pituitary and hippocampus. Endocrinology *127*, 431-439.

Sholter, D. E., and Armstrong, P. W. (2000). Adverse effects of corticosteroids on the cardiovascular system. Can J Cardiol *16*, 505-511.

Silva, C. M., Powell-Oliver, F. E., Jewell, C. M., Sar, M., Allgood, V. E., and Cidlowski, J. A. (1994). Regulation of the human glucocorticoid receptor by long-term and chronic treatment with glucocorticoid. Steroids *59*, 436-442.

Singer CJ, K. M., Rosner W (1988). Characteristics of the binding of corticosteroid-binding globulin to rat cell membranes. Endocrinology *122*, 89-96.

Skarnes W.C, Auerbach B.A, Joyner A.L. (1992). A gene trap approach in mouse embryonic stem cells: the lacZ reported is activated by splicing, reflects endogenous gene expression, and is mutagenic in mice.
Genes Dev *6*:903-18.

Slavin, B. G., Ong, J. M., and Kern, P. A. (1994). Hormonal regulation of hormone-sensitive lipase activity and mRNA levels in isolated rat adipocytes. J Lipid Res *35*, 1535-1541.

Smart, J. L., and Low, M. J. (2003). Lack of proopiomelanocortin peptides results in obesity and defective adrenal function but normal melanocyte pigmentation in the murine C57BL/6 genetic background. Ann N Y Acad Sci *994*, 202-210.

Smart, J. L., Tolle, V., and Low, M. J. (2006). Glucocorticoids exacerbate obesity and insulin resistance in neuron-specific proopiomelanocortin-deficient mice. J Clin Invest.

Smith, A. G., Heath, J. K., Donaldson, D. D., Wong, G. G., Moreau, J., Stahl, M., and Rogers, D. (1988). Inhibition of pluripotential embryonic stem cell differentiation by purified polypeptides. Nature *336*, 688-690.

Smith, C. K., and Romsos, D. R. (1985). Effects of adrenalectomy on energy balance of obese mice are diet dependent. Am J Physiol *249*, R13-22.

Snijder, M. B., van Dam, R. M., Visser, M., and Seidell, J. C. (2006). What aspects of body fat are particularly hazardous and how do we measure them? Int J Epidemiol *35*, 83-92.

Soumano, K., Desbiens, S., Rabelo, R., Bakopanos, E., Camirand, A., and Silva, J. E. (2000). Glucocorticoids inhibit the transcriptional response of the uncoupling protein-1 gene to adrenergic stimulation in a brown adipose cell line. Mol Cell Endocrinol *165*, 7-15.

Sowers, J. R. (2004). Insulin resistance and hypertension. Am J Physiol Heart Circ Physiol *286*, H1597-1602.

Stahn, C., Lowenberg, M., Hommes, D. W., and Buttgereit, F. (2007). Molecular mechanisms of glucocorticoid action and selective glucocorticoid receptor agonists. Mol Cell Endocrinol *275*, 71-78.

Stanton, M. E., Gutierrez, Y. R., and Levine, S. (1988). Maternal deprivation potentiates pituitary-adrenal stress responses in infant rats. Behav Neurosci *102*, 692-700.

Stewart, P. M. (2005). Tissue-specific Cushing's syndrome uncovers a new target in treating the metabolic syndrome--11beta-hydroxysteroid dehydrogenase type 1. Clin Med *5*, 142-146.

Strack, A. M., Sebastian, R. J., Schwartz, M. W., and Dallman, M. F. (1995). Glucocorticoids and insulin: reciprocal signals for energy balance. Am J Physiol *268*, R142-149.

Stratford, S., Hoehn, K. L., Liu, F., and Summers, S. A. (2004). Regulation of insulin action by ceramide: dual mechanisms linking ceramide accumulation to the inhibition of Akt/protein kinase B. J Biol Chem *279*, 36608-36615.

Strickland, I., Kisich, K., Hauk, P. J., Vottero, A., Chrousos, G. P., Klemm, D. J., and Leung, D. Y. (2001). High constitutive glucocorticoid receptor beta in human neutrophils enables them to reduce their spontaneous rate of cell death in response to corticosteroids. J Exp Med *193*, 585-593.

Strickland, S., and Mahdavi, V. (1978). The induction of differentiation in teratocarcinoma stem cells by retinoic acid. Cell *15*, 393-403.

Subramanian, G., Paterlini, M. G., Larson, D. L., Portoghese, P. S., and Ferguson, D. M. (1998). Conformational analysis and automated receptor docking of selective arylacetamide-based kappa-opioid agonists. J Med Chem *41*, 4777-4789.

Suen, K. K., Lewis, W. H., and Lai, K. N. (1997). Analysis of charge distribution of lambda- and kappa-IgA in IgA nephropathy by focused antigen capture immunoassay. Scand J Urol Nephrol *31*, 289-293.

Summers, L. K., Arner, P., Ilic, V., Clark, M. L., Humphreys, S. M., and Frayn, K. N. (1998). Adipose tissue metabolism in the postprandial period: microdialysis and arteriovenous techniques compared. Am J Physiol *274*, E651-655.

Sutherland, H. G., Mumford, G. K., Newton, K., Ford, L. V., Farrall, R., Dellaire, G., Caceres, J. F., and Bickmore, W. A. (2001). Large-scale identification of mammalian proteins localized to nuclear sub-compartments. Hum Mol Genet *10*, 1995-2011.

Syed, A. A., Irving, J. A., Redfern, C. P., Hall, A. G., Unwin, N. C., White, M., Bhopal, R. S., Alberti, K. G., and Weaver, J. U. (2004). Low prevalence of the N363S polymorphism of the glucocorticoid receptor in South Asians living in the United Kingdom. J Clin Endocrinol Metab *89*, 232-235.

Takeda, Y., Miyamori, I., Yoneda, T., Furukawa, K., Hatakeyama, H., Inaba, S., Ito, Y., Takeda, R., and Mabuchi, H. (1996). Effect of adrenocorticotropin stimulation on the synthesis of 19-noraldosterone in man. J Clin Endocrinol Metab *81*, 1852-1855.

Tamura, K., Umemura, S., Fukamizu, A., Ishii, M., and Murakami, K. (1995). Recent advances in the study of renin and angiotensinogen genes: from molecules to the whole body. Hypertens Res *18*, 7-18.

Tannenbaum, B. M., Brindley, D. N., Tannenbaum, G. S., Dallman, M. F., McArthur, M. D., and Meaney, M. J. (1997). High-fat feeding alters both basal and stress-induced hypothalamic- pituitary-adrenal activity in the rat. Am J Physiol *273*, E1168-E1177.

Tasker, J. G. (2006). Rapid glucocorticoid actions in the hypothalamus as a mechanism of homeostatic integration. Obesity (Silver Spring) *14 Suppl 5*, 259S-265S.

Tate, P., Lee, M., Tweedie, S., Skarnes, W. C., and Bickmore, W. A. (1998). Capturing novel mouse genes encoding chromosomal and other nuclear proteins. J Cell Sci *111 (Pt 17)*, 2575-2585.

Tchernof, A., Belanger, C., Morisset, A. S., Richard, C., Mailloux, J., Laberge, P., and Dupont, P. (2006). Regional differences in adipose tissue metabolism in women: minor effect of obesity and body fat distribution. Diabetes *55*, 1353-1360.

Tchoukalova, Y. D., Harteneck, D. A., Karwoski, R. A., Tarara, J., and Jensen, M. D. (2003). A quick, reliable, and automated method for fat cell sizing. J Lipid Res *44*, 1795-1801.

Tomlinson, J. W., Draper, N., Mackie, J., Johnson, A. P., Holder, G., Wood, P., and Stewart, P. M. (2002). Absence of Cushingoid phenotype in a patient with Cushing's disease due to defective cortisone to cortisol conversion. J Clin Endocrinol Metab *87*, 57-62.

Tremblay, A., Bouchard, L., Bouchard, C., Despres, J. P., Drapeau, V., and Perusse, L. (2003). Long-term adiposity changes are related to a glucocorticoid receptor polymorphism in young females. J Clin Endocrinol Metab *88*, 3141-3145.

Tronche, F., Kellendonk, C., Kretz, O., Gass, P., Anlag, K., Orban, P. C., Bock, R., Klein, R., and Schutz, G. (1999). Disruption of the glucocorticoid receptor gene in the nervous system results in reduced anxiety. Nature Genetics *23*, 99-103.

Tronche, F., Kellendonk, C., Reichardt, H. M., and Schütz, G. (1998). Genetic dissection of glucocorticoid receptor function in mice. Curr Opin Genet Dev *8*, 532-538.

Trousson, A., Grenier, J., Fonte, C., Massaad-Massade, L., Schumacher, M., and Massaad, C. (2007). Recruitment of the p160 coactivators by the glucocorticoid receptor: dependence on the promoter context and cell type but not hypoxic conditions. J Steroid Biochem Mol Biol *104*, 305-311.

Tsai, S. Y., Carlstedt-Duke, J., Weigel, N. L., Dahlman, K., Gustafsson, J.-Å., Tsai, M.-J., and O'Malley, B. W. (1988). Molecular interactions of steroid hormone receptor with its enhancer element: evidence for receptor dimer formation. Cell *55*, 361-369.

Ucker, D. S., and Yamamoto, K. R. (1984). Early events in the stimulation of mammary tumor virus RNA synthesis by glucocorticoids. Novel assays of transcription rates. J Biol Chem *259*, 7416-7420.

Udelsman, R., Ramp, J., Gallucci, W. T., Gordon, A., Lipford, E., Norton, J. A., Loriaux, D. L., and Chrousos, G. P. (1986). Adaptation during surgical stress. A reevaluation of the role of glucocorticoids. J Clin Invest *77*, 1377-1381.

Ukkola, O., Rosmond, R., Tremblay, A., and Bouchard, C. (2001). Glucocorticoid receptor Bcl I variant is associated with an increased atherogenic profile in response to long-term overfeeding. Atherosclerosis *157*, 221-224.

Unsicker, K., Krisch, B., Otten, U., and Thoenen, H. (1978). Nerve growth factor-induced fiber outgrowth from isolated rat adrenal chromaffin cells: impairment by glucocorticoids. Proc Natl Acad Sci USA *75*, 3498-3502.

van Rossum, E. F., Binder, E. B., Majer, M., Koper, J. W., Ising, M., Modell, S., Salyakina, D., Lamberts, S. W., and Holsboer, F. (2006a). Polymorphisms of the glucocorticoid receptor gene and major depression. Biol Psychiatry *59*, 681-688.

van Rossum, E. F., de Jong, F. J., Koper, J. W., Uitterlinden, A. G., Prins, N. D., van Dijk, E. J., Koudstaal, P. J., Hofman, A., de Jong, F. H., Lamberts, S. W., and Breteler, M. M. (2006b). Glucocorticoid receptor variant and risk of dementia and white matter lesions. Neurobiol Aging.

van Rossum, E. F., Feelders, R. A., van den Beld, A. W., Uitterlinden, A. G., Janssen, J. A., Ester, W., Brinkmann, A. O., Grobbee, D. E., de Jong, F. H., Pols, H. A.*, et al.* (2004a). Association of the ER22/23EK polymorphism in the glucocorticoid receptor gene with survival and C-reactive protein levels in elderly men. Am J Med *117*, 158-162.

van Rossum, E. F., Koper, J. W., van den Beld, A. W., Uitterlinden, A. G., Arp, P., Ester, W., Janssen, J. A., Brinkmann, A. O., de Jong, F. H., Grobbee, D. E.*, et al.* (2003). Identification of the BclI polymorphism in the glucocorticoid receptor gene: association with sensitivity to glucocorticoids in vivo and body mass index. Clin Endocrinol *59*, 585-592.

van Rossum, E. F., and Lamberts, S. W. (2004). Polymorphisms in the glucocorticoid receptor gene and their associations with metabolic parameters and body composition. Recent Prog Horm Res *59*, 333-357.

van Rossum, E. F., and Lamberts, S. W. (2006). Glucocorticoid resistance syndrome: A diagnostic and therapeutic approach. Best Pract Res Clin Endocrinol Metab *20*, 611-626.

van Rossum, E. F., Roks, P. H., de Jong, F. H., Brinkmann, A. O., Pols, H. A., Koper, J. W., and Lamberts, S. W. (2004b). Characterization of a promoter polymorphism in the glucocorticoid receptor gene and its relationship to three other polymorphisms. Clin Endocrinol (Oxf) *61*, 573-581.

van Rossum, E. F., Voorhoeve, P. G., te Velde, S. J., Koper, J. W., Delemarre-van de Waal, H. A., Kemper, H. C., and Lamberts, S. W. (2004c). The ER22/23EK polymorphism in the glucocorticoid receptor gene is associated with a beneficial body composition and muscle strength in young adults. J Clin Endocrinol Metab *89*, 4004-4009.

van Steensel, B., Brink, M., van der Meulen, K., van Binnendijk, E. P., Wansink, D. G., de Jong, L., de Kloet, E. R., and van Driel, R. (1995). Localization of the glucocorticoid receptor in discrete clusters in the cell nucleus. J Cell Sci *108 (Pt 9)*, 3003-3011.

van Winsen, L. M., Hooper-van Veen, T., van Rossum, E. F., Koper, J. W., Barkhof, F., Polman, C. H., and Uitdehaag, B. M. (2007). Glucocorticoid receptor gene polymorphisms associated with more aggressive disease phenotype in MS. J Neuroimmunol *186*, 150-155.

Vanderbilt, J. N., Miesfeld, R., Maler, B. A., and Yamamoto, K. R. (1987). Intracellular receptor concentration limits glucocorticoid-dependent enhancer activity. Mol Endocrinol *1*, 68-74.

Vegiopoulos, A., and Herzig, S. (2007). Glucocorticoids, metabolism and metabolic diseases. Mol Cell Endocrinol *275*, 43-61.

Vehaskari, V. M., Aviles, D. H., and Manning, J. (2001). Prenatal programming of adult hypertension in the rat. Kidney Int *59*, 238-245.

Vig, E., Barrett, T. J., and Vedeckis, W. V. (1994). Coordinate Regulation of Glucocorticoid Receptor and C-Jun Messenger- Rna Levels - Evidence For Cross-Talk Between 2 Signaling Pathways At the Transcriptional Level. Molecular Endocrinology *8*, 1336-1346.

Villarreal, D., Reams, G., Freeman, R. H., and Taraben, A. (1998). Renal effects of leptin in normotensive, hypertensive, and obese rats. Am J Physiol *275*, R2056-2060.

Voice, M. W., Seckl, J. R., Edwards, C. R. W., and Chapman, K. E. (1996). 11®-hydroxysteroid dehydrogenase type 1 expression in 2S-FAZA hepatoma cells is hormonally regulated; a model system for the study of hepatic glucocorticoid metabolism. Biochem J *317*, 621-625.

Wajchenberg, B. L. (2000). Subcutaneous and visceral adipose tissue: their relation to the metabolic syndrome. Endocr Rev *21*, 697-738.

Wake, D. J., Rask, E., Livingstone, D. E., Soderberg, S., Olsson, T., and Walker, B. R. (2003). Local and systemic impact of transcriptional up-regulation of 11β-hydroxysteroid dehydrogenase type 1 in adipose tissue in human obesity. J Clin Endocrinol Metab *88*, 3983-3988.

Wake, D. J., and Walker, B. R. (2004). 11 beta-hydroxysteroid dehydrogenase type 1 in obesity and the metabolic syndrome. Mol Cell Endocrinol *215*, 45-54.

Walker, B. R., and Andrew, R. (2006). Tissue production of cortisol by 11beta-hydroxysteroid dehydrogenase type 1 and metabolic disease. Ann N Y Acad Sci *1083*, 165-184.

Wallace, A. D., and Cidlowski, J. A. (2001). Proteasome-mediated glucocorticoid receptor degradation restricts transcriptional signaling by glucocorticoids. J Biol Chem *276*, 42714-42721.

Wallerath, T., Godecke, A., Molojavyi, A., Li, H., Schrader, J., and Forstermann, U. (2004). Dexamethasone lacks effect on blood pressure in mice with a disrupted endothelial NO synthase gene. Nitric Oxide *10*, 36-41.

Wang, L., Feng, Z. P., and Duff, H. J. (1999). Glucocorticoid regulation of cardiac K+ currents and L-type Ca2+ current in neonatal mice. Circ Res *85*, 168-173.

Wansink, D. G., Schul, W., van der Kraan, I., van Steensel, B., van Driel, R., and de Jong, L. (1993). Fluorescent labeling of nascent RNA reveals transcription by RNA polymerase II in domains scattered throughout the nucleus. J Cell Biol *122*, 283-293.

Warriar, N., Yu, C., and Govindan, M. V. (1994). Hormone binding domain of human glucocorticoid receptor. Enhancement of transactivation function by substitution mutants M565R and A573Q. J Biol Chem *269*, 29010-29015.

Watt, G. C., Harrap, S. B., Foy, C. J., Holton, D. W., Edwards, H. V., Davidson, H. R., Connor, J. M., Lever, A. F., and Fraser, R. (1992). Abnormalities of glucocorticoid metabolism and the renin-angiotensin system: a four-corners approach

to the identification of genetic determinants of blood pressure. J Hypertens *10*, 473-482.

Webster, J. C., Jewell, C. M., Bodwell, J. E., Munck, A., Sar, M., and Cidlowski, J. A. (1997). Mouse glucocorticoid receptor phosphorylation status influences multiple functions of the receptor protein. J Biol Chem *272*, 9287-9293.

Webster, N. J. G., Green, S., Jin, J. R., and Chambon, P. (1988). The hormone-binding domains of the estrogen and glucocorticoid receptors contain an inducible transcription activation function. Cell *54*, 199-107.

Wei, Q., Lu, X. Y., Liu, L., Schafer, G., Shieh, K. R., Burke, S., Robinson, T. E., Watson, S. J., Seasholtz, A. F., and Akil, H. (2004). Glucocorticoid receptor overexpression in forebrain: a mouse model of increased emotional lability. Proc Natl Acad Sci U S A *101*, 11851-11856.

Whitesall, S. E., Hoff, J. B., Vollmer, A. P., and D'Alecy, L. G. (2004). Comparison of simultaneous measurement of mouse systolic arterial blood pressure by radiotelemetry and tail-cuff methods. Am J Physiol Heart Circ Physiol *286*, H2408-2415.

Whitworth, J. A., Brown, M. A., Kelly, J. J., and Williamson, P. M. (1995). Mechanisms of cortisol-induced hypertension in humans. Steroids *60*, 76-80.

Widmaier, E. P., Rosen, K., and Abbott, B. (1992). Free fatty acids activate the hypothalamic-pituitary-adrenocortical axis in rats. Endocrinology *131*, 2313-2318.

Williams, T. D., Chambers, J. B., Roberts, L. M., Henderson, R. P., and Overton, J. M. (2003). Diet-induced obesity and cardiovascular regulation in C57BL/6J mice. Clin Exp Pharmacol Physiol *30*, 769-778.

Wrange, Ö., Eriksson, P., and Perlmann, T. (1989). The purified activated glucocorticoid receptor is a homodimer. J Biol Chem *264*, 5253-5259.

Wu, Y. Q., Wang, X. D., Fang, H., Wang, Y. L., Zhang, Y. C., and Su, L. J. (2007). [The relation between angiotensin II receptors 1 and 2, and CYP11B2 and atrial structural remodeling in patients with atrial fibrillation]. Zhonghua Yi Xue Za Zhi *87*, 2281-2284.

Wust, S., Van Rossum, E. F., Federenko, I. S., Koper, J. W., Kumsta, R., and Hellhammer, D. H. (2004). Common polymorphisms in the glucocorticoid receptor gene are associated with adrenocortical responses to psychosocial stress. J Clin Endocrinol Metab *89*, 565-573.

Xu, X., and Björntorp, P. (1990). Effects of dexamethasone on multiplication and differentiation of rat adipose precursor cells. Exp Cell Res *189*, 247-252.

Yaswen, L., Diehl, N., Brennan, M. B., and Hochgeschwender, U. (1999). Obesity in the mouse model of pro-opiomelanocortin deficiency responds to peripheral melanocortin. Nat Med *5*, 1066-1070.

Young, E. A., Kwak, S. P., and Kottak, J. (1995). Negative Feedback-Regulation Following Administration of Chronic Exogenous Corticosterone. Journal of Neuroendocrinology *7*, 37-45.

Young, W. F., and Hogan, M. J. (1994). Renin-Independent Hypermineralocorticoidism. Trends in Endocrinology and Metabolism *5*, 97-106.

Yudt, M. R., and Cidlowski, J. A. (2001). Molecular identification and characterization of a and b forms of the glucocorticoid receptor. Mol Endocrinol *15*, 1093-1103.

Zakrzewska, K. E., Cusin, I., Stricker-Krongrad, A., Boss, O., Ricquier, D., Jeanrenaud, B., and Rohner-Jeanrenaud, F. (1999). Induction of obesity and hyperleptinemia by central glucocorticoid infusion in the rat. Diabetes *48*, 365-370.

Zierath, J. R. (2007). The path to insulin resistance: paved with ceramides? Cell Metab *5*, 161-163.

(1996). Mutant mice in neuroscience:recommentations concerning genetic background, Paper presented at: Banbury Conference on genetic background in mice (Neuron).

Peripheral mechanisms contributing to the glucocorticoid hypersensitivity in proopiomelanocortin null mice treated with corticosterone

Zoi Michailidou, Anthony P Coll[1], Christopher J Kenyon, Nicholas M Morton, Stephen O'Rahilly[1], Jonathan R Seckl and **Karen E Chapman**

Endocrine Unit, Queen's Medical Research Institute, Centre for Cardiovascular Sciences, University of Edinburgh, 47 Little France Crescent, Edinburgh EH16 4TJ, UK

[1]Departments of Clinical Biochemistry and Medicine, Cambridge Institute for Medical Research, Addenbrooke's Hospital, Cambridge CB2 2XY, UK

(Requests for offprints should be addressed to K E Chapman; Email: karen.chapman@ed.ac.uk)

Abstract

Proopiomelanocortin (POMC) deficiency causes severe obesity through hyperphagia of hypothalamic origin. However, low glucocorticoid levels caused by adrenal insufficiency mitigate against insulin resistance, hyperphagia and fat accretion in *Pomc*$^{-/-}$ mice. Upon exogenous glucocorticoid replacement, corticosterone-supplemented (CORT) *Pomc*$^{-/-}$ mice show exaggerated responses, including excessive fat accumulation, hyperleptinaemia and insulin resistance. To investigate the peripheral mechanisms underlying this glucocorticoid hypersensitivity, we examined the expression levels of key determinants and targets of glucocorticoid action in adipose tissue and liver. Despite lower basal expression of 11β-hydroxysteroid dehydrogenase type 1 (11β-HSD1), which generates active glucocorticoids within cells, CORT-mediated induction of 11β-HSD1 mRNA levels was more pronounced in adipose tissues of *Pomc*$^{-/-}$ mice. Similarly, CORT treatment increased lipoprotein lipase mRNA levels in all fat depots in *Pomc*$^{-/-}$ mice, consistent with exaggerated fat accumulation. Glucocorticoid receptor (GR) mRNA levels were selectively elevated in liver and retroperitoneal fat of *Pomc*$^{-/-}$ mice but were corrected by CORT in the latter depot. In liver, CORT increased phosphoenolpyruvate carboxykinase mRNA levels specifically in *Pomc*$^{-/-}$ mice, consistent with their insulin-resistant phenotype. Furthermore, CORT induced hypertension in *Pomc*$^{-/-}$ mice, independently of adipose or liver renin–angiotensin system activation. These data suggest that CORT-inducible 11β-HSD1 expression in fat contributes to the adverse cardiometabolic effects of CORT in POMC deficiency, whereas higher GR levels may be more important in liver.

Journal of Endocrinology (2007) **194,** 161–170

Introduction

Glucocorticoids exert pleiotrophic effects on metabolism and energy partitioning. Centrally, they increase food intake and reduce energy expenditure, whilst peripherally, they promote insulin resistance, fat accumulation (Dallman *et al.* 1993, Kellendonk *et al.* 2002) and hypertension (Saruta 1996, Whitworth *et al.* 2001). Polymorphisms in the human glucocorticoid receptor *NR3c1* gene (GR) are associated with glucocorticoid hypersensitivity, visceral obesity, hypertension and increased cardiovascular disease risk (Buemann *et al.* 1997, Rosmond *et al.* 2000, Dobson *et al.* 2001, Ukkola *et al.* 2001*a*,*b*, van Rossum *et al.* 2003). Many rodent models of obesity are characterised by hypercorticosteronaemia, with weight gain normalised following adrenalectomy and reinstated by glucocorticoid replacement (Debons *et al.*1982, Freedman *et al.* 1986, Sainsbury *et al.*1997, Makimura *et al.* 2000). Although plasma glucocorticoid levels are normal in human idiopathic obesity (Flier 2004), it has been proposed that intra-adipose glucocorticoid action is selectively increased, through increased adipose expression of 11β-hydroxysteroid dehydrogenase type 1 (11β-HSD1), the intracellular enzyme that regenerates active glucocorticoids from intrinsically inert 11-keto-glucocorticoids (Kotelevtsev *et al.* 1997, Jamieson *et al.* 2000, Andrew *et al.* 2002).

Obese humans (Rask *et al.* 2001, Paulmyer-Lacroix *et al.* 2002, Lindsay *et al.* 2003, Kannisto *et al.* 2004) and some rodent models of obesity (Livingstone *et al.* 2000, Masuzaki *et al.* 2001) have selectively increased adipose levels of 11β-HSD1 and transgenic overexpression of 11β-HSD1 in adipocytes causes hyperphagia, obesity, insulin resistance and hypertension despite unchanged systemic glucocorticoid levels (Masuzaki *et al.* 2001, 2003). Hepatic overexpression of 11β-HSD1 has no effect on adiposity, but causes hypertension and insulin resistance (Paterson *et al.* 2004). Conversely, mice deficient in 11β-HSD1 are insulin sensitised and resist the adverse metabolic effects of a high-fat diet (Kotelevtsev *et al.* 1997, Morton *et al.* 2001, 2004).

DOI: 10.1677/JOE-07-0090
0022–0795/07/0194–161 © 2007 Society for Endocrinology *Printed in Great Britain*
Online version via http://www.endocrinology-journals.org

Proopiomelanocortin (POMC) is a polypeptide precursor which undergoes extensive post-translational modification to yield a range of smaller, biological active peptides. These include α-, β- and γ-melanocyte-stimulating hormone and adrenocorticotrophic hormone (ACTH), collectively known as melanocortins. Inactivating mutations of the *POMC* gene in humans and mice result in a complex phenotype. Loss of melanocortin signalling within the hypothalamus causes hyperphagia and obesity (Krude *et al.* 1998, Yaswen *et al.*1999, Challis *et al.* 2004). Further, a failure to produce ACTH within the anterior pituitary causes adrenal insufficiency with low or absent circulating glucocorticoids (Krude *et al.* 1998, Yaswen *et al.*1999, Challis *et al.* 2004). *Pomc*$^{-/-}$ mice are therefore unusual amongst rodent models in that obesity develops in the absence of circulating glucocorticoids. However, glucocorticoid treatment exacerbates hyperphagia and obesity in adult *Pomc*$^{-/-}$ mice and induces severe insulin resistance, hyperleptinaemia and diabetes (Coll *et al.* 2005).

We have tested the hypothesis that increased glucocorticoid action in peripheral tissues of glucocorticoid-treated *Pomc*$^{-/-}$ mice contributes to their apparent glucocorticoid hypersensitivity and exaggerated metabolic syndrome-like phenotype. We further demonstrate that glucocorticoid replacement induces hypertension in *Pomc*$^{-/-}$ mice, independently of renin–angiotensin system (RAS) activation.

Materials and Methods

Animals and CORT replacement

The generation of *Pomc*$^{-/-}$ mice on a 129/SvEv background has been described previously (Challis *et al.* 2004). All mice were housed in standard conditions on a 12 h light:12 h darkness cycle (lights on 0070 h) with *ad libitum* access to water and chow (4·5% fat diet, Special Diet Services, Witham, UK). Eight-week-old male mice ($n=5$ per group) were treated with corticosterone (25 μg/ml) in their drinking water, a dose that results in similar plasma glucocorticoid levels and hypothalamic corticotrophin releasing hormone (CRH) mRNA levels in *Pomc*$^{-/-}$ and wild-type mice (Coll *et al.* 2005). All animal protocols used in these studies were approved under the auspices of the UK Home Office Animals (Scientific Procedures) Act 1986.

Blood pressure measurement

Systolic blood pressure was measured photoelectrically in the tail of restrained conscious mice using an IITC model 179 analyser (Woodland Hills, CA, USA). Prior to recording measurements, all mice underwent three periods of training to accustom them to the procedure. Mice were warmed at 32 °C for 30 min before taking ten consecutive readings. The first five were discounted and a mean value of systolic blood pressure was calculated from the last five readings. Five mice from each treatment group were measured. All analogue recordings were analysed by an independent observer who was blinded to the genotype of the mice and any treatment they had received.

Plasma hormone and lipid measurements

Animals were killed between 0800 and 0900 h by cervical dislocation. Trunk blood samples were collected into EDTA-coated tubes (Sarstedt, Leicester, UK), centrifuged at 6000 ***g*** for 10 min and plasma stored at −80 °C until required for assay. Non-esterified fatty acid (NEFA) and triglyceride levels were determined by commercial kits (NEFA, Roche Diagnostics; triglyceride, Dade Behring, Marburg, Germany). Plasma renin and angiotensinogen concentrations were determined as previously described (Morton *et al.* 2005).

Tissue morphology and hepatic triglyceride levels

Neutral lipids, cholesterol and fatty acids were identified by light microscopy at 40× magnification in cryostat liver sections (30 μm) stained with oil red O (Sigma) and counter stained with haematoxylin as previously described (Morton *et al.* 2005). Hepatic triglycerides were extracted by homogenisation in isopropanol (ten volumes) and then incubated at 37 °C for 45 min and measured spectrophotometrically in supernatants (3000 ***g*** for 10 min) using reagent TR224221 (Alpha Laboratories, Eastleigh, Hampshire, UK).

RNA extraction and northern blot analysis

Pieces of liver and adipose tissues (inguinal, retroperitoneal and epididymal) were rapidly frozen in dry ice, stored at −80 °C and then homogenised in Trizol reagent (Invitrogen). Total RNA was purified using a binding matrix (RNaid Plus kit, BIO 101; Anachem, UK) and eluted in diethylpyrocarbonate-treated water containing 400 U/ml RNasin (Promega) and 10 mmol/l dithiothreitol. RNA (5–10 μg) was blotted and hybridised to ^{32}P-labelled cDNA probes for mouse 11β-HSD1, GR, angiotensinogen, phosphoenolpyruvate carboxykinase (PEPCK), lipoprotein lipase (LPL) and 18S as previously described (Morton *et al.* 2005). Specific mRNAs were quantified using a phosphorimager (Fuji BAS FLA 2000, Raytek, Sheffield,

Figure 1 Mediators of GC action in adipose tissue of *Pomc*$^{-/-}$ mice and effects of CORT treatment on GC target genes. (A) Representative northern blot showing levels of 11β-HSD1 mRNA and 18S RNA in epididymal adipose tissue of *Pomc*$^{-/-}$ (−/−) and wild-type (+/+) mice, either untreated or treated for 10 days with corticosterone (cort). (B–E) Quantitation of adipose tissue-specific 11β-HSD1 (B), GR (C), LPL (D) and PEPCK (E) mRNA levels in experimental mice. Epi, epididymal fat; ing, inguinal fat; retro, retroperitoneal fat. Data are presented as percentage of the value in untreated wild-type mice (100%) and are the means±S.E.M.; $n=5$ per group. Significance $^{*}P<0{\cdot}05$, $^{**}P<0{\cdot}01$ and $^{***}P<0{\cdot}001$.

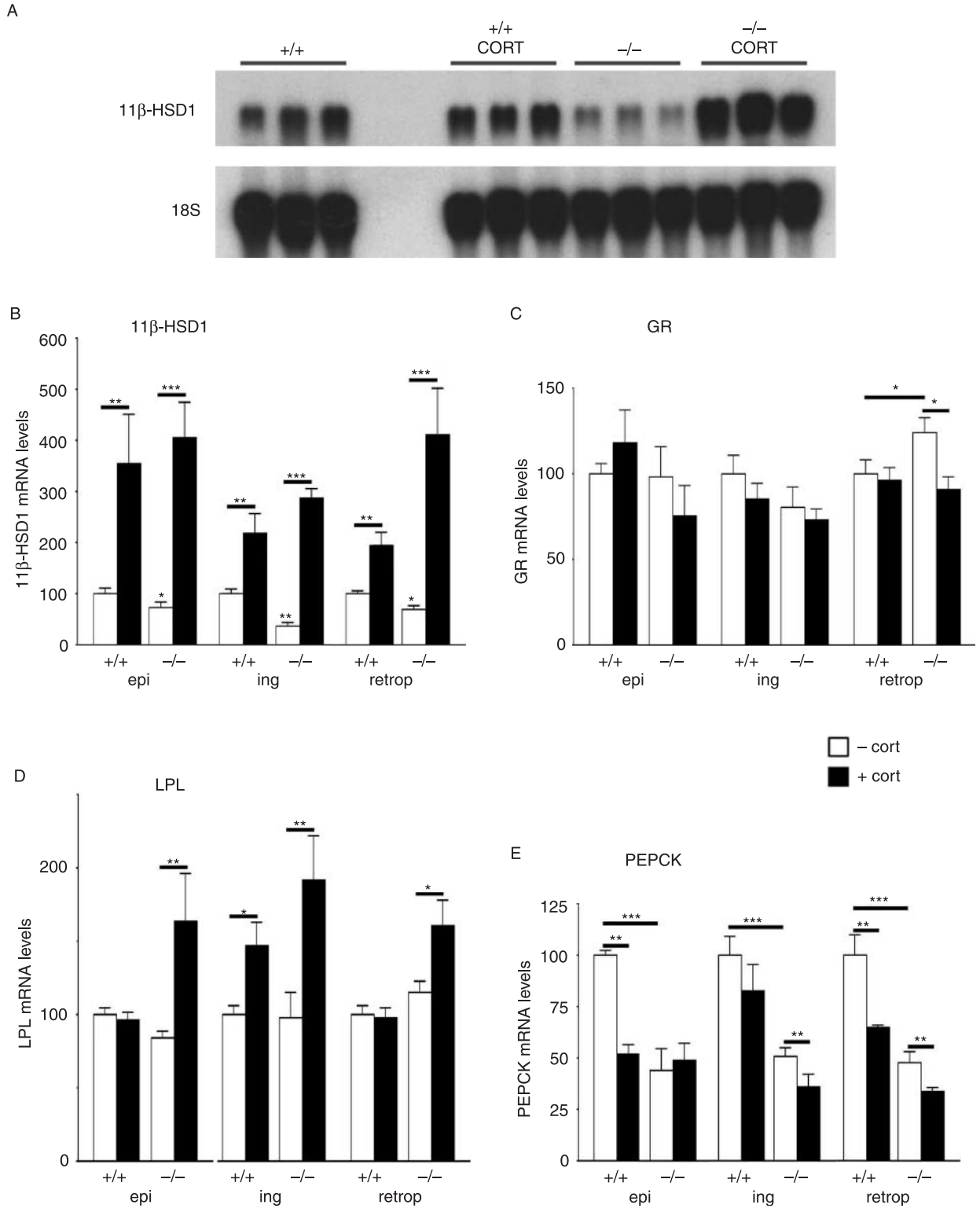
A
+/+
+/+ CORT
–/–
–/– CORT
11β-HSD1
18S
B
11β-HSD1
11β-HSD1 mRNA levels
epi
ing
retrop
C
GR
GR mRNA levels
– cort
+ cort
D
LPL
LPL mRNA levels
E
PEPCK
PEPCK mRNA levels

UK) and Aida image analysis software (Raytek) and are expressed in arbitrary units relative to 18S RNA.

Statistical analyses

The effects of genotype and corticosterone interactions were assessed by two-way ANOVA followed by *post hoc* Tukey's tests for group differences. Significance was set at $P<0{\cdot}05$. Values are means ± S.E.M.

Results

Pomc$^{-/-}$ *mice have reduced intra-adipose GC action but exaggerated CORT-mediated GC amplification*

Corticosterone-treated *Pomc*$^{-/-}$ and wild-type mice had similar plasma corticosterone levels and hypothalamic CRH mRNA levels (Coll *et al.* 2005). To examine potential mechanisms of corticosterone hypersensitivity in *Pomc*$^{-/-}$ mice, 11β-HSD1 and GR mRNA levels were measured in epididymal, inguinal and retroperitoneal adipose depots. Adipose 11β-HSD1 mRNA expression was lower in all untreated *Pomc*$^{-/-}$ compared with wild-type mice (Fig. 1A) and was dramatically increased by corticosterone in both genotypes (Fig. 1A), with larger increases (two- to four-fold greater) in *Pomc*$^{-/-}$ mice.

Adipose expression of GR mRNA was higher in the retroperitoneal fat of *Pomc*$^{-/-}$ mice and restored to wild-type levels by corticosterone treatment (Fig. 1B). GR mRNA levels did not differ in inguinal and epididymal fat between *Pomc*$^{-/-}$ and wild-type mice, and were unaffected by corticosterone treatment in either genotype (Fig. 1B).

To investigate mechanisms downstream of 11β-HSD1/GR by which corticosterone treatment selectively increases fat mass in *Pomc*$^{-/-}$ mice, adipose levels of mRNA encoding LPL, a glucocorticoid-regulated gene (Fried *et al.* 1993), were measured. Although LPL mRNA levels were the same in untreated *Pomc*$^{-/-}$ and wild-type mice in all depots, adipose LPL expression in *Pomc*$^{-/-}$ mice was markedly increased by corticosterone treatment (Fig. 1C) consistent with increased triglyceride uptake, and fat mass in *Pomc*$^{-/-}$ mice. In wild-type mice, corticosterone treatment increased LPL mRNA only in the inguinal depot, and to a lesser extent than in *Pomc*$^{-/-}$ mice (Fig. 1C), suggesting adipose depot-dependent regulation of LPL by glucocorticoids in non-obese mice, consistent with previous data in rats (Freedman *et al.* 1986).

PEPCK is an enzyme essential for gluconeogenesis in liver and glycerol synthesis in adipose tissue (Pilkis & Granner 1992, Reshef *et al.* 2003). PEPCK is a classical glucocorticoid target gene which is positively regulated by glucocorticoids in hepatocytes and negatively regulated in adipocytes (Sasaki *et al.*1984, Nechushtan *et al.* 1987). Consistent with this, adipose PEPCK mRNA levels were decreased in epididymal and retroperitoneal fat by corticosterone treatment in wild-type mice (Fig. 1D). Surprisingly, given their glucocorticoid deficiency, *Pomc*$^{-/-}$ mice had lower levels of PEPCK mRNA in adipose tissue than in wild-type (Fig. 1D). However, although corticosterone treatment in *Pomc*$^{-/-}$ mice decreased PEPCK expression in inguinal and retroperitoneal adipose tissue (significantly lower than in corticosterone-treated wild-type mice; $P=0{\cdot}01$), it had no effect on PEPCK mRNA levels in epididymal adipose tissue, suggesting that other regulatory factors dominate PEPCK expression in adipose tissue of *Pomc*$^{-/-}$ mice (Fig. 1D).

Pomc$^{-/-}$ *mice are dyslipidaemic, and have unaltered hepatic 11β-HSD1 but higher GR mRNA levels*

Hepatic 11β-HSD1 mRNA levels were similar between the two genotypes (Fig. 2A) and unaffected by corticosterone (Fig. 2A). Hepatic GR mRNA levels were higher in *Pomc*$^{-/-}$ compared with wild-type mice (Fig. 2B), but again corticosterone had no effect on GR mRNA levels (Fig. 2B).

Hepatic PEPCK expression was lower in *Pomc*$^{-/-}$ than in wild-type mice (Fig. 2C) and was increased by corticosterone treatment to levels equivalent to untreated wild-type mice. In contrast, corticosterone decreased hepatic PEPCK mRNA levels in wild-type mice (Fig. 2C).

Pomc$^{-/-}$ mice showed markedly higher circulating triglyceride levels (Fig. 3A) and hepatic lipid accumulation than wild-type mice (Fig. 3B), with sixfold higher levels of hepatic triglyceride ($P<0{\cdot}001$; Fig. 3C). However, corticosterone had no effect on plasma triglyceride levels in either genotype (Fig. 3A), nor did it worsen the liver phenotype (Fig. 3C). *Pomc*$^{-/-}$ and wild-type mice had similar plasma NEFA levels which were unaffected by corticosterone (Fig. 3D).

CORT drives hypertension in Pomc$^{-/-}$ *mice independently of adipose and liver RAS activation*

Pomc$^{-/-}$ mice had similar blood pressure to wild-type mice (Fig. 4A). Corticosterone markedly increased blood pressure only in *Pomc*$^{-/-}$ mice (Fig. 4A). Since hypertension following transgenic expression of 11β-HSD1 in adipose or liver is associated with increased levels of angiotensinogen in each of these tissues respectively (Masuzaki *et al.* 2001, Paterson *et al.* 2004), we hypothesised that a similar mechanism may drive corticosterone-mediated hypertension in *Pomc*$^{-/-}$ mice. We therefore examined key components of the RAS (Guyton 1991). *Pomc*$^{-/-}$ mice had higher hepatic angiotensinogen mRNA levels than controls (Fig. 4B). However, corticosterone did not alter hepatic angiotensinogen mRNA levels in either genotype (Fig. 4B). Consistent with lower intra-adipose GC action, adipose angiotensinogen mRNA levels were lower in *Pomc*$^{-/-}$ mice in all adipose depots (Fig. 4C). Corticosterone increased angiotensinogen mRNA levels specifically in epididymal adipose tissue of both genotypes (twofold increase; $P<0{\cdot}001$; Fig. 4C) but had no effect on angiotensinogen mRNA levels in inguinal or retroperitoneal adipose tissue of either genotype (Fig. 4C). Plasma angiotensinogen

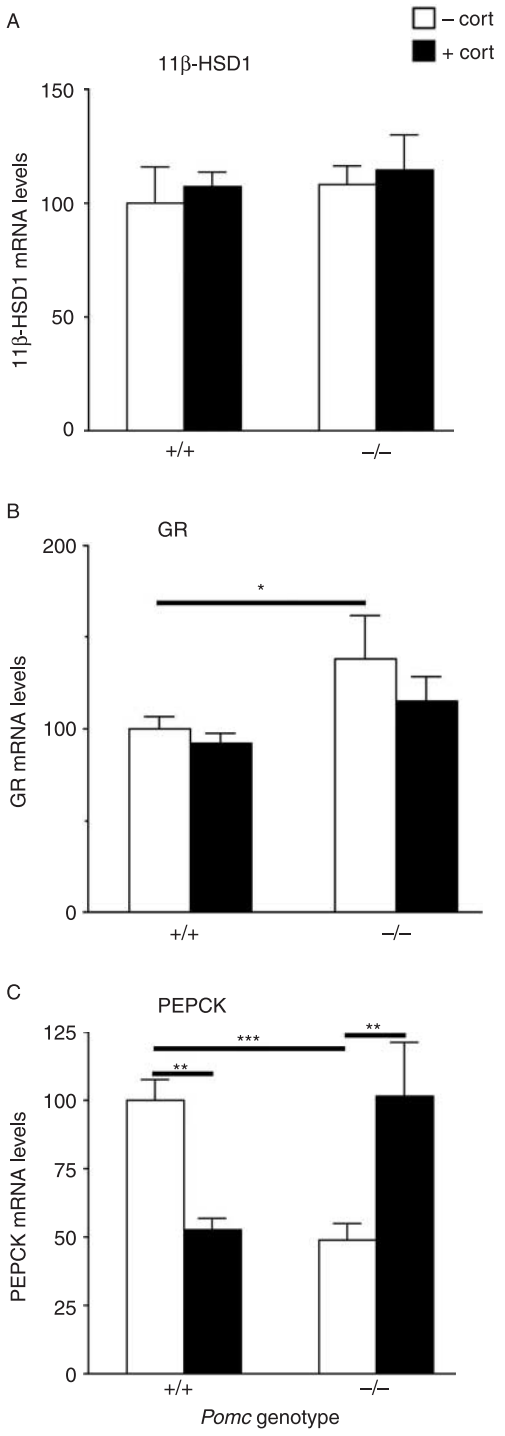

Figure 2 Mediators of GC action in the liver of *Pomc*$^{-/-}$ mice and effects of CORT treatment on GC target genes. Liver mRNA expression of (A) 11β-HSD1, (B) GR and (C) PEPCK in *Pomc*$^{-/-}$ (−/−) and wild-type (+/+) mice, either untreated or treated for 10 days with corticosterone (cort). Data are presented as percentages of the value in untreated control mice (100%) and are the means±S.E.M.; $n=5$ per group. Significance $^{*}P<0{\cdot}05$, $^{**}P<0{\cdot}01$ and $^{***}P<0{\cdot}001$.

concentrations did not differ with genotype or corticosterone (Fig. 4D). As has been found in another model of glucocorticoid-deficient obesity (Morton *et al.* 2005), plasma renin concentration was markedly higher in *Pomc*$^{-/-}$ mice (Fig. 4E) but this was unaffected by corticosterone (Fig. 4E).

Discussion

Increased glucocorticoid action specifically in adipose (Masuzaki *et al.* 2001) or liver (Paterson *et al.* 2004) produces distinct metabolic syndromes with hypertension. Increased GR sensitivity is also associated with altered fat distribution, hypertension and cardiometabolic disease (Buemann *et al.* 1997, Rosmond *et al.* 2000, Dobson *et al.* 2001, Ukkola *et al.* 2001*a*,*b*, van Rossum *et al.* 2003). We hypothesised that altered tissue regeneration of active glucocorticoid and/or peripheral tissue sensitivity to GCs might explain in part the exaggerated fat accumulation, insulin resistance (Coll *et al.* 2005) and the hypertension observed in *Pomc*$^{-/-}$ mice with glucocorticoid replacement.

With fixed circulating glucocorticoid levels, 11β-HSD1 and GR expression levels are the key determinants of GC action. *Pomc*$^{-/-}$ mice had lower adipose but similar hepatic levels of 11β-HSD1 mRNA levels to wild-type mice. Corticosterone treatment dramatically and more markedly increased 11β-HSD1 in the adipose tissue of *Pomc*$^{-/-}$ mice. This was accompanied by a marked increase in the expression of the glucocorticoid-inducible (Fried *et al.* 1993) gene *LPL*, which is consistent with the exaggerated accumulation of fat in these mice. Intriguingly, these data suggest that, at least in adipose tissue, 11β-HSD1 itself is a glucocorticoid target gene. This finding is consistent with most (Hammami & Siteri 1991, Jamieson *et al.* 1995, Voice *et al.* 1996, Bujalska *et al.* 1999), but not all (Napolitano *et al.* 1998) previous reports of glucocorticoid induction of 11β-HSD1 in a variety of cell types. Although not specifically measured here, increased adipose 11β-HSD1 activity is predicted to selectively amplify intra-adipose glucocorticoid concentrations, particularly when circulating levels of substrate are high. On the other hand, our data suggest that congenital glucocorticoid deficiency has little impact upon hepatic 11β-HSD1 levels *in vivo* and is not regulated by corticosterone. In contrast, 11β-HSD1 mRNA levels are highly and positively regulated by glucocorticoids in adipose tissue.

GR levels are another major determinant of cellular glucocorticoid sensitivity (Vanderbilt *et al.* 1987, Geley *et al.* 1996). Small differences in GR mRNA levels can markedly alter glucocorticoid responsiveness (Geley *et al.* 1996, Reichardt *et al.* 2000). *Pomc*$^{-/-}$ mice had elevated GR mRNA levels in liver and retroperitoneal adipose tissue, suggesting increased glucocorticoid sensitivity selectively in these depots. Following corticosterone replacement in *Pomc*$^{-/-}$ mice, GR mRNA levels were restored to wild-type levels in retroperitoneal adipose tissue but not in liver, consistent with tissue- and time-specific differences in GR

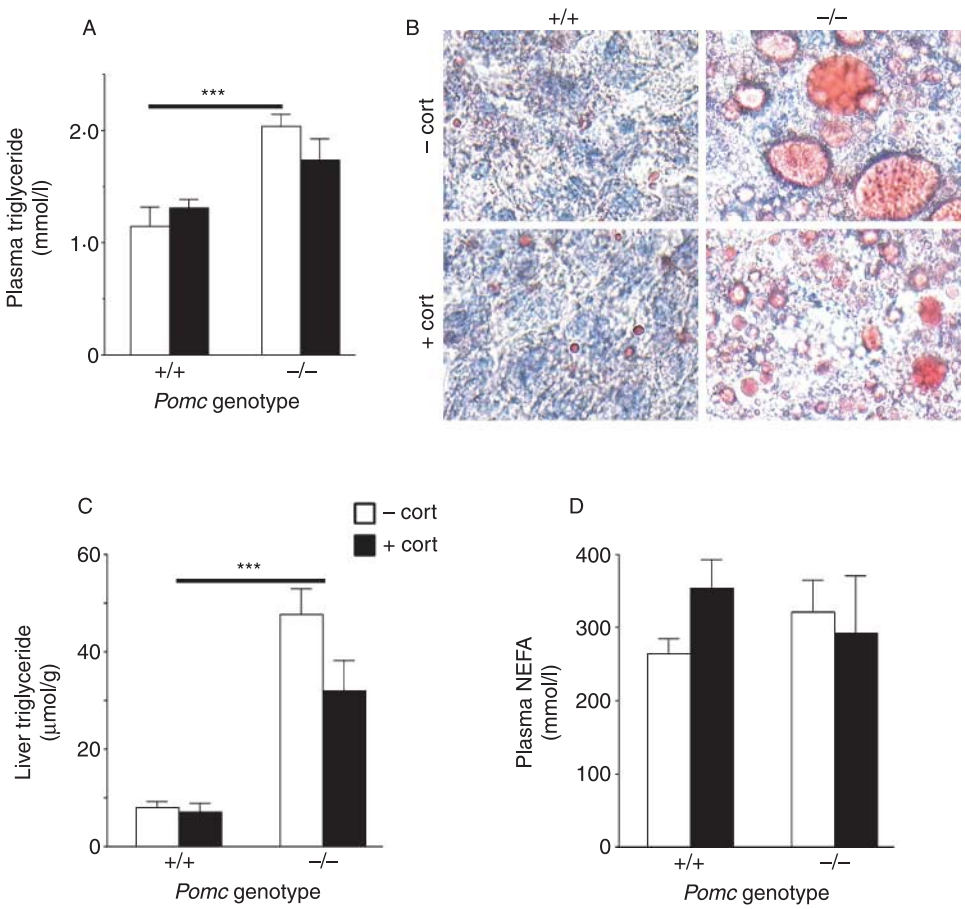

Figure 3 Dyslipidaemia and fatty liver in *Pomc*$^{-/-}$ mice. (A) Plasma triglyceride levels in *Pomc*$^{-/-}$ (−/−) and wild-type (+/+) mice, either untreated or treated for 10 days with corticosterone (cort). (B) Oil Red O staining of neutral lipid in liver sections of wild-type mice (+/+, left upper panel), CORT-treated wild-type mice (+/+, left bottom panel), *Pomc*$^{-/-}$ (−/−, right upper panel) and CORT-treated *Pomc*$^{-/-}$ (−/−, right bottom panel). Magnification is 40×; red, oil red O; blue, haematoxylin (nuclei). (C) Hepatic triglyceride content in *Pomc*$^{-/-}$ (−/−) and wild-type (+/+) mice, either untreated or treated for 10 days with corticosterone (cort). (D) Plasma levels of non-esterified fatty acids (NEFA) in *Pomc*$^{-/-}$ (−/−) and wild-type (+/+) mice, either untreated or treated for 10 days with corticosterone (cort). Data are means±S.E.M.; (n=6 per group). Significance ***$P<0{\cdot}001$.

autoregulation (Kalinyak *et al.* 1987, Dong *et al.* 1988, Sheppard *et al.* 1990, Holmes *et al.*, 1995, 1997, Reichardt *et al.* 2000).

Corticosterone had no additional effects on the hypertriglyceridaemia and fatty liver of the *Pomc*$^{-/-}$ mice, and did not affect plasma NEFAs, which were normal in *Pomc*$^{-/-}$ mice. The corticosterone-driven caloric excess in *Pomc*$^{-/-}$ mice may drive a further increase in the flux of triglycerides from the liver, that, coupled with increased adipose uptake via LPL, maintains the circulating and liver triglyceride levels constant and is consistent with increased adipose tissue mass in corticosterone-treated *Pomc*$^{-/-}$ mice (Coll *et al.* 2005).

Adipose PEPCK is critical for glyceroneogenesis and is thus a key regulator of the level of fatty acid re-esterification (reviewed in Reshef *et al.* 2003). Unexpectedly, since glucocorticoids reduce adipose PEPCK, glucocorticoid-deficient *Pomc*$^{-/-}$ mice had lower levels of PEPCK mRNA in all adipose depots. This was further decreased by corticosterone treatment. The lower level of PEPCK mRNA in untreated *Pomc*$^{-/-}$ mice may be due to their higher fed blood glucose levels (Nechushtan *et al.* 1987, Opherk *et al.* 2004), thus reducing the need for glyceroneogenesis to generate glycerol phosphate for fatty acid re-esterification. *Pomc*$^{-/-}$ mice have lower hepatic expression of PEPCK. This may not be due to the lack of glucocorticoid signalling in liver, as mice with a liver-specific knockout of GR have normal levels of PEPCK in liver (Opherk *et al.* 2004), but may be related to the higher circulating levels of insulin in *Pomc*$^{-/-}$ mice compared with wild-type (Coll *et al.* 2005). Insulin dominantly and negatively suppresses hepatic PEPCK in the fed state (Pilkis & Granner 1992). In corticosterone-treated wild-type mice, the repressive effect of insulin

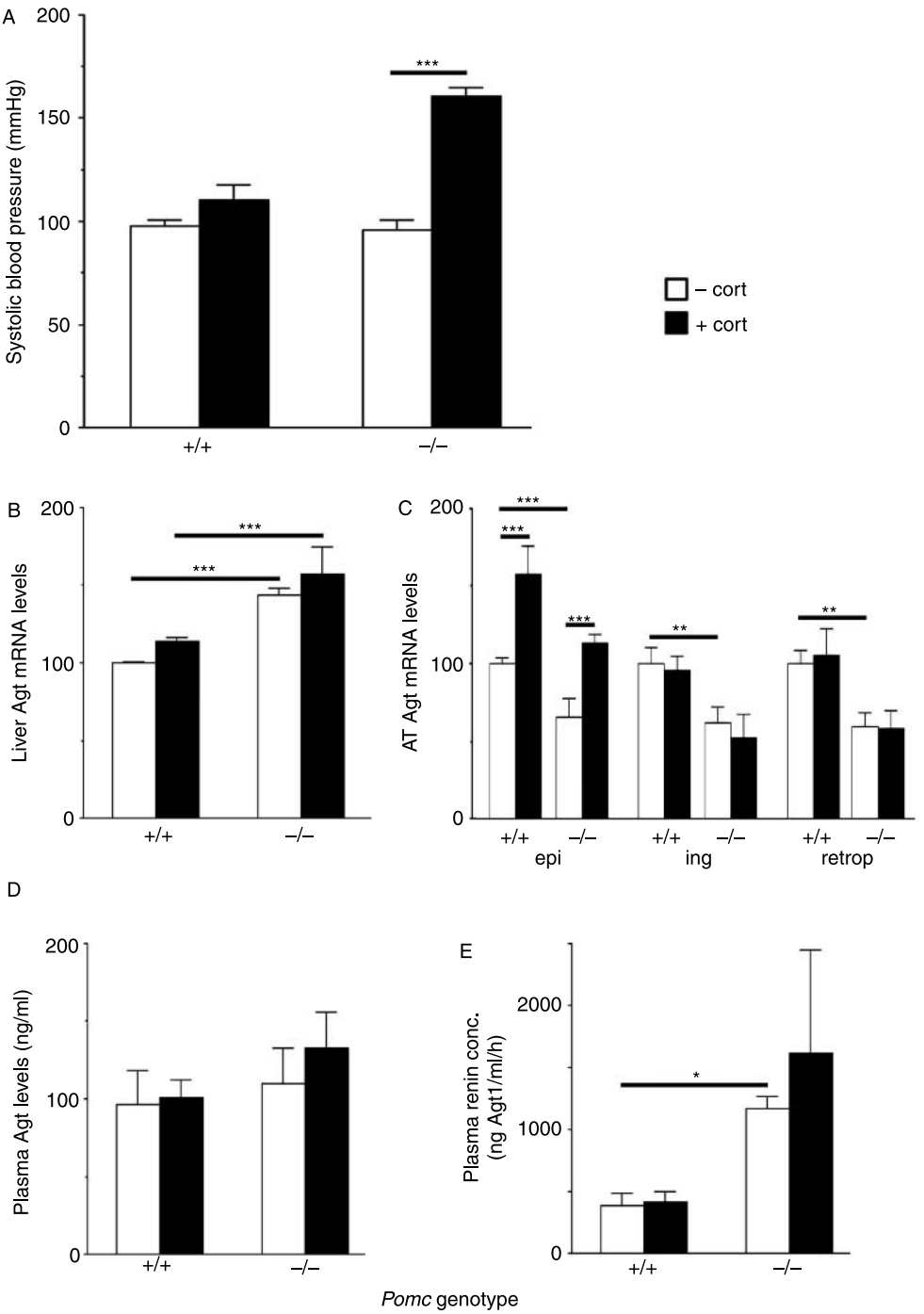

Figure 4 Corticosterone treatment increases blood pressure in *Pomc*$^{-/-}$ mice: effect of CORT treatment on the Renin-angiotensin system. Effect of 10 days corticosterone treatment (cort) on (A) systolic blood pressure, (B) renin concentration, (C) plasma angiotensinogen, (D) angiotensinogen (Agt) mRNA in adipose tissue (AT), and (E) angiotensinogen (Agt) mRNA levels in liver in wild-type (+/+) and *Pomc*$^{-/-}$ (−/−) mice. Epi, epididymal fat; ing, inguinal fat; retro, retroperitoneal fat. Data are means ± S.E.M., and for transcript levels are expressed relative to levels in untreated wild-type mice (100%); $n=5$ per group. Significance $^{*}P<0{\cdot}05$, $^{**}P<0{\cdot}01$ and $^{***}P<0{\cdot}001$.

predominated. Indeed, the decreased levels of PEPCK in these mice compared with untreated wild-type mice may reflect the increase in insulin levels following corticosterone (Coll *et al.* 2005). In contrast, hepatic PEPCK mRNA levels doubled following corticosterone treatment in *Pomc*$^{-/-}$ mice, consistent with hepatic insulin resistance and marked hyperinsulinaemia (Coll *et al.* 2005).

Blood pressure in *Pomc*$^{-/-}$ mice is normal despite their hypoadrenal state. This implies that secondary mechanisms are invoked to maintain cardiovascular function when circulating aldosterone and corticosterone concentrations are chronically reduced (Coll *et al.* 2004). It seems likely that the increased renin activity which we have observed in *Pomc*$^{-/-}$ mice is part of this adaptive process. However, corticosterone replacement did not normalise renin activity and selectively increased blood pressure in *Pomc*$^{-/-}$ mice. This was not attributed to a further activation of the circulating RAS, since neither renin nor its substrate angiotensinogen was increased. Indeed, the expression of angiotensinogen mRNA in liver and adipose tissues did not correlate with blood pressure. It seems likely that corticosterone augmented existing mechanisms that were already sustaining vascular function. Apart from renin, these secondary processes are likely to involve the hyperinsulinaemic (Sowers 2004) state of *Pomc*$^{-/-}$ mice (which is exacerbated by corticosterone treatment; Coll *et al.* 2005), the sympathetic nervous system (Rascher *et al.* 1979; which is thought to explain glucocorticoid-induced hypertension in normal mice) or structural adaptation of the vasculature (Wallerath *et al.* 2004).

In summary, we show that increased adipose tissue-specific sensitivity to glucocorticoids in *Pomc*$^{-/-}$ mice may result in part from exaggerated induction of 11β-HSD1 in adipose tissue with corticosterone administration. Whilst acknowledging that mRNA changes do not always translate to altered protein (or enzyme activity) levels, these data nevertheless suggest that 11β-HSD1 might be a more potent mediator of intra-adipose GC action than the GR levels, whereas in liver, higher GR levels contribute to the diabetogenic phenotype of the *Pomc*$^{-/-}$ mice.

Acknowledgements

We thank Keith Burling for assistance with plasma hormone and lipid measurements and members of the Endocrinology Unit, QMRI for helpful comments and discussions. The authors declare that there is no conflict of interest that would prejudice the impartiality of this scientific work.

Funding

This work has been supported by the Wellcome Trust Programme grant (J R S and K EC), by separate MRC Programme grants to S O'R and C J K and by the EU Sixth Framework Programme Diabesity. Z M is supported by the Wellcome Trust PhD studentship, A P C by an MRC Clinician Scientist Award and N M M by the Wellcome Trust Research Career Development Fellowship.

References

Andrew R, Smith K, Jones GC & Walker BR 2002 Distinguishing the activities of 11β-hydroxysteroid dehydrogenases *in vivo* using isotopically labeled cortisol. *Journal of Clinical Endocrinology and Metabolism* **87** 277–285.

Buemann B, Vohl MC, Chagnon M, Chagnon YC, Gagnon J, Perusse L, Dionne F, Despres JP, Tremblay A, Nadeau A *et al.* 1997 Abdominal visceral fat is associated with a BclI restriction fragment length polymorphism at the glucocorticoid receptor gene locus. *Obesity Research* **5** 186–192.

Bujalska IJ, Kumar S, Hewison M & Stewart PM 1999 Differentiation of adipose stromal cells: the roles of glucocorticoids and 11β-hydroxysteroid dehydrogenase. *Endocrinology* **140** 3188–3196.

Challis BG, Coll AP, Yeo GS, Pinnock SB, Dickson SL, Thresher RR, Dixon J, Zahn D, Rochford JJ, White A *et al.* 2004 Mice lacking pro-opiomelanocortin are sensitive to high-fat feeding but respond normally to the acute anorectic effects of peptide-YY3-36. *PNAS* **101** 4695–4700.

Coll AP, Challis BG, Yeo GS, Snell K, Piper SJ, Halsall D, Thresher RR & O'Rahilly S 2004 The effects of pro-opiomelanocortin deficiency on murine adrenal development and responsiveness to adrenocorticotropin. *Endocrinology* **145** 4721–4727.

Coll AP, Challis BG, Lopez M, Piper S, Yeo GS & O'Rahilly S 2005 Proopiomelanocortin-deficient mice are hypersensitive to the adverse metabolic effects of glucocorticoids. *Diabetes* **54** 2269–2276.

Dallman MF, Strack AM, Akana SF, Bradbury MJ, Hanson ES, Scribner KA & Smith M 1993 Feast and famine: critical role of glucocorticoids with insulin in daily energy flow. *Frontiers in Neuroendocrinology* **14** 303–347.

Debons AF, Siclari E, Das KC & Fuhr B 1982 Gold thioglucose-induced hypothalamic damage, hyperphagia, and obesity: dependence on the adrenal gland. *Endocrinology* **110** 2024–2029.

Dobson MG, Redfern CP, Unwin N & Weaver JU 2001 The N363S polymorphism of the glucocorticoid receptor: potential contribution to central obesity in men and lack of association with other risk factors for coronary heart disease and diabetes mellitus. *Journal of Clinical Endocrinology and Metabolism* **86** 2270–2274.

Dong Y, Poellinger L, Gustafsson J-Å & Okret S 1988 Regulation of glucocorticoid receptor expression: evidence for transcriptional and posttranslational mechanisms. *Molecular Endocrinology* **2** 1256–1264.

Flier JS 2004 Obesity wars: molecular progress confronts an expanding epidemic. *Cell* **116** 337–350.

Freedman MR, Horwitz BA & Stern JS 1986 Effect of adrenalectomy and glucocorticoid replacement on development of obesity. *American Journal of Physiology* **250** R595–R607.

Fried SK, Russell CD, Grauso NL & Brolin RE 1993 Lipoprotein lipase regulation by insulin and glucocorticoid in subcutaneous and omental adipose tissues of obese women and men. *Journal of Clinical Investigation* **92** 2191–2198.

Geley S, Hartmann BL, Hala M, Strasser-Wozak EM, Kapelari K & Kofler R 1996 Resistance to glucocorticoid-induced apoptosis in human T-cell acute lymphoblastic leukemia CEM-C1 cells is due to insufficient glucocorticoid receptor expression. *Cancer Research* **56** 5033–5038.

Guyton AC 1991 Blood pressure control: special role of the kidneys and body fluids. *Science* **252** 1813–1816.

Hammami MM & Siiteri PK 1991 Regulation of 11β-hydroxysteroid dehydrogenase activity in human skin fibroblasts: enzymatic modulation of glucocorticoid action. *Journal of Clinical Endocrinology and Metabolism* **73** 326–334.

Holmes MC, Yau JLW, French KL & Seckl JR 1995 The effect of adrenalectomy on 5-hydroxytryptamine and corticosteroid receptor subtype messenger RNA expression in rat hippocampus. *Neuroscience* **64** 327–337.

Holmes MC, French KL & Seckl JR 1997 Dysregulation of diurnal rhythms of serotonin 5-HT2C and corticosteroid receptor gene expression in the hippocampus with food restriction and glucocorticoids. *Journal of Neuroscience* **17** 4056–4065.

Jamieson PM, Chapman KE, Edwards CRW & Seckl JR 1995 11β-Hydroxysteroid dehydrogenase is an exclusive 11β-reductase in primary cultures of rat hepatocytes: effect of physicochemical and hormonal manipulations. *Endocrinology* **136** 4754–4761.

Jamieson PM, Walker BR, Chapman KE, Andrew R, Rossiter S & Seckl JR 2000 11β-Hydroxysteroid dehydrogenase type 1 is a predominant 11β-reductase in the intact perfused rat liver. *Journal of Endocrinology* **165** 685–692.

Kalinyak JE, Dorin RI, Hoffman AR & Perlman AJ 1987 Tissue-specific regulation of glucocorticoid receptor mRNA by dexamethasone. *Journal of Biological Chemistry* **262** 10441–10444.

Kannisto K, Pietilainen KH, Ehrenborg E, Rissanen A, Kaprio J, Hamsten A & Yki-Jarvinen H 2004 Overexpression of 11β-hydroxysteroid dehydrogenase-1 in adipose tissue is associated with acquired obesity andfeatures of insulin resistance: studies in young adult monozygotic twins. *Journal of Clinical Endocrinology and Metabolism* **89** 4414–4421.

Kellendonk C, Eiden S, Kretz O, Schutz G, Schmidt I, Tronche F & Simon E 2002 Inactivation of the GR in the nervous system affects energy accumulation. *Endocrinology* **143** 2333–2340.

Kotelevtsev Y, Holmes MC, Burchell A, Houston PM, Schmoll D, Jamieson P, Best R, Brown R, Edwards CRW, Seckl JR *et al.* 1997 11β-Hydroxysteroid dehydrogenase type 1 knockout mice show attenuated glucocorticoid inducible responses and resist hyperglycaemia on obesity or stress. *PNAS* **94** 14924–14929.

Krude H, Biebermann H, Luck W, Horn R, Brabant G & Gruters A 1998 Severe early-onset obesity, adrenal insufficiency and red hair pigmentation caused by POMC mutations in humans. *Nature Genetics* **19** 155–157.

Lindsay RS, Wake DJ, Nair S, Bunt J, Livingstone DE, Permana PA, Tataranni PA & Walker BR 2003 Subcutaneous adipose 11β-hydroxysteroid dehydrogenase type 1 activity and messenger ribonucleic acid levels are associated with adiposity and insulinemia in Pima Indians and Caucasians. *Journal of Clinical Endocrinology and Metabolism* **88** 2738–2744.

Livingstone DEW, Jones GC, Smith K, Jamieson PM, Andrew R, Kenyon CJ & Walker BR 2000 Understanding the role of glucocorticoids in obesity: tissue-specific alterations of corticosterone metabolism in obese Zucker rats. *Endocrinology* **141** 560–563.

Makimura H, Mizuno TM, Roberts J, Silverstein J, Beasley J & Mobbs CV 2000 Adrenalectomy reverses obese phenotype and restores hypothalamic melanocortin tone in leptin-deficient ob/ob mice. *Diabetes* **49** 1917–1923.

Masuzaki H, Paterson J, Shinyama H, Morton NM, Mullins JJ, Seckl JR & Flier JS 2001 A transgenic model of visceral obesity and the metabolic syndrome. *Science* **294** 2166–2170.

Masuzaki H, Yamamoto H, Kenyon CJ, Elmquist JK, Morton NM, Paterson JM, Shinyama H, Sharp MG, Fleming S, Mullins JJ *et al.* 2003 Transgenic amplification of glucocorticoid action in adipose tissue causes high blood pressure in mice. *Journal of Clinical Investigation* **112** 83–90.

Morton NM, Holmes MC, Fiévet C, Staels B, Tailleux A, Mullins JJ & Seckl JR 2001 Improved lipid and lipoprotein profile, hepatic insulin sensitivity, and glucose tolerance in 11β-hydroxysteroid dehydrogenase type 1 null mice. *Journal of Biological Chemistry* **276** 41293–41300.

Morton NM, Paterson JM, Masuzaki H, Holmes MC, Staels B, Fievet C, Walker BR, Flier JS, Mullins JJ & Seckl JR 2004 Novel adipose tissue mediated resistance to diet-induced visceral obesity in 11β-hydroxysteroid dehydrogenase type 1-deficient mice. *Diabetes* **53** 931–938.

Morton NM, Densmore V, Wamil M, Ramage L, Nichol K, Bunger L, Seckl JR & Kenyon CJ 2005 A polygenic model of the metabolic syndrome with reduced circulating and intra-adipose glucocorticoid action. *Diabetes* **54** 3371–3378.

Napolitano A, Voice MW, Edwards CRW, Seckl JR & Chapman KE 1998 11β-Hydroxysteroid dehydrogenase 1 in adipocytes: expression is differentiation-dependent and hormonally regulated. *Journal of Steroid Biochemistry and Molecular Biology* **64** 251–260.

Nechushtan H, Benvenisty N, Brandeis R & Reshef L 1987 Glucocorticoids control phosphoenolpyruvate carboxykinase gene expression in a tissue specific manner. *Nucleic Acids Research* **15** 6405–6417.

Opherk C, Tronche F, Kellendonk C, Kohlmuller D, Schulze A, Schmid W & Schutz G 2004 Inactivation of the glucocorticoid receptor in hepatocytes leads to fasting hypoglycemia and ameliorates hyperglycemia in streptozotocin-induced diabetes mellitus. *Molecular Endocrinology* **18** 1346–1353.

Paterson JM, Morton NM, Fiévet C, Kenyon CJ, Holmes MC, Staels B, Seckl JR & Mullins JJ 2004 Metabolic syndrome without obesity: hepatic overexpression of 11β-hydroxysteroid dehydrogenase type 1 in transgenic mice. *PNAS* **101** 7088–7093.

Paulmyer-Lacroix O, Boullu S, Oliver C, Alessi MC & Grino M 2002 Expression of the mRNA coding for 11β-hydroxysteroid dehydrogenase type 1 in adipose tissue from obese patients: an *in situ* hybridization study. *Journal of Clinical Endocrinology and Metabolism* **87** 2701–2705.

Pilkis SJ & Granner DK 1992 Molecular physiology of the regulation of hepatic gluconeogenesis and glycolysis. *Annual Review of Physiology* **54** 885–909.

Rascher W, Dietz R, Schomig A, Burkart G, Luth JB, Mann JF & Weber J 1979 Modulation of sympathetic vascular tone by prostaglandins in corticosterone-induced hypertension in rats. *Clinical Science* **57** 235s–237s.

Rask E, Olsson T, Söderberg S, Andrew R, Livingstone DE, Johnson O & Walker BR 2001 Tissue-specific dysregulation of cortisol metabolism in human obesity. *Journal of Clinical Endocrinology and Metabolism* **86** 1418–1421.

Reichardt HM, Umland T, Bauer A, Kretz O & Schütz G 2000 Mice with an increased glucocorticoid receptor gene dosage show enhanced resistance to stress and endotoxic shock. *Molecular and Cellular Biology* **20** 9009–9017.

Reshef L, Olswang Y, Cassuto H, Blum B, Croniger CM, Kalhan SC, Tilghman SM & Hanson RW 2003 Glyceroneogenesis and the triglyceride/fatty acid cycle. *Journal of Biological Chemistry* **278** 30413–31416.

Rosmond R, Chagnon YC, Holm G, Chagnon M, Pérusse L, Lindell K, Carlsson B, Bouchard C & Björntorp P 2000 A glucocorticoid receptor gene marker is associated with abdominal obesity, leptin, and dysregulation of the hypothalamic–pituitary–adrenal axis. *Obesity Research* **8** 211–218.

van Rossum EF, Koper JW, van den Beld AW, Uitterlinden AG, Arp P, Ester W, Janssen JA, Brinkmann AO, de Jong FH, Grobbee DE *et al.* 2003 Identification of the BclI polymorphism in the glucocorticoid receptor gene: association with sensitivity to glucocorticoids *in vivo* and body mass index. *Clinical Endocrinology* **59** 585–592.

Sainsbury A, Cusin I, Rohner-Jeanrenaud F & Jeanrenaud B 1997 Adrenalectomy prevents the obesity syndrome produced by chronic central neuropeptide Y infusion in normal rats. *Diabetes* **46** 209–214.

Saruta T 1996 Mechanism of glucocorticoid-induced hypertension. *Hypertension Research* **19** 1–8.

Sasaki K, Cripe TP, Koch SR, Andreone TL, Petersen DD, Beale EG & Granner DK 1984 Multihormonal regulation of phosphoenolpyruvate carboxykinase gene transcription. The dominant role of insulin. *Journal of Biological Chemistry* **259** 15242–15251.

Sheppard KE, Roberts JL & Blum M 1990 Differential regulation of type II corticosteroid receptor messenger ribonucleic acid expression in the rat anterior pituitary and hippocampus. *Endocrinology* **127** 431–439.

Sowers JR 2004 Insulin resistance and hypertension. *American Journal of Physiology. Heart and Circulatory Physiology* **286** H1597–H1602.

Ukkola O, Pérusse L, Weisnagel SJ, Bergeron J, Després JP, Rao DC & Bouchard C 2001*a* Interactions among the glucocorticoid receptor, lipoprotein lipase, and adrenergic receptor genes and plasma insulin and lipid levels in the Quebec Family Study. *Metabolism* **50** 246–252.

Ukkola O, Rosmond R, Tremblay A & Bouchard C 2001*b* Glucocorticoid receptor Bcl I variant is associated with an increased atherogenic profile in response to long-term overfeeding. *Atherosclerosis* **157** 221–224.

Vanderbilt JN, Miesfeld R, Maler BA & Yamamoto KR 1987 Intracellular receptor concentration limits glucocorticoid-dependent enhancer activity. *Molecular Endocrinology* **1** 68–74.

Voice MW, Seckl JR, Edwards CRW & Chapman KE 1996 11β-Hydroxysteroid dehydrogenase type 1 expression in 2S-FAZA hepatoma cells is hormonally regulated; a model system for the study of hepatic glucocorticoid metabolism. *Biochemical Journal* **317** 621–625.

Wallerath T, Godecke A, Molojavyi A, Li H, Schrader J & Forstermann U 2004 Dexamethasone lacks effect on blood pressure in mice with a disrupted endothelial NO synthase gene. *Nitric Oxide* **10** 36–41.

Whitworth JA, Schyvens CG, Zhang Y, Mangos GJ & Kelly JJ 2001 Glucocorticoid-induced hypertension: from mouse to man. *Clinical and Experimental Pharmacology and Physiology* **28** 993–996.

Yaswen L, Diehl N, Brennan MB & Hochgeschwender U 1999 Obesity in the mouse model of pro-opiomelanocortin deficiency responds to peripheral melanocortin. *Nature Medicine* **5** 1066–1070.

Received in final form 16 April 2007
Accepted 1 May 2007
Made available online as an Accepted Preprint
8 May 2007

Omental 11β-hydroxysteroid Dehydrogenase 1 Correlates with Fat Cell Size Independently of Obesity

Zoi Michailidou, Michael D. Jensen,† Daniel A. Dumesic,† Karen E. Chapman,* Jonathan R. Seckl,* Brian R. Walker,* and Nicholas M. Morton**

Abstract

MICHAILIDOU, ZOI, MICHAEL D. JENSEN, DANIEL A. DUMESIC, KAREN E. CHAPMAN, JONATHAN R. SECKL, BRIAN R. WALKER, AND NICHOLAS M. MORTON. Omental 11β-hydroxysteroid dehydrogenase 1 correlates with fat cell size independently of obesity. *Obesity.* 2007;15:1155–1163.

Objectives: In ideopathic obesity, there is evidence that enhanced cortisol regeneration within abdominal subcutaneous adipose tissue may contribute to adiposity and metabolic disease. Whether the cortisol regenerating enzyme, 11β-hydroxysteroid dehydrogenase type 1 (11βHSD1), or glucocorticoid receptor (GRα) levels are altered in other adipose depots remains uncertain. Our objective was to determine the association between 11βHSD1 and GRα mRNA levels in four distinct adipose depots and measures of obesity and the metabolic syndrome.

Research Methods and Procedures: Adipose tissue biopsies were collected from subcutaneous (abdominal, thigh, gluteal) and intra-abdominal (omental) adipose depots from 21 women. 11βHSD1 and GRα mRNA levels were measured by real-time polymerase chain reaction. Body composition, fat distribution, fat cell size, and blood lipid, glucose, and insulin levels were measured.

Results: 11βHSD1 mRNA was highest in abdominal subcutaneous ($p < 0.001$) and omental ($p < 0.001$) depots and was positively correlated with BMI and visceral adiposity in all depots. Omental 11βHSD1 correlated with percent body fat ($R = 0.462$, $p < 0.05$), fat cell size ($R = 0.72$, $p < 0.001$), and plasma triglycerides ($R = 0.46$, $p < 0.05$). Conversely, GRα mRNA was highest in omental fat ($p < 0.001$). GRα mRNA was negatively correlated with BMI in the abdominal subcutaneous ($R = -0.589$, $p < 0.05$) and omental depots ($R = -0.627$, $p < 0.05$). Omental GRα mRNA was inversely associated with visceral adiposity ($R = -0.507$, $p < 0.05$), fat cell size ($R = -0.52$, $p < 0.01$), and triglycerides ($R = -0.50$, $p < 0.05$).

Discussion: Obesity was associated with elevated 11βHSD1 mRNA in all adipose compartments. GRα mRNA is reduced in the omental depot with obesity. The novel correlation of 11βHSD1 with omental fat cell size, independent of obesity, suggests that intracellular cortisol regeneration is a strong predictor of hypertrophy in the omentum.

Key words: abdominal obesity, omental, adipose tissue, 11β-hydroxysteroid

Introduction

Visceral obesity is associated with an increased risk for type 2 diabetes, hyperlipidemia, and hypertension (the metabolic syndrome) (1,2). In contrast, comparable amounts of fat stored preferentially in gluteal or femoral depots (lower body obesity) showed lower risk of morbidity and mortality from metabolic abnormalities (3). Exposure to high circulating glucocorticoid (GC)[1] levels, as found in Cushing's syndrome, causes a metabolic disease that resembles features of idiopathic metabolic syndrome including pro-

Received for review July 30, 2006.

Accepted in final form November 15, 2006.

The costs of publication of this article were defrayed, in part, by the payment of page charges. This article must, therefore, be hereby marked "advertisement" in accordance with 18 U.S.C. Section 1734 solely to indicate this fact.

*Endocrinology Unit, Centre for Cardiovascular Science, Queen's Medical Research Institute, University of Edinburgh, Edinburgh, United Kingdom; and †Division of Endocrinology and Metabolism, Department of Internal Medicine, the Mayo Clinic, Rochester, Minnesota. Address correspondence to Nicholas M. Morton, Endocrinology Unit, Centre for Cardiovascular Science, Queen's Medical Research Institute, University of Edinburgh, 47 Little France Crescent, Edinburgh EH16 4TJ, UK.

E-mail: Nik.Morton@ed.ac.uk

Copyright © 2007 NAASO

[1] Nonstandard abbreviations: GC, glucocorticoid; 11βHSD1, 11β-hydroxysteroid dehydrogenase type 1; GRα, glucocorticoid receptor α; HOMA-IR, homeostasis model of assessment insulin resistance index; VAT, visceral adipose tissue; SAT, subcutaneous adipose tissue.

nounced visceral obesity (4). However, idiopathic obesity is not associated with high circulating GC levels (4). Rather, it seems that intracellular generation of active from inactive GCs by the enzyme 11β-hydroxysteroid dehydrogenase type 1 (11βHSD1) is aberrantly elevated in adipose tissue of obese individuals (4). Thus, we and others have shown that 11βHSD1 mRNA and activity are elevated in abdominal subcutaneous adipose tissue from obese compared with non-obese individuals (5–10) and in adipose depots in monogenic obesity in rodents (11,12). In vivo microdialysis confirmed increased abdominal subcutaneous adipose regeneration of cortisol from cortisone in human obesity (13). Given the key association of intra-abdominal (visceral) adipose tissue in metabolic and cardiovascular risk, it has been hypothesized that increased 11βHSD1 in the visceral, rather than subcutaneous, adipose depot causes the adverse metabolic consequences of idiopathic obesity and the metabolic syndrome (14). This hypothesis has been supported by the observation that transgenic mice overexpressing 11βHSD1 in adipose tissue develop visceral obesity and the phenotype of the metabolic syndrome (12,15). Conversely, global 11βHSD1 knockout mice are protected from the metabolic consequences of dietary obesity, at least in part, through adipose tissue insulin sensitization and fat redistribution away from the visceral depot (16,17). However, Tomlinson et al. (18) reported a negative association between omental 11βHSD1 activity and BMI in primary omental human adipocytes cultured in vitro, although there was no correlation in whole adipose biopsies. A further study could not detect increased portal vein cortisol (19) or increased splanchnic cortisol production rates (20) in obesity, suggesting that if cortisol generation is indeed elevated in visceral fat, it is further metabolized or is not released at higher rates from adipocytes. Together, these data have engendered some confusion as to whether visceral and subcutaneous 11βHSD1 is elevated in human obesity. Mechanistically, GCs induce adipose tissue expansion by stimulating preadipocyte differentiation (21) and lipoprotein lipase-mediated triglyceride accumulation (22,23). A key factor in this process is tissue levels of the intracellular glucocorticoid receptor α (GRα). In contrast to the plethora of studies (5–10,14) of 11βHSD1 in adipose tissue and metabolic syndrome, curiously few studies have examined associations between GR and such parameters. Genetic studies strongly support the role of the GC receptor in determining body composition and fat distribution (24,25). Higher levels of GR found in omental compared with subcutaneous fat (26) would further be expected to have a more pronounced effect on GC action in the omental depot. However, our previous study showed no correlation between adipose tissue GR mRNA in abdominal subcutaneous adipose tissue and obesity (10), whereas Kannisto et al. (9) reported an inverse correlation between subcutaneous adipose GRα mRNA and BMI. Here we hypothesized that high adipose 11βHSD1, but not GR, mRNA levels predicts obesity in visceral and subcutaneous fat depots in women.

Research Methods and Procedures

Subjects

Informed, written consent was obtained from 21 women undergoing elective, laparoscopic tubal ligation surgery; the study was approved by the Mayo Clinic Institutional Review Board. Tubal ligation surgery was done routinely in the follicular phase of the menstrual cycle to eliminate the risk of pregnancy. Before surgery, body composition was assessed by measuring weight, height, body fatness (% fat) using DXA (DPX-IQ; Lunar Radiation, Madison, WI), and abdominal fat distribution using a single sliced computerized tomography scan at the L_2–L_3 level (27,28). Visceral and subcutaneous adipose tissue areas were calculated as previously described (28). Although 8 of 21 subjects were taking oral contraceptives, there was no effect on our variables by Student's *t* test, and the data were pooled.

Blood Assays. Fasting plasma triglycerides, glucose, and insulin levels were assayed as previously described (29). Homeostasis model of assessment insulin resistance index (HOMA-IR) was calculated by the following equation: fasting insulin (μU/mL) $\times$ fasting glucose (mM)/22.5 (30).

Adipose Tissue Biopsies. Subcutaneous fat from abdominal ($n = 13$), thigh ($n = 16$), and gluteal ($n = 18$) regions were collected just before surgery and omental ($n = 21$) adipose biopsies were obtained intraoperatively. The tissue was washed to remove blood and snap frozen in liquid nitrogen and stored at -80 °C. Biopsies were homogenized in 1 to 2 mL Trizol (Gibco BRL, Paisley, United Kingdom). RNA was extracted using RNAid+ binding matrix (Anachem, Luton, UK) and eluted in diethylpyrocarbonate-treated water, containing 10 mM dithiothreitoland 400 U/mL RNasin (Promega, Southampton, UK). Total RNA was quantified using a spectrophotometer at A_{260}.

RNA integrity was verified by agarose gel electrophoresis. Oligo dT-primed cDNA was synthesized from 0.5 μg of RNA samples using the Promega Reverse Transcription System (Promega, Madison, WI). GRα and 11βHSD1 mRNA levels were quantified by real-time polymerase chain reaction primer-probe sets using the ABI PRISM 7700/7900 Sequence Detection System (Applied Biosystems, Foster City, CA). The primers and probes used are as follows: 11βHSD1, 5′-GGAATATTCAGTGTCCAGGGTCAA-3′ (forward), 5′-TGATCTCCAGGGCACATTCCT-3′ (reverse) and 5′-6-FAM-ACATTGACAACCTTCGCTGGGAGG-TAMRA-3′ (probe); GRα, 5′-CATTGTCAAGAGGGAA-GGAAACTC-3′ (forward), 5′-ATTTTCAACCACTTCAT-GCATAGAA-3′ (reverse), and 5′-6-FAM-TTGTCAGT-TGATAAAACCGCTGCCAGTTCT-TAMRA-3′ (probe). Levels of GRα or 11βHSD1 mRNA are reported relative to human cyclophilin A RNA (Applied Biosystems, Cheshire,

United Kingdom) as previously optimized (10) and are expressed in arbitrary units. Standard curves for primer-probe sets and real-time polymerase chain reaction analysis were performed as previously described (10). Fat cell size (mean diameter of mature adipocytes in micrometers) was determined using the AdCount (Biomedical Imaging Resource, Rochester, MN) approach as previously described (31).

Statistical Analysis

Repeated-measures ANOVA followed by Tukey post hoc test were performed to determine differences in transcript levels in paired adipose compartments. Pearson correlation was performed to examine the relationships between anthropometric and metabolic parameters with 11βHSD1 or GRα mRNA levels in different fat depots according to a priori hypotheses to minimize multiple interdependent variables. Multiple linear regression was performed to test whether relationships between fat cell sizes or triglycerides with transcript levels are independent of obesity. Data were tested for normality and were normalized by log transformation where appropriate.

Data are means ± standard error unless otherwise stated. Differences were considered significant at $p < 0.05$. All statistical analyses were performed using Sigma Stat 3.1 software (Systat Software Inc., San Jose, CA).

Results

Subject Characteristics

Volunteers were white women 35 ± 1 years of age with a mean BMI of 32.7 ± 1.5 kg/m^2 (Table 1), indicating an obese group. Their median ± interquartile range fasting insulin was 15.6 ± 19.6 μU/mL, and HOMA-IR as 3.3 ± 4.6 (range, 0.42 to 47). Median fasting glucose and mean triglyceride concentrations averaged 4.9 ± 0.44 mM and 148 ± 19 mg/dL, respectively (Table 1).

Comparison of 11βHSD1 and GRα mRNA Levels in Multiple Fat Depots

11βHSD1 mRNA levels were greater in subcutaneous abdominal and omental adipose tissues than in other subcutaneous tissues (gluteal, thigh; Figure 1A). 11βHSD1 mRNA levels were positively correlated in the three subcutaneous depots: abdominal subcutaneous vs. thigh ($R = 0.83$, $p < 0.005$) and abdominal vs. gluteal ($R = 0.86$, $p < 0.005$). There were no associations between abdominal subcutaneous and omental 11βHSD1 mRNA levels. GRα mRNA expression levels were highest in omental and lowest in thigh subcutaneous adipose tissue (Figure 1B) but were not correlated between any compartments. No correlation was found between 11βHSD1 and GRα mRNA levels in any depot (data not shown).

Table 1. Anthropometric and metabolic characteristics of study participants

	Women ($n = 21$)
Anthropometry	
Age (yrs)	35.3 ± 1.4 (20 to 44)
BMI (kg/m^2)	32.7 ± 1.5 (20 to 42)
Body fat (%)	46 ± 2 (23 to 56)
VAT area (cm^2)	96 ± 16.3 (23 to 236)
SAT area (cm^2)	326 ± 35 (59 to 577)
VAT/SAT	0.28 ± 0.03 (0.11 to 0.64)
Plasma biochemistry	
Fasting glucose (mM)	4.9 ± 0.44 (4.1 to 7.0)
Fasting insulin (μU/mL)	16.5 ± 3.5 (2.2 to 64.3)
Fasting triglyceride (mg/dL)	146.7 ± 18.7 (38 to 278)

VAT, visceral adipose tissue; SAT, subcutaneous adipose tissue. Data are presented as mean ± standard error. For glucose, data are presented as median ± interquartile range. Range values in parentheses.

Association of Obesity with Elevated 11βHSD1 but Reduced GRα mRNA in Omental Fat

A strong positive association between BMI and omental adipose 11βHSD1 mRNA levels was observed ($R = 0.570$; Figure 2A; Table 2; $p < 0.01$). Moreover, visceral fat tissue [visceral adipose tissue (VAT)] area by computed tomography was correlated with increased 11βHSD1 mRNA levels in the omentum (Figure 2B; Table 2). Omental 11βHSD1 mRNA levels were consistently and positively associated with general adiposity (as defined by percent of body fat; $R = 0.462$, $p < 0.05$) and with subcutaneous/peripheral adiposity (Table 2). In contrast, obesity was associated with decreased GRα mRNA levels in the omental depot ($R = -0.627$, $p < 0.001$; Figure 2D; Table 2). Visceral adiposity (Figure 2E) was negatively correlated with omental GRα mRNA levels (VAT; $R = -0.507$, $p < 0.05$).

Association of Omental Fat Cell Hypertrophy with Increased 11βHSD1 but Reduced GRα

Fat cells were smaller in the omental depot than in subcutaneous adipose tissue (SAT) (omental, 84 ± 4 μm; vs. abdominal subcutaneous, thigh, gluteal, 104 ± 3, 109 ± 3, and 106 ± 2 μm, respectively; $p < 0.0001$). Omental fat cell size was positively correlated ($R = 0.72$, $p < 0.001$) with 11βHSD1 mRNA levels (Figure 2C; Table 2). In contrast, GRα transcript levels were negatively correlated with omental fat cell size (Figure 2F; Table 2). To test for independent effects, multiple regression analyses were performed to understand the effects of obesity (BMI) and fat cell size on 11βHSD1 or GRα mRNA. Omental fat cell size

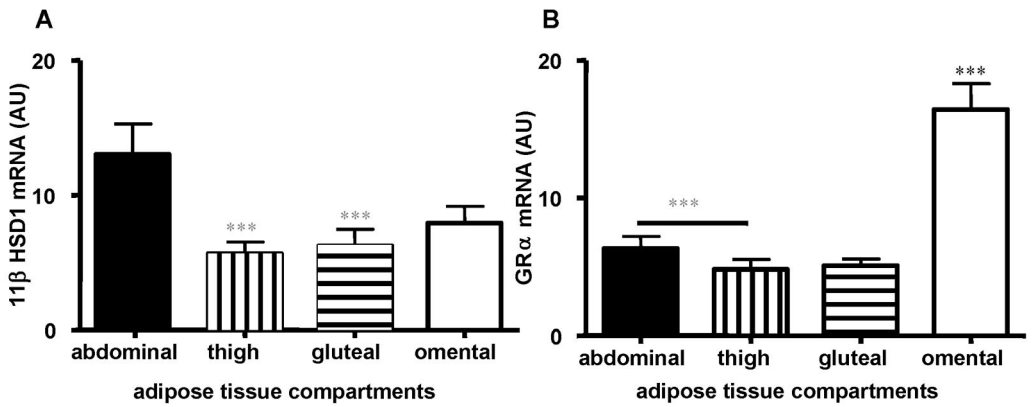

Figure 1: 11βHSD1 and GRα mRNA levels in multiple adipose tissue compartments in women. (A) 11βHSD1 mRNA levels were higher in abdominal and omental compared with thigh and gluteal adipose tissues. (B) GRα mRNA levels were higher in omental and lower in thigh compared with the other adipose tissue compartments. Data are presented as mean ± standard error.

was strongly and independently correlated with 11βHSD1 (standardized β coefficient, 1.2; $p < 0.05$), whereas GRα was not associated with fat cell size independently of obesity.

Association of Obesity with Increased 11βHSD1 mRNA Levels in Subcutaneous Depots but Reduced GRα mRNA in the Abdominal Subcutaneous Fat

Because reporting on glucocorticoid action has been largely in the abdominal subcutaneous depot, we extended our subcutaneous depots to gluteal and thigh to test whether the expected relationships held in these distinct compartments. Positive associations with BMI and 11βHSD1 mRNA levels were detected in all subcutaneous adipose compartments examined (e.g., abdominal subcutaneous adipose: $R = 0.584$, $p < 0.05$; Table 2). Thigh adipose 11βHSD1 mRNA correlated positively with SAT, and this relationship showed a consistent trend in the other depots (Table 2). In contrast, abdominal subcutaneous GRα mRNA levels were inversely correlated with BMI ($R = -0.589$, $p < 0.05$; Table 2). No significant associations were observed between SAT and abdominal subcutaneous GRα mRNA levels (Figure 3B) or GRα mRNA levels in any other subcutaneous depots (Table 2).

Abdominal Subcutaneous Hypertrophy is Associated with Reduced GRα mRNA Levels

Although multiple regression analysis with small numbers of abdominal subcutaneous biopsies should be interpreted cautiously, our data nevertheless indicate the following. Surprisingly, in subcutaneous abdominal adipose tissue, 11βHSD1 mRNA levels were not associated with fat cell size (Figure 3C). In contrast, abdominal subcutaneous GRα transcript levels were negatively correlated with fat cell size (Figure 3D). Multiple regression analysis confirmed that GRα mRNA levels were independently and negatively correlated with abdominal subcutaneous fat cell size (standardized β coefficient, -0.014; $p < 0.05$). Although GRα levels were negatively correlated with fat cell size in the thigh, this relationship did not hold when tested by multiple regression analysis.

Associations of Depot-specific Glucocorticoid Action with Metabolic Parameters

Pearson correlation was used to examine interrelationships between transcript levels and metabolic parameters (Table 2). Higher omental and thigh 11βHSD1 levels were associated with increased triglycerides levels (omental: $R = 0.46$, $p < 0.05$; thigh: $R = 0.57$, $p < 0.01$). This effect was not independent of obesity as confirmed by multiple linear regression analysis. There were no significant associations between fasting glucose, insulin, or HOMA-IR and 11βHSD1 transcript levels. In contrast, there was a negative correlation between GRα mRNA levels and plasma triglycerides levels selectively in the omental compartment ($R = -0.50$, $p < 0.05$). Moreover, there was a trend for inverse associations between omental GRα and fasting plasma insulin levels ($R = -0.48$, $p = 0.052$).

Discussion

This study examined relationships between two major determinants of tissue glucocorticoid action in multiple adipose tissue depots in lean and obese women. The key findings were 1) 11βHSD1 mRNA is most highly expressed in subcutaneous abdominal and omental tissues, whereas GRα mRNA is highest in omental adipose tissue; 2) within individuals, there are positive associations between 11βHSD1 mRNA levels in subcutaneous adipose depots but not omental fat, whereas GRα mRNA levels do not correlate between depots; 3) between individuals, 11βHSD1 mRNA levels in all adipose depots, including omentum, are

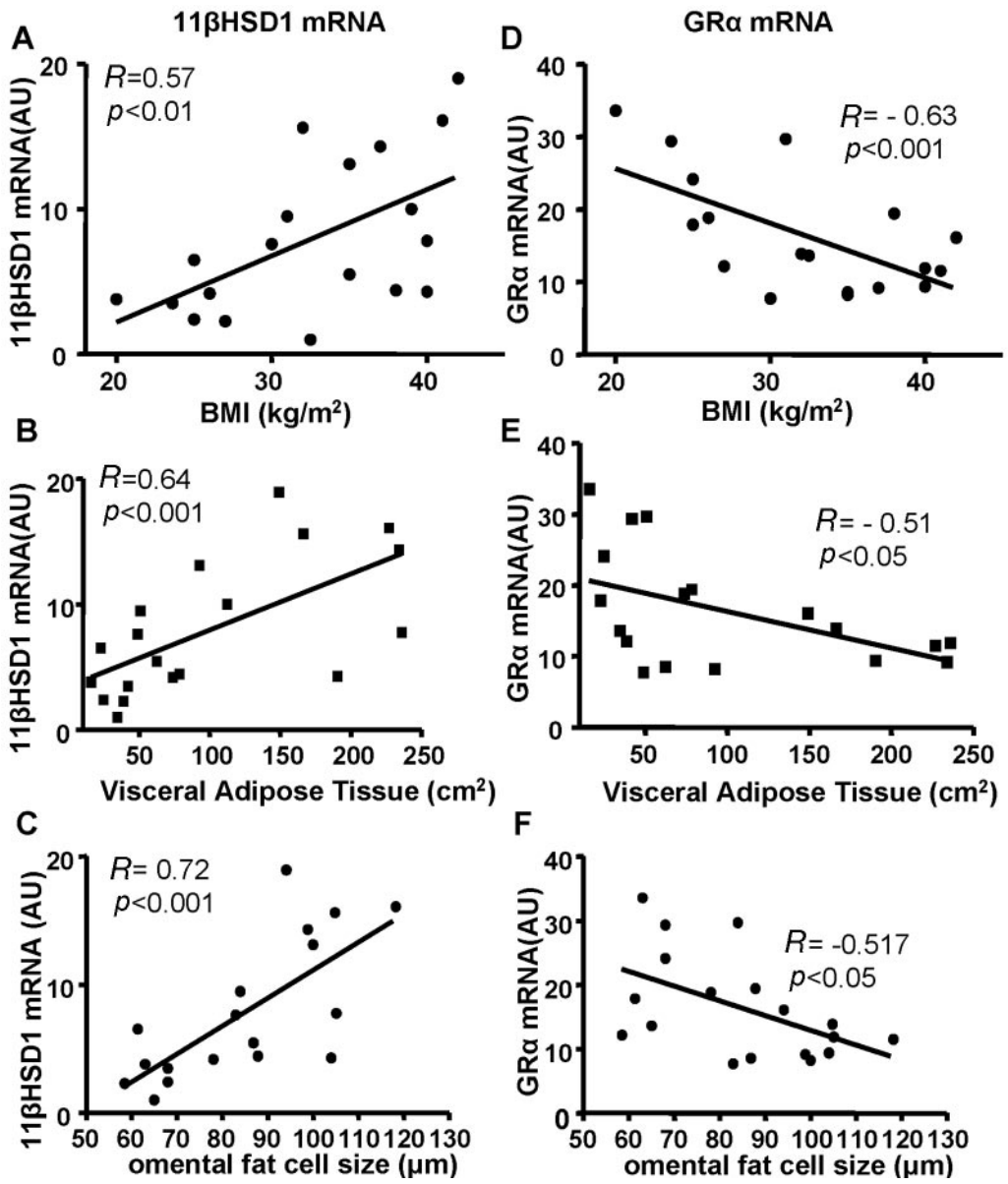

Figure 2: Correlation of 11βHSD1 and GRα transcript levels with anthropometric parameters and fat cell size in the omental adipose compartment. Correlation of (A) BMI with 11βHSD1, (B) VAT with 11β-HSD1, (C) fat cell size with 11βHSD1, (D) BMI with GRα mRNA levels, (E) VAT with GRα mRNA levels, and (F) fat cell size with GRα mRNA levels. Regression lines and *R* and *p* values are indicated in each graph. NS, non-significant correlation.

positively associated with BMI and local fat mass, whereas for GRα mRNA the main relationships were negative associations in the omentum; 4) increased fat cell size strongly associates with increased 11βHSD1 but reduced GRα in the omentum.

Here we extend our (4,6,8,10) and others (5,7,9) previous observations on abdominal subcutaneous adipose to show a positive relationship between BMI and 11βHSD1 mRNA levels in all four adipose compartments examined. This implies an up-regulation of glucocorticoid production in multiple adipose tissue compartments, including the visceral fat depot. Increased visceral fat is a better predictor of metabolic abnormalities compared with upper-body subcutaneous fat (1,2) and is independently correlated with increased morbidity and mortality (32). In contrast, lower-body obesity may even show a protective effect with respect to metabolic abnormalities (33). In our cohort, omental 11βHSD1 mRNA levels were also most strongly associated with increased general adiposity (% body fat). Kannisto et al. (9) previously reported a positive association between percent body fat and 11βHSD1 mRNA levels in subcutaneous in obese male and female monozygotic twins. In our

Table 2. Pearson correlation (R) of 11βHSD1 and GRα mRNA levels in multiple adipose tissue depots with body composition, metabolic parameters, and fat cell sizes

	11βHSD1 mRNA				GRα mRNA			
	Abdominal	Log thigh	Log gluteal	Omental	Abdominal	Log thigh	Gluteal	Omental
BMI	0.58*	0.53*	0.54*	0.57†	−0.59*	−0.24	−0.20	−0.63‡
Percent body fat	0.22	0.41	0.44	0.46*	−0.50	−0.24	−0.01	−0.41
VAT	0.55*	0.73‡	0.71‡	0.64‡	−0.30	−0.05	−0.32	−0.51*
SAT	0.36	0.55†	0.40	0.63‡	−0.57	−0.15	−0.13	−0.60‡
Log fasting glucose	0.20	−0.29	−0.32	−0.18	0.14	−0.41	−0.04	−0.27
Fasting insulin	0.1	0.09	0.26	0.33	−0.38	−0.12	0.01	−0.41
Fasting triglycerides	0.21	0.57†	0.46	0.46*	−0.44	0.01	0.2	−0.50*
Log FCS abdominal	0.19				−0.80†			
FCS thigh		0.28				−0.51*		
FCS gluteal			0.40				0.03	
FCS omental				0.72‡				−0.52†

11β HSD1, 11β-hydroxysteroid dehydrogenase type 1; GRα, glucocorticoid receptor α; VAT, visceral adipose tissue; SAT, subcutaneous adipose tissue; FSC, fat cell size. Percent body fat was measured using DXA. VAT and SAT were measured by computed tomography scan. FCS was determined by measuring the mean adipocyte diameter. Plasma glucose values, abdominal FCS, and 11βHSD1 mRNA levels in thigh and gluteal regions and GRα mRNA levels in thigh showed inhomogeneity of variance and were log-transformed before analysis.
* $p < 0.05$.
† $p < 0.01$.
‡ $p < 0.001$.

study, subcutaneous adipose expression of 11βHSD1 mRNA did not correlate with percent body fat. Differences between these studies may be caused by the distinct populations studied and/or our limited power to detect this interaction because 11βHSD1 did correlate with other markers of generalized obesity such as BMI. Although in this study we did not measure 11βHSD1 activity levels because of limited sizes of biopsies, we expect, from previous studies (7,10), that activity and mRNA levels are correlated in abdominal subcutaneous adipose tissue biopsies.

GRα transcript levels were highest in omental (visceral) fat, as previously reported in humans (26) and mice (12). The major new finding is that in omental and abdominal subcutaneous adipose, GRα is inversely associated with adiposity and fat cell size. A previous study also reported lower GRα mRNA levels in subcutaneous adipose tissue in severely obese women (34). Moreover, omental GRα mRNA levels were negatively associated with plasma triglyceride and, albeit as a trend, insulin levels. This finding is perhaps counterintuitive because GR polymorphisms causing increased glucocorticoid sensitivity lead to increased visceral fat accumulation (25). Our data suggest that reduction of GR levels to the degree we observe in obesity does not sufficiently compensate for the hypertrophy caused by increased ligand regeneration (i.e., 11βHSD1). This notion is supported by data from transgenic animal models. Thus, fat-specific 11βHSD1 overexpressing mice (12) have increased visceral adiposity, and 11βHSD1 null mice have reduced visceral adiposity (16), despite unaltered GR levels. In contrast in humans, to our knowledge, this is the first study describing a consistent opposing change in 11βHSD1 and GRα mRNA in multiple adipose compartments with obesity. However, because the two transcripts were not correlated in any depot, consistent with previous observations in subcutaneous adipose tissue (9), it seems unlikely that GRα and 11βHSD1 directly regulate each other. Naturally, there are clearly limitations with association studies, which do not test causality, and further direct study is needed to elucidate possible mechanisms involved.

The volunteers who participated in our study had normal glucose and triglyceride levels but impaired insulin sensitivity. Increased plasma triglycerides were associated with increased 11βHSD1 in both thigh and omental regions but with reduced GRα mRNA levels selectively in the omental compartment. Neither 11βHSD1 nor GRα mRNA levels were associated with fasting glucose, which is consistent with our previous report (7). However, there seemed to be a

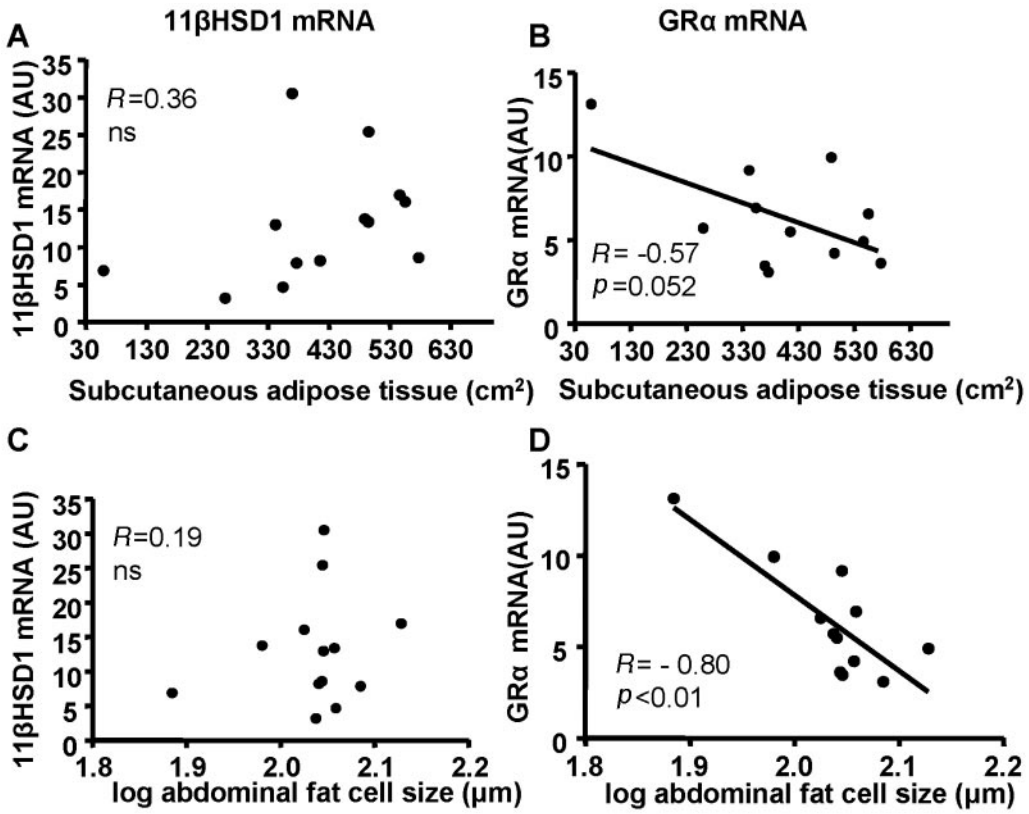

Figure 3: Correlation of 11βHSD1 and GRα transcript levels with peripheral adiposity and fat cell size in abdominal subcutaneous compartment. Correlation of (A) SAT with 11βHSD1 mRNA levels, (B) SAT with GRα mRNA levels, (C) fat cell size (FCS) with 11βHSD1 mRNA levels, and (D) FCS with GRα mRNA levels. Regression lines and *R* and *p* values are indicated in each graph. NS, non-significant correlation.

trend for a negative association of omental and thigh GRα mRNA with fasting insulin levels that would be interesting to confirm in larger cohorts.

Visceral fat adipocytes are more resistant to insulin's anti-lipolytic effects compared with subcutaneous adipocytes (35). Transgenic mice overexpressing 11βHSD1 in fat develop central obesity attributed to adipocyte hypertrophy, particularly in the mesenteric depot (12). To our knowledge, this is the first study that addressed the relationship of 11βHSD1 or GRα mRNA levels with regional fat cell size. Consistent with previous studies (36–38), we found larger adipocytes in the abdominal subcutaneous compared with omental depot, indicating higher fat storage in this depot in women. We showed a strong positive correlation between 11βHSD1 and adipocyte size in the omental depot, independent of obesity. Despite the negative association of GRα mRNA with omental fat cell size, this was not independent of obesity. Although 11βHSD1 was equally high in the abdominal subcutaneous and omental depot, we did not find an association between 11βHSD1 mRNA levels and abdominal fat cell size, despite the strong positive correlation with BMI. This may seem counterintuitive. The reasons for this might be our limited power to detect a possible correlation because we had fewer abdominal subcutaneous compared with omental depot biopsies. Alternatively, 11βHSD1 is not a strong predictor of subcutaneous hypertrophy in our cohort. This is supported by the lack of correlation between 11βHSD1 and fat cell size in the thigh and gluteal depots. In contrast to findings in the omental depot, GRα mRNA was negatively associated with fat cell size in the abdominal subcutaneous depot, independent of obesity. It would seem that obesity is associated with a down-regulation of GRα that is expected to limit the hypertrophic effects of GCs in adipose tissue (21–23). However, our data suggest that this GR down-regulation cannot entirely counteract increased ligand levels, particularly in the omental depot. It will be important to determine whether and how altered GR levels can indeed reach a functionally limiting state with respect to adipose hypertrophy in obesity.

In conclusion, 11βHSD1 mRNA is a strong predictor of omental fat hypertrophy, whereas GR mRNA is negatively associated with obesity.

Acknowledgments

This work was supported by the Wellcome Trust (PhD studentship awarded to ZM; Programme Grant to J.R.S., B.R.W., and K.E.C.; Intermediate Fellowship to N.M.M.), DK45343 (P.I.M. Jensen), DK50456, and RR-0585 from the U.S. Public Health Service and by the Mayo Foundation. We are grateful to the staff of the Genetics Core Laboratory, Wellcome Trust CRF, Western General Hospital, Edinburgh, for assistance in the real-time polymerase chain reaction assays and to members of the Endocrinology Unit for helpful discussions.

References

1. **Fujioka S, Matsuzawa Y, Tokunaga K, Tarui S.** Contribution of intra-abdominal fat accumulation to the impairment of glucose and lipid metabolism in human obesity. *Metabolism.* 1987;36:54–9.
2. **Despres JP, Nadeau A, Tremblay A, et al.** Role of deep abdominal fat in the association between regional adipose tissue distribution and glucose tolerance in obese women. *Diabetes.* 1989;38:304–9.
3. **Kennel WB, Cupples LA, Ramaswami R, Stokes J, Kreger BE, Higgins M.** Regional obesity and risk of cardiovascular disease; the Framingham Study. *J Clin Epidemiol.* 1991;44: 183–90.
4. **Seckl JR, Morton NM, Chapman KE, Walker BR.** Glucocorticoids and 11beta- hydroxysteroid dehydrogenase in adipose tissue. *Recent Prog Horm Res.* 2004;59:359–93.
5. **Rask E, Walker BR, Soderberg S, et al.** Tissue-specific changes in peripheral cortisol metabolism in obese women: increased adipose 11beta-hydroxysteroid dehydrogenase type 1 activity. *J Clin Endocrinol Metab.* 2002;87:3330–6.
6. **Paulmyer-Lacroix O, Boullu S, Oliver C, Alessi MC, Grino M.** Expression of the mRNA coding for 11beta-hydroxysteroid dehydrogenase type 1 in adipose tissue from obese patients: an in situ hybridization study. *J Clin Endocrinol Metab.* 2002;87:2701–5.
7. **Lindsay RS, Wake DJ, Nair S, et al.** Subcutaneous adipose 11 beta-hydroxysteroid dehydrogenase type 1 activity and messenger ribonucleic acid levels are associated with adiposity and insulinemia in Pima Indians and Caucasians. *J Clin Endocrinol Metab.* 2003;88:2738–44.
8. **Engeli S, Bohnke J, Feldpausch M, et al.** Regulation of 11beta-HSD genes in human adipose tissue: influence of central obesity and weight loss. *Obes Res.* 2004;12:9–17.
9. **Kannisto K, Pietilainen KH, Ehrenborg E, et al.** Overexpression of 11beta-hydroxysteroid dehydrogenase-1 in adipose tissue is associated with acquired obesity and features of insulin resistance: studies in young adult monozygotic twins. *J Clin Endocrinol Metab.* 2004;89:4414–21.
10. **Wake DJ, Rask E, Livingstone DE, Soderberg S, Olsson T, Walker BR.** Local and systemic impact of transcriptional up-regulation of 11beta-hydroxysteroid dehydrogenase type 1 in adipose tissue in human obesity. *J Clin Endocrinol Metab.* 2003;88:3983–8.
11. **Livingstone DE, Jones GC, Smith K, et al.** Understanding the role of glucocorticoids in obesity: tissue-specific alterations of corticosterone metabolism in obese Zucker rats. *Endocrinology.* 2000;141:560–3.
12. **Masuzaki H, Paterson J, Shinyama H, et al.** A transgenic model of visceral obesity and the metabolic syndrome. *Science.* 2001;294:2166–70.
13. **Sandeep TC, Andrew R, Homer NZ, Andrews RC, Smith K, Walker BR.** Increased in vivo regeneration of cortisol in adipose tissue in human obesity and effects of the 11beta-hydroxysteroid dehydrogenase type 1 inhibitor carbenoxolone. *Diabetes.* 2005;54:872–9.
14. **Bujalska IJ, Kumar S, Stewart PM.** Does central obesity reflect "Cushing's disease of the omentum"? *Lancet.* 1997; 349:1210–3.
15. **Masuzaki H, Yamamoto H, Kenyon CJ, et al.** Transgenic amplification of glucocorticoid action in adipose tissue causes high blood pressure in mice. *J Clin Invest.* 2003;112:83–90.
16. **Morton NM, Holmes MC, Fievet C, et al.** Improved lipid and lipoprotein profile, hepatic insulin sensitivity, and glucose tolerance in 11beta-hydroxysteroid dehydrogenase type 1 null mice. *J Biol Chem.* 2001;276:41293–300.
17. **Morton NM, Paterson JM, Masuzaki H, et al.** Novel adipose tissue-mediated resistance to diet-induced visceral obesity in 11 beta-hydroxysteroid dehydrogenase type 1-deficient mice. *Diabetes.* 2004;53:931–8.
18. **Tomlinson JW, Sinha B, Bujalska I, Hewison M, Stewart PM.** Expression of 11beta- hydroxysteroid dehydrogenase type 1 in adipose tissue is not increased in human obesity. *J Clin Endocrinol Metab.* 2002;87:5630–5.
19. **Aldhahi W, Mun E, Goldfine AB.** Portal and peripheral cortisol levels in obese humans. *Diabetologia.* 2004;47:833–6.
20. **Basu R, Singh RJ, Basu A, et al.** Obesity and type 2 diabetes do not alter splachnic cortisol production in humans. *J Clin Endocrinol Metab.* 2005;90:3919–26.
21. **Xu X, Björntorp P.** Effects of dexamethasone on multiplication and differentiation of rat adipose adipose precursor cells. *Exp Cell Res.* 1990;189:242–52.
22. **Cigolini M, Smith U.** Human adipose tissue in culture.VIII. Studies of the insulin-antagonistic effect of glucocorticoids. *Metabolism.* 1979;28:502–10.
23. **Fried SK, Russell CD, Grauso NL, Brolin RE.** Lipoprotein lipase regulation by insulin and glucocorticoid in subcutaneous and omental adipose tissue of obese women and men. *J Clin Invest.* 1993;92:2191–8.
24. **van Rossum EF, Lamberts SW.** Polymorphisms in the glucocorticoid receptor gene and their associations with metabolic parameters and body composition. *Recent Prog Horm Res.* 2004;59:333–57.
25. **Tremblay A, Bouchard L, Bouchard C, Despres JP, Drapeau V, Perusse L.** Long-term adiposity changes are related to a glucocorticoid receptor polymorphism in young females. *J Clin Endocrinol Metab.* 2003;88:3147–5.
26. **Rebuffe-Scrive M, Bronnegard M, Nilsson A, Eldh J, Gustafsson JA, Björntorp P.** Steroid hormone receptors in human adipose tissues. *J Clin Endocrinol Metab.* 1990;71: 1215–9.
27. **Jensen MD, Kanaley JA, Reed JE, Sheedy PF.** Measurement of abdominal and visceral fat with computed tomography and dual-energy X-ray absorptiometry. *Am J Clin Nutr.* 1995;61:274–8.

28. **Jensen MD, Kanaley JA, Roust LR, et al.** Assessment of body composition with use of dual-energy x-ray absorptiometry: evaluation and comparison with other methods. *Mayo Clin Proc.* 1993;68:867–73.
29. **Jensen MD, Sarr MG, Dumesic DA, Southorn PA, Levine JA.** Regional uptake of meal fatty acids in humans. *Am J Physiol Endocrinol Metab.* 2003;285:E1282–8.
30. **Matthews DR, Hosker JP, Rudenski AS, Naylor BA, Treacher DF, Turner RC.** Homeostasis model assessment: insulin resistance and beta-cell function from fasting plasma glucose and insulin concentrations in man. *Diabetologia.* 1985;28:412–9.
31. **Tchoukalova YD, Harteneck DA, Karwoski RA, Tarara J, Jensen MD.** A quick, reliable, and automated method for fat cell sizing. *J Lipid Res.* 2003;44:1795–801.
32. **Kuk JL, Katzmarzyk PT, Nichamann Z, Church TS, Blair SN, Ross R.** Visceral fat is an independent predictor of all-cause mortality in men. 2006;14:336–41.
33. **Snijder MB, van Dam RM, Seidell JC.** What aspects of body fat are particularly hazardous and how do we measure them? *Int J Epidemiol.* 2006;35:83–92.
34. **Boullu-Ciocca S, Paulmyer-Lacroix O, Fina F, et al.** Expression of the mRNAs coding for the glucocorticoid receptor isoforms in obesity. *Obes Res.* 2003;11:925–9.
35. **Richelsen B, Pedersen SB, Moller-Pedersen T, Balk JF.** Regional differences in triglyceride breakdown in human adipose tissue effects of catecholamins, insulin and prostaglandin E2. *Metabolism.* 1991;40:990–6.
36. **Ostman J, Arner P, Engfeldt P, Kager L.** Regional differences in the control of lipolysis in human adipose tissue. *Metabolism.* 1979;28:1198–205.
37. **Rebuffe-Scrive M, Andersson B, Olbe L, Bjorntrop P.** Metabolism of adipose tissue in intraabdominal depots of nonobese men and women. *Metabolism.* 1990;38:453–8.
38. **Tchernof A, Belanger C, Morisset A, et al.** Regional differences in adipose tissue metabolism in women. Minor effect of obesity and body fat distribution. *Diabetes.* 2006; 55:1353–60.